University of Stavanger

FACULTY OF SCIENCE AND TECHNOLOGY

MASTER'S THESIS

Study program / Specialization: Petroleum Engineering / Well Engineering	Spring semester, 2019 Open access
Writer: Hadi Tranggono	…… (Writer's signature)
Supervisor: Bernt Sigve Aadnøy & Eirik Kårstad	
Thesis title: Wellbore Collapse Failure Criteria and Drilling Optimization	
Credits (ECTS): 30	
Keywords: Pore Pressure Fracture Pressure Insitu Stress Rock Mechanics Collapse Pressure Formation Casing Design Cutting Transport & Hydraulic Methods	Pages : 122 + enclosure : 20 Stavanger, 15 June 2019

ACKNOWLEDGEMENTS

This master's thesis is completed as one of the requirement to accomplish master degree in Petroleum Engineering with specialization in Well engineering in University of Stavanger, Norway.

I would like to express my thankfullness to God Almighty for giving me the opportunity and bless me to finish my study in Well Engineering. It is not easy to complete master degree in different environtment and far away from my country (Indonesia) but God have a different ways to help His children.

I would like to thank to my family that give me a freedom to continue my study. I would like to thank to my fiance, Anggi Novia Regina that support and help me to finish my master's thesis.

Special thank to my internal supervisor, Bernt S. Aadnøy that always have a time to meet and discuss about my master thesis. I also would like to thank to my external supervisor, Eirik Kårstad that help me to finish my master thesis.

Last but not least, I would like to thank to indonesian community in Stavanger for their support during my study in Stavanger.

ABSTRACT

Design and planning in drilling a well are a key for successful before to execute drilling operation. A good understanding of wellbore stability, design mud, casing, cementing, BHA & drillstring, drilling bit, hole cleaning & hydraulic are an important process in well planning. Good design and planning can keep drilling activity on track based on schedule and it can avoid non-productive time during drilling.

By knowing the rock mechanics properties is important in the drilling design. Many problems happen during drilling relate to rock mechanics. One of the problem during drilling relates to rock mechanics is wellbore instability. Before drilling, rock in equilibrium condition but after drilling, there is a disturbance in the rock formation and it changes stress distribution. Knowing the insitu stresses (vertical stress, maximum horizontal stress, minimum horizontal stress) and stresses around the borehole wall (radial stress, axial stress and tangential stress) are important. With knowing these parameters, wellbore collapse caused by shear stress can be avoided. In this thesis will analyze the sensitivity of the failure criteria with respect to horizontal stress anisotropy and depth, in order to evaluate which failure criteria to recommend under which stress conditions. Mohr-Coulomb, Modified Lade and Stassi d' Alia models will be used to figure out the failure criteria. The result of these models is used to estimate critical mud weight to prevent wellbore collapse.

This study also will analyze drilling optimization through casing design, hole cleaning and hydraulic design, drillstring and bottom hole assembly (BHA) design. Landmark drilling software is used to design drilling optimization. With a good well design, it is expected that it can manage drilling on the track based on budget and it can mitigate problems during drilling.

TABLE OF CONTENTS

LIST OF FIGURES

LIST OF TABLES

1. INTRODUCTION

1.1 Background

Wellbore instability is one of serious problems during drilling in oil and gas company. Based on Bernt S. Aadnøy (Aadnøy, 2003), the overall drilling cost is increase by 10 % due to wellbore instability problems. Two kinds of wellbore instability problems are wellbore collapse and fracture. Wellbore collapse is happen when mud weight in the wellbore does not enough to support external pressure from formation (collapse pressure) so that wellbore under compression. On the other hand, wellbore fracture is happen when mud weight is larger than fracture pressure so that wellbore in tension condition.

Rock formation remain stable and in equilibrium condition before drilling. After drilling, there is a disturbance and it change the stability condition. Wellbore stability is dominated by insitu stress system. When drilling a well, the rock surrounding the wellbore must take the load that was previously taken by the removed rock. As a result, the insitu stress is change in the borehole wall. This stress can lead to rock failure. This problem can be avoided by adjust the mud density so that stress concentration around the borehole wall can be managed to minimize borehole failure.

In this study will use three models to analyze shear failure criteria, they are Modified Lade, Stassi d' Alia and Mohr Coulomb. Modified Lade and Stassi d' Alia methods using three principal stresses where where $\sigma_1 \neq \sigma_2 \neq \sigma_3$. On the other hand, Mohr-Coulomb method using two principal stresses where $\sigma_1 \neq \sigma_2 = \sigma_3$. The value of these stresses (σ) are different with depth so that in this thesis will analyze the failure criteria with respect to stress anisotrophy and depth.

In this study, the data are derived from seismic interval velocity, logging data and well data. These data are used to calculate pore pressure, fracture pressure, rock mechanic properties, stress distribution and collapse pressure formation. From all of these data, the optimum mud weight to avoid wellbore failure can be estimated. By generating mud safe window, problems during drilling related to wellbore instability can be avoided.

Furthermore, data from this wellbore stability can be used as an input to estimate casing setting depth, casing design, cutting transport and hydraulic system design. Landmark drilling software like Compass, Stress check, Wellplan are used to analyze casing design, cutting transport and hydraulic system design. With good planning and design of wellbore, problem during drilling can be avoided and it can minimize drilling cost.

1.2 Thesis Objective

The main objective of this thesis are:

1. Calculate pore pressure and fracture pressure
2. Calculate insitu stresses
3. Calculate rock mechanics Properties
4. Analyze wellbore failure criteria using Mohr-Coulomb, Modified Lade and Stassi d' Alia.
5. Calculate formation collapse pressure
6. Drilling Optimization using Landmark drilling software to design casing, hole cleaning & hydraulic systems.

2. BASIC THEORY WELLBORE COLLAPSE FAILURE CRITERIA

2.1 Rock Mechanical Properties

2.1.1. Stress

Stress is defined as force acting over an area. The SI unit is Pascal (N/m^2) and the field unit is pound per square inch (psi). Stress is not dependent on the size and shape of a body but it is dependent on its orientation (Aadnøy and Looyeh, 2011). Mathematically, stress is defined as below :

$$\sigma = \frac{F}{A} \tag{1}$$

Where

σ = Stress (Pound per square inch, psi)

F = Force (Pound, Lb)

A = Surface Area (Square inch, $inch^2$)

There are two types of stress. Stress that acts perpendicular to the plane, it is called normal stress (σ) and stress that act parallel to the plane, it is called shear stress (τ). this stress can be seen in the figure below.

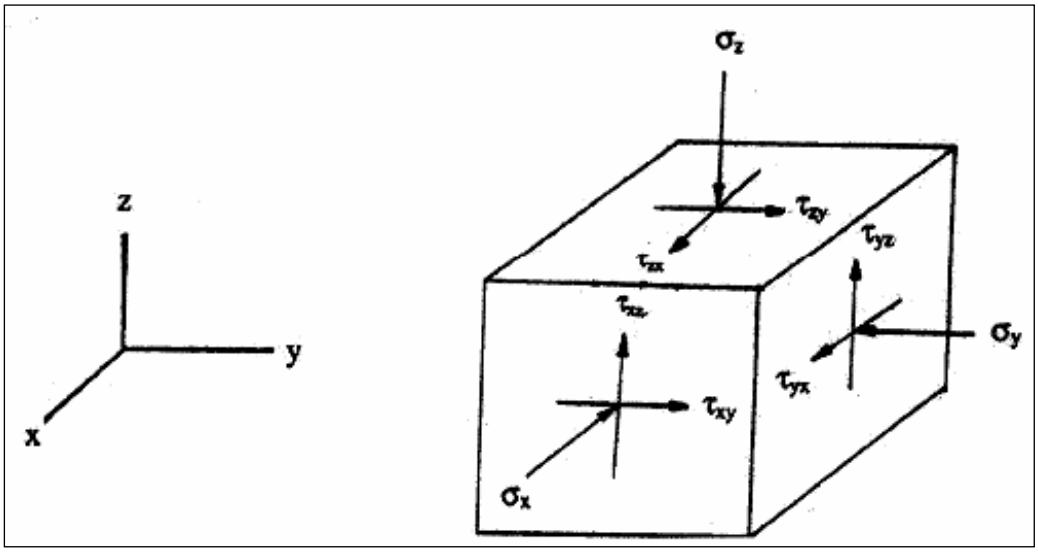

Figure 1 Stresses acting on the cube (Aadnøy & Looyeh, 2011)

Based on figure above, there are nine components that act on the cube, these are :

Normal stresses : σ_x, σ_y, σ_z

Shear stresses : τ_{xy}, τ_{yx}, τ_{xz}, τ_{zx}, τ_{yz}, τ_{zy}

According to the Newton's second law, all forces acting on the body can cancel each other when the stress body reamin at rest. There is no translation or rotation force acting on it so that it can be simplified like this :

$$\tau_{xy} = \tau_{yx} \tag{2}$$

$$\tau_{xz} = \tau_{zx} \tag{3}$$

$$\tau_{yz} = \tau_{zy} \tag{4}$$

And the stress tensor becomes :

$$[\sigma] = \begin{matrix} \sigma_x & \tau_{xy} & \tau_{xz} \\ \tau_{xy} & \sigma_y & \tau_{yz} \\ \tau_{xz} & \tau_{yx} & \sigma_z \end{matrix} \quad (5)$$

The stresses consist of three normal stresses and three shear stresses now. Generally in rock mechanics, compressive stresses is defined as negative value and tensile stresses as positive value.

2.1.2. Strain

Strain is the ratio of the change in length per original length due to an applied load. Strain is determined by applying load to the body of material and the change in dimension is measured.

Mathematically,

$$\varepsilon = \frac{l - l_o}{l_o} \quad (6)$$

Where,

ε = strain

l = new length

lo = original length

In elastic deformation, the rock deforms as stress is applied but it will come to the original shape when stress is relieved. In elastic deformation, the strain is proportional to the stress (Hooke's Law). The plastic deformation is formed when applied stress reaches the elastic limit. In plastic deformation, the rock only partially returns to its original shape when stress is relieved. If more stress is applied, the fractures will be formed and the rock become fails (ultimate failure). Rock become fail in brittle condition in low confining stress and it will become in ductile condition in higher confining stress. The Ultimate tensile strength is the maximum load where the material can be exposed to before it fails. The yield point is the stress at transition zone between elastic and plastic zone.

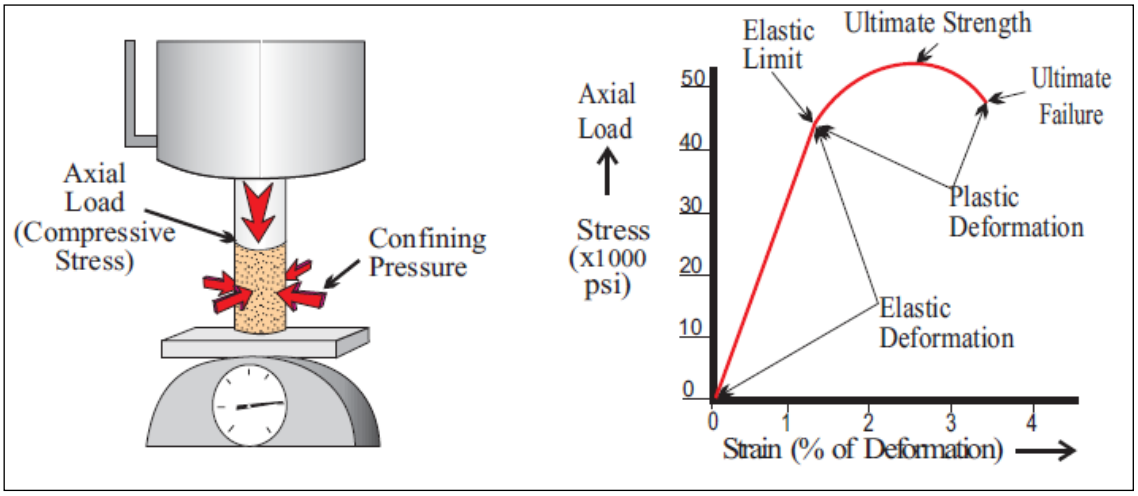

Figure 2 Typical stress-strain behavior of a material (Amoco, 2010)

2.1.3. Young's Modulus

Young's modulus (E) measure the stiffness of material. Young's modulus can be applied only in the elastic region.

Mathematically,

$$E = \frac{\Delta\sigma}{\Delta\varepsilon} \tag{7}$$

Young's modulus also can be calculated from linear slope in relation between stress and strain as shown in figure below

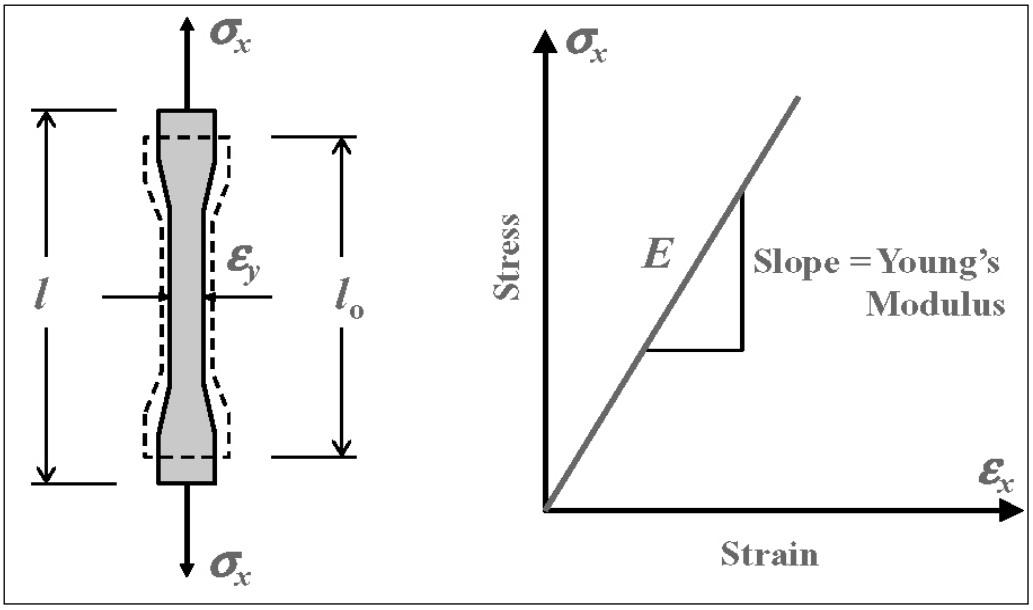

Figure 3 Stress-strain diagram showing linear elastic deformation (Aadnøy & Looyeh, 2011)

Young's modulus (E) also can be calculated from field data using compressional velocity (V_p), shear velocity (V_s), and bulk density (ρ). Mathematically, Young's modulus (E) can be obtained as :

$$E = \rho\, V_s^2\, \frac{3V_p^2 - 4V_s^2}{V_p^2 - V_s^2} \tag{8}$$

2.1.4. Poisson Ratio

Poisson ratio is ratio between lateral strains to axial strain. It can be calculated through laboratory test with this equation:

$$\upsilon = -\frac{\varepsilon_x}{\varepsilon_y} \tag{9}$$

Poisson ratio also can be determined using log data with this equation :

$$\upsilon = \frac{V_p^2 - 2V_s^2}{2(V_p^2 - V_s^2)} \tag{10}$$

Where

V_p = compressional waves

V_s = shear waves

2.1.5. Angle of Internal Friction

PoissonThe angle of internal friction is defined as "a measure of the ability of a unit of rock or soil to withstand a shear stress. It is the angle (ϕ), measured between normal force (N) and resultant force (R), that is attained when failure just occurs in response to a shearing stress (τ). Its tangent (τ/N) is the coefficient of sliding friction. Its value is determined experimentally" (Allaby and Allaby, 1999a). This angle of internal friction is used to calculate coefficient of friction (μ) with this equation:

$$\mu = \tan \phi \tag{11}$$

The angle of internal friction (ϕ) are obtained from conducting laboratory tests on core samples or from logging data. There are many empirical equations to calculate internal friction of angle. These are some empirical equation to calculate angle of internal friction:

1. Chang and Zoback, 2003

$$\phi = 18.532 V_p^{0.5148} \tag{12}$$

ϕ is in degrees and Vp is in km/sec

2. Manohar Lal correlation (Lal et al., 1999)

$$\text{Sin } \phi = \frac{V_p - 1}{V_p + 1} \tag{13}$$

ϕ is in degrees and Vp is in km/sec

3. Horsruds correlation (Horsrud et al., 2001)

$$\beta = 39.9^0 + 5.5 V_p \tag{14}$$

ϕ is in degrees and Vp is in km/sec

2.1.6. Cohesive Strength

Cohesive strength (So) is the bond strength between the grains in the rock. The frictional resistance between the grains is the product of the coefficient friction (μ) and the effective compressive stress (σ). If the shear stress greater than cohesive strength and the frictional resistance between the grains ($\mu\sigma$) so the rock will fail.

Shear Stress = Cohesive strength + Frictional Resistance

$$\tau = S_0 + \mu\sigma \tag{15}$$

Several core tests in laboratory are needed to determine the failure envelope. The higher the confining pressure, the greater compressive stress is needed to fail the rock. This figure below expresses how to get cohesive strength and the angle of internal friction from core test in laboratory.

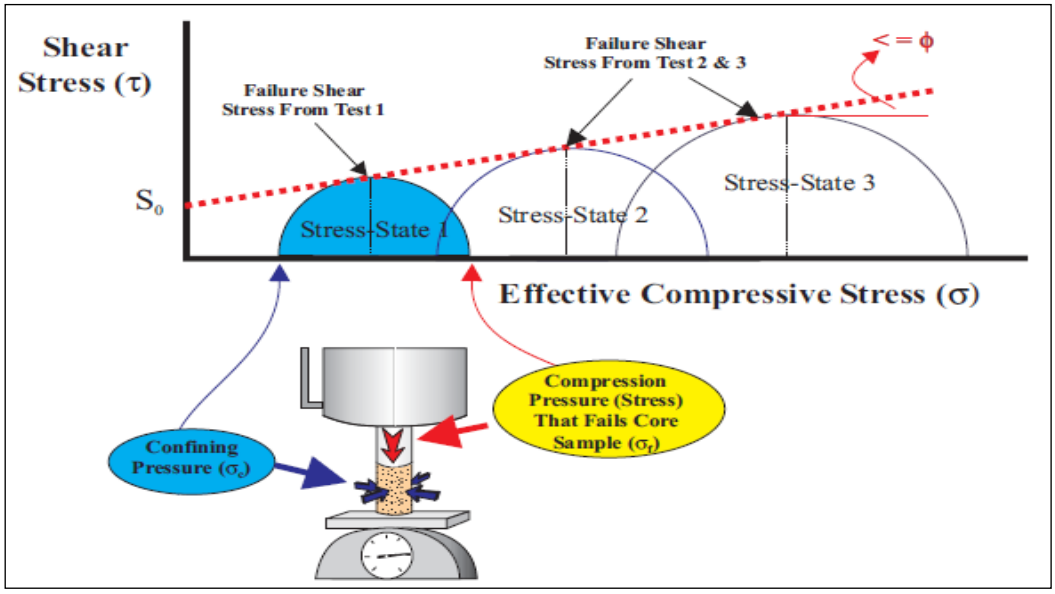

Figure 4 Core test laboratory (Amoco, 2010)

Generally, weak rock with low cohesive strength have relatively high angle of internal friction and higher young's modulus. The relationship of this paramater can be seen in the figure below.

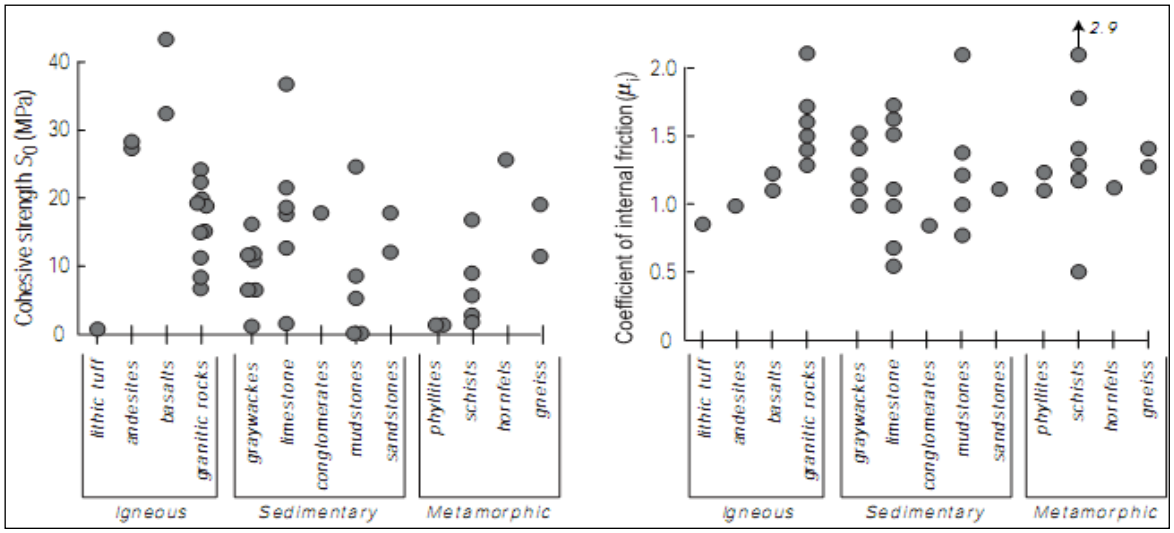

Figure 5 Cohesion and internal friction data for a variety rocks (Carmichael, 1982)

Cohesion (S_0) is not a physically measureable parameter. This parameter can be determined using correlation between coefficient of internal friction (μ) and unconfined compressive strength (C_0).

$$S_0 = \frac{C_0}{2\,[(\mu^2+1)^{0.5}+\mu]} \tag{16}$$

2.1.7. Unconfined Compressive Strength, UCS

The unconfined compressive strength (UCS) is defined as "The strength of a rock or soil sample when crushed in one direction (uniaxial) without lateral restraint" (Allaby and Allaby, 1999b). Mathematically, it can be written with this equation :

$$UCS = C_0 = 2S_0 \tan \beta. \quad (17)$$

where

β = the orientation of failure plane (Fjaer et al., 2008)

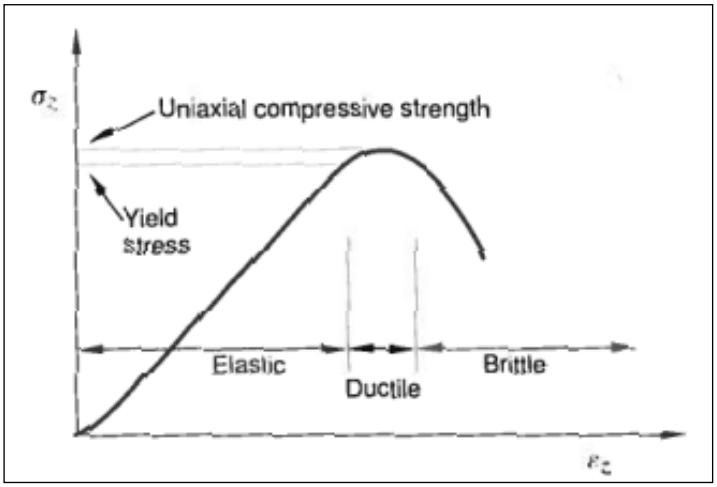

Figure 6 Stress Vs Deformation in Uniaxial Compression test (Zoback, 2010)

Unconfined compressive strength also can be determined using log data. UCS can be estimated using some correlation or equation based on types of lithologies. Some of the correlation that are used in this thesis are :

1. Horsrud, 2001 create an equation to calculate UCS for mosltly high porosity, tertiary shales using sonic log

$$UCS = 0.77\left(\frac{304.8}{\Delta t}\right)^{2.93} \quad (18)$$

2. Mc Nally, 1987 derive an empirical relationship in sandstone for fine grained, both consolidated and unconsolidated sandstone with wide porosity range

$$UCS = 1200 \exp(-0.036\, \Delta t) \quad (19)$$

3. Militzer, 1973 derive an empirical relationship to calculate UCS for limestone using sonic log

$$UCS = \frac{(7682/\Delta t)^{1.82}}{145} \quad (20)$$

Unit used for above calculation : UCS in MPa, Δt in ($\mu s/ft$)

2.2 Insitu Stress

The insitu stress, it is also called as far field stress is stress of rock formation in its original , relaxed and undisturbed position, before drilling a well. generally this stress under compression in nature due to the weight of the overburden. The earth stress are related to a number of some parameter including :

- Tectonic setting
- Depth
- Pore pressure
- Lithology
- Temperature
- Structure

The relationship between stress and some parameters above is complicated due to local geographical differences between basins and interdependence of the above parameters. However, it can be simplified like this :

a. Intrabasin stress variations are correlated with lithology and pore pressure
b. Interbasin stress variations are correlated with tectonic setting and diagenesis (consolidation and cementation).

Insitu stress consist of vertical stress, minimum horizontal stress and maximum horizontal stress. Based on insitu stress magnitudes and tectonic setting, Anderson (1951) classified into three categories :

a. Normal fault regime, the vertical stress (σ_v) is the maximum principal stress (σ_1).
   $\sigma_v > \sigma_H > \sigma_h$
b. Thrust (reverse) fault regime, the horizontal stress (σ_H) is the maximum principal stress (σ_1).
   $\sigma_H > \sigma_h > \sigma_v$
c. Slip fault regime, the horizontal stress (σ_H) is the maximum principal stress (σ_1).
   $\sigma_H > \sigma_v > \sigma_h$

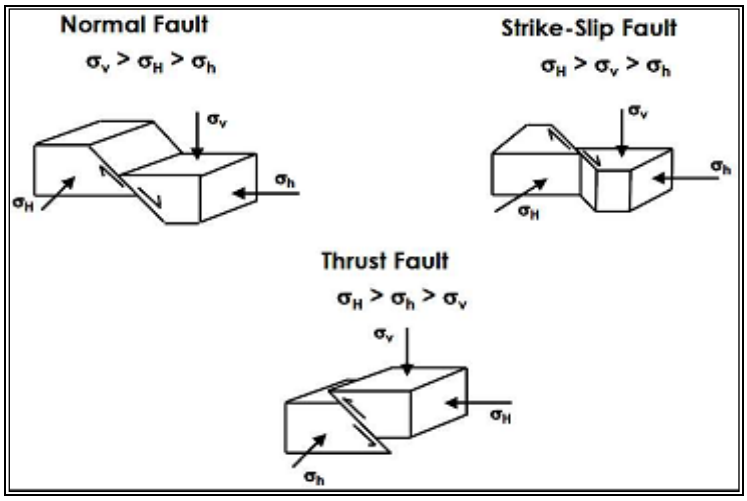

Figure 7 Fault Classifications (SPE 99644)

2.2.1. Vertical Stress

Vertical stress also called as overburden stress. Overburden stress is stress that caused by overlaying of weight from rock matrix and fluid above that depth. Factors that influence the over-burden stress are porosity, fluid density and rock density. Overburden stress can be calculated with this equation :

$$\sigma_v = \left(\sum_{0}^{Depth} \rho sediment \right) x \, \Delta Z \qquad (21)$$

Where

σ_v = Overburden stress
$\rho_{sediment}$ = Density of sediment
Δz = Depth

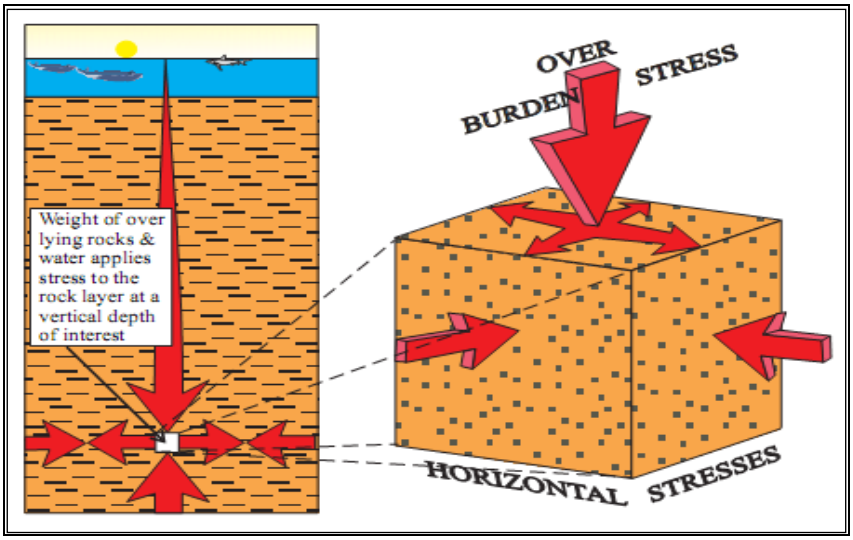

Figure 8 Overburden Stress(Amoco, 2010)

Most formation are formed from sedimentation or compaction. Density of the formation may vary from the earth's surface to the certain depth. Generally with increasing the depth, the rock is compacted and the density trend is increase.

Overburden stress can be calculated using data from density log. If the density log data is missing, the overburden stress can be estimated using Eaton's variable density curve or Wylie time average equation using sonic travel time, bulk density and porosity. Typically the overburden stress is 1 psi/ft.

2.2.2. Minimum Horizontal Stress

As the overburden squeezes the vertically, this stress also will push the sediment in horizontal direction and by constrain from the surrounding rock can create horizontal stress. In relaxaxed formation, two horizontal stress are same ($\sigma_h = \sigma_H$). But in the salt domes area or in the tectonic areas, minimum horizontal stress is not same with maximum horizontal stress ($\sigma_h \neq \sigma_H$).

Generally minimum horizontal stress normally determined from extended leak off test (XLOT). Minimum horizontal stress also can be estimated from other data like leak off test, minifrac, lost circulation and balooning.

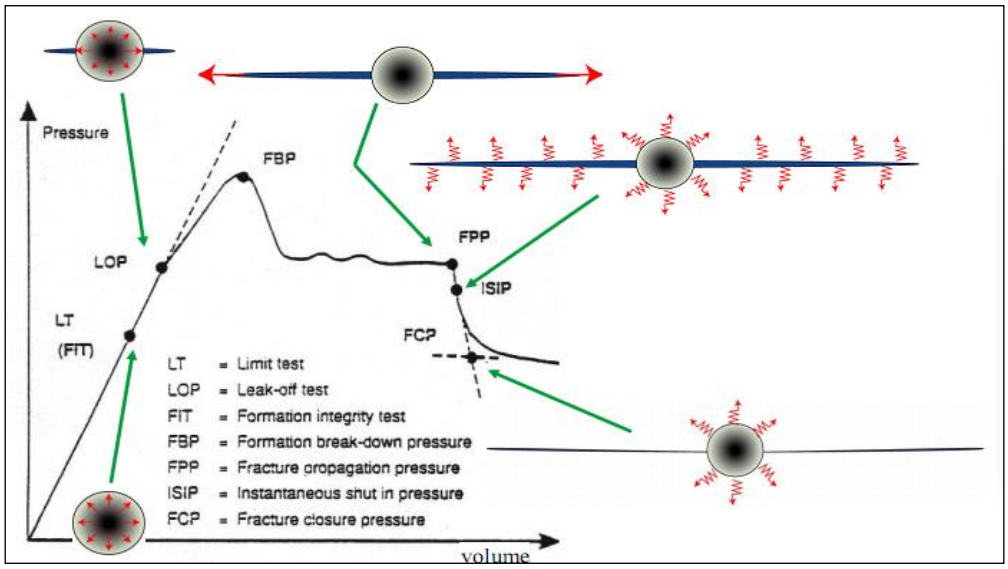

Figure 9 Extended Leaks off Test (After Gaarenstroom et al., 1993)

From figure above, leak off point (LOP) is identic with fracture pressure. During extended leak off test, mud is pumped to the wellbore with low flowrate, for example 1 barrel per minute (1 BPM) and pressure is plotted versus cumulative volume. Pressure where there is a distinct departure from a linier increase with increasing cumulative volume is called leak off point. Formation break-down pressure (FBP) is a peak formation where it form fracture propagation. At formation break-down pressure, fluid will flow faster from wellbore to formation than pump rate and pressure become drops. If pumping continues at constant pump rate, pressure will drop to relatively contant value and it is called fracture propagation pressure (FPP). The Instantaneous shut in pressure (ISIP) is determined from deviation in the rate of rapid pressure decrease to a more gradual decay on the linear plot of pressure as a function of time.

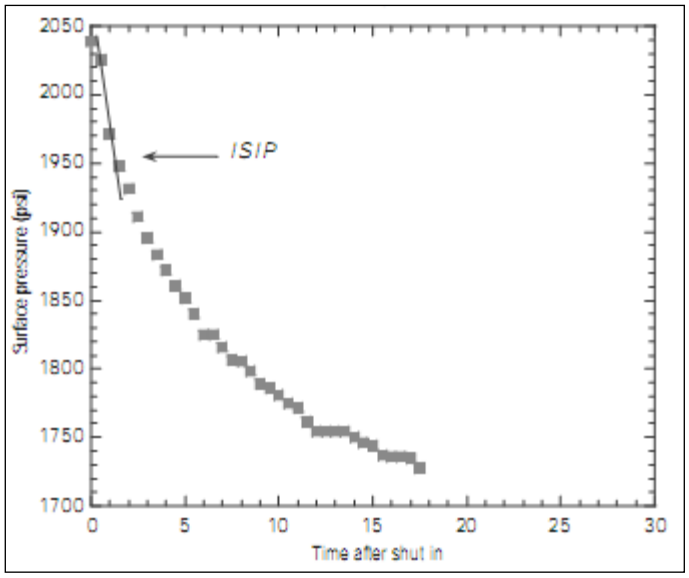

Figure 10 ISIP Determination (Zoback, 2010)

Whereas fracture closure pressure (FCP) is determined from deviation from the deviation from the linearity surface pressure versus $t^{0.5}$ as shown by figure below.

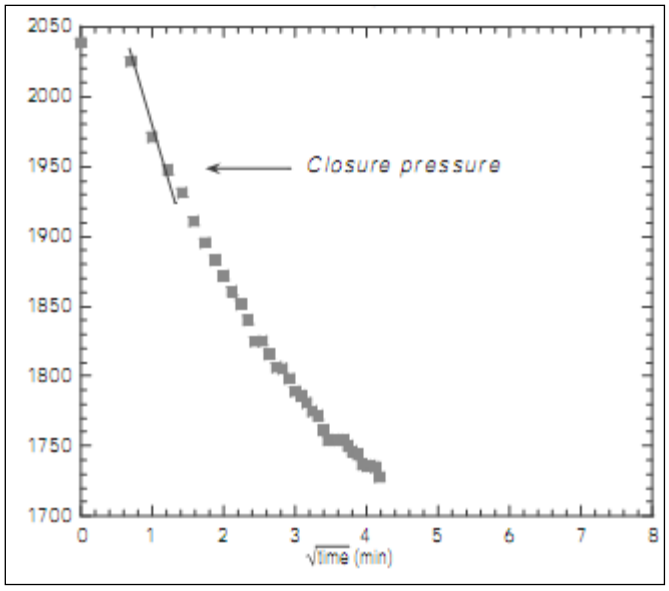

Figure 11 Closure Pressure Determinations (Zoback, 2010)

The minimum horizontal stress (S_h) is the first point after permanent decrease after ISIP in the slope and this value usually equal to or less than LOP. But in some case the the value of leak off pressure (LOP), fracture propagation pressure (FPP), and instantaneous shut in pressure (ISIP) approximately are same and can be used to determine the magnitude of minimum horizontal stress.

Minimum horizontal stress also can be estimated using empirical method by Zoback and Healy (1984) in normal faulting area:

$$S_h = \left(\frac{(S_v - P_p)}{[(1+\mu^2)^{0.5} + \mu]^2}\right) + P_p \qquad (22)$$

2.2.3. Maximum Horizontal Stress

Maximum horizontal stress can be seen in salt formation, in active tectonic area or in active geological structure. In north sea, the tectonic activity or geological structure is not too active so that the magnitude of maximum horizontal stress is almost same or not too far with magnitude minimum horizontal stress. The orientation of maximum horizontal stress can be determined from breakout using image log. The orientation of maximum horizontal stress is perpendicular with breakout. Breakout is happen when the stress concentration around the wellbore exceeds the rock strength. Breakout is happen in the direction of minimum horizontal stress. Whereas tensile failure or fractue is happen in the dirention of maximum horizontal stress.

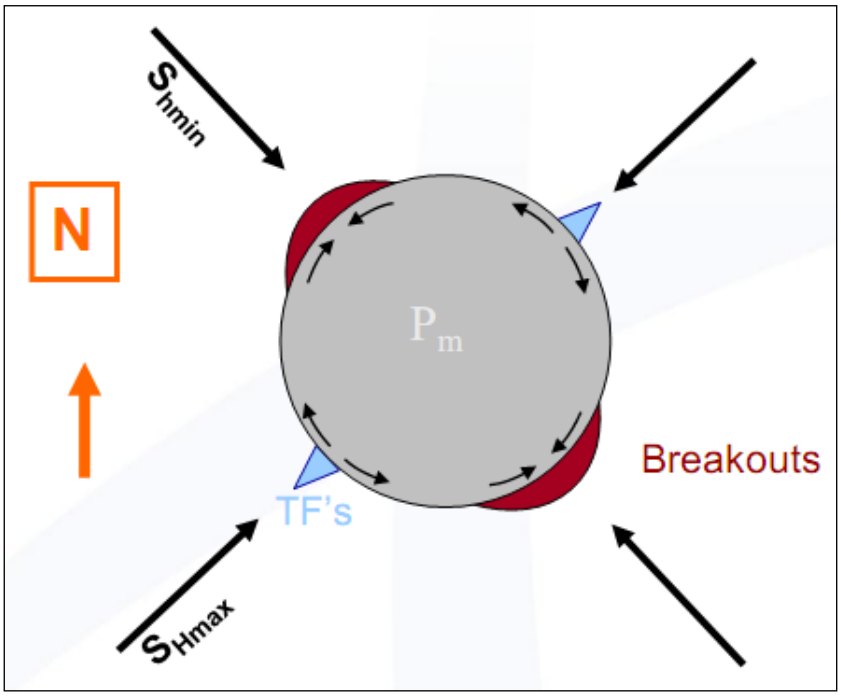

Figure 12 $S_H$max Orientations and Breakout (Baker, 2012)

Zoback et al. (1998) proposed a methodology to calculate S_{Hmax} with assumption that the stess concentration at the edge of a breakout is in equillibrium with the rock strength.

$$S_H = \frac{(C_0 + 2P_p + \Delta P + \sigma^{\Delta T}) - S_{hmin}(1 + 2\cos 2\theta_b)}{1 - 2\cos 2\theta_b} \quad (23)$$

This figure below will explain how to determine θ_b

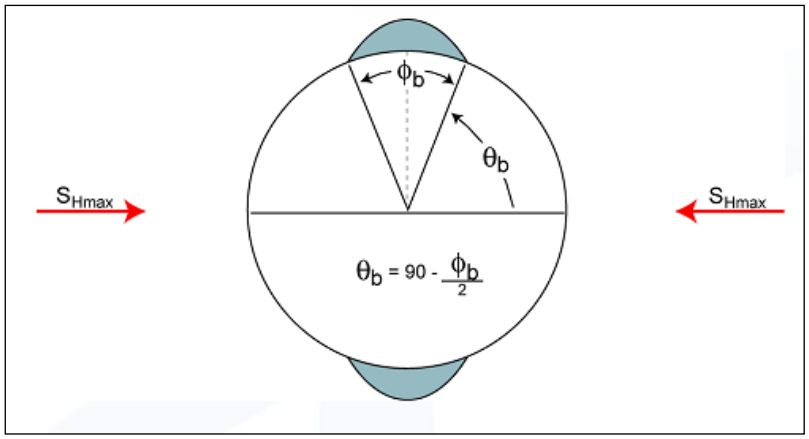

Figure 13 S_{Hmax} magnitudes from breakout width (Zoback, 2010)

The magnitude of maximum horizontal stress also can be determined using frictional faulting theory in strike-slip and reverse faulting stress states using this equation :

- In strike-slip faulting

$$S_{Hmax} \leq (S_{hmin} - P_p)[(\mu^2 + 1)^{0.5} + \mu]^2 + P_p \quad (24)$$

- In reverse faulting

$$S_{Hmax} \leq (S_v - P_p)[(\mu^2 + 1)^{0.5} + \mu]^2 + P_p \quad (25)$$

2.3 Stresses Orientation in Three Dimension

Many wells in development field are drilled using deviated well or horizontal well to exploit hydrocarbon and to get big drainage radius. In deviated well, these stresses orientation must be transformed into a new coordinate system x, y and z. The well have direction and orientation with inclination (γ) from vertical and azimuth (φ) so the stress orientation can be transformed using this equation:

$$\sigma_x = (\sigma_H \cos^2\varphi + \sigma_h \sin^2\varphi)\cos^2\gamma + \sigma_v \sin^2\gamma \quad (26)$$

$$\sigma_y = (\sigma_H \sin^2\varphi + \sigma_h \cos^2\varphi) \quad (27)$$

$$\sigma_z = (\sigma_H \cos^2\varphi + \sigma_h \sin^2\varphi)\sin^2\gamma + \sigma_v \cos^2\gamma \quad (28)$$

$$\tau_{yz} = \frac{1}{2}(\sigma_h - \sigma_H) \sin(2\varphi) \sin\gamma \quad (29)$$

$$\tau_{xz} = \frac{1}{2}(\sigma_H \cos^2\varphi + \sigma_h \sin^2\varphi - \sigma_v) \sin 2\gamma \quad (30)$$

$$\tau_{xy} = \frac{1}{2}(\sigma_h - \sigma_H) \sin(2\varphi) \cos\gamma \quad (31)$$

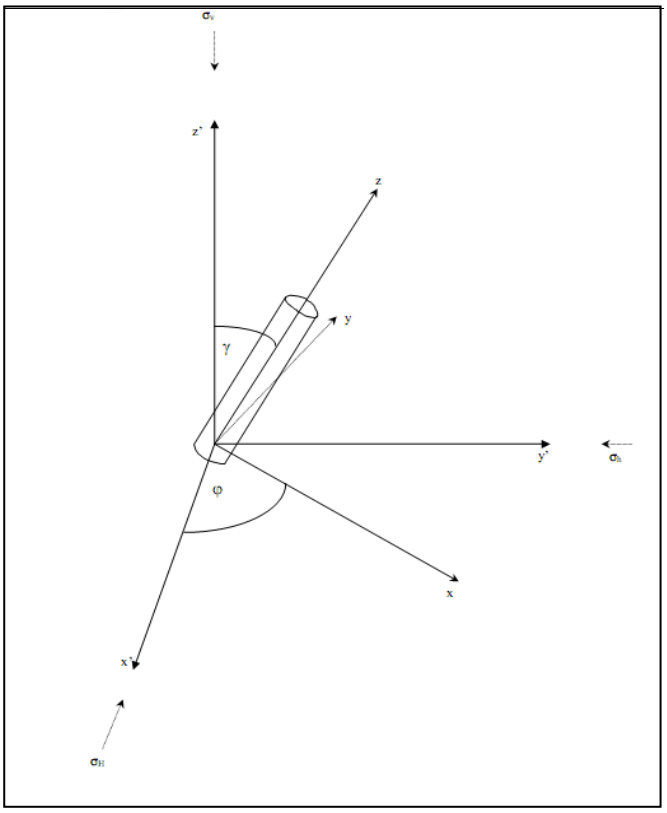

Figure 14 Deviated Boreholes in an Anisotropic Stress Field (Aadnøy & Looyeh, 2011)

A brief explanation from figure above:

- x' is parallel with σ_H
- y' is parallel with σ_h
- z' is parallel with σ_v
- x is parallel to the low side of the hole
- y is perpendicular to x (and perpendicular to the axis of the borehole)
- z is parallel to the axis of the borehole

2.4 Stress At Borehole Wall

Before drilling a well, rock stress is described by the insitu stresses. But after drilled a well, stress distribution around wellbore are change. The support which provided by rock is removed and replaced by hydrostatic pressure. Stress around the wellbore are described as radial stress, hoop (tangential) stress and axial stress. There are additional shear stress components that called as $\sigma_{r\theta}$, σ_{rz}, $\sigma_{\theta z}$. These stress are perpendicular to each other.

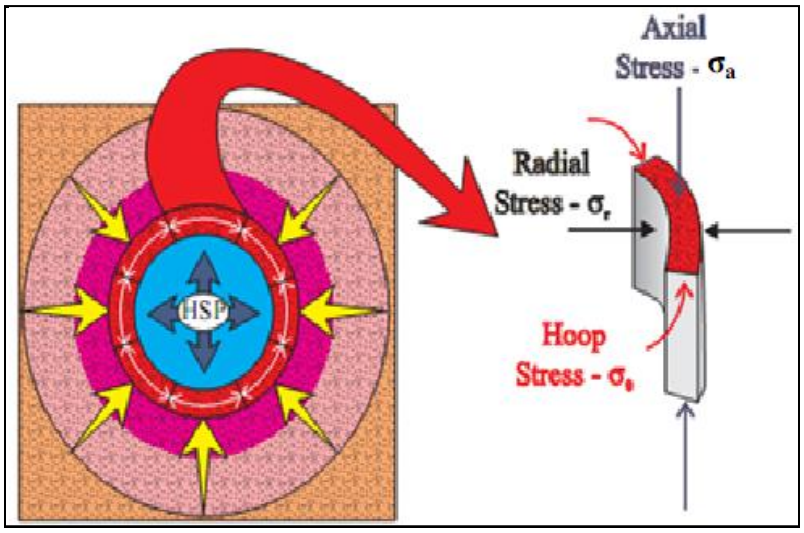

Figure 15 Stress Distributions around Borehole Wall (Amoco,2010)

Density of mud also determine the magnitude of stress distribution around the wellbore wall. Low mud density can cause tangential stress (θ_t) in the wellbore wall become high and high density mud can cause radial stress (θ_r) around the wellbore wall become higher.

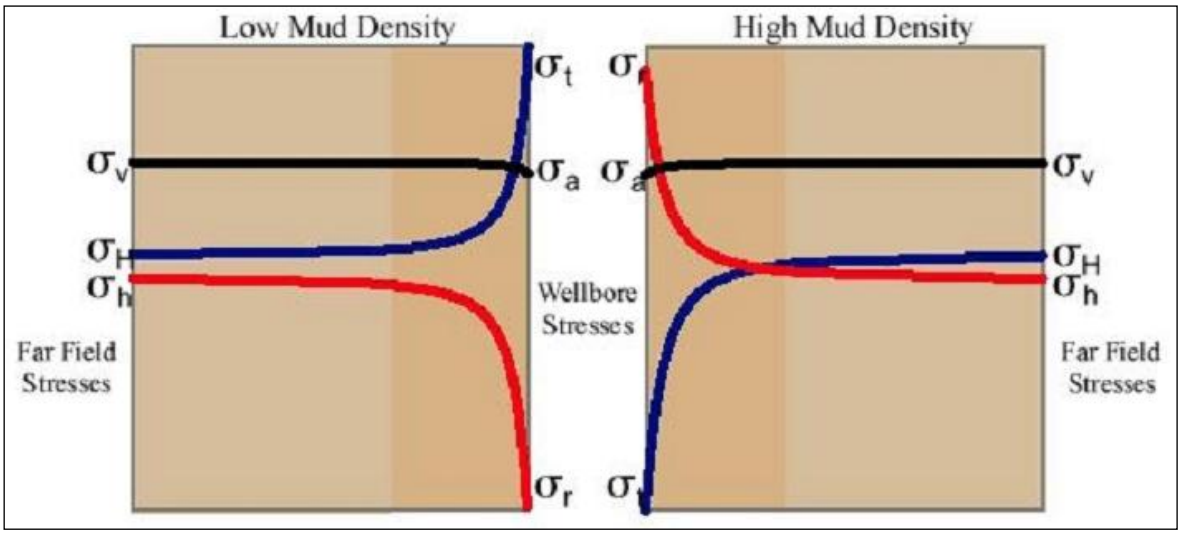

Figure 16 Variations of Wellbore Stresses Away from the Wellbore Wall (Sugar Land Learning Centre)

2.4.1. Radial Stress

Radial stress is a stress that acting along the radius of the wellbore. Radial stress can be calculated using Kirsch equation with assumption that rock remain linear elastic and the wellbore fluid pressure (P_w) does not penetrate the rock, it means that there is a mud cake in the borehole wall.

$$\sigma_r = \frac{1}{2}(\sigma_x + \sigma_y)\left(1 - \frac{a^2}{r^2}\right) + \frac{1}{2}(\sigma_x - \sigma_y)\left(1 + 3\frac{a^4}{r^4} - 4\frac{a^2}{r^2}\right)\cos 2\theta + \tau_{xy}\left(1 + 3\frac{a^4}{r^4} - 4\frac{a^2}{r^2}\right)\sin 2\theta + \frac{a^2}{r^2}P_w \quad (32)$$

where

a = radius of the hole

r = position radially outwards from the center

θ = angle between a point on the circumference of the wellbore and the direction of maximum horizontal stress

v = poisson's ratio

These notation can be explain with the figure below :

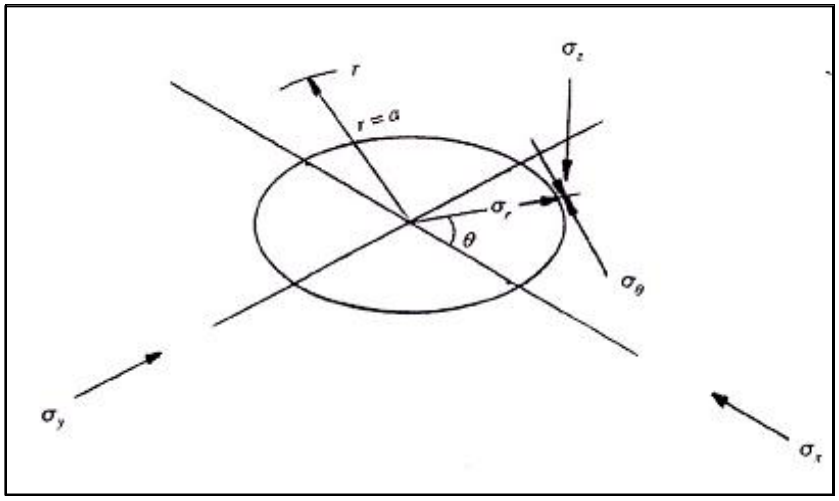

Figure 17 Stress Acting on the borehole wall (Aadnøy & Looyeh, 2011)

At the borehole wall (r=a), the equation can be simplified to :

$$\sigma_r = P_w \quad (33)$$

At the far distance from the borehole wall (r→ ∞ and $\frac{a}{r}\longrightarrow 0$), the radial stress can be simplified to :

$$\sigma_r = \frac{1}{2}(\sigma_H + \sigma_h) + \frac{1}{2}(\sigma_H - \sigma_h)\cos 2\theta \quad (34)$$

This stress show that the wellbore stress diminish rapidly from the borehole wall converting to far field stress. This is make sense because at large distance from the wellbore, the rock is in an unperturbed condition.

For example

at $\theta = 0$ ($\cos 2\theta = 1$) And then $\sigma_r = \sigma_H$

at $\theta = 90^0$ And then $\sigma_r = \sigma_h$

2.4.2. Axial Stress

Axial stress is a stress that acting parallel to the well path. Axial stress can be calculated using Kirsch equation.

$$\sigma_a = \sigma_z - v\left(2(\sigma_x - \sigma_y)\frac{a^2}{r^2}\cos 2\theta + 4\tau_{xy}\frac{a^2}{r^2}\sin 2\theta\right) \quad (35)$$

At the borehole wall (r=a), the equation can be simplified to:

$$\sigma_a = \sigma_v - 2(\sigma_H - \sigma_h)\, v \cos 2\theta \quad (36)$$

At the far distance from the borehole wall (r→ ∞ and $\frac{a}{r}\longrightarrow 0$), the axial stress can be simplified to :

$$\sigma_a = \sigma_v \quad (37)$$

This stress show that the wellbore stress diminish rapidly from the borehole wall converting to far field stress. This is make sense because at large distance from the wellbore, the rock is in an unperturbed condition.

For example

at $\theta = 0$ ($\cos 2\theta = 1$) And then $\sigma_a = \sigma_v$

at $\theta = 90^0$ And then $\sigma_a = \sigma_v$

2.4.3. Tangential Stress

Tangential (hoop) stress is a stress that acting around the circumference of the wellbore. Tangential stress can be calculated using Kirsch equation.

$$\sigma_\theta = \frac{1}{2}(\sigma_x + \sigma_y)\left(1 + \frac{a^2}{r^2}\right) - \frac{1}{2}(\sigma_x - \sigma_y)\left(1 + 3\frac{a^4}{r^4}\right)\cos 2\theta - \tau_{xy}\left(1 + 3\frac{a^4}{r^4}\right)\sin 2\theta - \frac{a^2}{r^2}P_w \quad (38)$$

At the borehole wall (r=a), the equation can be simplified to:

$$\sigma_\theta = (\sigma_H + \sigma_h) - 2(\sigma_H - \sigma_h)\cos 2\theta - P_w \quad (39)$$

At the far distance from the borehole wall ($r \rightarrow \infty$ and $\frac{a}{r} \rightarrow 0$), the radial stress can be simplified to:

$$\sigma_\theta = \frac{1}{2}(\sigma_H + \sigma_h) - \frac{1}{2}(\sigma_H - \sigma_h)\cos 2\theta \quad (40)$$

This stress show that the wellbore stress diminish rapidly from the borehole wall converting to far field stress. This is make sense because at large distance from the wellbore, the rock is in an unperturbed condition.

For example

at $\theta = 0$ ($\cos 2\theta = 1$) And then $\sigma_\theta = \sigma_h$

at $\theta = 90^0$ And then $\sigma_\theta = \sigma_H$

2.4.4. Shear Stress

Generally the stresses are comressive and create shear stress within the rock. If these stress are equal so the rock will be stable. For example radial stress is resisting shear caused by the hoop stress.

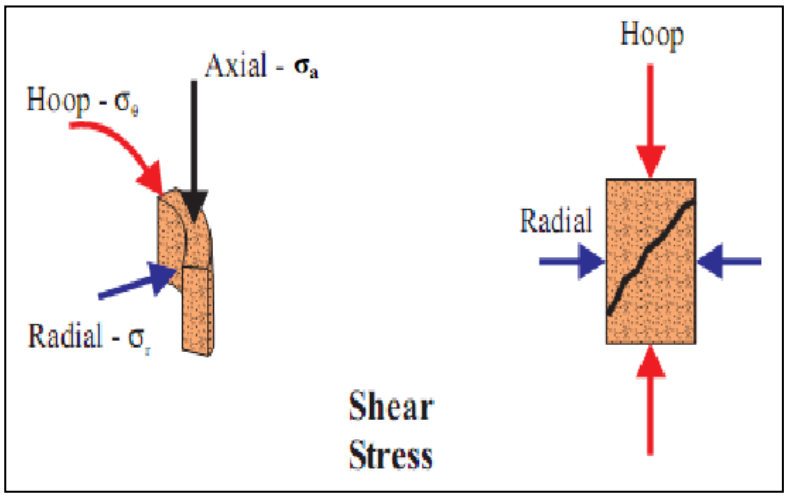

Figure 18 Radial Stress Resisting Shear Stress (Sugar Land Learning Centre)

Mathematically, shear stress can be calculated using Kirsch equation as below :

$$\tau_{r\theta} = \left\{\frac{1}{2}(\sigma_x - \sigma_y)sin2\theta + \tau_{xy}cos2\theta\right\}\left\{1 - 3\frac{a^4}{r^4} + 2\frac{a^2}{r^2}\right\} \quad (41)$$

$$\tau_{ra} = \{\tau_{xz}cos\theta + \tau_{yz}\sin\theta\}\left\{1 - \frac{a^2}{r^2}\right\} \quad (42)$$

$$\tau_{\theta a} = \{-\tau_{xz}cos\theta + \tau_{yz}\sin\theta\}\left\{1 + \frac{a^2}{r^2}\right\} \quad (43)$$

Shear stress at borehole wall (r=a), the above equation can be simplified as below :

$$\tau_{\theta a} = 2\{\tau_{yz}\cos\theta - \tau_{xz}sin\theta\} \quad (44)$$

$$\tau_{ra} = \tau_{r\theta} = 0 \quad (45)$$

2.5 The Geometry of Borehole Shear Failure

The geometry of borehole shear failure can be categorized into 6 based on the magnitude of axial stress (σ_a), radial stress (σ_r) and tangential stress (σ_θ):

a. Shear Failure Shallow Knockout (ssko) where $\sigma_a > \sigma_\theta > \sigma_r$
b. Shear Failure Wide Breakout (swbo) where $\sigma_\theta > \sigma_a > \sigma_r$
c. Shear Failure High-Angle Echelon (shae) where $\sigma_a > \sigma_r > \sigma_\theta$
d. Shear Failure Narrow Breakout (snbo) where $\sigma_r > \sigma_a > \sigma_\theta$
e. Shear Failure Deep Knockout (sdko) where $\sigma_r > \sigma_\theta > \sigma_a$
f. Shear Failure Low-Angle Echelon (slae) where $\sigma_\theta > \sigma_r > \sigma_a$

2.5.1. Shear Failure Shallow Knockout (SSKO)

This shear failure criteria is happen when $\sigma_a > \sigma_\theta > \sigma_r$. The failure will occure in the radial / axial plane because the maximum (σ_a) and minimum (σ_r) stresses are oriented in this plane (a vertical plane). The orientation of shear failure shallow knockout (ssko) failure can be encountered in the direction of minimum horizontal stress (σ_h). In image log, ssko can be seen ass dark vertical feature with narrow width (around 20^0).

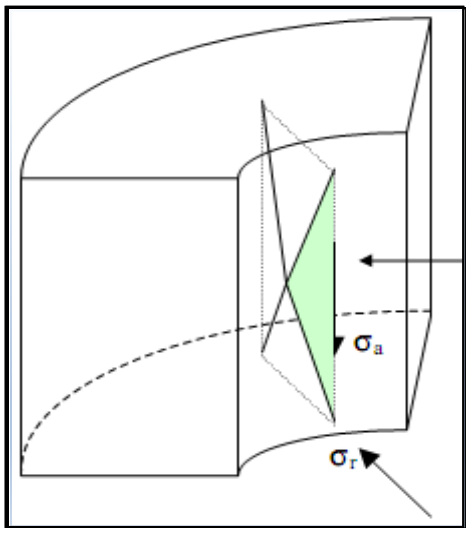

Figure 19 Shear Failure Shallow Knockout (Sugar Land Learning Centre)

2.5.2. Shear Failure Wide Breakout (SWBO)

This shear failure criteria is happen when $\sigma_\theta > \sigma_a > \sigma_r$. This mode of failure occur in the radial / tangential plane. It also called as breakout because the failure covers a large arc, from 30^o to 90^o. The orientation of swbo failure is in the direction of minimum horizontal stress. In image log, it can be seen as dark vertical features with wide width (around 30^o to 90^o).

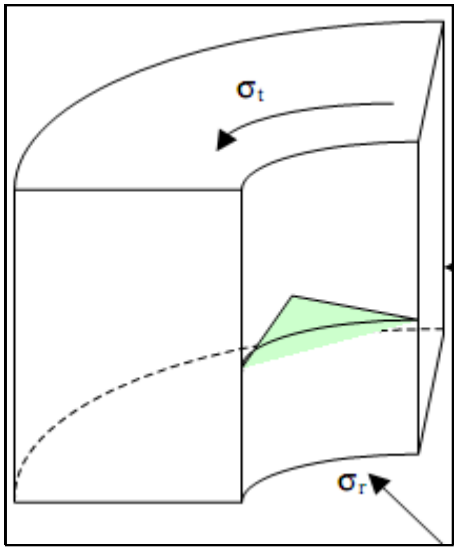

Figure 20 Shear Failure Wide Breakout (Sugar Land Learning Centre)

2.5.3. Shear Failure High-Angle Echelon (SHAE)

This shear failure criteria is happen when $\sigma_a > \sigma_r > \sigma_\theta$. This failure occur in axial / tangential arc. Shae form high-angle fractures that cover up to a quarter of the borehole circumference. The orientation of shae can be determined when σ_a is maximum with $\theta = 90^o$ and σ_t is minimum with $\theta = 45^o$ or originate at σ_H and extending away at angle. In image Log, it appears as dark feature inclined at high angle ($>50^o$).

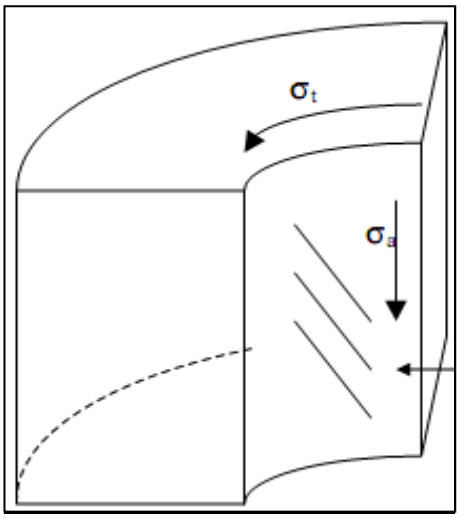

Figure 21 Shear Failure High-Angle Echelon (Sugar Land Learning Centre)

2.5.4. Shear Failure Narrow Breakout (SNBO)

This shear failure criteria is happen when $\sigma_r > \sigma_a > \sigma_\theta$. This failure occur in radial / tangential plane. Snbo also called as breakout and it is generally narrow because the failure covers an

arc about less than 30°. The orientation of snbo is in the direction of maximum horizontal stress (σ_H). In Image log, it appears as dark vertical feature with narrow width (around 20°).

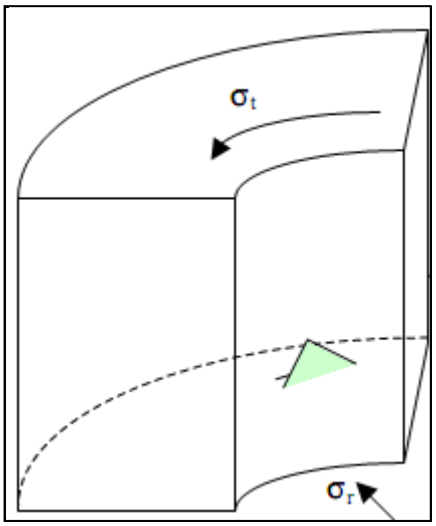

Figure 22 Shear Failure Narrow Breakout (Sugar Land Learning Centre)

2.5.5. Shear Failure Deep Knockout (SDKO)

This shear failure criteria is happen when $\sigma_r > \sigma_\theta > \sigma_a$. Sdko occur in the radial / axial plane. The orientation of sdko is in the direction of maximum horizontal stress (σ_H). In Image log, it appears as dark vertical feature with narrow width (around 20°).

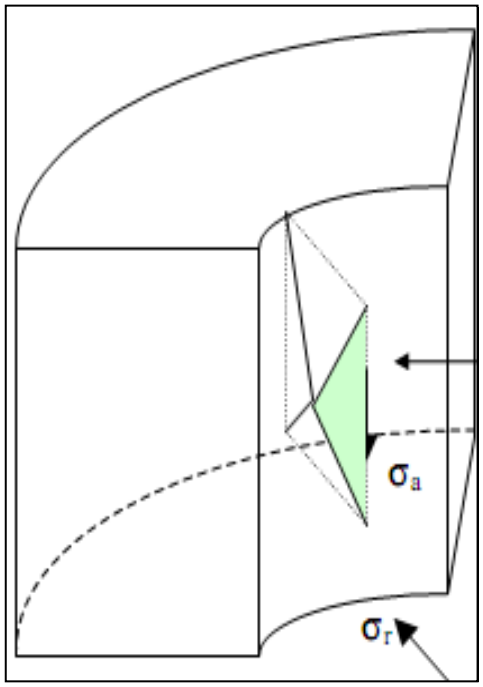

Figure 23 Shear Failure Deep Knockout (Sugar Land Learning Centre)

2.5.6. Shear Failure Low-Angle Echelon (SLAE)

This shear failure criteria is happen when $\sigma_\theta > \sigma_r > \sigma_a$. Slae occur in the axial / tangential plane. This failure forms low-angle fractures. The orientation of slae is determined when σ_t is maximum with $\theta = 90^o$ and σ_a is minimum with $\theta = 0^o$. This is the reason why the high - angle echelon failures are spread over a larger circumferential area than knockouts or

breakouts. The orientation of this failure is in the sirection of minimum horizontal stress (σ_h) and it extend away at low angle.

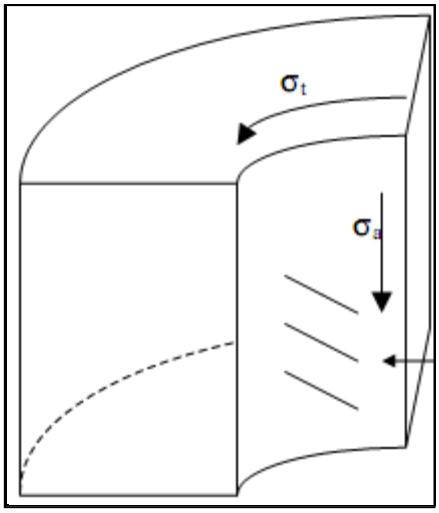

Figure 24 Shear Failure Low-Angle Echelon (Sugar Land Learning Centre)

2.6 The Geometry of Borehole Tensile Failure

Tensile failure will occur when tensile stress are applied in the formation and consequently grains will be pulled apart in the direction of the tensile stress. Because formation fails under tension, crack will appear perpendicular to the tensile stress. Tensile strength of formation can be estimated from extended leak off test (XLOT). Usually, tensile strength of formation (T_0) less than 10% of the unconfined compressive strength (C_0).

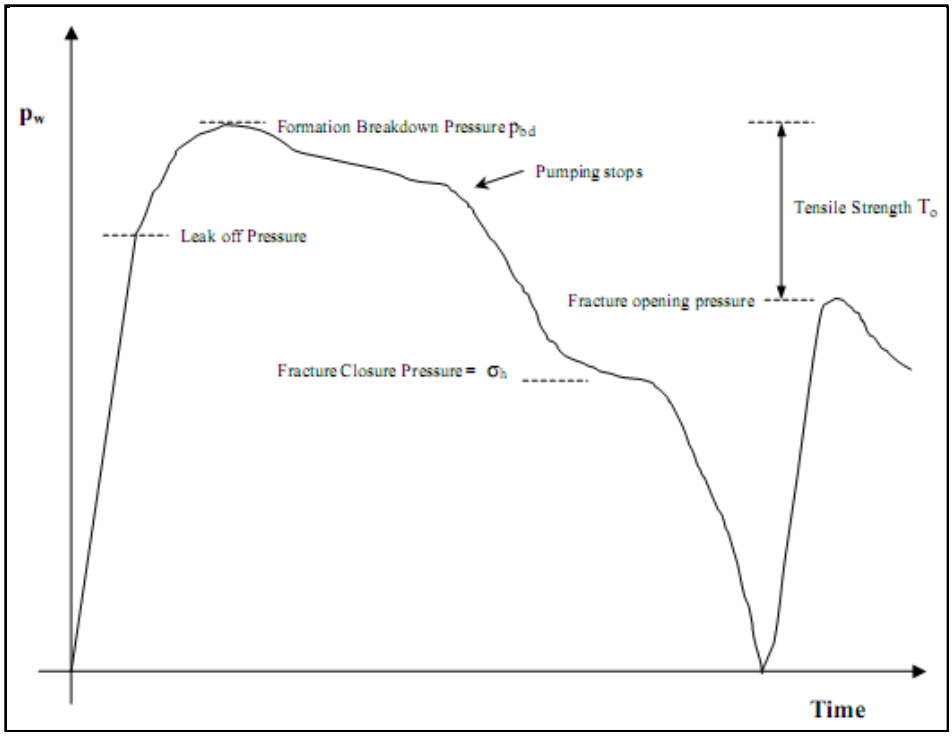

Figure 25 Extended Leaks off Test (Sugar Land Learning Centre)

There are 3 types of tensile failure geometry when tensile stress exceed the tensile strength of formation (T_0) :

a. Tensile failure cylindrical (tcyl) when $\sigma_r \leq - T_0$
b. Tensile failure horizontal (thor) when $\sigma_a \leq - T_0$
c. Tensile failure vertical (tver) when $\sigma_\theta \leq - T_0$

2.6.1. Tensile Failure Cylindrical (tcyl)

This failure occure when radial stress lower than the negative of tensile strength formation ($\sigma_r \leq - T_0$). Tcyl is concentric with borehole wall and it does not appear in image log.

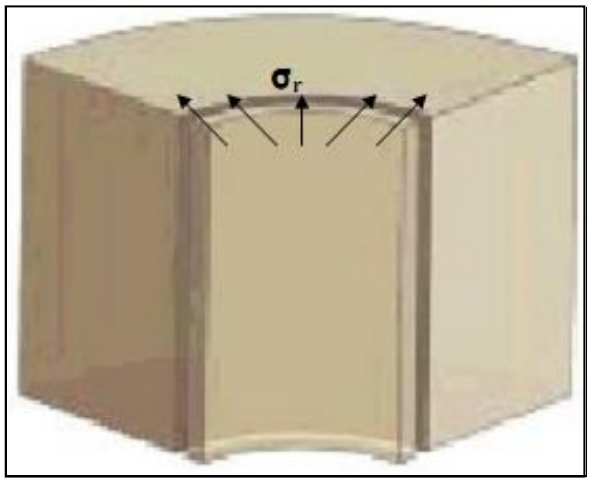

Figure 26 Tensile Failures Cylindrical (Sugar Land Learning Centre)

2.6.2. Tensile Failure Horizontal (thor)

This failure occure when axial stress lower than the negative of tensile strength formation ($\sigma_a \leq - T_0$). In image log, this failure can be seen as a thin black horizontal line throughout all azimuthal orientations.

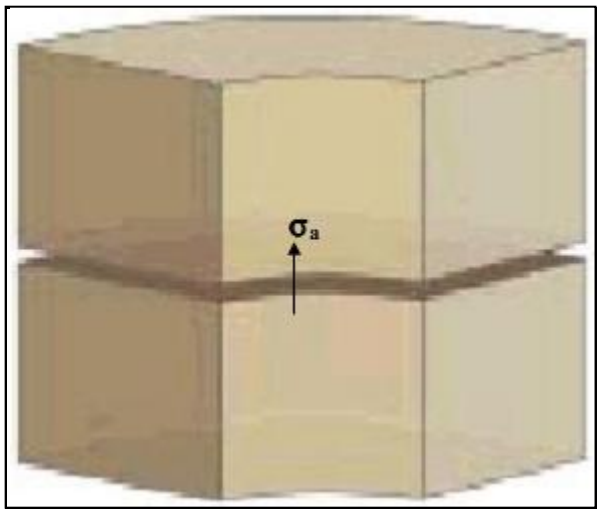

Figure 27 Tensile Failure Horizontal (Sugar Land Learning Centre)

2.6.3. Tensile Failure Vertical (tver)

This failure occure when tangential stress lower than the negative of tensile strength formation ($\sigma_\theta \leq - T_0$). The orientation of tver is in the direction of maximum horizontal stress (σ_H). In image log, this tensile failure appears as dark vertical feature with very width (more than 20^o).

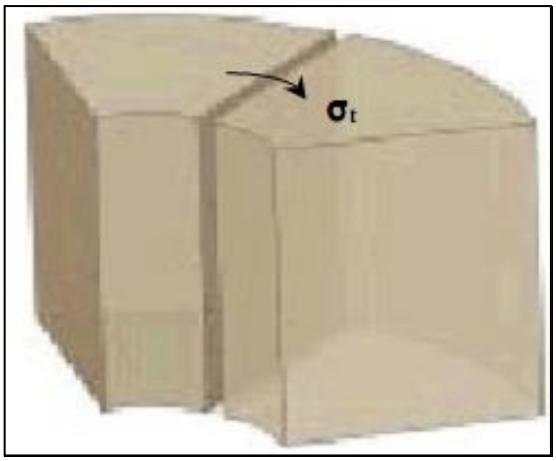

Figure 28 Tensile Failure Vertical (Sugar Land Learning Centre)

2.7 Wellbore Stability Monitoring

The openhole wellbore must be kept in good condition so it can allow drilling and casing can be run. Monitoring in wellbore stability is very important. During drilling, design wellbore stability can be compared with the real time drilling data and can be updated and analyzed to avoid drilling problems during drilling. This monitoring data from real time data can be used as lesson learn to design the next well.

In wellbore stability monitoring can use some of drilling data parameters. These are some of drilling data parameters to control wellbore stability :

a. Surface signature :
   - Caving analysis - Wellbore failure
   - Cutting volume - Hole cleaning
   - Pit volume - Mud gains (overpressured zone), mud losses
   - Surface drilling parameters

b. MWD Data :
   - Downhole drilling parameters
   - DWOB, DTORQ - Friction / drag
   - ECD behaviour - Hole cleaning, pack off

c. LWD Data :
   - Gamma ray, resistivity - To identify zone of potential instability
   - Sonic - Pore pressure prediction
   - Caliper measurements - if pattern is forming in some intervals

The easy ways to observe wellbore stability is by caving analysis. There are three types of caving :

a. Tabular caving

   Tabular caving happen in natural fractures or weak planes. It is caused by wellbore pressure exceeds the minimum horizontal stress, resulting in mud invasion of fracture network around the wellbore. This caving can be characterized by its form like flat, parallel, faces caving.

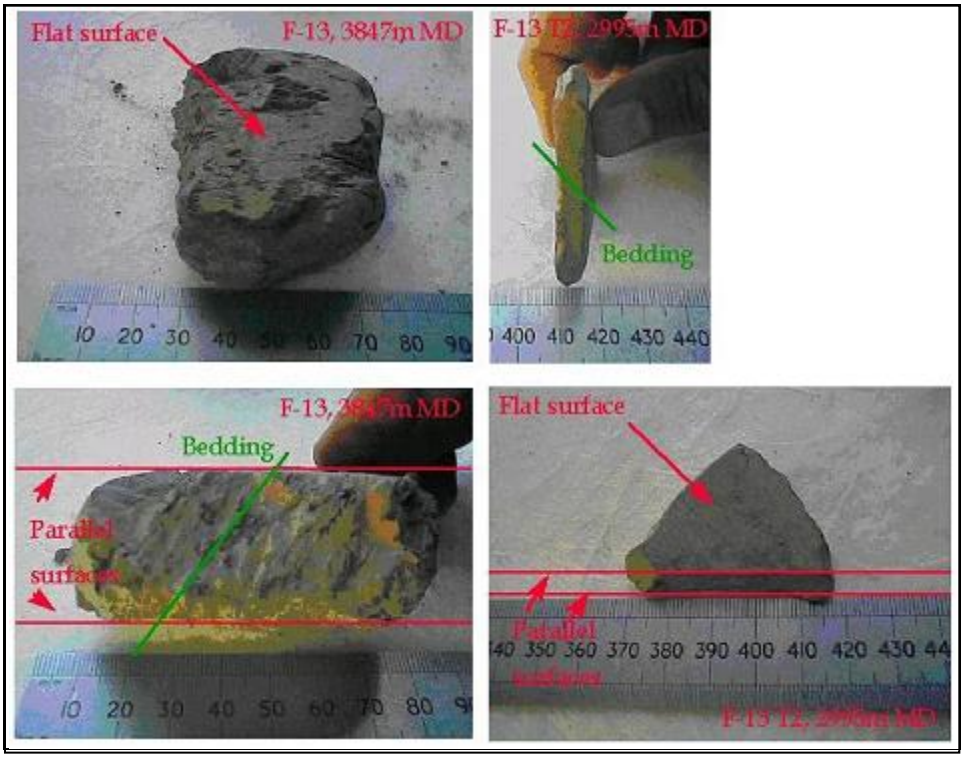

Figure 29 Tabular Cavings (Sugar Land Learning Centre)

b. Angular cavings

These caving are formed as the consequence of breakout. Angular caving can be characterized by curved faces with a rough surface structure.

Figure 30 Angular Cavings (Sugar Land Learning Centre)

c. Splintered cavings

These caving have form as two nearly-parallel faces with plume structures. Its happen due to tensile failure (tcyl) and occure parallel to borehole wall. Splintered caving normally happen in over pressure formation and with wellbore pressure a slightly or almost same with pore pressure.

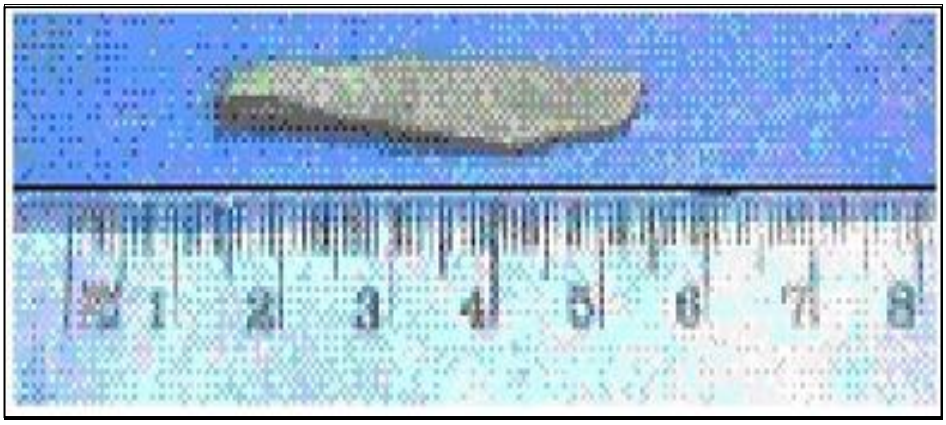

Figure 31 Splintered Cavings (Sugar Land Learning Centre)

2.8 Wellbore Collapse Failure Criteria Model

Failure criteria on the material depend on the type of material (brittle or ductile). If the material is ductile, the stresses are compared to the yield strength since the permanent deformation can cause failure. And if material is brittle, this material does not have yield point so the stresses are compared to the ultimate strength of the material. This rule is applicable to almost for all materials, but you will find an exception (Aadnøy and Looyeh, 2011).

Rock failure happens when stress exceeds the formation strength of rock . The failure criteria are different in the different lithologies. Sandstone will fail in shear, while a claystone may fail due to plastic deformation. Aadnøy and Looyeh (2011) highlighted some of the mechanisms which can affect the wellbore stability and eventually lead to rock formation failure as follows:

- Rock formation part due to Tensile failure
- Shear failure without appreciable plastic deformation
- Plastic deformation that may result to pore collapse
- Erosion or cohesive failure
- Creep failure which may lead to a tight hole situation during drilling
- Pore collapse or complete failure which may occur during production

There are many failure criteria model but in this thesis will presents three failure criteria models, they are Mohr - Coulomb, Modified Lade and Stassi d' Alia. Each model will be explained briefly separately.

2.8.1. Mohr - Coulomb

Shear failure occurs when the shear stress along a plane is too large. The Mohr-Coulomb criterion makes an assumption that shear stress (τ) is a linear function of stress (σ). From this relationship, Mohr-Coulomb describes a curve (function) that separates a safe region from the failure region.

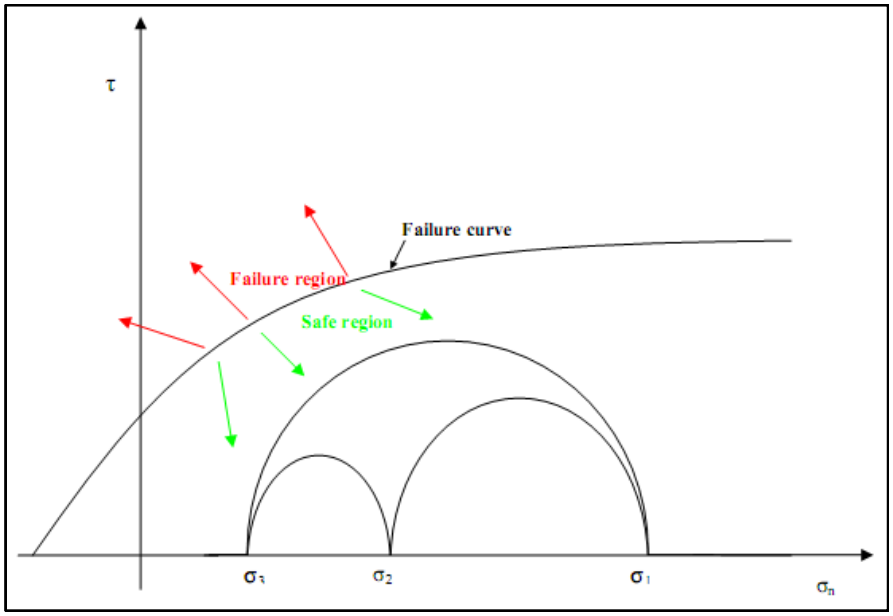

Figure 32 Three Principal Stresses and the Mohr Circles (Sugar Land Learning Centre)

From the figure above, if σ1 is increased, the circle connecting σ1 and σ3 will expand and consequently touch the failure curve causing a failure. The value of intermediate principal stress σ2 does not affect this process. it means that if σ2 is increased up to a maximum value of σ1 but not exceed σ1 so based on that figure, it does not affect the failure. By these experiments, Mohr-Coulomb model failure criterion only depends on the minimum principal stress (σ3) and maximum principal stress (σ1). The failure condition will happen if the difference between minimum principal stress (σ3) and maximum principal stress (σ1) become larger (the diameter of the hemisphere is increased).

Based on Coulomb (1773), a rock will undergo failure if the shear stress (τ) has a magnitude that exceeds the inherent shear strength of the rock (S_0) plus the opposing friction force ($\mu\sigma_n$). Mathematically this is can be written as :

$$\tau = S_0 + \mu\sigma_n \qquad (46)$$

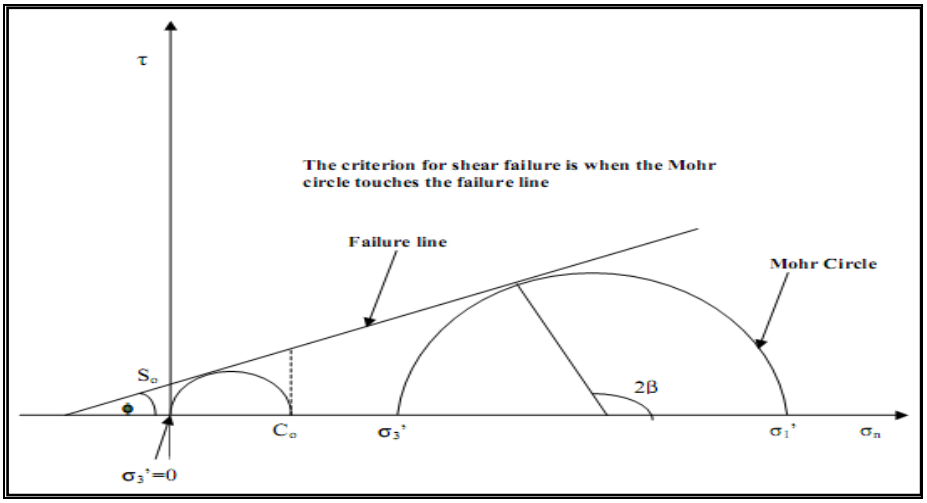

Figure 33 Mohr- Coulomb Shear Failure Criterions (Sugar Land Learning Centre)

In this thesis, Mohr - Coulomb failure criterion model is only used for fundamental understanding to figure out Modified Lade failure criterion and Stassi d' Alia failure criterion.

2.8.2. Modified Lade

Modified Lade requires requires same parameters for rock strength (cohesion and friction angle) as Mohr-Coulomb criterion but in this models involves the influence of intermediate principal stress (σ_2). In Modified Lade for rock failure criterion, the three principal stress are not same ($\sigma_1 \neq \sigma_2 \neq \sigma_3$). This corrective model give a better results in rock failure criteria. The Lade failure criterion is given by :

$$\left(\frac{I_1^3}{I_3} - 27\right)\left(\frac{I_1}{P_a}\right)^m = \eta_1 \tag{47}$$

where

$$I_1 = \sigma_1 + \sigma_2 + \sigma_3 \tag{48}$$

and

$$I_3 = (\sigma_1)\,(\sigma_2)\,(\sigma_3) \tag{49}$$

σ_1 , σ_2 , σ_3 are the three principal stresses and P_a is atmospheric pressure. The parameters η_1 and m are the material constants.

Ewy (1999) develope modified Lade criterion with set parameter "m" equal to zero. If "m" is zero so that equation will become linear equation and this relationship can be used to predict a linier shear strength with mean stress ($I_1/3$). To handle materials with cohesion or non-zero tensile strength so the stress axes be shifted into the tensile region by a dimensionless constant multuplied by P_a. For this reason, a shift constant with units of cohesion is more applicable and this will be defined as S_1. Pore pressure also must be substracted in order to handle effective stress. Performing these changes and defining appropriate stress invariant I_1" and I_3", the equation for modified lade criterion is developed :

$$\frac{\left(I_1^{"}\right)^3}{I_3^{"}} = 27 + \eta \tag{50}$$

Where

$$I_1" = (\sigma_1 + S_1 - p_0) + (\sigma_2 + S_1 - p_0) + (\sigma_3 + S_1 - p_0) \tag{51}$$

$$I_3" = (\sigma_1 + S_1 - p_0)\,(\sigma_2 + S_1 - p_0)\,(\sigma_3 + S_1 - p_0) \tag{52}$$

S_1 and η are material constant and p_0 is pore pressure. The invarians I_1" and I_3" can also be computed using the following equation :

$$I_1" = (\sigma_x + S_1 - p_0) + (\sigma_y + S_1 - p_0) + (\sigma_z + S_1 - p_0) \tag{53}$$

$$I_3" = (\sigma_x + S_1 - p_0)\,(\sigma_y + S_1 - p_0)\,(\sigma_z + S_1 - p_0) + 2\tau_{xy}\,\tau_{yz}\,\tau_{zx} - (\sigma_x + S_1 - p_0)\,\tau^2_{yz} - (\sigma_y + S_1 - p_0)\,\tau^2_{zx} - (\sigma_z + S_1 - p_0)\,\tau^2_{xy} \tag{54}$$

The parameter S_1 is related to the cohesion of the rock and η represents the internal friction. These parameters are obtained with this equation :

$$S_1 = S_0 / \tan\phi \tag{55}$$

$$\eta = 4\tan^2\phi\,(9 - 7\sin\phi) / (1 - \sin\phi) \tag{56}$$

where S_0 is cohesion and ϕ is friction angle.

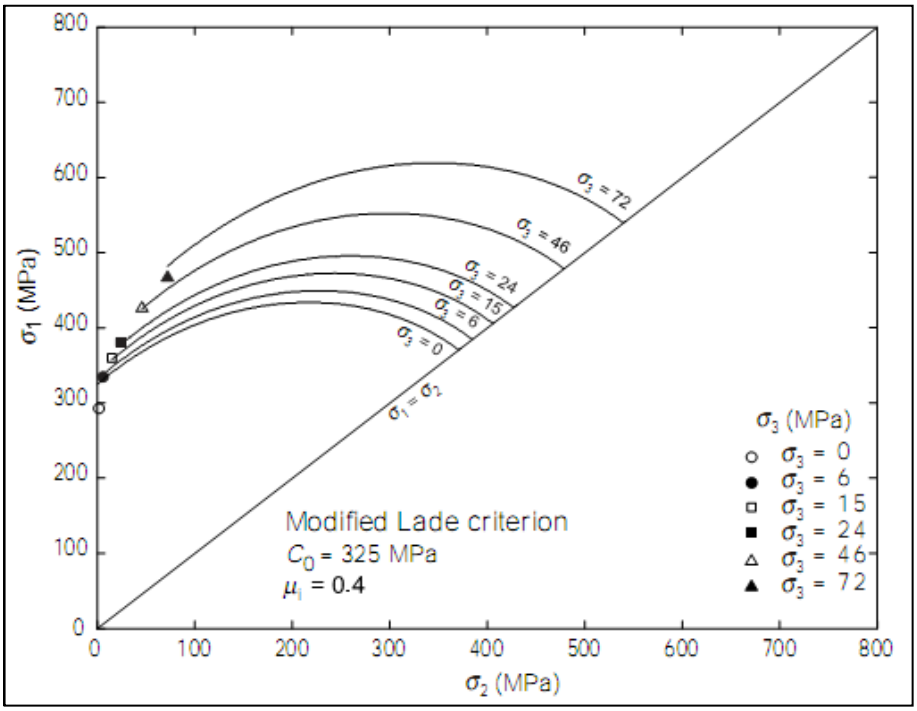

Figure 34 Modified Lade Criterion (SPE 56862)

2.8.3. Stassi d' Alia

Stassi d' Alia developed the rock failure criterion based on the tensile strength and uniaxial compressive strength. This model is mostly used in the north sea to figure out shear failure criterion. This criterion is expressed as below :

$$(\sigma_1 - \sigma_3)^2 + (\sigma_1 - \sigma_2)^2 + (\sigma_2 - \sigma_3)^2 = 2\,(C_0 - T_0)(\,\sigma_1 + \sigma_2 + \sigma_3) + 2C_0T_0 \qquad (57)$$

where C_0 is the uniaxial compressive strength, T_0 is the uniaxial tensile strength and σ_1, σ_2, σ_3 are the three principal stresses. The tensile strength (T_0) is commonly set equal to zero to avoid unexpected and peculiar effect which may happen if the tensile strength is increased. So the equation above can be simplified as below:

$$(\sigma_1 - \sigma_3)^2 + (\sigma_1 - \sigma_2)^2 + (\sigma_2 - \sigma_3)^2 = 2C_0\,(\sigma_1 + \sigma_2 + \sigma_3) \qquad (58)$$

The results of shear failure calculation from this equation is used to design mud weight when drilling a well.

3. BASIC THEORY WELL OPTIMIZATION

3.1 Wellbore Stability

There are two causes where wellbore instability can happen in the wellbore, it can be caused by mechanical stability or chemical stability. Mechanical stability related to insitu stress and rock strength of formation whereas chemical stability related to control of drilling fluid/rock formation, usually most problematic when drilling in shales. This study will learn about wellbore instability caused by mechanical stability where the impact of chemical stability can be neglected with the selection of appropriate drilling fluid and this drilling fluid is compatible with formation without causing problems with formation. For example, using KCl polymer or oil-based mud as drilling fluid to prevent reactive shale during drilling a wellbore. Wellbore instability caused by mechanical stability can be obtained by controlling stability problems. There are many controls in mechanical stability that can provide for a stable wellbore. Maintaining a balance between rock stress and rock strength is very important to reach wellbore stability.

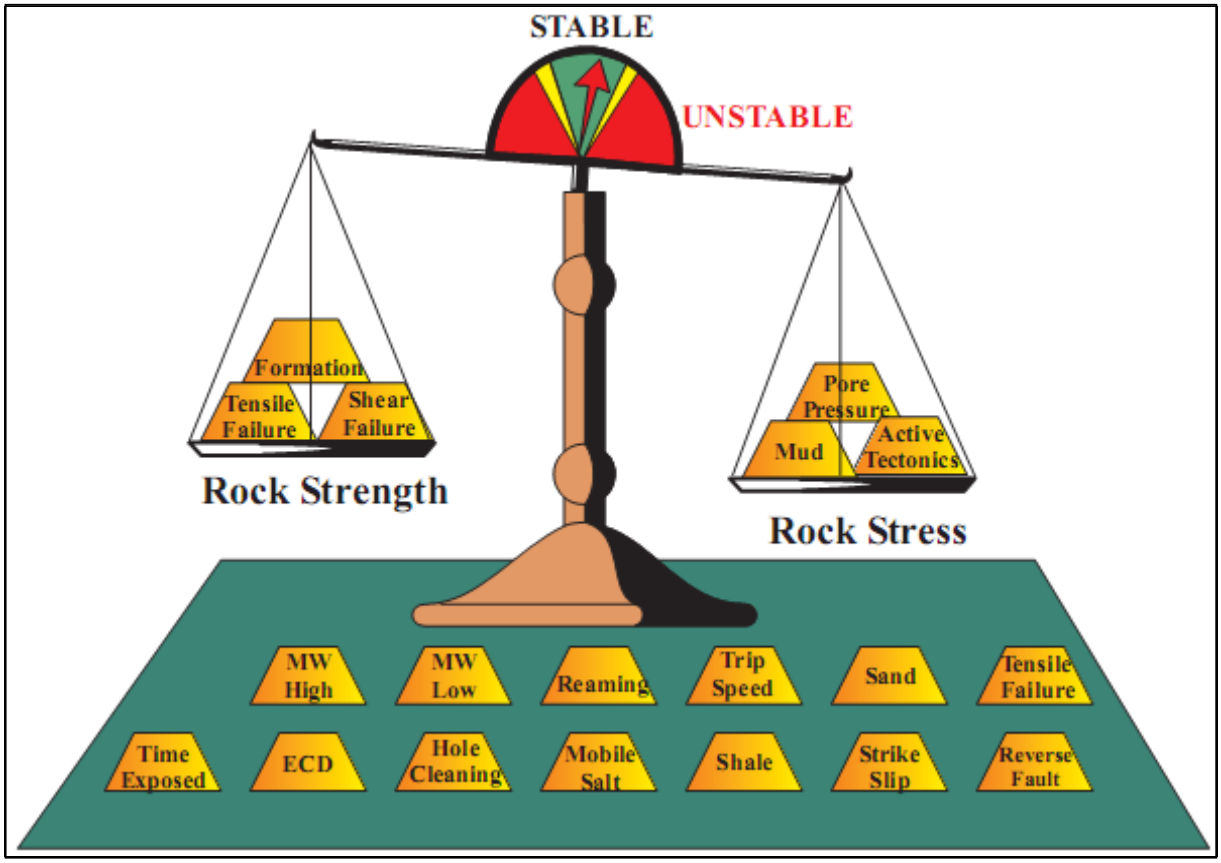

Figure 35 Maintaining Balance in Wellbore Stability (Amoco, 2010)

Maintaining a stable wellbore is important during drilling because it can avoid many problems related to wellbore instability and it can reduce drilling cost. These are some problems related to wellbore instability :

- Pack offs (formation failure leading to excess of cuttings)
- Excessive trip and reaming time
- Mud losses
- Stuck Pipe and BHAs → Loss of equipment / Fishing / Sidetracks

- Inability to land casing, casing collapse
- Poor logging and cementing conditions

These are some ways to design wellbore stability :

- Optimizing mud weight and mud properties
- Minimizing casing strings
- Optimizing wellbore trajectory
- Optimizing surface location

In case of optimizing mud weight, it is very important to design mud weight located in safe mud weight window to avoid problems from shear failure and tensile failure. This explanation can be seen in the figure below :

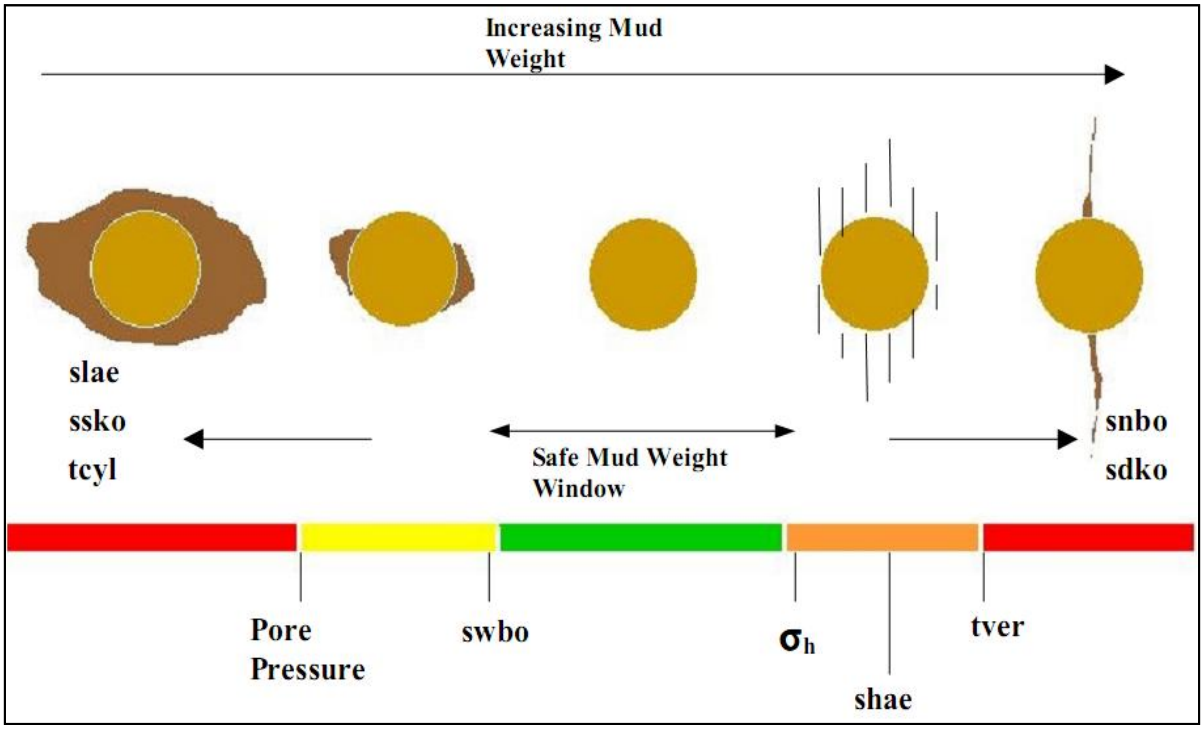

Figure 36 Design Safe Mud Weight Window (Sugar Land Learning Centre)

From figure above, it can be seen that if the mud weight is in the yellow area so shear failure wide breakout (swbo) can occur and the cavings from the wellbore will fall into the wellbore leaving a washed out zone (in the direction of σ_h). On the other hand, when there are natural fractures, using mud weight too high and above minimum horizontal stress (σ_h) can trigger lost circulation. Furthermore, if mud weight exceed minimum horizontal stress (σ_h), so it can trigger shear failure high angle echelon (shae), tensile failure vertical (tver), shear failure narrow breakout (snbo) and shear failure deep knockout (sdko). Design mud weight with too low mud weight also can trigger some rock failure problems like shear failure low angle echelon (slae), shear failure shallow knockout (ssko) and tensile failure cylindrical (tcyl). So it is very important to determine mud weight window to avoid wellbore instability problems.

3.1.1. Pore Pressure

Pore pressure is a pressure caused by the weight of the fluid that fills the cavity of the rock pores. Pore pressure is also called formation pressure. Pore pressure has psi units in field units. As long as the increase in overburden pressure does not exceed the rate at which fluid can escape from the pore so the fluid connection exists from surface to the depth of interest. this pressure equal to hydrostatic pressure of water (0.465 psi / ft).

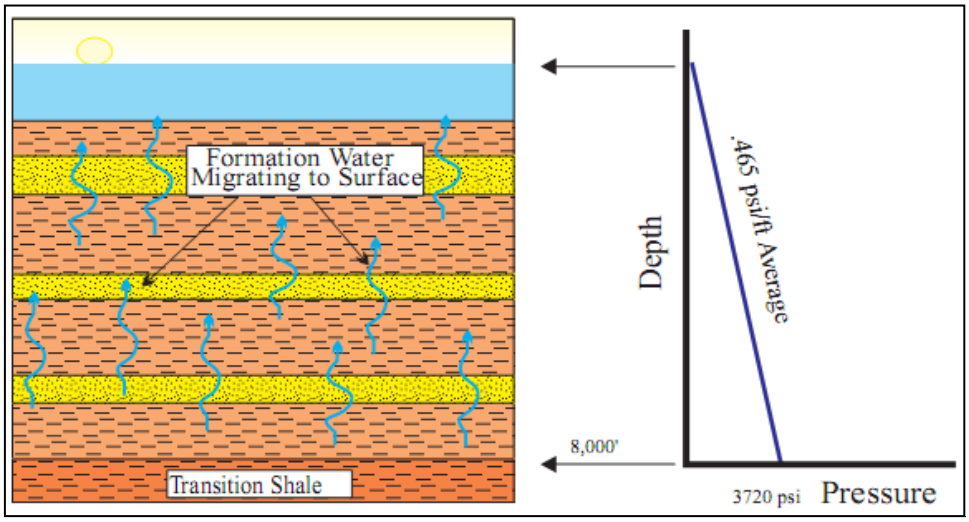

Figure 37 Normal Formation Pressure (Amoco, 2010)

If the fluid can not escape the pore so the the fluid will urge in all direction and pore pressure will increase. In certain circumstances, sometime the value of formation pressure is greater than the pressure of the fluid that fills the pore cavity, this pressure is called abnormal pressure. Meanwhile, if the formation pressure is smaller than the hydrostatic pressure of the fluid that fills the cavity in the rock, it is called subnormal pressure. The magnitude of this pore pressure which deviate from the normal are caused by the height of hydrocarbons column in the reservoir rock and because of the sedimentation process too fast.

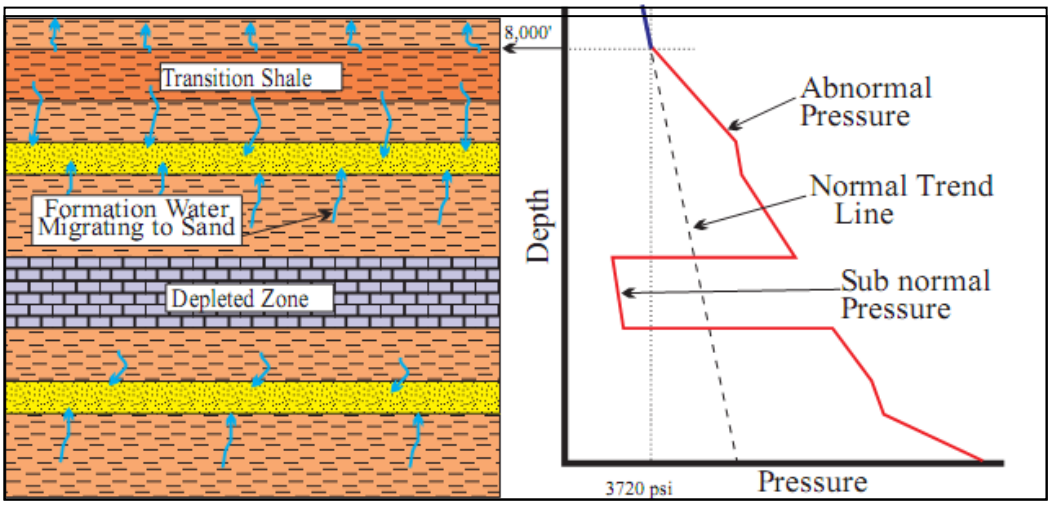

Figure 38 Abnormal Formation Pressure (Amoco, 2010)

Formation pore pressure prediction is a highly specialized process. Seismic data from interval velocity can be used to predict pore pressure. Interval velocity (V_{Int}) is the velocity in a single layer and it can be calculated from root mean square velocity (V_{RMS}) where V_{RMS} calculate the velocity to the bottom of the layer. This is the equation to determine interval velocity from V_{RMS} :

$$V_{int}^2 (Z_i) = [(V_{rms}^2 (Z_i) \times Z_i - V_{rms}^2(Z_{i-1}) \times Z_{i-1})] / (Z_i - Z_{i-1}) \quad (59)$$

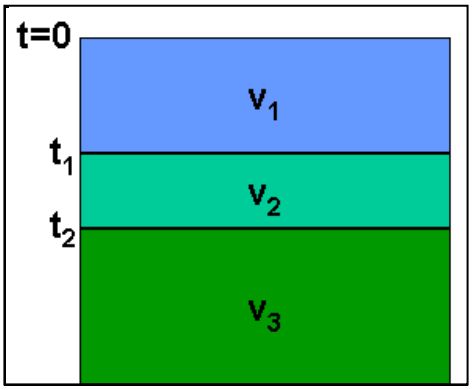

Figure 39 Interval Velocity (www.xsgeo.com)

Interval velocity can be used to detect abnormal pressure or subnormal pressure after. If the interval velocity is greater than normal compacted trend velocity (V_{nct}) so pore pressure in this formation can be estimated as subnormal pressure. On the other hand if interval velocity is less than normal compacted trend velocity (V_{nct}) so pore pressure in this formation can be estimated as abnormal pressure. Normal compacted trend velocity (V_{nct}) can be determined from compacted shale as shallow as possible in the the formation. At normal compacted trend velocity (V_{nct}), the pore pressure is same with the pressure gradient of water formation (0.465 psi / ft).

This interval velocity is used to predict pore pressure in the formation as function with depth using Eaton's equation.

$$PP = OBP - \left[(OBP - HP) \times \left(\frac{Vint}{Vnct}\right)^N\right] \quad (60)$$

Where :

PP = Pore pressure (psi)
OBP = Overburden pressure (psi)
HP = Hydrostatic pressure (psi)
V_{int} = Interval velocity (m/s)
V_{nct} = Normal compacted velocity (m/s)
N = Exponential factor

Overburden pressure is obtained from integral of bulk density from surface to depth of interest. Hydrostatic pressure can be obtained from formation water density for example 8.4 ppg. Exponential factor (N) can be obtained from plot between Log vertical effective stress (VES) Vs Log V_{int} from exploration well. From linier function plot between Log VES Vs Log V_{int} , exponential factor (N) can be calculated where N = 1 / slope. From all of these parameters, pore pressure profile from surface until depth of drilling target can be estimated.

While drilling, several MWD / LWD log give real time data to estimate pore pressure. By using this tools, the pore pressure can be determined precisely.

3.1.2. Fracture Pressure

Fracture pressure is the maximum pressure that can be applied to the formation without breaking the formation. The magnitude of fracture pressure depends on several parameters like overburden pressure, pore pressure, and rock strength conditions. In drilling, fracture pressure can be obtained from leak off test data. This test is applied to determine the strength of rock formation. Leak off test is done through drill out formation about 10 feet after installed casing and cemented casing. During the test, the well is shut in and mud is slowly pumped into the formation with rate 0.25 barrel per minute. The pressure will gradually increase during pumping mud. A plot between surface pressure vs a number of barrel mud pumped to the formation will give information about fracture pressure. In leak off test, fracture pressure is leak off pressure where there is a deviation line from plot surface pressure vs a number of barrel mud pumped to the formation.

$$\mathrm{FP} = \left(\frac{\mathrm{LOP}}{0.052 \text{ x } \mathrm{TVD}}\right) + \mathrm{MW} \tag{61}$$

where :

FP : Fracture presure (ppg)
LOP : Leak off pressure (psi)
TVD : Total vertical depth (feet)
MW : Mud weight that used during leak off test (ppg)

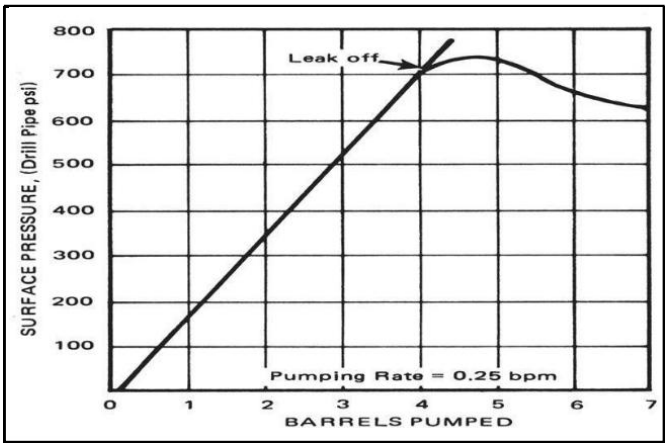

Figure 40 Figure 3.5 Leak Off Test (Zoback, 2010)

Leak off test only knows at a certain point of fracture pressure at a certain depth. In this thesis, Tarzaghi's equation is used to estimate fracture pressure profile from surface to depth target of drilling.

$$\mathrm{FP} = \mathrm{PP} + \mathrm{HES} \tag{62}$$

$$\mathrm{HES} = \frac{\upsilon}{(1-\upsilon)}\mathrm{VES} \tag{63}$$

$$\mathrm{VES} = (\mathrm{OBP} - \mathrm{PP})\left(\frac{\mathrm{Vint}}{\mathrm{Vnct}}\right)^{\mathrm{N}} \tag{64}$$

Where :

FP = Fracture pressure (psi)

PP = Pore pressure (psi)
HES = Horizontal effective stress
VES = Vertical effective stress
υ = poisson's ratio

3.1.3. Collapse Pressure

Determining collapse pressure formation to prevent rock failure is important in wellbore stability. By determining collapse pressure formation, appropriate mud weight window can be generated to prevent rock failure. Rock failure can happen in shear failure and tensile failure. In shear failure, the rock under compression and high compression in one side can make a breakout. On the other side, tensile failure happens when rock under tension and this can trigger for lost circulation.

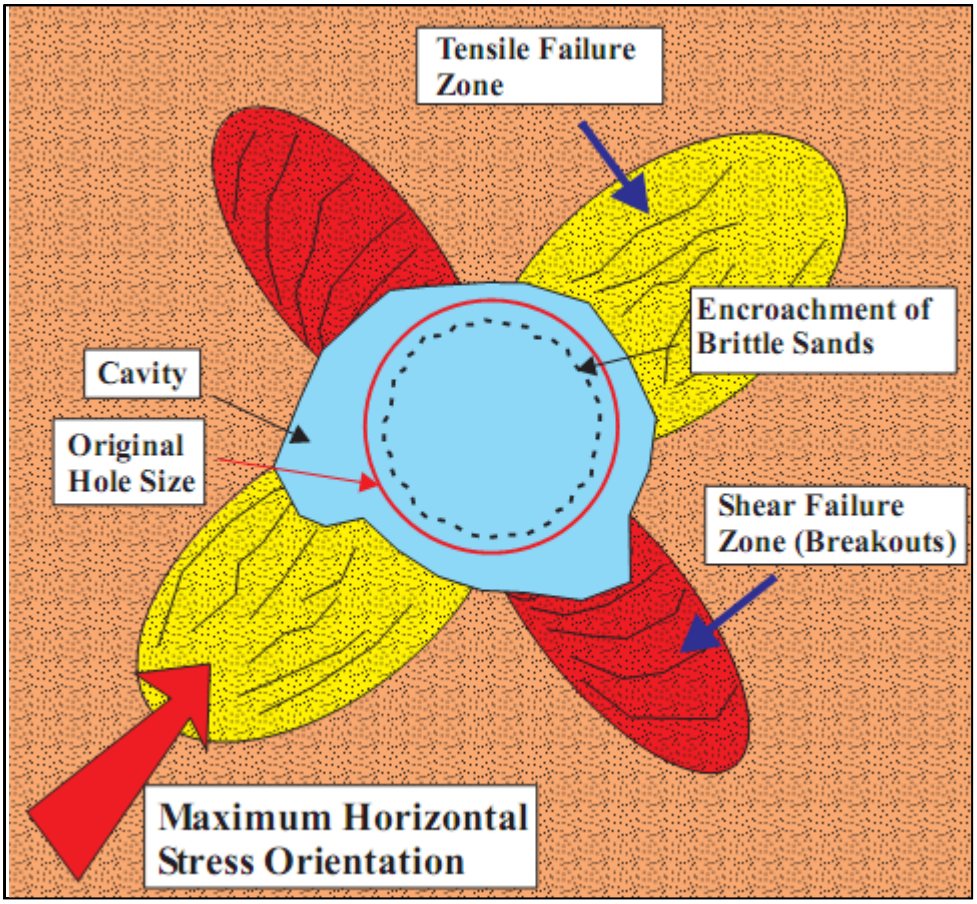

Figure 41 Wellbore Failure (Amoco, 2010)

In this study use three models to calculate collapse pressure to prevent rock failure. They are Mohr Coulomb, Modified Lade and Stassi D' Alia. Basen on Kirch equation with assumption $\theta = 90^0$, it means that there is no breakout in the borehole wall because breakout is avoided during drilling or can be minimalize as small as possible to reach wellbore stability. So stress around borehole wall can be described as below :

$$\sigma_\theta = 3\sigma_x - \sigma_y - P_{wc} \quad (65)$$

$$\sigma_a = \sigma_{zz} + 2\upsilon\,(\sigma_x - \sigma_y) \quad (66)$$

$$\sigma_r = P_{wc} \quad (67)$$

$$\tau_{\theta z} = -2\,\tau_{zx} \quad (68)$$

Rock failure is governed by principal stresses and the solution for principal stress are below :

$$\sigma_i = P_{wc} \quad (69)$$

$$\sigma_j = \frac{1}{2}(\sigma_\theta + \sigma_a) + \frac{1}{2}\sqrt{(\sigma_\theta - \sigma_a)^2 + 4\tau_{\theta z}^2} \quad (70)$$

$$\sigma_k = \frac{1}{2}(\sigma_\theta + \sigma_a) - \frac{1}{2}\sqrt{(\sigma_\theta - \sigma_a)^2 + 4\tau_{\theta z}^2} \quad (71)$$

The way how to calculate collapse pressure can be simplify using chart in the figure below:

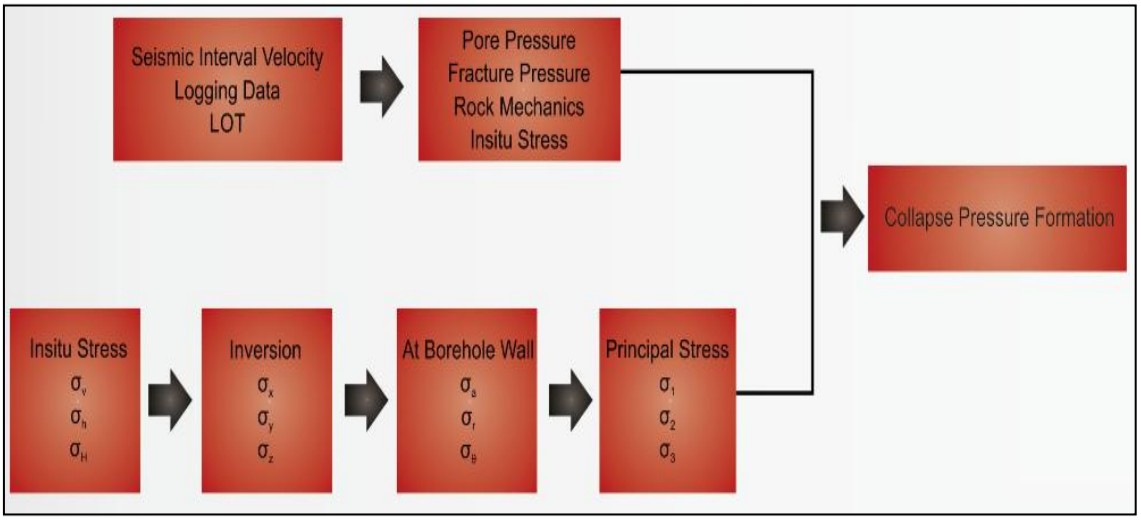

Figure 42 Collapse Pressure Determination

3.1.3.1.Collapse Pressure Using Mohr Coulomb Model

In Mohr Coulomb failure model only use maximum and minimum principal stress. The failure model can be described below :

$$\tau = \tau_0 + \sigma' \tan\mu \quad (72)$$

where

$$\tau = \frac{1}{2}(\sigma_1' - \sigma_3')\cos\mu \quad (73)$$

$$\sigma' = \frac{1}{2}(\sigma_1' + \sigma_3') - \frac{1}{2}(\sigma_1' - \sigma_3')\sin\mu \quad (74)$$

$$\sigma' = \sigma - P_0 \quad (75)$$

Combining this equation together to get σ_3'

$$(\sigma_1' - \sigma_3') - (\sigma_1' + \sigma_3')\sin\mu = 2\,\tau_0\,\cos\mu \quad (76)$$

$$\sigma_3^{'} = \frac{\sigma_1^{'}(1-\sin\mu) - 2\tau_0\cos\mu}{1+\sin\mu} \quad (77)$$

Because Mohr Coulomb only use two principal stress so :

$$\sigma_1 = \sigma_j = \frac{1}{2}(\sigma_\theta + \sigma_a) + \frac{1}{2}\sqrt{(\sigma_\theta - \sigma_a)^2 + 4\tau_{\theta z}^2} \quad (78)$$

$$\sigma_3 = \sigma_i = P_{wc} \quad (79)$$

a. Vertical Well

$$\tau_{\theta z} = 0 \quad (80)$$

$$\sigma_1 = \sigma_\theta = 3\sigma_x - \sigma_y - P_{wc} \quad (81)$$

$$\sigma_3 = P_{wc} \quad (82)$$

$$\sigma_1' = 3\sigma_x - \sigma_y - P_{wc} - P_0 \quad (83)$$

$$\sigma_3' = P_{wc} - P_0 \quad (84)$$

From previous equation

$$\sigma_3^{'} = \frac{\sigma_1^{'}(1-\sin\mu) - 2\tau_0\cos\mu}{1+\sin\mu} \quad (85)$$

$$P_{wc} - P_0 = \frac{(3\sigma_x - \sigma_y - P_{wc} - P_0)(1-\sin\mu) - 2\tau_0\cos\mu}{1+\sin\mu} \quad (86)$$

$$P_{wc} = \frac{1}{2}(3\sigma_x - \sigma_y)(1-\sin\mu) + P_0\sin\mu - \tau_0\cos\mu \quad (87)$$

b. Directional Well

$$\sigma_\theta = 3\sigma_x - \sigma_y - P_{wc} = R - P_{wc} \quad (88)$$

$$\sigma_a = \sigma_{zz} + 2\upsilon(\sigma_x - \sigma_y) \quad (89)$$

$$\sigma_1 = \sigma_j = \frac{1}{2}(\sigma_\theta + \sigma_a) + \frac{1}{2}\sqrt{(\sigma_\theta - \sigma_a)^2 + 4\tau_{\theta z}^2} \quad (90)$$

$$\sigma_3 = P_{wc} \quad (91)$$

$$\sigma_3' = \frac{\sigma_1'(1-\sin\mu) - 2\tau_0\cos\mu}{1+\sin\mu} \quad (92)$$

$$P_{wc} - P_0 = \frac{\left[\left(\frac{1}{2}(\sigma_\theta + \sigma_a) + \frac{1}{2}\sqrt{(\sigma_\theta - \sigma_a)^2 + 4\tau_{\theta z}^2}\right) - P_0\right](1-\sin\mu) - 2\tau_0\cos\mu}{1+\sin\mu} \quad (93)$$

Substitute σ_θ and σ_a into above equation to get equation in P_{wc} :

$$(4+4sin^2\mu)P_{wc}^2 - 2(\sigma_a - R - \sigma_a sin^2\mu)P_{wc} + 2R\sigma_a(1-sin^2\mu) + 16\tau_0^2 cos^2\mu - 8P_0^2 sin^2\mu - 2R^2(1-sin^2\mu) - 2\sigma_a^2(1-sin^2\mu) - 4\tau_{\theta z}^2(1-sin^2\mu) = 0 \quad (94)$$

The equation above can be simplified with this equation:

$ax^2 + bx + c$ (95)

where

$$a = (4 + 4sin^2\mu) \quad (96)$$

$$b = -2(\sigma_a - R - \sigma_a sin^2\mu) \quad (97)$$

$$c = 2R\sigma_a(1 - sin^2\mu) + 16\tau_0^2 cos^2\mu - 8P_0^2 sin^2\mu - 2R^2(1 - sin^2\mu) - 2\sigma_a^2(1 - sin^2\mu) - 4\tau_{\theta z}^2(1 - sin^2\mu) \quad (98)$$

The above equation have a solution :

$$x_{1,2} = \frac{-b \pm \sqrt{b^2 - 4ac}}{2a} \quad (99)$$

3.1.3.2.Collapse Pressure Using Modified Lade Model

This model assume that there is no communication between the wellbore pressure and pore pressure. It means that a stable mud cake is formed at the borehole wall. The collapse pressure (P_{wc}) to prevent wellbore instability is given by :

$$P_{wc} = \frac{\left(B - C^{\frac{1}{2}}\right)}{2A} \quad (100)$$

Where

$$A = \sigma_a + S_1 - P_0 \quad (101)$$

$$B = A\sigma_{\theta n} - \tau_{\theta z}^2 \quad (102)$$

$$C = B^2 - 4A\{D - (S_1 - P_0)[A(\sigma_{\theta n} + S_1 - P_0) - \tau_{\theta z}^2]\} \quad (103)$$

$$D = \frac{(\sigma_{\theta n} + \sigma_a + 3S_1 - 3P_0)^3}{27 + \eta} \quad (104)$$

$$\sigma_{\theta n} = \sigma_x + \sigma_y - 2(\sigma_x - \sigma_y)cos2\theta - 4\tau_{xy}sin2\theta \quad (105)$$

$$\sigma_a = \sigma_{zz} - \upsilon[2(\sigma_x - \sigma_y)cos2\theta + 4\tau_{xy}sin2\theta] \quad (106)$$

$$\tau_{\theta z} = 2(\tau_{yz}cos\theta - \tau_{zx}sin\theta) \quad (107)$$

3.1.3.3.Collapse Pressure Using Stassi D' Alia Model

Stassi D' Alia use three principal stress (σ_1, σ_2, σ_3) to estimate wellbore failure criteria where:

$$\sigma_1 = \sigma_j = \frac{1}{2}(\sigma_\theta + \sigma_a) + \frac{1}{2}\sqrt{(\sigma_\theta - \sigma_a)^2 + 4\tau_{\theta z}^2} \quad (108)$$

$$\sigma_2 = \sigma_k = \frac{1}{2}(\sigma_\theta + \sigma_a) - \frac{1}{2}\sqrt{(\sigma_\theta - \sigma_a)^2 + 4\tau_{\theta z}^2} \quad (109)$$

$$\sigma_3 = \sigma_i = P_{wc} \quad (110)$$

Beside three pricipal stress, Stassi D' Alia also use uniaxial compressive strength (C_0) and tensile strength (T_0) in his calculation. Tensile strength (T_0) can be estimated using modified Griffith equation where:

$$T_0 = \frac{C_0\sqrt{\mu^2 + 1} - \mu}{4} \quad (111)$$

From all of these parameters, wellbore collapse pressure can be obtained using this equation :

$$12P_{wc}^2 - 6(U + Y)P_{wc} + 3Y^2 + 12\tau_{\theta z}^2 + U^2 - 4(C_0 - T_0)U - 4C_0T_0 = 0 \quad (112)$$

The equation above can be simplified with this equation

$$ax^2 + bx + c \quad (113)$$

where

$$a = 12 \quad (114)$$

$$b = -6(U + Y) \quad (115)$$

$$c = 3Y^2 + 12\tau_{\theta z}^2 + U^2 - 4(C_0 - T_0)U - 4C_0T_0 \quad (116)$$

$$U = 3\sigma_x - \sigma_y + \sigma_a \quad (117)$$

$$Y = 3\sigma_x - \sigma_y - \sigma_a$$

This equation have a solution :

$$x_{1,2} = \frac{-b \pm \sqrt{b^2 - 4ac}}{2a} \quad (118)$$

3.2 Casing Design

Casing shoe should be set in shale formation to reach the integrity criteria and to make sure that gas does not migrate through casing shoe in case there is a gas kick during drilling in open hole section below casing shoe. There are some parameters to determine casing shoe depth and the number of casing strings :

- Regulatory requirements
- Kick tolerance
- Zonal isolation
- Hole stability and rock strength
- Well trajectory and wear consideration

Casing must have enough mechanical strength to withstand burst, collapse and tension loads. Burst in pipe is happen when internal pressure inside casing is bigger than pressure at the outside and this pressure difference exceed the mechanical strength of casing. On the other side, collapse is happen when the external pressure is bigger than internal pressure inside the casing and this pressure difference exceed the mechanical strength of casing. And the next criteria is tension which tension failure will occure when the axial load exceed the material strength of casing.

According to Bernt S. Aadnøy (Aadnøy, 2003), there are some situations where burst can occure in the casing :

a. The hydrostatic mud pressure inside the casing exceeds the formation pressure or hydrostatic pressure outside the casing.
b. During well shut-in, the differential borehole pressure allows formation fluid to enter the wellbore.
c. A gas bubble, caused by a kick, is allowed to migrate up the casing with or without

limited expansion.

d. During kick circulation.
e. The casing is filled with gas migrating up the wellbore during a temporary abandonment or disconnect in an emergency situation.
f. During testing or production a leak occurs in the tubing just below the wellhead.
g. Temperature expansion of fluid in closed annuli between casing strings.
h. When squeeze cementing.

In simulation using stress check (Landmark) software, burst will occure when the difference between internal pressure and extrenal pressure exceed the mechanical strength of casing. This is the parameter that are used for internal pressure and external pressure in stress check software :

a. Internal pressure :
   - Displacement to gas

     $$P_{gas/mud} = P_{pore} - \{g \text{ x } \rho_{gas} \text{x} (TVD_{influx\ depth} - TVD_{gas/mud})\} \quad (119)$$

     $$P_{internal} = P_{gas/mud} + \{g \text{ x } \rho_{gas} \text{x} (TVD - TVD_{gas/mud})\} \quad (120)$$

   - Gas kick profile

     $$P_{bh} = g\ x\ (\rho_{mud} + EMW_{kick\ intensity})\ x\ TVD_{influx\ depth} \quad (121)$$

   - Fracture at shoe with gas gradient above

     $$P_{internal} = P_{frac} - \{g\ x\ \rho_{gas} x (TVD_{shoe\ above\ open\ hole\ TD} - TVD)\} \quad (122)$$

   - Lost return with water

     $$P_{internal} = P_{frac} - \{g\ x\ \rho_{mud} x (TVD_{shoe\ above\ open\ hole\ TD} - TVD)\} \quad (123)$$

   - Surface protection (BOP)

     $$P_{hanger} = P_{frac} - \{g \text{ x } \rho_{water} \text{x} (TVD_{shoe\ above\ open\ hole\ TD} - TVD_{hanger})\} \quad (124)$$

     $$P_{internal} = P_{hanger} + \{g \text{ x } \rho_{gas} \text{x} (TVD - TVD_{hanger})\} \quad (125)$$

   - Pressure test

     $$P_{internal} = P_{test} + (g \text{ x } \rho_{mud} \text{ x } TVD) \quad (126)$$

   - Green cement pressure test

     Internal pressure profile from hanger to the float collar

     $$P_{internal} = P_{test} + (g \text{ x } \rho_{displacement\ fluid} \text{ x } TVD) \quad (127)$$

     Internal pressure profile from float collar to the casing shoe

     $$P_{shoe} = P_{tail\ slurry\ top} + \{g \text{ x } \rho_{tail\ slurry} \text{x} (TVD_{shoe} - TVD_{tail\ slurry\ top})\} \quad (128)$$

     $$P_{internal} = P_{shoe} - \{g \text{ x } \rho_{tail\ slurry} \text{x} (TVD_{shoe} - TVD)\} \quad (129)$$

b. External pressure :
   - Mud and cement mix-water

     External pressure profile from hanger to top of cement :

     $$P_{external} = g \text{ x } \rho_{mud} \text{ x } TVD \quad (130)$$

     External pressure profile from top of cement to casing shoe :

$$P_{toc} = g \text{ x } \rho_{mud} \text{ x } TVD_{toc} \quad (131)$$

$$P_{external} = P_{toc} + \{g \text{ x } \rho_{mix-water} \text{ x } (TVD - TVD_{toc}) \} \quad (132)$$

- Minimum formation pore pressure

$$P_{external} = g \text{ x } EMW_{min} \text{ x } TVD \quad (133)$$

- Pore pressure with seawater gradient

$$P_{external} = g \text{ x } \rho_{sea\ water} \text{ x } (TVD - TVD_{msl}) \quad (134)$$

- Fluid gradient with pore pressure

$$P_{external} = \text{Pore pressure profile} \quad (135)$$

Only for production casing, the internal pressure for production load in stress check software consist of :

- Tubing leak

$$P_{prod\ cas\ hanger} = P_{res} - \{g \text{ x } \rho_{res\ fluid} \text{ x } (TVD_{perf.} - TVD_{prod.casing\ hanger})\} \quad (136)$$

$$P_{internal} = P_{prod\ cas\ hanger} + \{g \text{ x } \rho_{packer\ fluid} \text{ x } (TVD - TVD_{hanger})\} \quad (137)$$

- Stimulation surface leak

  If the shoe is deeper than the packer

$$P_{internal} = P_{injection} + (g \text{ x } \rho_{injection\ fluid} \text{ x } TVD) \quad (138)$$

- Injection down casing

$$P_{internal} = P_{injection} + (g \text{ x } \rho_{injection\ fluid} \text{ x } TVD) \quad (139)$$

- Gas migration

$$P_{shoe} = P_{res.} + \{g \text{ x } \rho_{annulus\ fluid} \text{ x } (TVD_{shoe} - TVD_{prod\ casing\ hanger})\} \quad (140)$$

If $P_{shoe} > P_{fracture}$

$$P_{internal} = P_{frac} - \{g \text{ x } \rho_{annulus\ fluid} \text{ x } (TVD_{shoe} - TVD)\} \quad (141)$$

Otherwise

$$P_{internal} = P_{res.} + \{g \text{ x } \rho_{annulus\ fluid} \text{ x } (TVD - TVD_{prod\ casing\ hanger})\} \quad (142)$$

In the other hand, casing collapse also can occure in some of situations. These are situations where casing collapse occure in the well :

- Lost circulation where mud level inside the casing is drop until wellbore pressure equivalent with pore pressure.
- During cement squeeze job through perforation where high pressure may arise behind the casing
- Drilling through salt formation
- The casing string is not properly filled with mud
- Temperature expansion on closed liquid-filled annuli between casing string

In simulation using stress check software, the internal and external pressure consist of some parameters :

a. Internal profile

- Fluid or partial evacuation

$$P_{internal} = P_{atm} \quad (143)$$

- Lost return with mud drop

$$TVD_{mud\ level} = \frac{TVD_{pore} \text{ x } P_{pore}}{(g \text{ x } \rho_{mud})} \quad (144)$$

$$P_{internal} = (P_{atm} + P_{pore}) - \{g \text{ x } \rho_{mud} \text{ x } (TVD_{pore} - TVD)\} \quad (145)$$

- Cementing

$$P_{internal} = g \text{ x } \rho_{displacement\ fluid} \text{ x } TVD \quad (146)$$

b. External profile

- Mud and cement mix-water

$$P_{toc} = g \text{ x } \rho_{mud} \text{ x } TVD_{toc} \quad (147)$$

$$P_{external} = P_{toc} + \{g \text{ x } \rho_{mix-water} \text{x } (TVD - TVD_{toc})\} g \text{ x } \rho_{mud} \text{ x } TVD_{toc} \quad (148)$$

- Mud and cement slurry

External pressure profile from hanger to top of cement :

$$P_{external} = g \text{ x } \rho_{mud} \text{ x } TVD \quad (149)$$

External pressure profile from top of cement to casing shoe :

$$P_{toc} = g \text{ x } \rho_{mud} \text{ x } TVD_{toc} \quad (150)$$

$$P_{external} = P_{toc} + \{g \text{ x } \rho_{cement} \text{ x } (TVD_{casing\ shoe} - TVD_{toc})\} \quad (151)$$

- Fracture at prior shoe with gas gradient above

$$P_{external} = P_{frac\ @\ prior\ shoe} + \{g \text{ x } \rho_{mud} \text{ x } (TVD - TVD_{prior\ shoe})\} \quad (152)$$

- Fluid gradients with pore pressure

$$P_{toc} = g \text{ x } \rho_{above\ toc} \text{ x } TVD_{toc} \quad (153)$$

$$P_{external} = P_{toc} + \{g \text{ x } \rho_{below\ toc} \text{ x } (TVD - TVD_{toc})\} \quad (154)$$

For collapse calculation in production casing, the internal profile consist of :

- Full evacuation

$$P_{external} = P_{atm} \quad (155)$$

- Above / below packer

$$P_{external} = (P_{atm} + P_{pore}) - \{g \text{ x } \rho_{fluid} \text{ x } (TVD_{perf.} - TVD)\} \quad (156)$$

- Gas migration

$$P_{shoe} = P_{res.} + \{g \text{ x } \rho_{mud} \text{ x } (TVD_{shoe} - TVD_{prod\ casing\ hanger})\} \quad (157)$$

If $P_{shoe} > P_{fracture}$

$$P_{external} = P_{frac} - \{g \text{ x } \rho_{mud} \text{ x } (TVD_{shoe} - TVD)\} \quad (158)$$

Otherwise

$$P_{external} = P_{res.} + \{g \text{ x } \rho_{mud} \text{ x } (TVD - TVD_{prod\ casing\ hanger})\} \quad (159)$$

Tension failure can occure because of the material strength can not withstand some of tension load. These conditions are some parameters which cause tension failure :

a. Dynamic forces or shock loads
b. Movements to free stuck pipe may induce considerable tensional loads
c. Pressure testing
d. The static weight of the casing string
e. Bouyancy that reduce the effective weight of the string so that it will reduce tension
f. Bending loads due to dog-leg severities
g. Drag forces

Axial load can be calculated based on weight of casing:

$$F_a = w_a x \text{ L x BF} \quad (160)$$

Where

w_a = Weight of casing (ppf)
L = Length of casing (feet)
BF = Bouyancy Factor

The casing also need to check for triaxial stress to make sure that casing yield strength can withstand from three principal stress (radial stress, tangential stress and axial stress). Triaxial stress often called as Von Mises equivalent stress (VME stress). Von Mises stress can be calculated using this equation:

$$\sigma_y^2 = \left(\frac{F_e}{\pi(r_0^2 - r_i^2)}\right)^2 + 3\left(\frac{r_0^2 \Delta p}{r_0^2 - r_i^2}\right)^2 \quad (161)$$

where

$$F_e = F_a - p_i r_i^2 \pi + p_o r_o^2 \pi \quad (162)$$

3.3 Hole Cleaning and Hydraulic Design

Cutting transport or hole cleaning is very important during drilling a well. Cutting must be transported to the surface. Poor hole cleaning will cause serious problem in drilling. These are several problems during drilling that caused by poor hole cleaning :

- Low rate of penetration (ROP)
- High drag and torque, it will impact on drillstring design
- Stuck pipe
- Difficulty in casing landing
- Problems during cementing, for example channeling
- Difficulty during run in hole logging tools

Cutting transport will be more difficult in directional well or horizontal well. If fluid flowrate does not enough to transport cutting to the surface, cutting will accumulate in the high angle of well and it will form cutting bed. On the other hand, if fluid flow rate too high, it will

cause higher equivalent circulating density (ECD), subsequently If ECD more than fracture pressure of formation, it will cause well fracturing. So to optimize hole cleaning, it is important to consider about mud properties like plastic viscosity (PV), yield point (YP), density, etc.

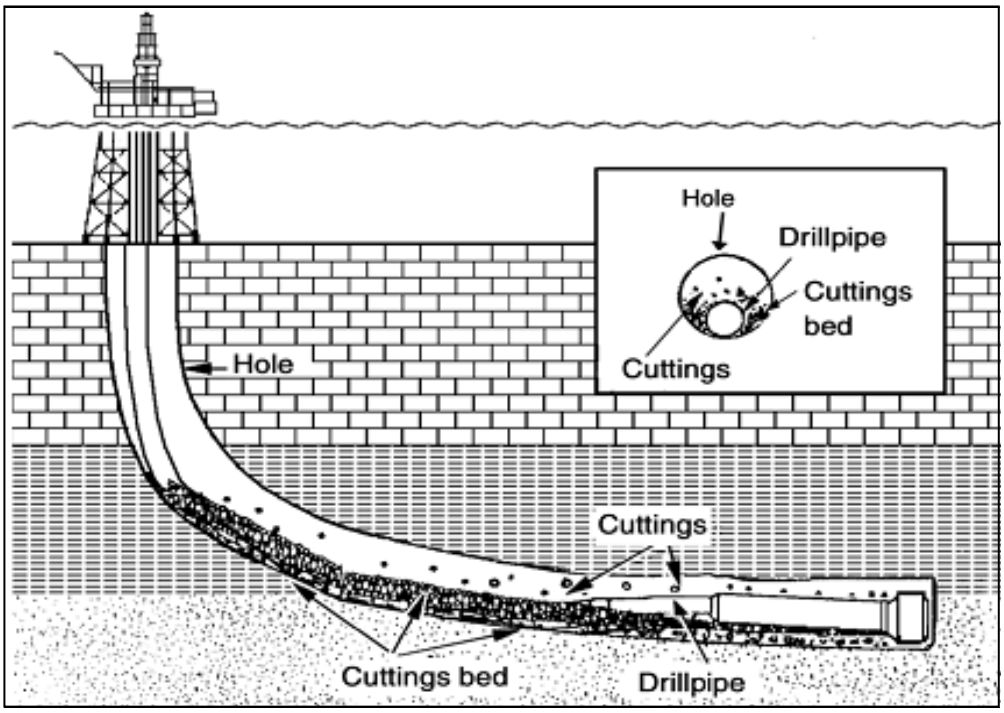

Figure 43 Cutting Bed in Directional Well (Lecture Note, Mesfin)

In this thesis, cutting transport calculation using wellplan software (Landmark, Halliburton). These are step by step in cutting transport calculation using wellplan software :

a. Calculate n, k,τ_y and Reynold's number

$$n = \frac{(3.32)(\log 10)(YP + 2PV)}{(YP + PV)} \quad (163)$$

$$k = \frac{(YP + PV)}{511} \quad (164)$$

$$\tau_y = (5.11)^n \quad (165)$$

$$R_A = \frac{\rho V_a^{(2-n)}(D_H - D_P)^n}{(2/3)G_{pl}K} \quad (166)$$

b. Calculate concentration based on ROP in flow channel

$$C_0 = \frac{(V_r D_B^2/1471)}{(V_r D_B^2/1471) + Q_m} \quad (167)$$

c. Calculate fluid velocity based on open flow channel

$$V_a = \frac{24.5\ Q_m}{D_H^2 - D_P^2} \quad (168)$$

d. Calculate coefficient of drag around sphere

If $R_e < 225$

then

$$C_D = \frac{22}{\sqrt{R_a}} \tag{169}$$

else,

$C_D = 1.5$

e. Calculate mud carrying capacity

$$C_M = \frac{4g\left(\frac{D_c}{12}\right)(\rho_c - \rho)}{3\rho C_D} \tag{170}$$

f. Calculate slip velocity

If $V_A < 53$, then

$$V_{sv} = (0.00516)V_A + 3.0006 \tag{171}$$

If $V_A \geq 53$, then

$$V_{sv} = (0.02554)(V_A - 53) + 3.28 \tag{172}$$

g. Calculate settling velocity in the plug in a mud with a yield stress

$$U_{sv} = \left[\frac{4gD_c^{1+bn}(\rho_c - \rho)}{3aK\rho_c^{1-b}}\right]^{\frac{1}{2-b(2-n)}} \tag{173}$$

where

$a = 42.9 - 23.9n$

$b = 1\text{-}0.33n$

h. Calculate angle of inclination correction factor

$$C_a = \left(\sin(1.33\alpha)\right)^{1.33}\left(\frac{5}{D_H}\right)^{0.66} \tag{174}$$

i. Calculate cutting size correction factor

$$C_s = 1.286 - 1.04\, D_c \tag{175}$$

j. Calculate mud weight correction factor

If $\rho < 7.7$ then $C_m = 1$

else

$$C_m = 1 - 0.0333\,(\rho - 7.7) \tag{176}$$

k. Calculate critical wall shear stress

$$\tau_{wc} = \left[a\, g \sin(\alpha)(\rho_c - \rho)D_c^{1+b}\rho^{b/2}\right]\frac{2n}{2n - 2b + bn} \tag{177}$$

where

$a = 1.732$

b = -0.744

l. Calculate critical pressure gradient

$$P_{gc} = \frac{2\tau_{wc}}{r_h\left[1 - \left(\frac{r_o}{r_h}\right)^2\right]} \quad (178)$$

m. Calculate total cross sectional area of the annulus without cutting bed

$$A_A = \frac{\pi\left(D_H^2 - D_p^2\right)}{4 \text{ x } 144} \quad (179)$$

n. Calculate dimentionless flow rate

$$\Pi g_b = \left[8 \text{ x } \frac{n}{\frac{2(1+2n)}{(a)\frac{1}{b}}}\right]^{\frac{1}{2-(2-n)^b}} \text{x}\left(1 - \left(\frac{r_p}{r_h}\right)^2\right)\left(1 - \left(\frac{r_p}{r_h}\right)^{\frac{b}{2-(2-n)b}}\right) \quad (180)$$

Where

a = 16

b = 1

o. Calculate critical Flow Rate (CFR)

$$Q_{crit} = r_h^2\left[\frac{\rho g b^{\frac{1}{b}} r_h^{\left(\frac{1}{b+n}\right)}}{K\rho^{\left(\frac{1}{b-1}\right)}}\right]^{\frac{b}{2-b(2-n)}} \Pi g_b \quad (181)$$

p. Calculate correction factor for cuttings concentration

$$C_{BED} = 0.97 - (0.00231\ \mu_a) \quad (182)$$

q. Calculate cutting concentration for a stationary bed by volume

$$C_{cons} = C_{BED}\left(1 - \frac{Q_m}{Q_{crit}}\right)(1 - \emptyset_B)(100) \quad (183)$$

After calculate the minimum flow rate to transport cutting to surface, the next step is to determine the optimization of hydraulic system by choosing the equipment to keep pressure losses at minimum in the drillstring and maximum in the drilling bit. The optimization of hydraulic system can be determined by these methods :

- Select the optimization methods : impact force or hydraulic horse power
- Determine the optimum flow rate
- Adjust flow rate to meet the requirements or limit
- Determine total flow area in the bit (TFA)

Generally, there are two methods in hydraulic optimization, they are jet impact force and maximum hydraulic horse power (HHP). The jet impact force can be maximized with maximize the momentum. Generally this occur when bit losses are about 49 % of the available pump pressure. On the other hand, the maximum horse power can be reached when the energy dissipated at the bit is maximized. Generally, this occur when 65% of pump

pressure is dissipated at the bit. Mathematically jet impact force and hydraulic horse power can be expressed as below :

- Impact Force (lbf) $= \left(\frac{\rho}{g_c}\right) VQ$ (184)

where ρ = Density of fluid (lb / ft^3)
Q = Flow rate (ft^3 / s)
g_c = Gravitational constant (32.17 ft / sec^2)
V = Velocity through the bit (ft / sec)

$$= \frac{Q\ (gpm)}{2.96\ A(in^2)} \quad (185)$$

- Bit Hydraulic Horse Power (hp) $= \frac{QP_b}{1714}$ (186)

where Q = Flow rate (gpm)
P_b = Pressure loss across bit nozzles (psi)

Pressure loss across the bit nozzle can be calculated using this equation

$$\Delta P_{bit} = \frac{\rho V^2}{2C_d^2 g_c} \quad (187)$$

where ρ = Density of fluid (lb / ft^3)
V = Fluid velocity (ft / s)
C_d = Nozzle coefficient (0.95)
g_c = 32.17 (ft / sec^2)
P = Pressurem (lb / ft^2)

Determination about the output from cutting transport and hydraulic system calculation can be simplified using chart below:

Figure 44 Output from Cutting Transport and Hydraulic System Calculation

4. CASE STUDY

4.1 Background

In this thesis use case study from X field. During the simulation, seismic interval velocity is used to estimate pore pressure. In propose well, well trajectory is made based on target reservoir that will be drilled. Interval velocity of this well can be exported to excel file from the interval velocity models. Pore pressure and fracture pressure can be calculated using this interval velocity and well logging from exploration wells.

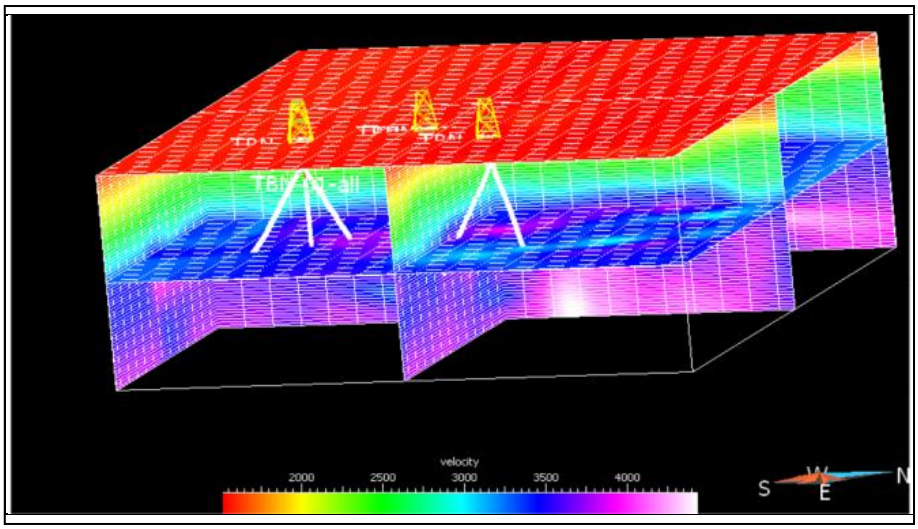

Figure 45 Interval Velocity Model from X Field

The formation of this field consists of shale, sand and limestone formation. The shale formation in this field is not reactive so using KCl polymer mud is enough to prevent swelling.

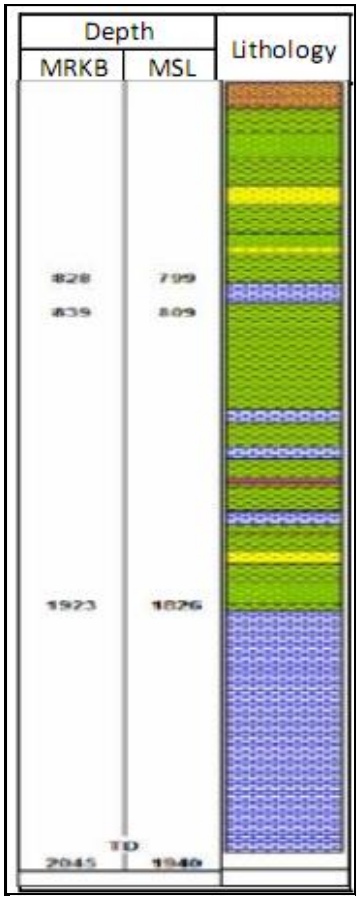

Figure 46 Lithology of X Field

In this case, data from offset exploration well T-1 is used to estimate wellbore stability parameter for directional well T-2. Figure below is vertical section for directional well T-2:

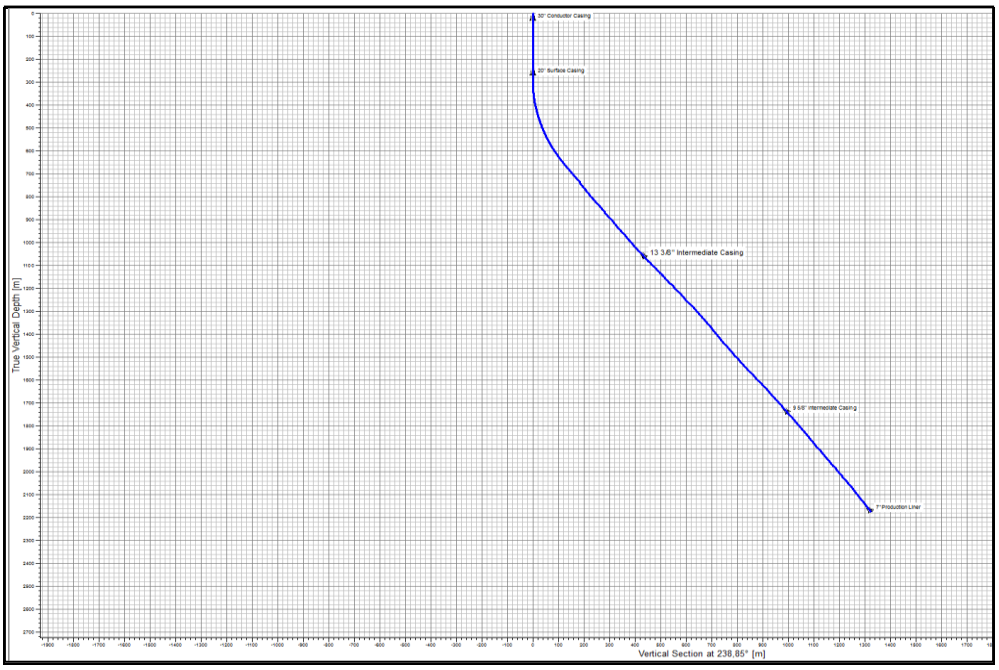

Figure 47 Vertical Section Well T-2

4.2 Pore Pressure Calculation

Pore pressure is estimated using Eaton equation. Eaton equation can be implemented in the compacted shale formation. In this case, it uses logging data from well T-1. This well is exploration well with vertical trajectory. To make sure that Eaton equation can be used in this well or in this field so it needs to plot density log (RHOB) vs. sonic log (DT). In compacted formation, density formation tends to increase with increasing depth and the value of the sonic log will decrease.

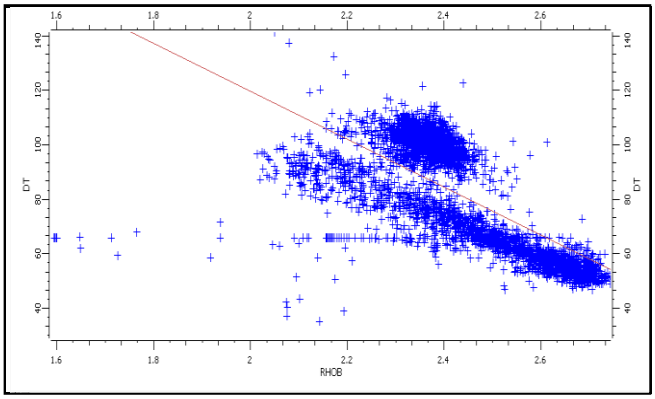

Figure 48 Plot DT Vs. RHOB from Well T-1

From figure above, it can be seen that Eaton equation can be used to estimate pore pressure in this field using this equation :

$$PP = OBP - \left[(OBP - HP)x \left(\frac{Vint}{Vnct}\right)^{N}\right] \quad (188)$$

Overburden pressure (OBP) can be calculated from density log and integrate it from surface until depth of interest.

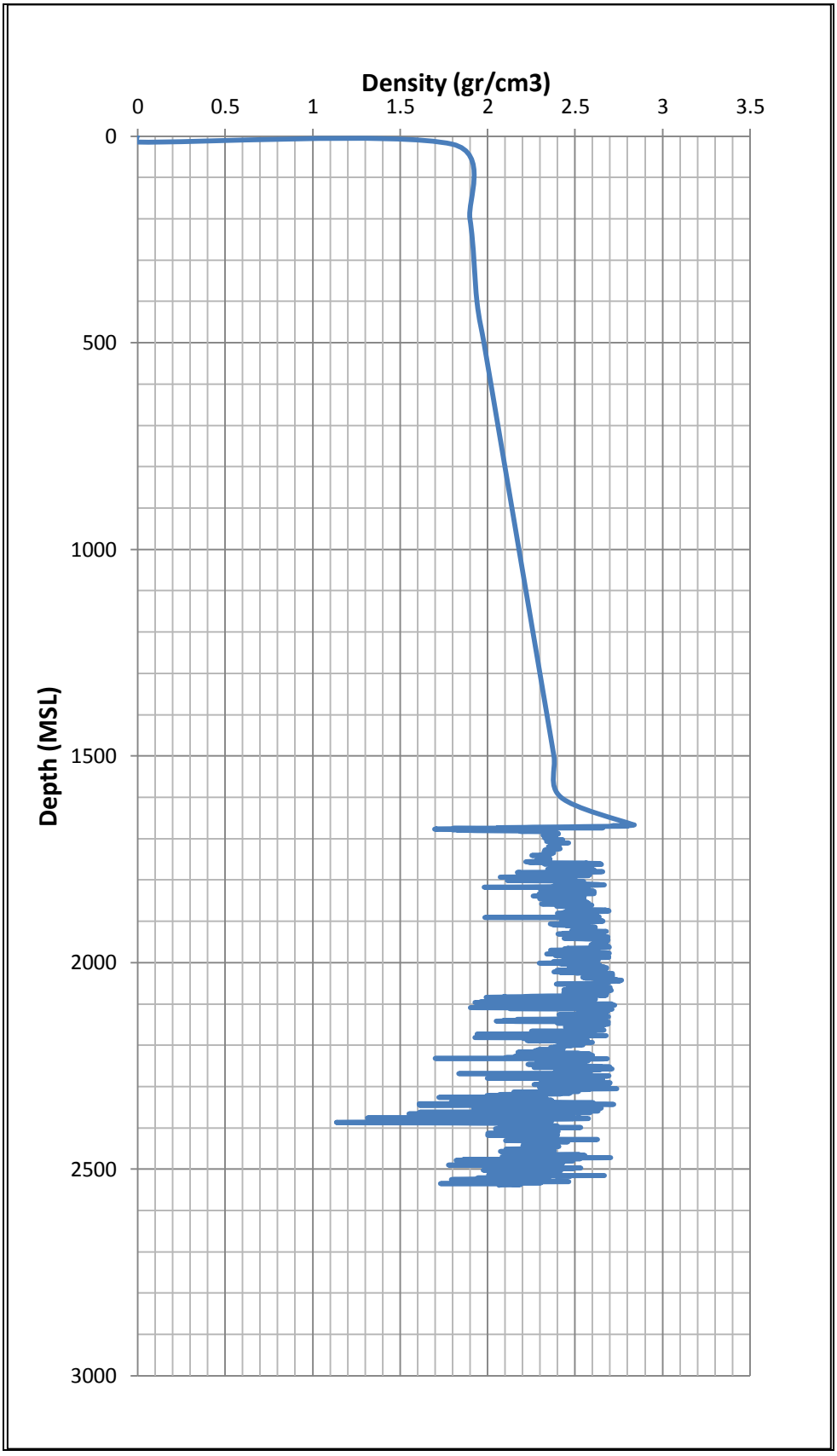

Figure 49 Density Profile Well T-1

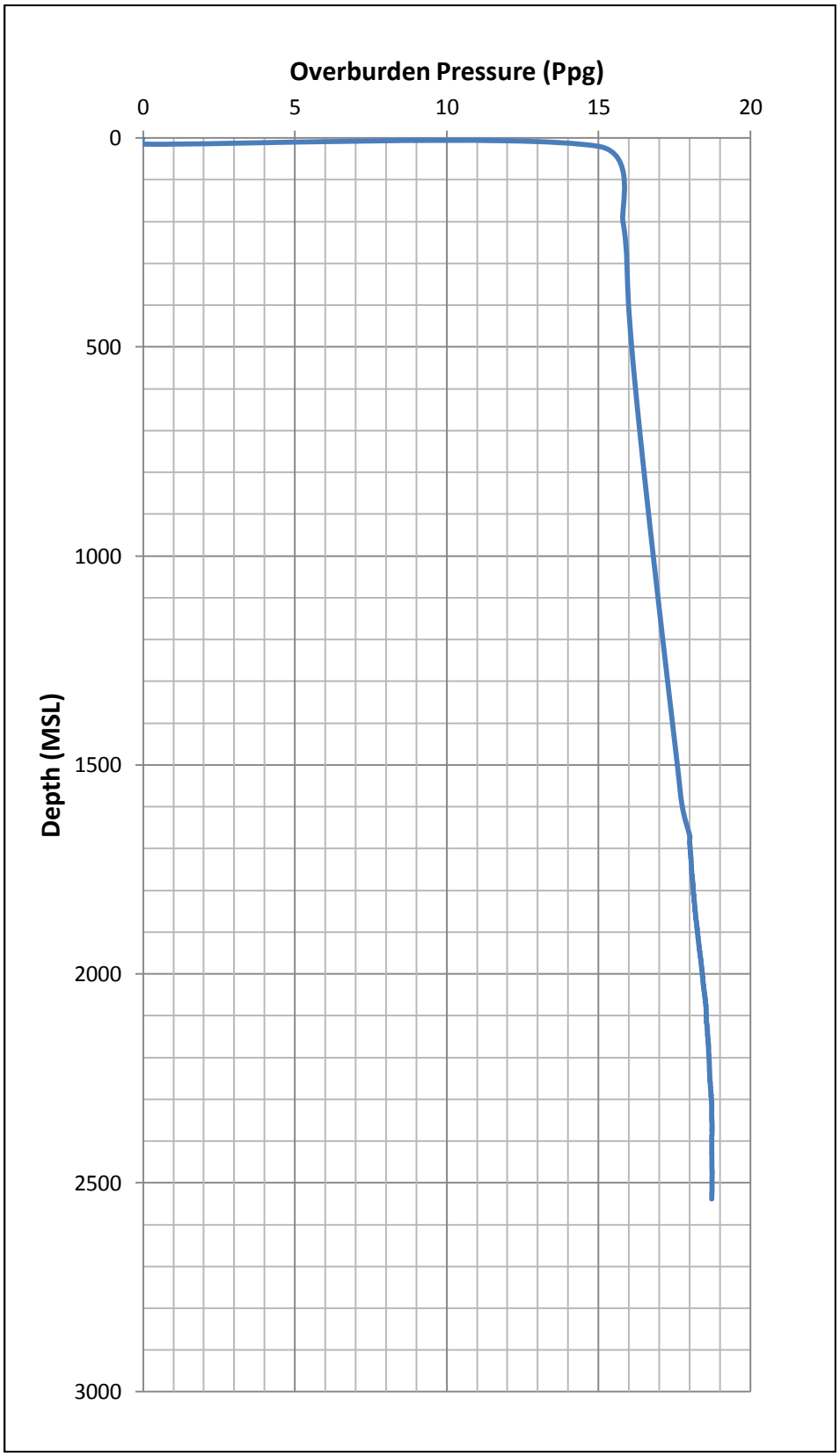

Figure 50 Overburden Pressure Profile Well T-1

Normal compacted trend velocity (Vnct) can be obtained through draw a line of interval velocity in compacted shale.

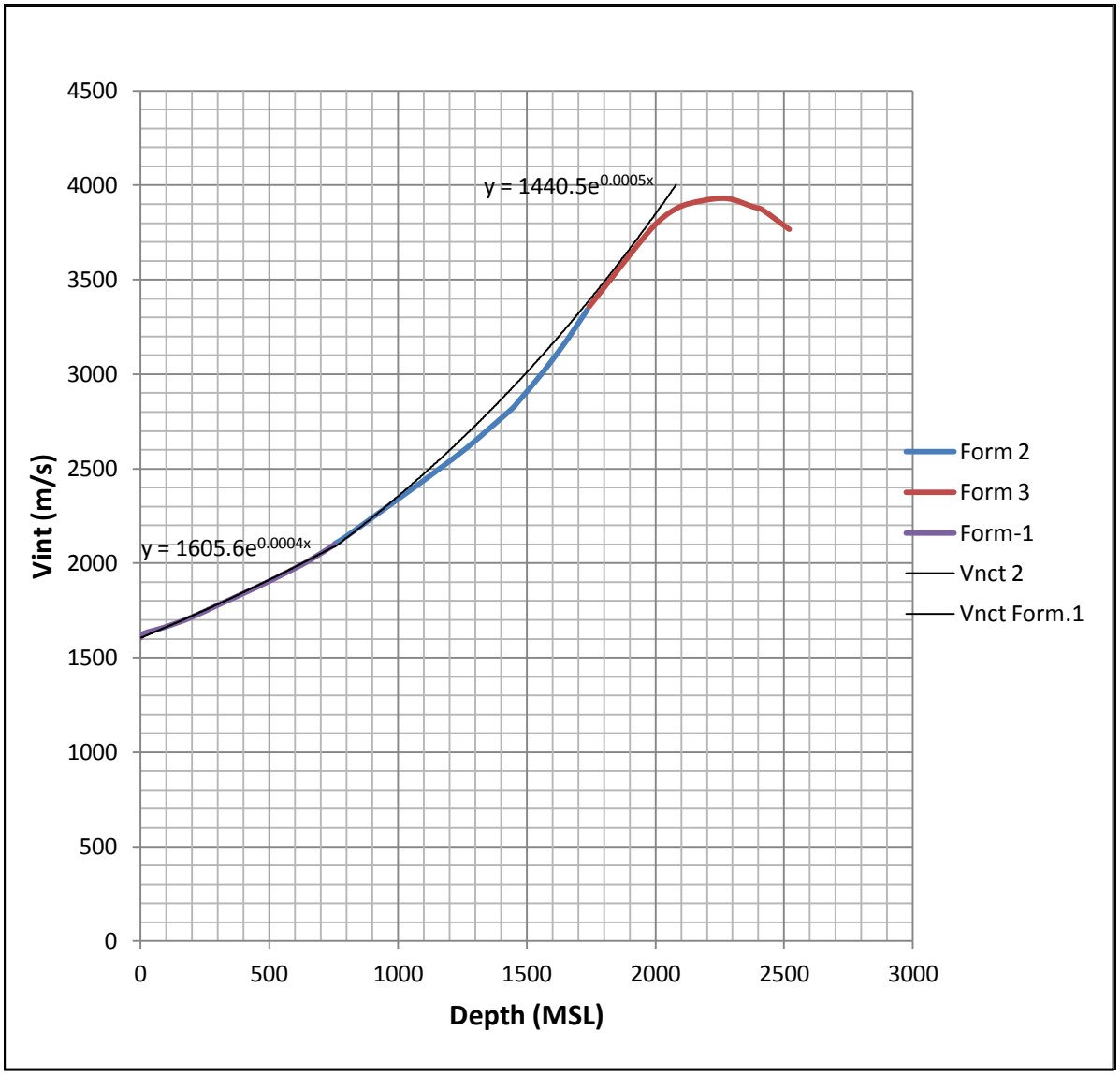

Figure 51 Vint and Vnct Profile Well T-1

Eksponential (N) is calculated based on properties from table below :

Table 1 Exponential (N) Properties Well T-1

Depth	PP	OBP	PP	OBP	Vint	VES	Log VES	Log Vint
(MSL)	Ppg	Ppg	Psi	Psi	m/s	Psi		
750.179	8.780	16.411	1123.710	2100.461	2097.489	976.752	2.990	3.322
1664.973	9.113	17.542	2588.651	4983.119	3198.973	2394.468	3.379	3.505

From table properties above and then plot Log VES Vs Log Vint

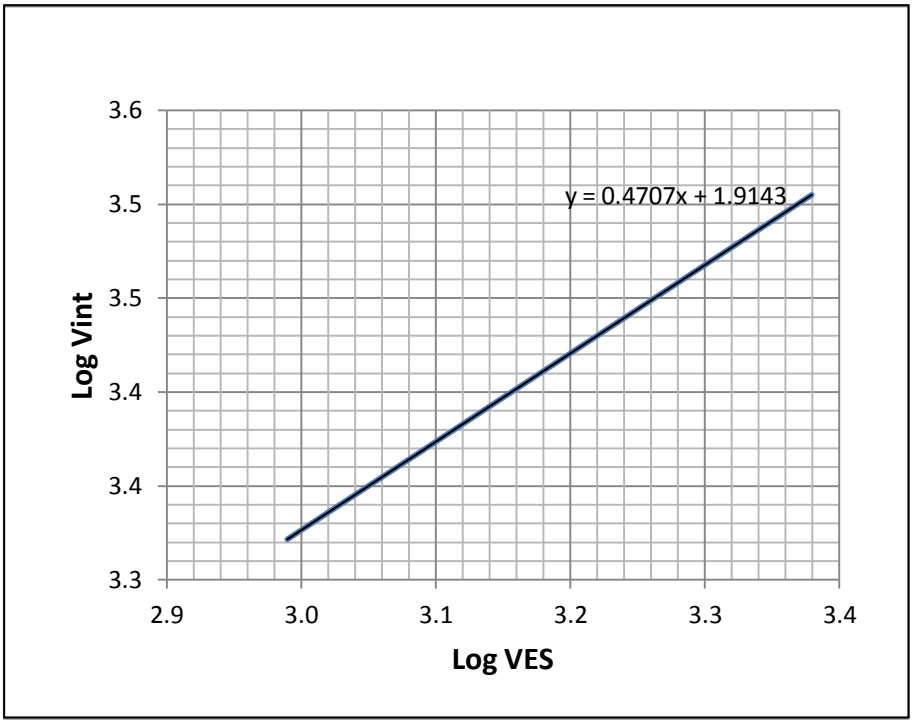

Figure 52 Plot Log VES Vs Log Vint

The value of exponential (N) is obtained from the slope

$$N = \frac{1}{Slope} = \frac{1}{0.4707} = 2.124$$

The value of HP can be estimated based on the density of water formation in this field. Based on the measurement , the water formation density has value 8.4 ppg.

From all of the parameter that defined above, pore pressure profile for well exploration T-1 can be estimated based on the value of interval velocity. Pore pressure based on calculation is corrected with mud density during drilling so that this method will give pore pressure value near real condition. For reservoir section, pore pressure is calculated based on pressure survey data at certain depth and fluid density from PVT analysis data. Table below show the mesurement of pore pressure in the reservoir section and PVT analysis data:

Table 2 PVT Analysis Data

Depth	Pressure	Fluid Density
meter	psi	gr/cm^3
2198	4002	0.82

From PVT anaylis data, pore pressure in the reservoir section can be calculated. Figure below show the output of the pore pressure profile from well T-1.

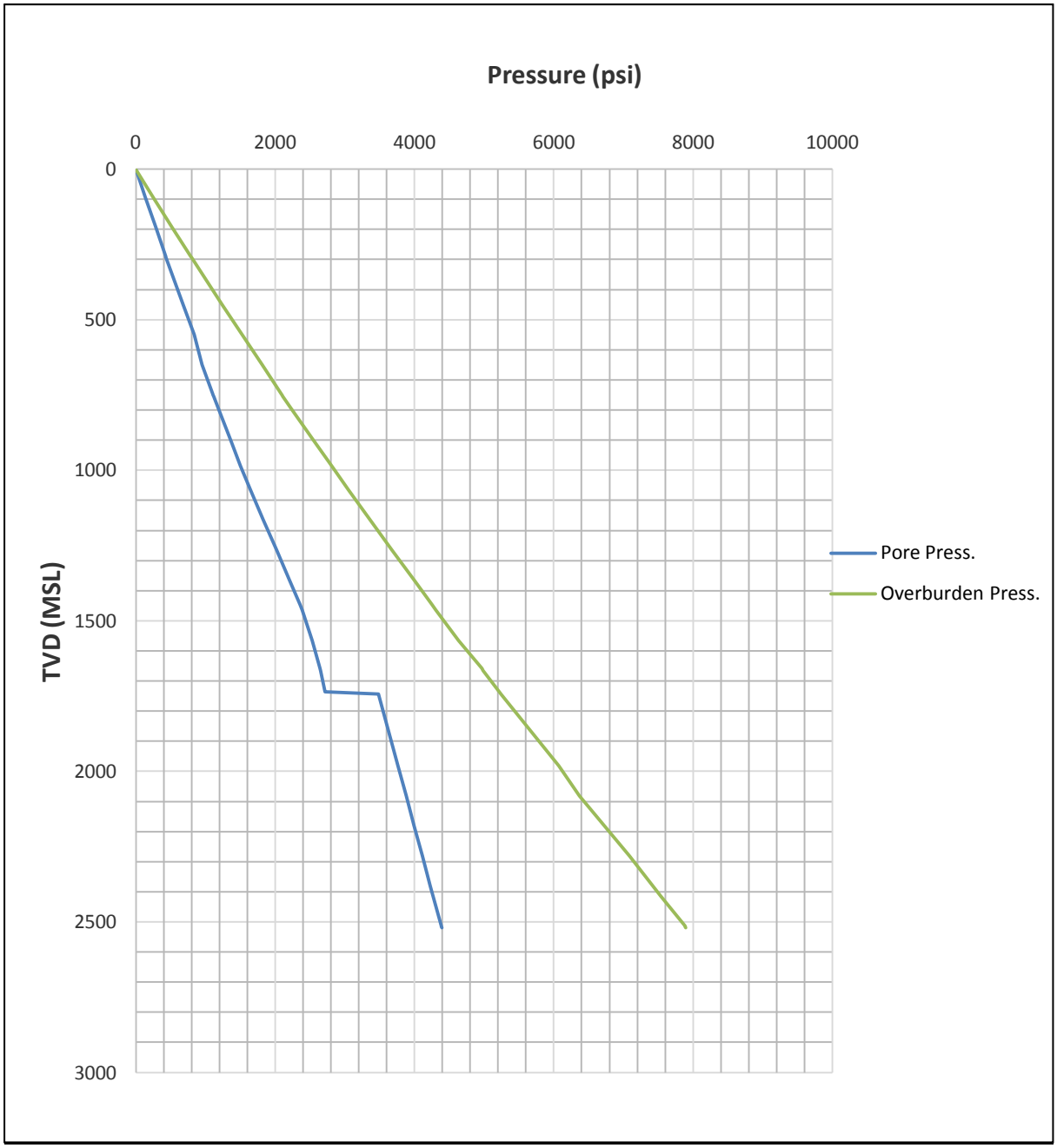

Figure 53 Pore Pressure Profile Well T-1

The same procedure can be followed to design the next well in this field. In this case, the propose T-2 well will be drilled to exploit oil and gas from this field. T-2 is directional well. Interval velocity from well T-2 is exported from the interval velocity model based on the trajectory from this well. Normal compacted trend velocity (Vnct) is estimated based on interval velocity profile in this well and it started to pick it up from compacted shale.

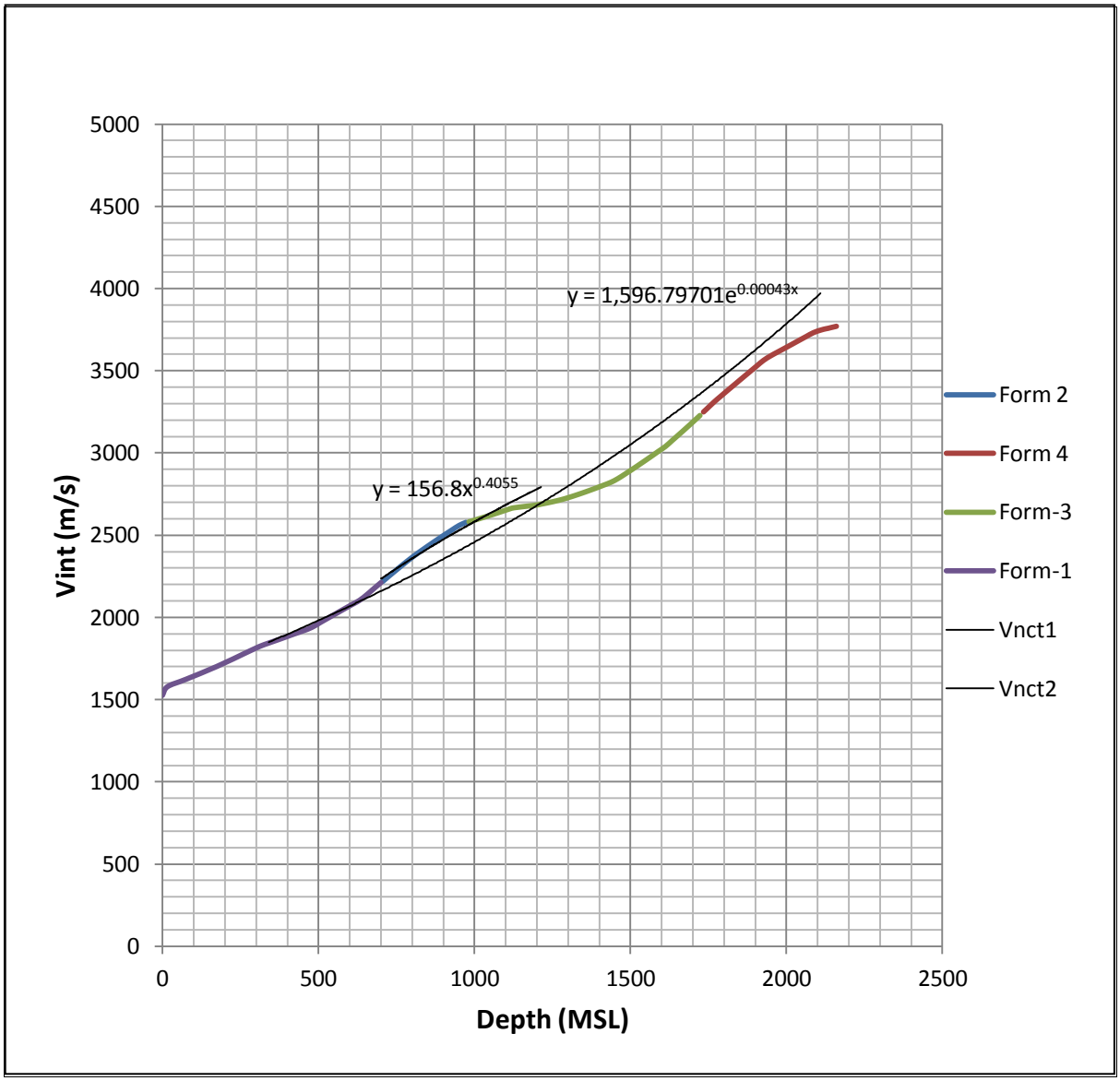

Figure 54 Vint and Vnct Profile Well T-2

Overburden pressure for well T-2 is obtained from the density model of this field and then the value of density is extracted based on well trajectory.

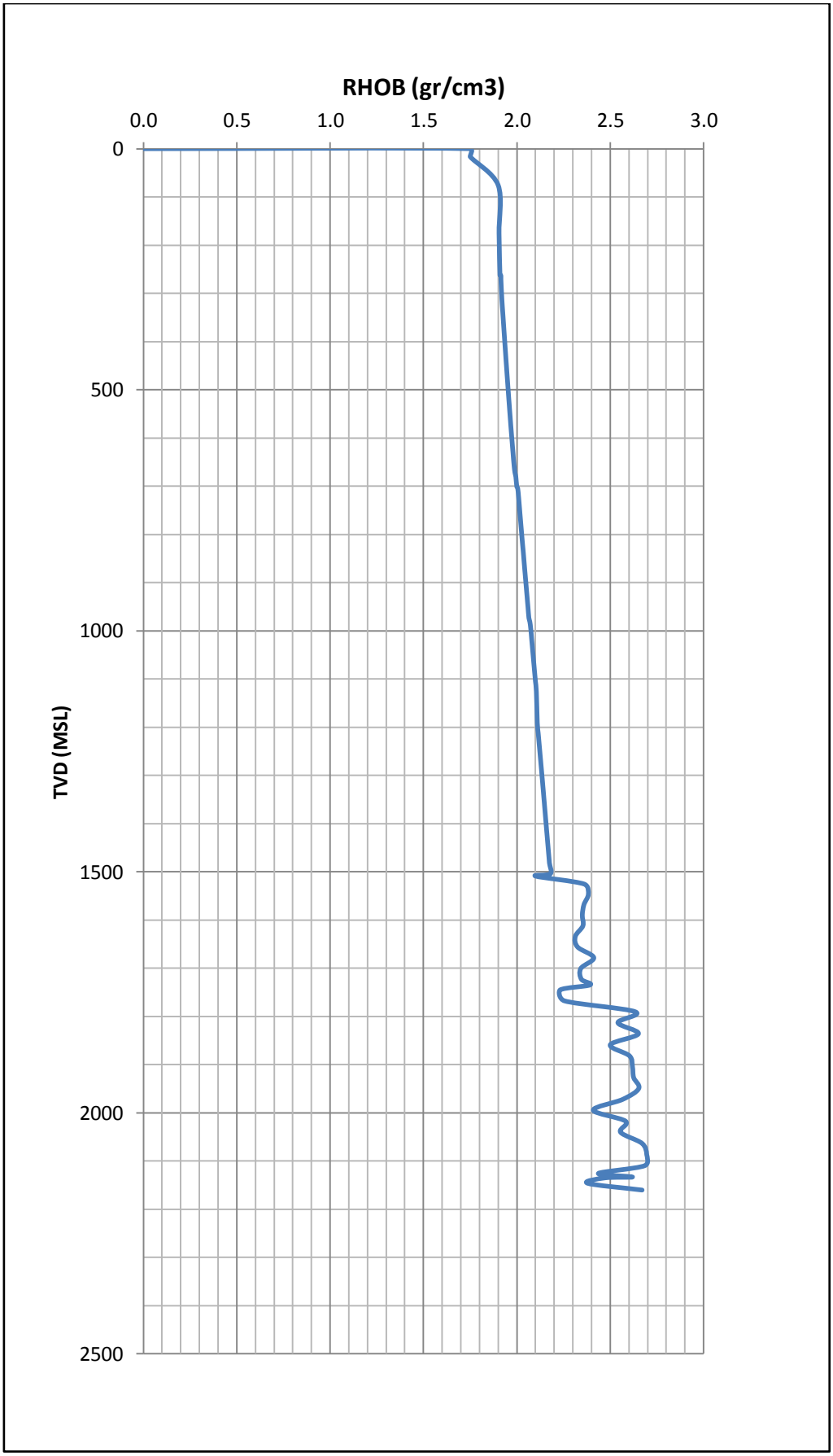

Figure 55 Density Profile Well T-2

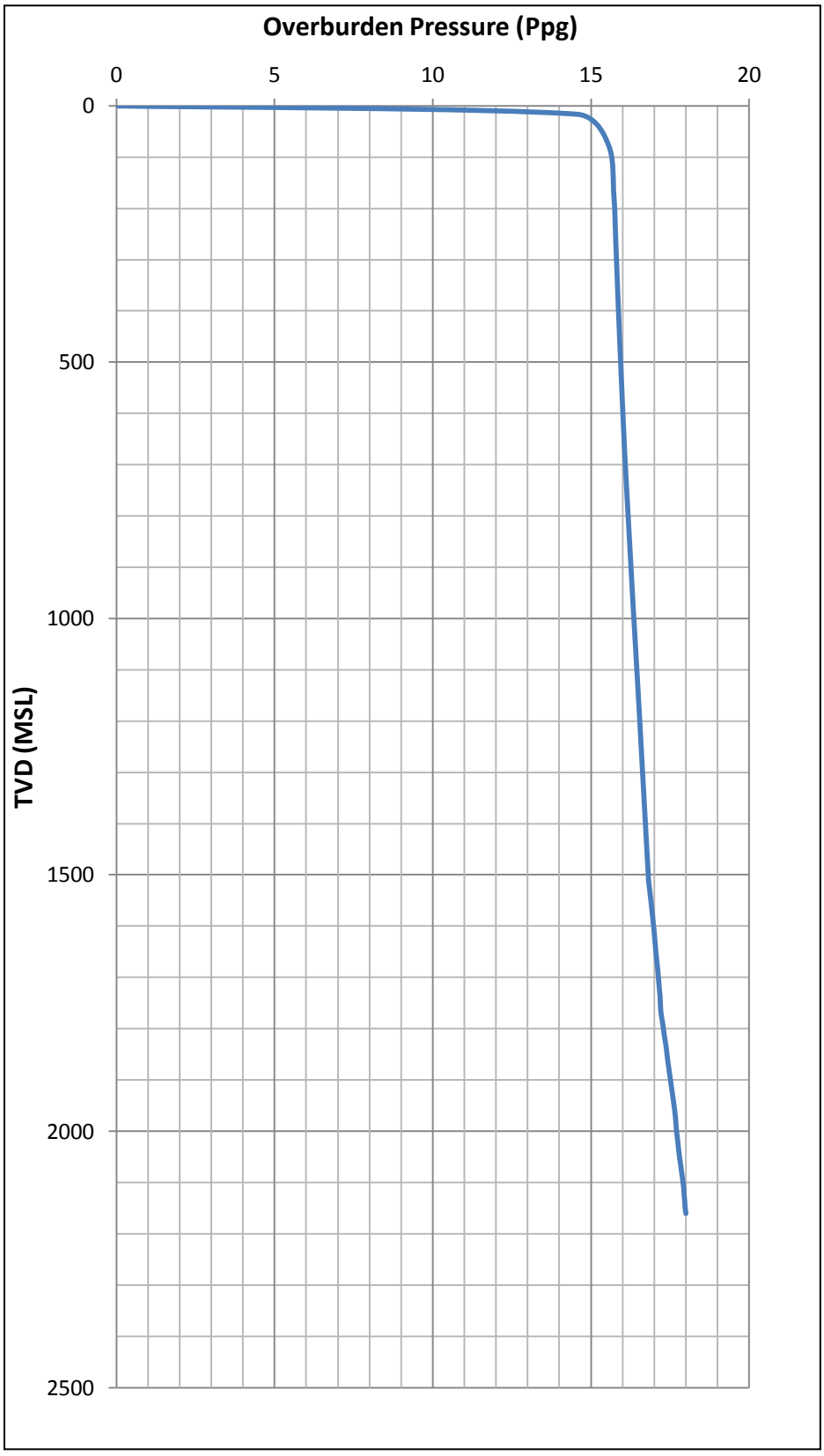

Figure 56 Overburden Pressure Profile Well T-2

From interval velocity data well T-2 and the other parameters so pore pressure for well T-2 can be estimated.

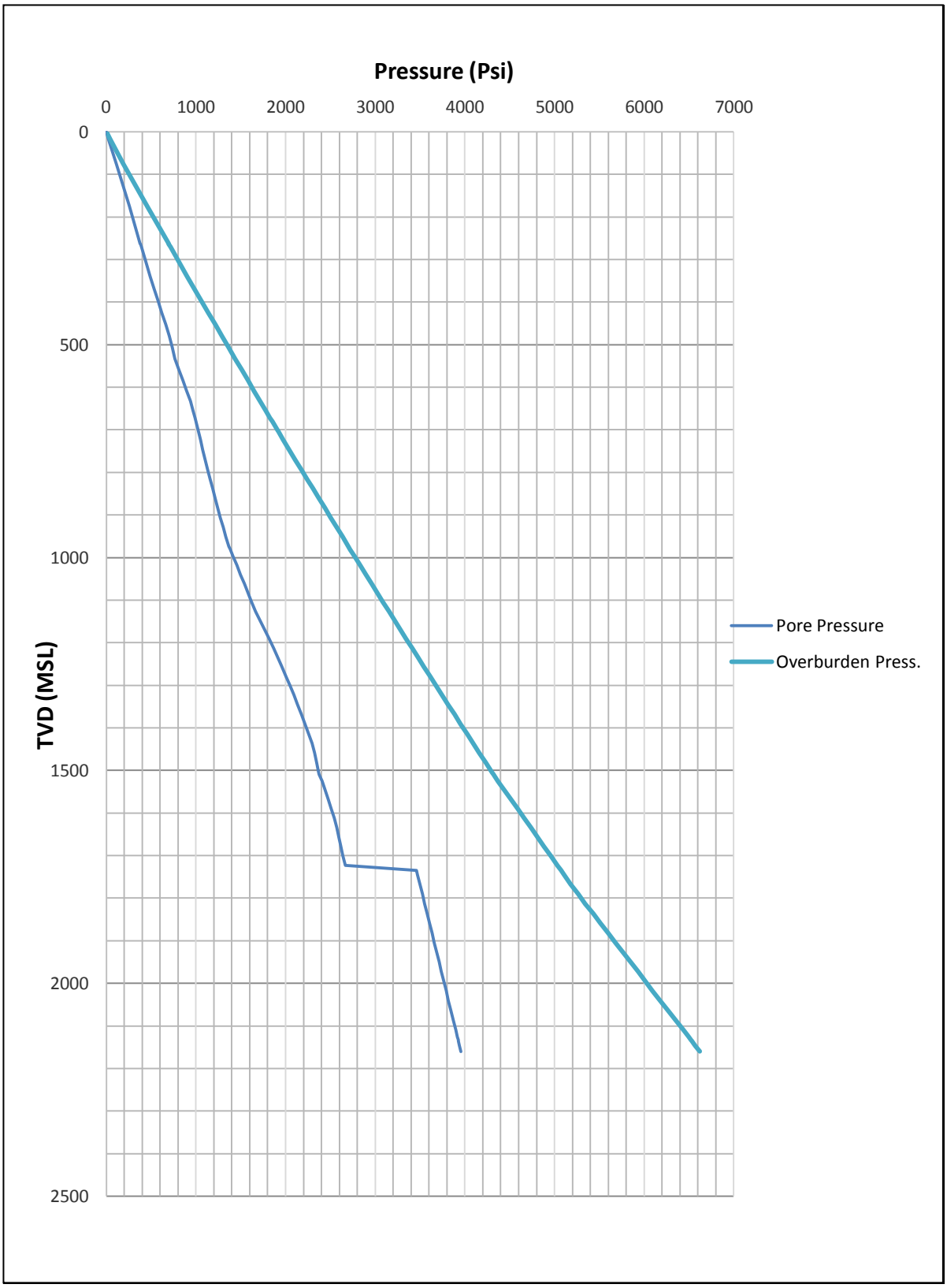

Figure 57 Pore Pressure Profile Well T-2

4.3 Fracture Pressure Calculation

In this study, fracture pressure is estimated using Tarzaghi equation.

$$FP = PP + \left[\left(\frac{\upsilon}{(1-\upsilon)}\right)(OBP - PP)\left(\frac{Vint}{Vnct}\right)^{N}\right] \quad (189)$$

Poisson ratio (υ) is estimated based on data from sonic velocity (V_p) and shear velocity (V_s). Because there is no shear velocity data (V_s) from well T-1 so shear velocity can be estimated using the relationship between sonic velocity and leak off test (LOT) data from well T-1.

Table 3 Synthetic Shear Velocity (Vs) from LOT

Depth	LOT	PP	HES	VES	HES/VES	poisson	Vp	Vs
MSL	Ppg	Ppg	Ppg	Ppg			m/s	m/s
750	12.162	8.689	3.473	7.733	0.449	0.310	2097.489	1100.858
1665	12.562	9.327	3.234	7.632	0.424	0.298	3198.973	1717.078

From 2 points LOT above and then Vp and Vs is plotted to get the relationship equation and to get synthetic shear velocity (Vs) from surface to depth of interest.

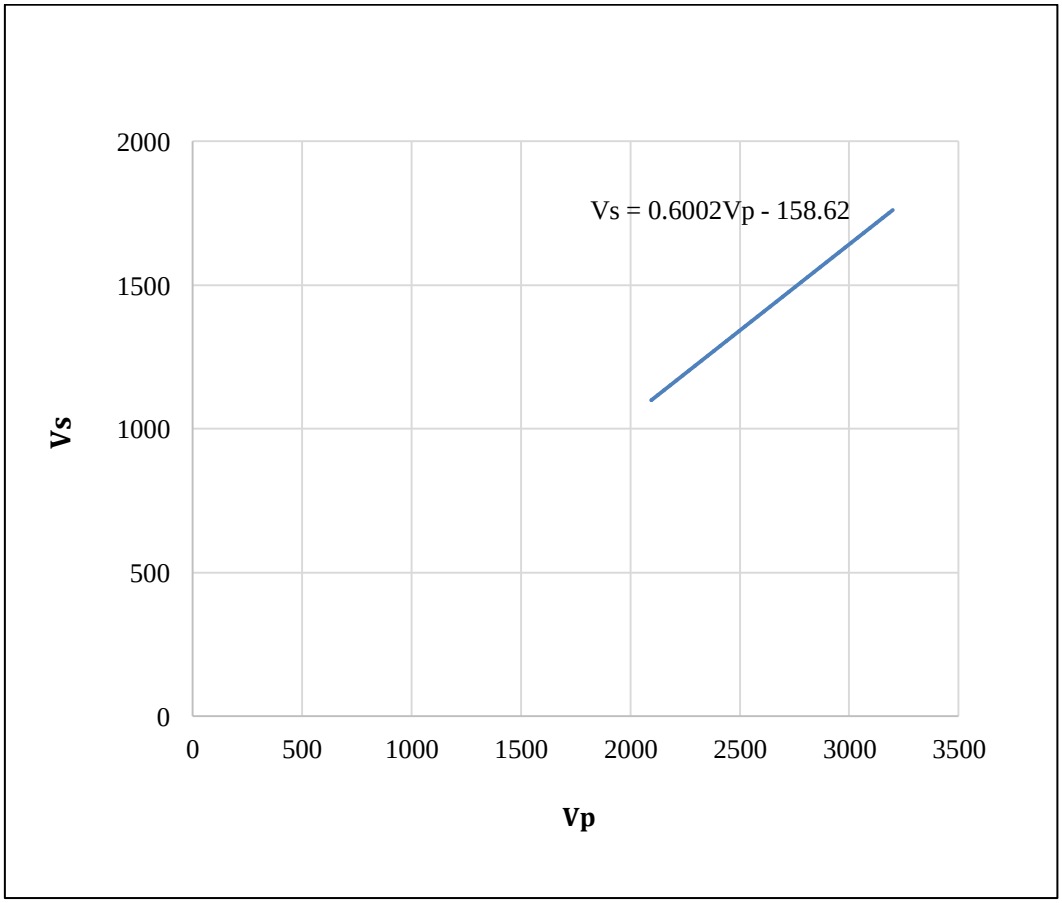

Figure 58 Shear Velocity from Data LOT Well T-1

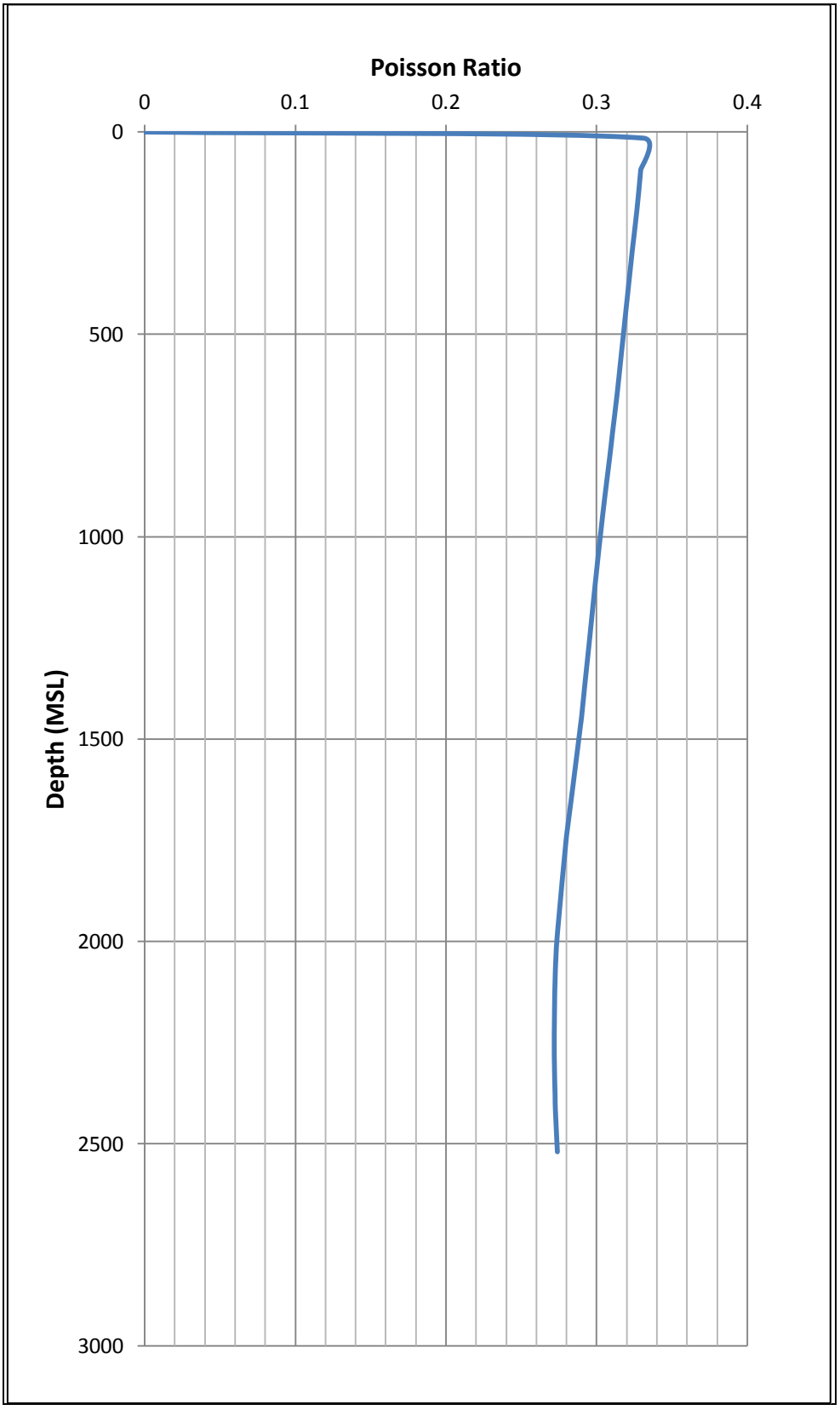

Figure 59 Poisson Ratio Well T-1

From poisson's ratio data and data from the previous calculation, fracture pressure can be estimated using Tarzaghi equation.

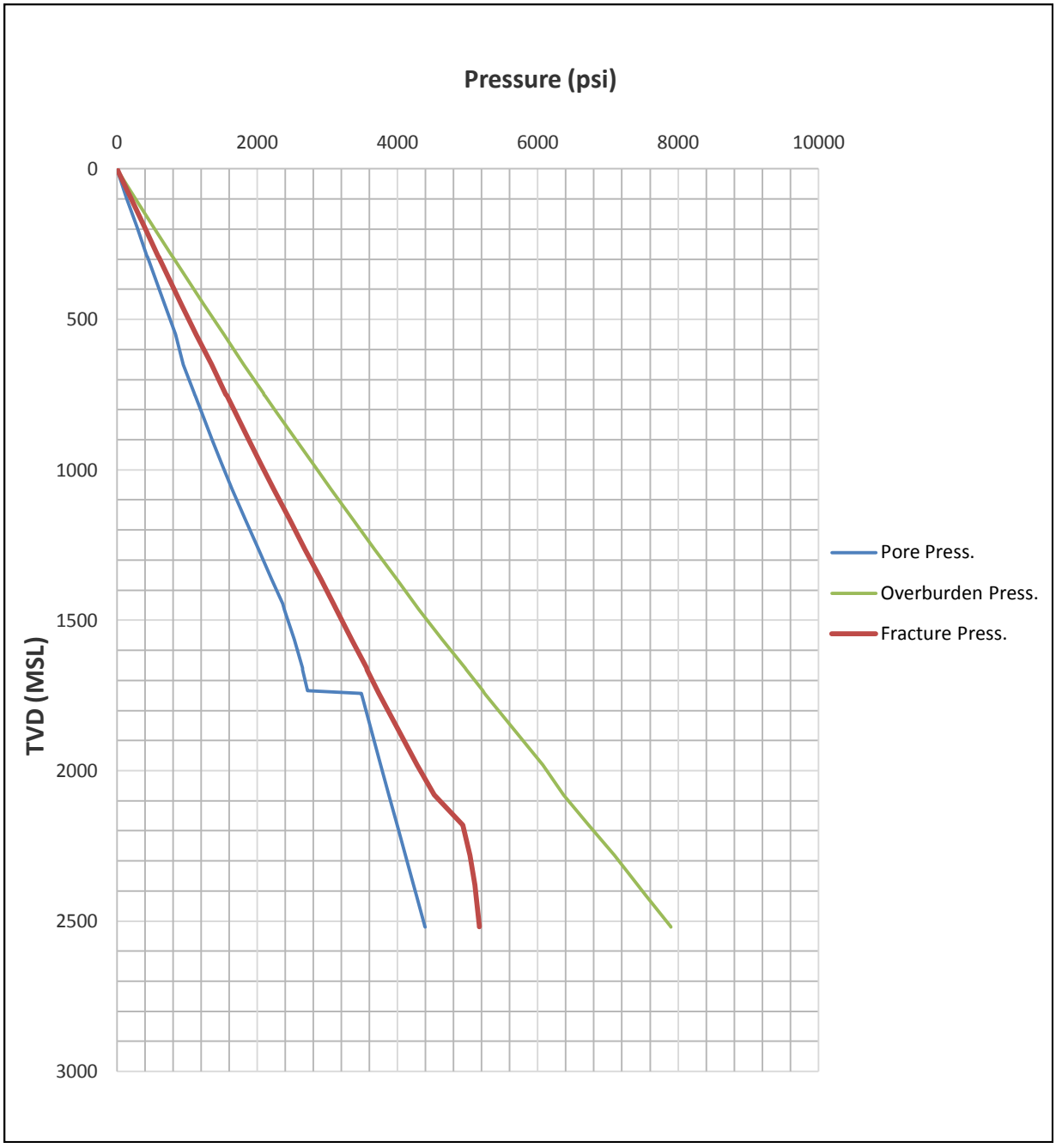

Figure 60 Fracture Pressure Profile Well T-1

With the same procedure, using poisson's ratio data from well T-1 and then can be estimated fracture pressure for directional well T-2.

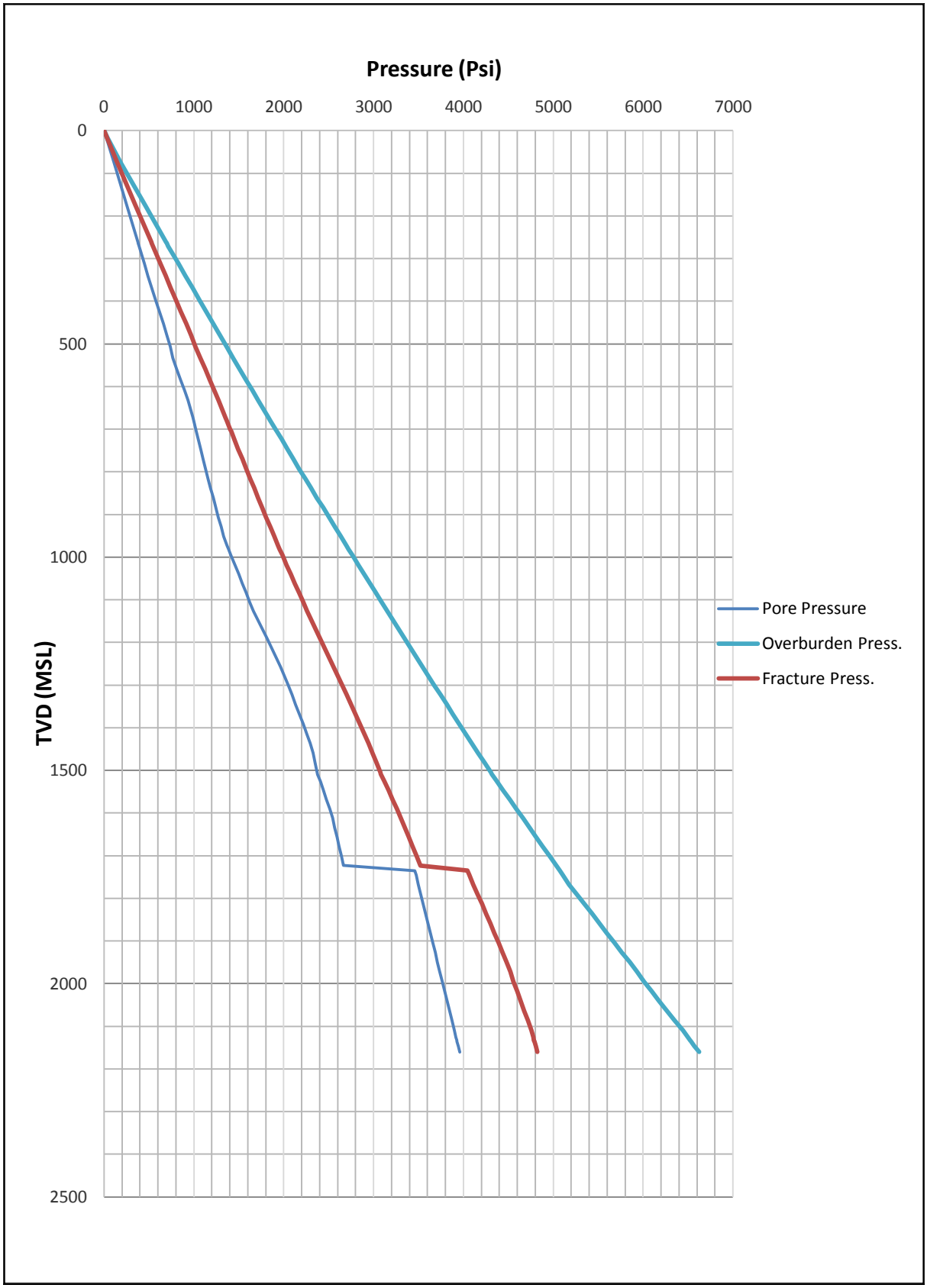

Figure 61 Fracture Pressure Profile Well T-2

4.4 Rock Mechanic and Insitu Stress Calculation

To calculate rock mechanics properties like cohesive strength (S_0), unconfined compressive strength (UCS), angle of friction, etc., it is important to know about the type of rock formation (shale, sand or limestone). The type of rock formation can be known from gamma-ray log and it can be corrected with drilling cutting. In this calculation, it is used logging data like gamma-ray log and sonic log to determine rock mechanics properties.

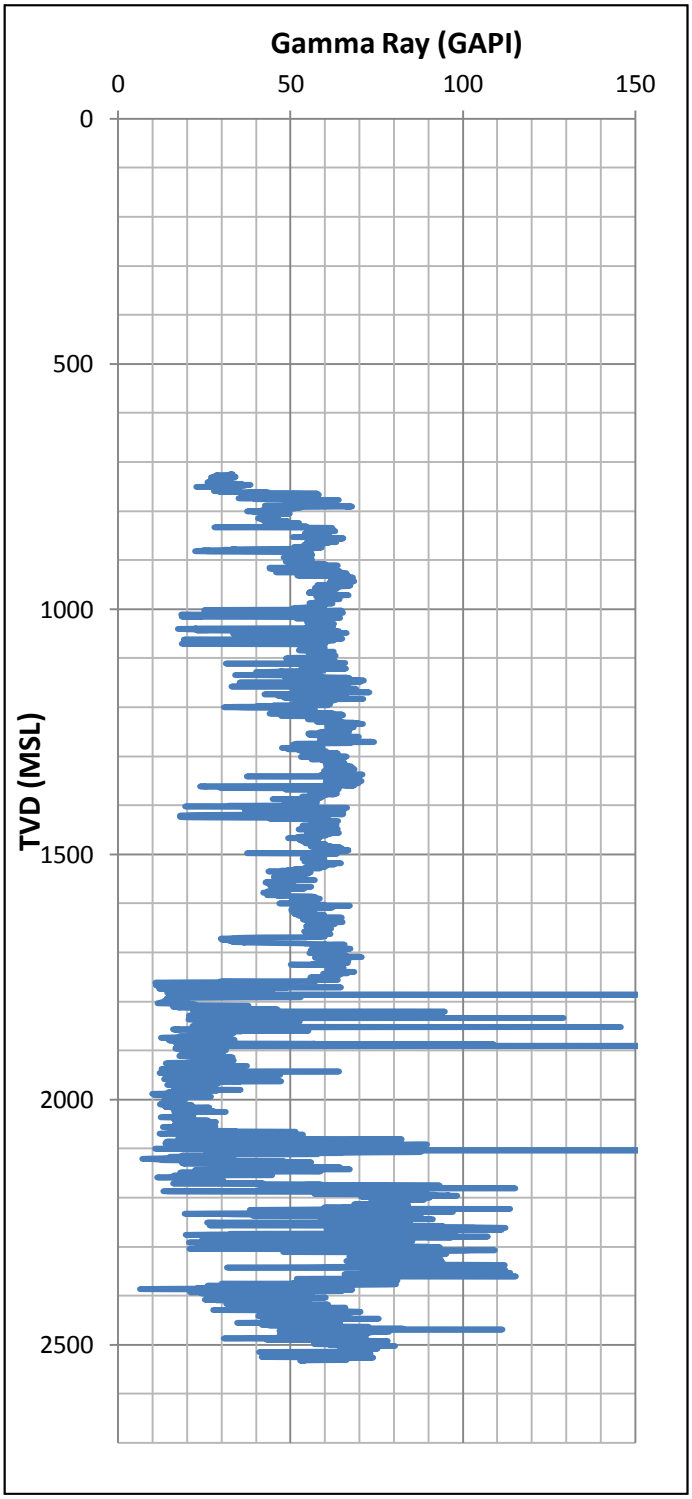

Figure 62 Gamma Ray Log from Well T-1

Unconfined compressive strength (UCS) is determined using empirical equation based on type of rock. Horsrud's equation is used to determine UCS in shale formation. Mc Nally's equation is used to determine UCS in sandstone formation. Militzer's equation is used to determine UCS in limestone formation.

The other rock mechanic properties is angle of internal friction (μ). These properties are calculated using Chang and Zoback equation. After UCS and μ are calculated, cohesive strength (S_0) can be calculated. Sonic logging data from well T-1 is used to estimate rock mechanic properties in well T-2. The results of these calculation can be seen in the figure below:

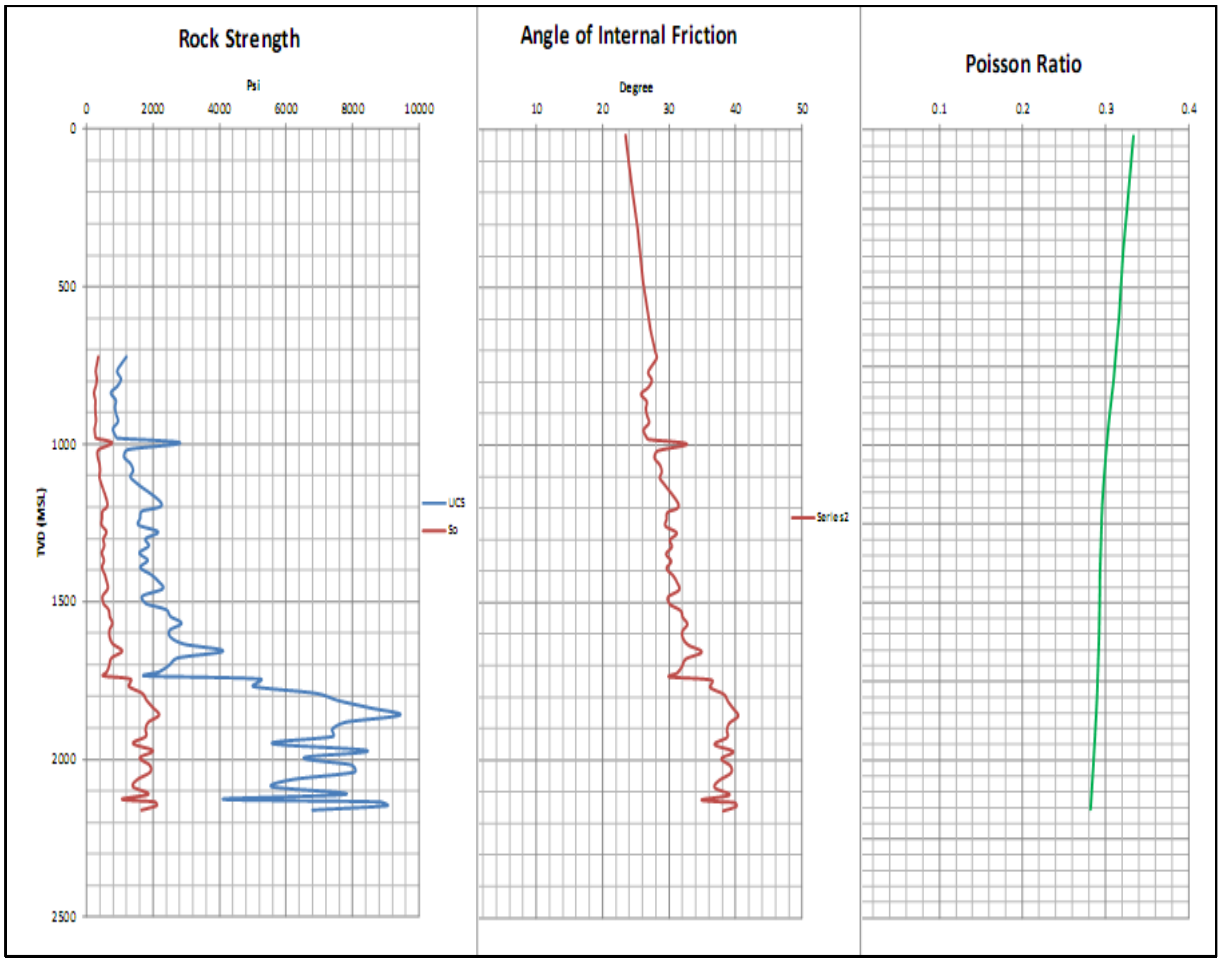

Figure 63 Estimation Rock Mechanics Properties Well T-2

4.5 Insitu Stress Calculation

Insitu stress consists of vertical stress (σ_v), minimum horizontal stress (σ_h) and maximum horizontal stress (σ_H). Vertical stress (σ_v) is same with overburden stress and can be calculated from the density log. Minimum horizontal stress (σ_h) can be estimated using Zoback and Healy equation. Maximum horizontal stress (σ_H) can be estimated using Zoback equation with assumption $\sigma^{\Delta T} = 0$ and $\theta_b = 90^0$, it means that in this case to prevent breakout happen during drilling. From this calculation, σ_H is plotted together with σ_h and σ_v.

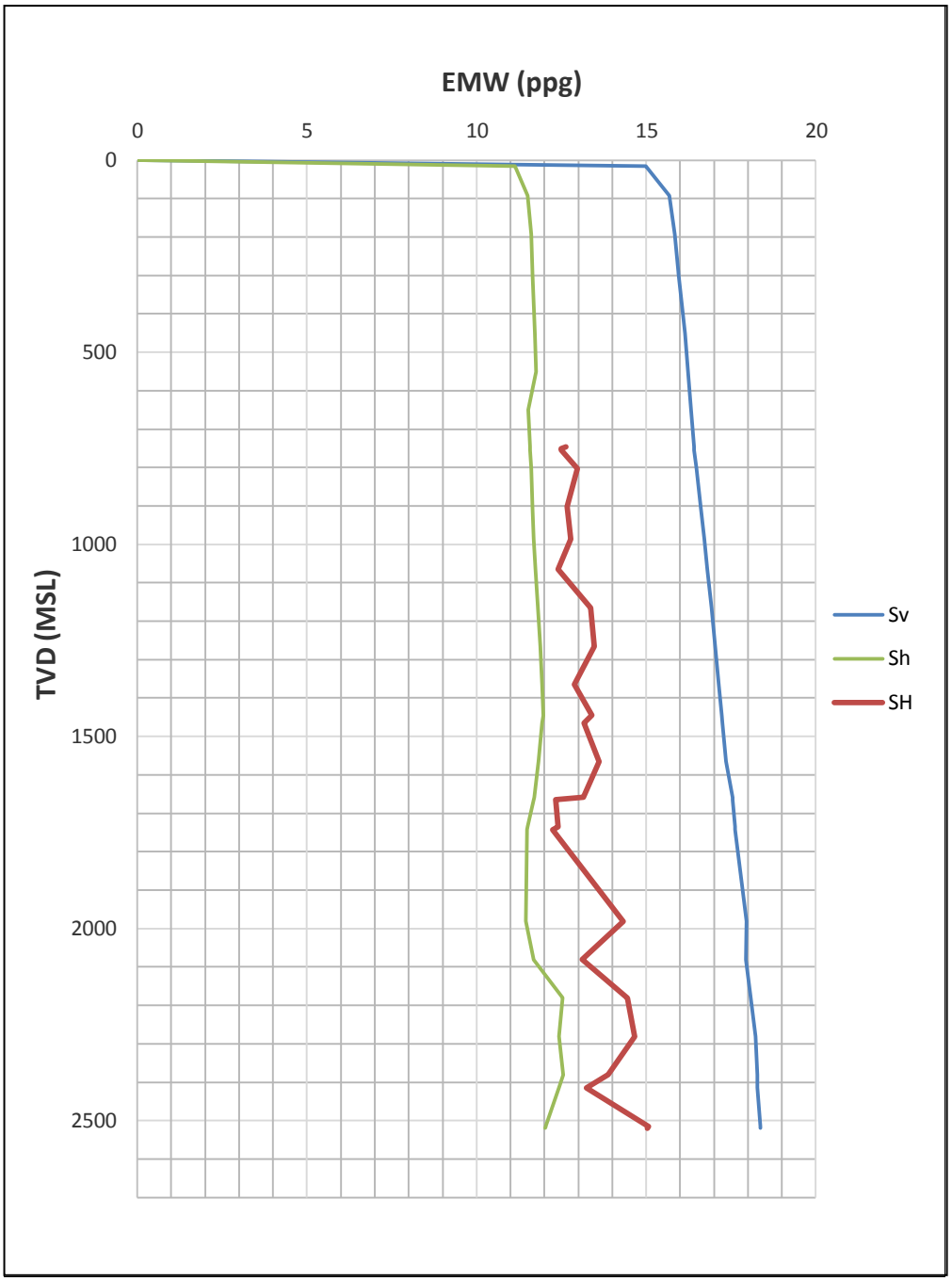

Figure 64 Insitu Stress Well T-1

Maximum horizontal stress (σ_H) from figure above also can be estimated using relationship ratio σ_H / σ_h and choose the biggest ratio σ_H / σ_h to make the value of σ_H become smoothly. This method is chosen because the biggest ratio σ_H / σ_h will give the worst case scenario during wellbore collapse failure criteria. From calculation ratio σ_H / σ_h, it is obtained σ_H = 1.25 σ_h. This value is plotted again with the other value insitu stress and convert these value into equivalent mud weight (EMW) in pound per gallon (ppg).

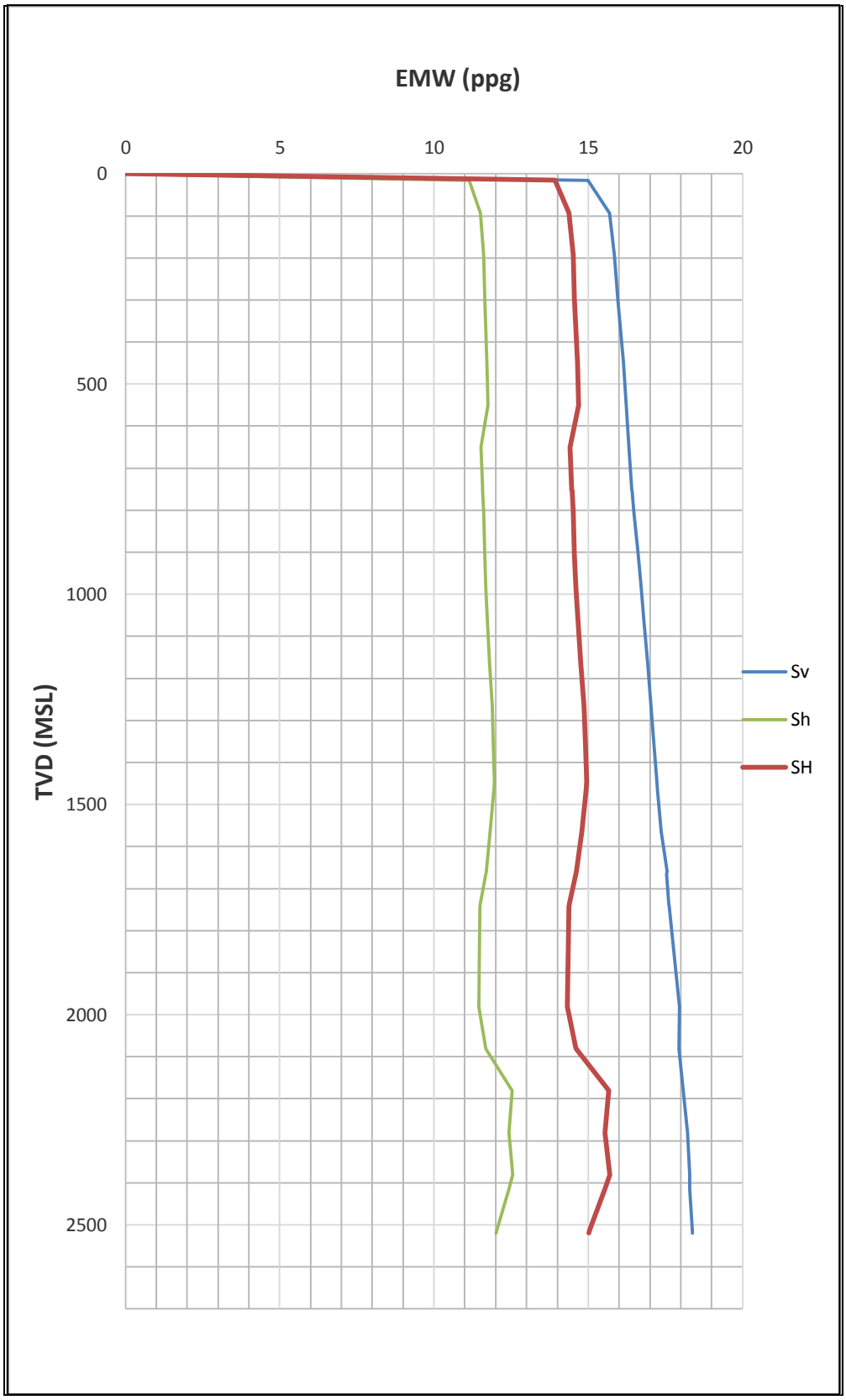

Figure 65 Corrected Insitu Stress Well T-1

The same procedure is used to calculate insitu stress for directional well T-2.

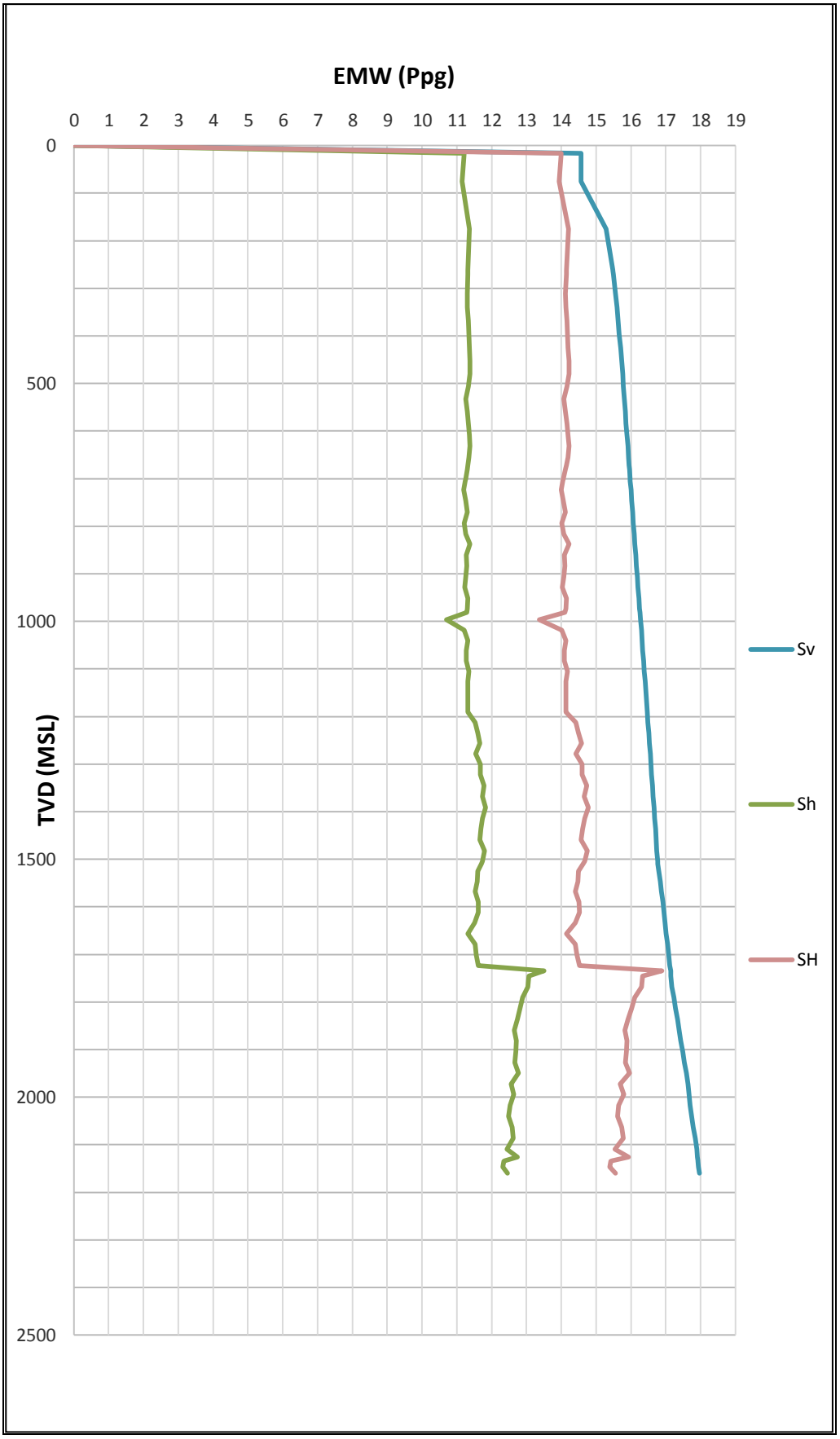

Figure 66 Insitu Stress Well T-2

4.6 Wellbore Collapse Calculation

Wellbore collapse happens when borehole wall under compression. Because wellbore takes any orientation so it needs to transform stress distribution into the new cartesian coordinate system (x, y, z). The new stress stresses transformation become σ_x, σ_y, σ_z. From these cartesian stresses and then it can be estimated stress around the borehole wall (σ_a, σ_r, σ_θ).

As wellbore failure condition is governed by the principal stresses so it needs to define three principal stresses (σ_1, σ_2, σ_3). From these three principal stress, wellbore collapse can be predicted. In this study will evaluate wellbore collapse failure criteria using three different methods, they are Mohr-Coulomb, Modified Lade and Stassi D' Alia. To prevent wellbore collapse, drilling activity should use mud weight greater than wellbore collapse equivalent mud weight. By knowing the wellbore collapse parameter, drilling problems related to wellbore instability can be avoided.

4.6.1. Wellbore Collapse Pressure Prediction Using Mohr Coulomb

Mohr Coulomb only involves two principal stresses, they are maximum principal stress (σ_1) and minimum principal stress (σ_2). In this calculation are used one exploration well which is vertical well (well T-1) and one directional well (well T-2). The figure below is the estimation of wellbore collapse using this method.

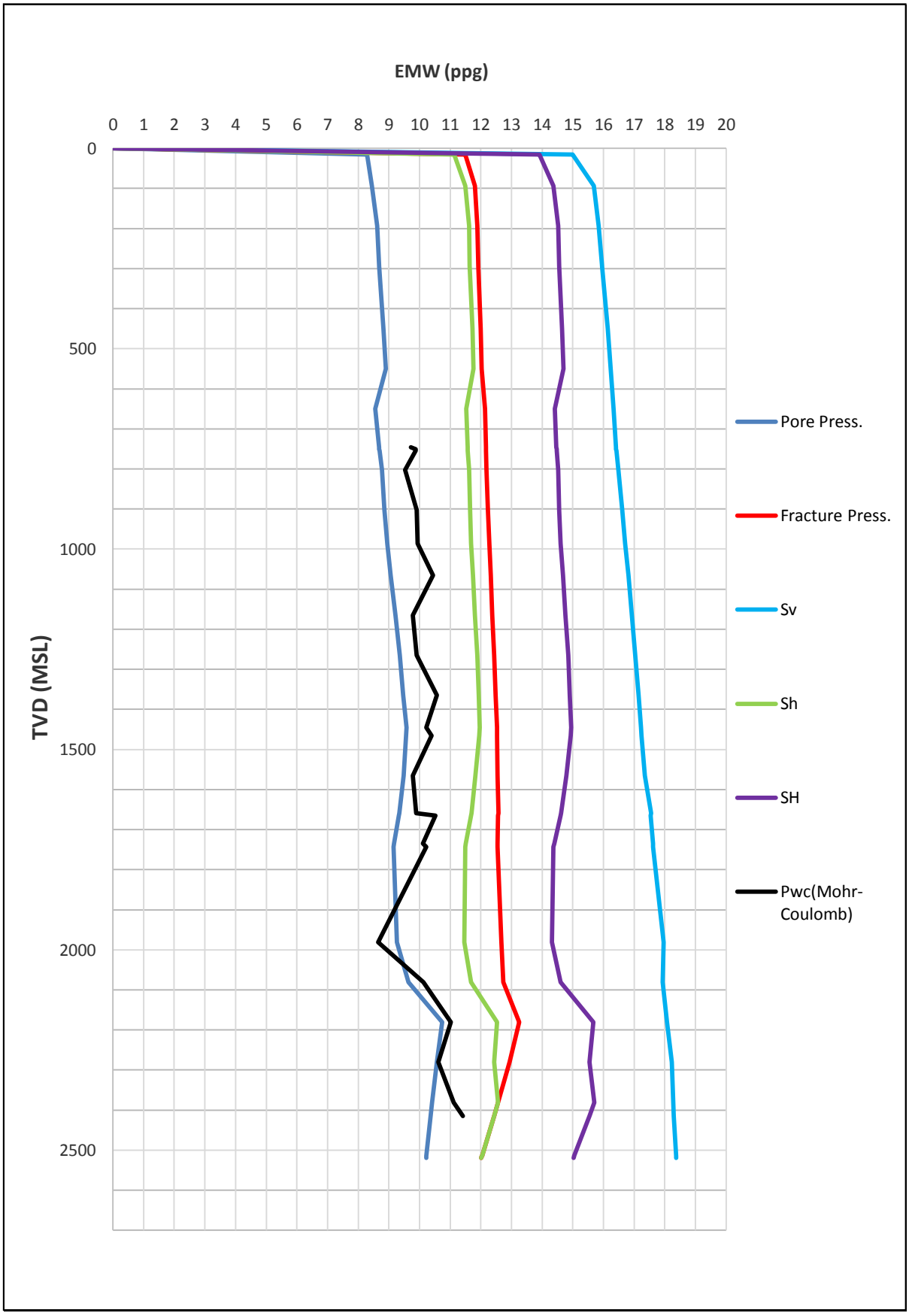

Figure 67 Mohr-Coulomb Collapse Pressure Well T-1

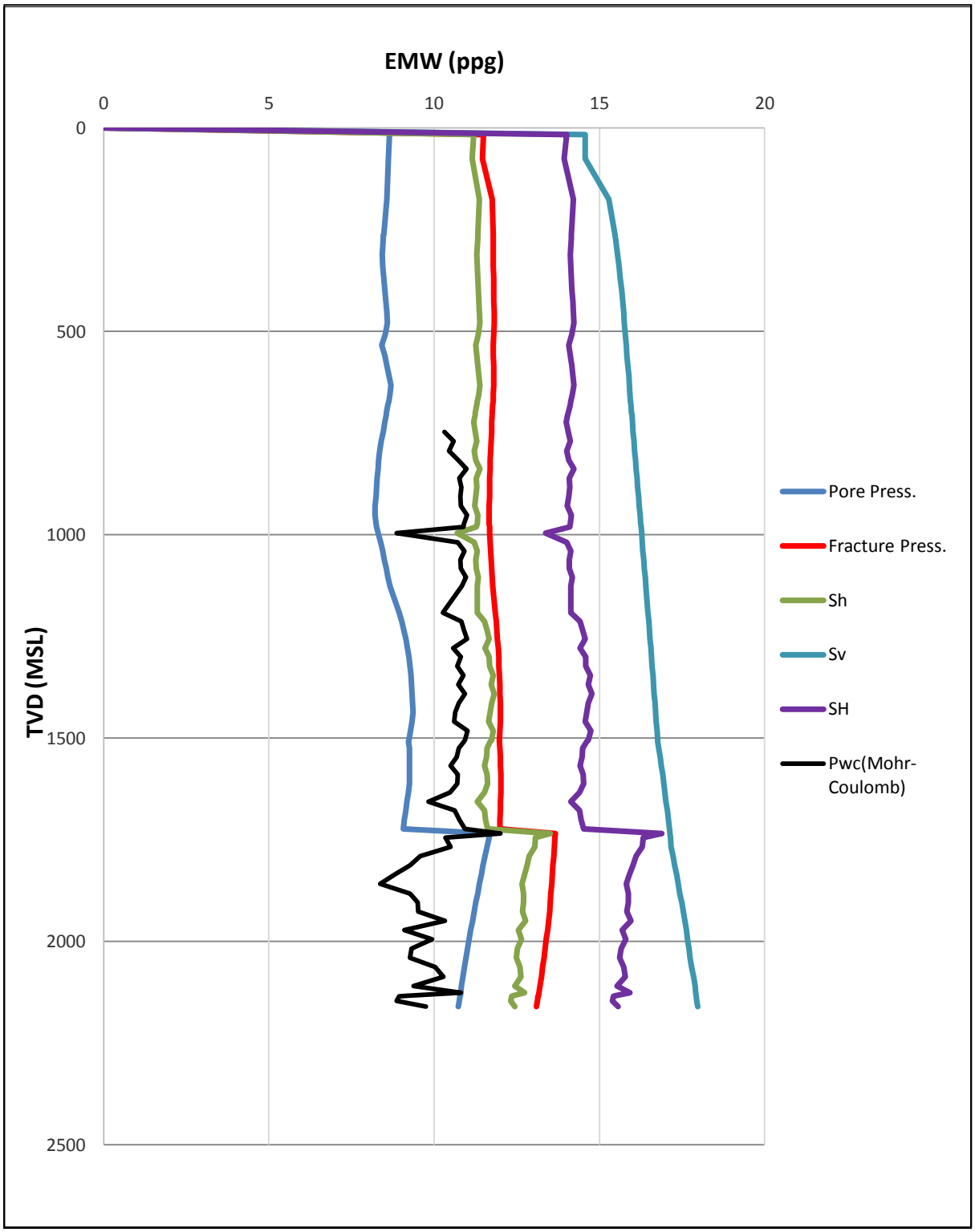

Figure 68 Mohr-Coulomb Collapse Pressure Well T-2

4.6.2. Wellbore Collapse Pressure Prediction Using Modified Lade

In Modified Lade, it involves three principal stress to calculate wellbore collapse. They are σ_1, σ_2 and σ_3. Modified Lade assumes that there is communication between wellbore and formation, it means that there is stable mud cake between this boundary. The results of collapse pressure formation to prevent well failure can be seen in the figure below.

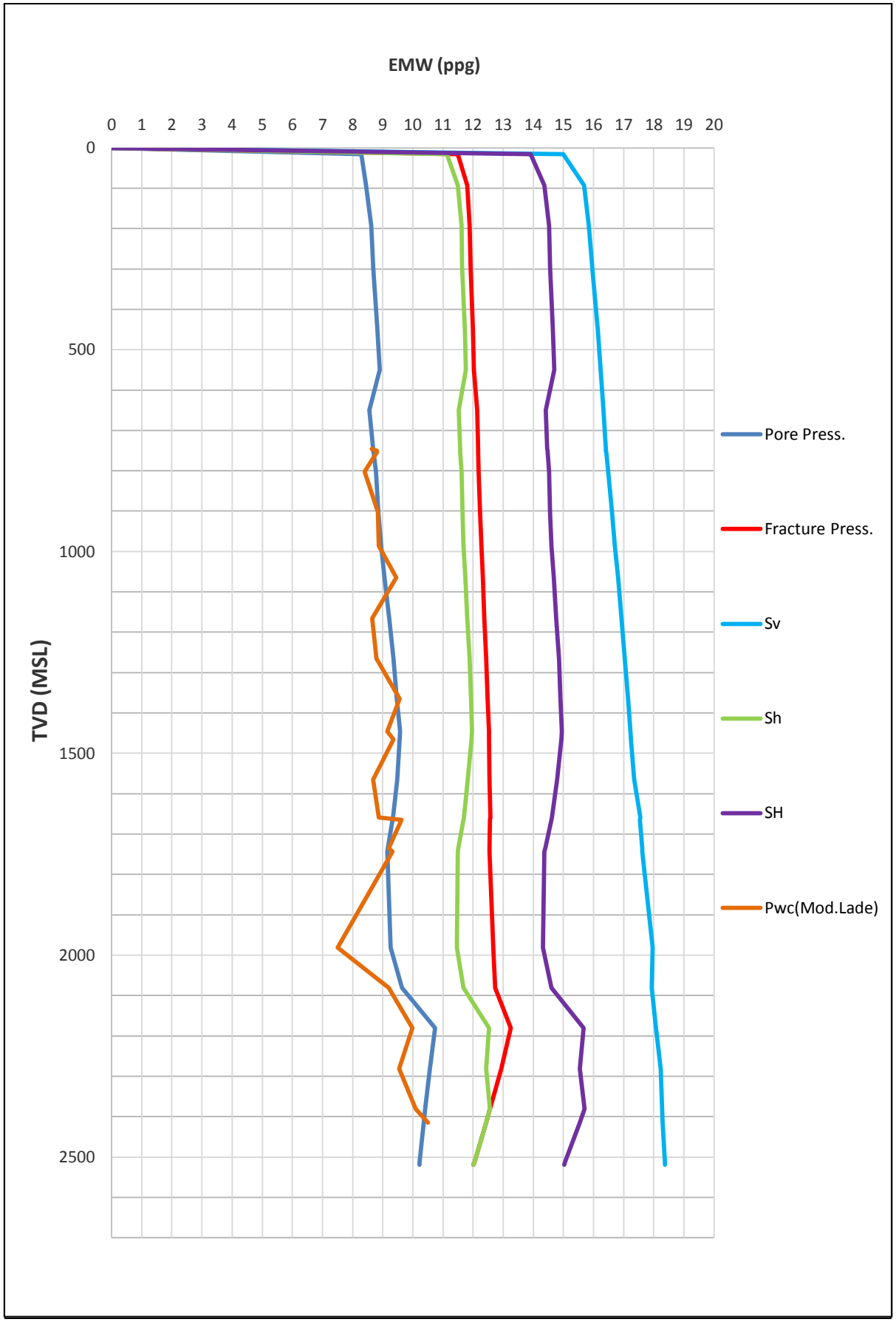

Figure 69 Modified Lade Collapse Pressure Well T-1

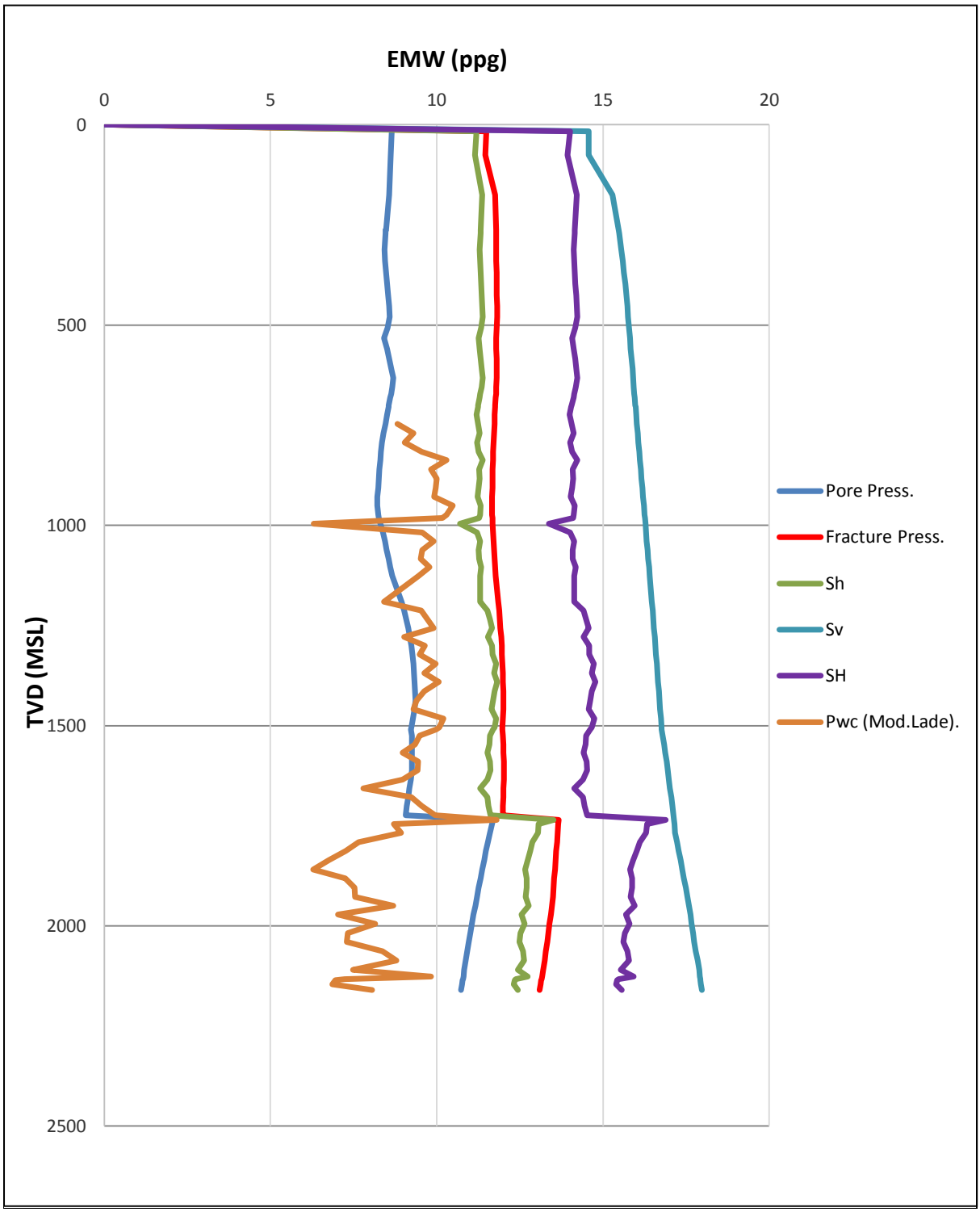

Figure 70 Modified Lade Collapse Pressure Well T-2

4.6.3. Wellbore Collapse Pressure Prediction Using Stassi D' Alia

Beside three principal stresses, Stassi D' Alia also uses uniaxial compressive strength (C_0) and tensile strength (T_0) in his calculation to predict wellbore failure criteria. The result calculation of wellbore collapse pressure from these well can be seen in the figure below :

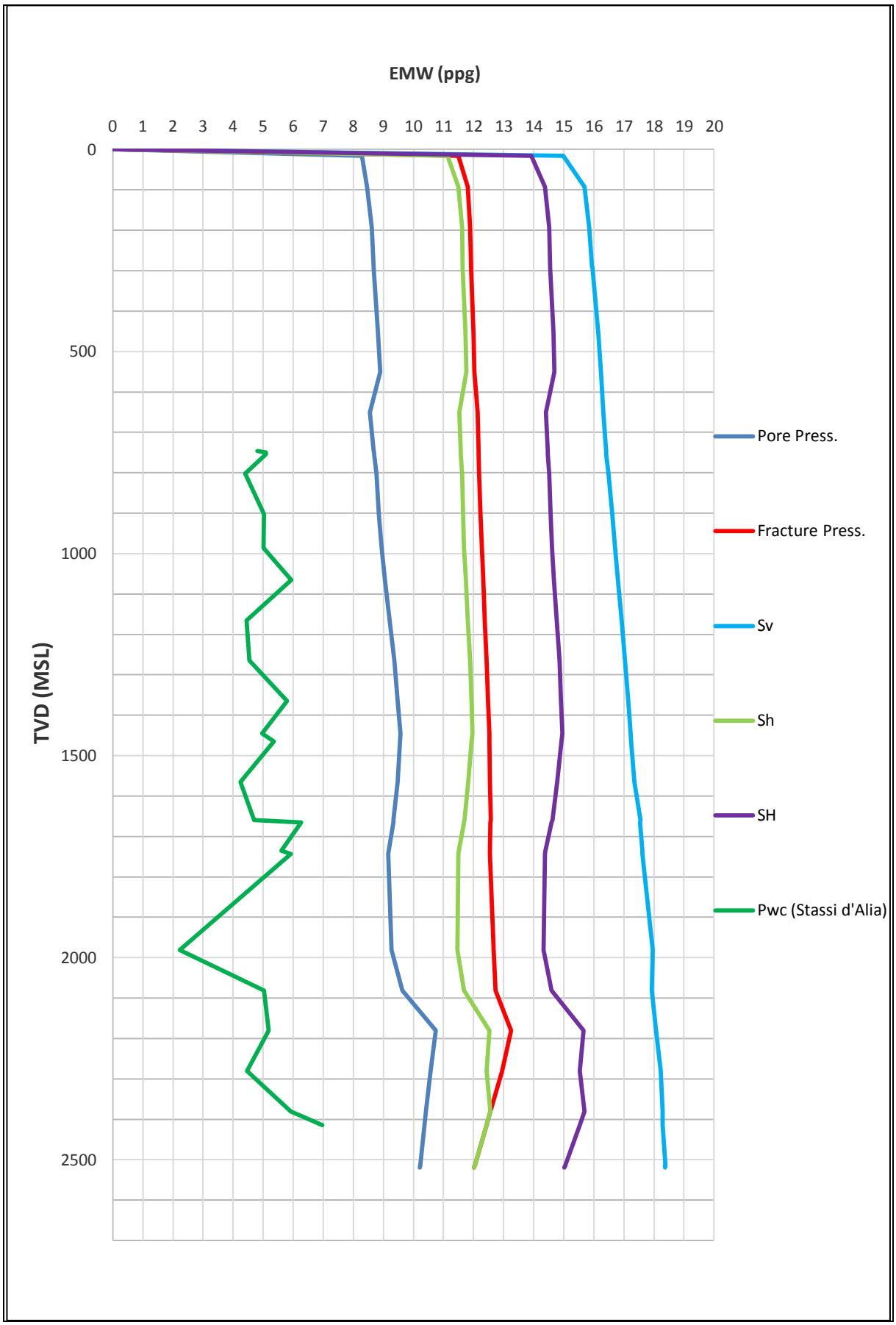

Figure 71 Stassi d' Alia Collapse Pressure Well T-1

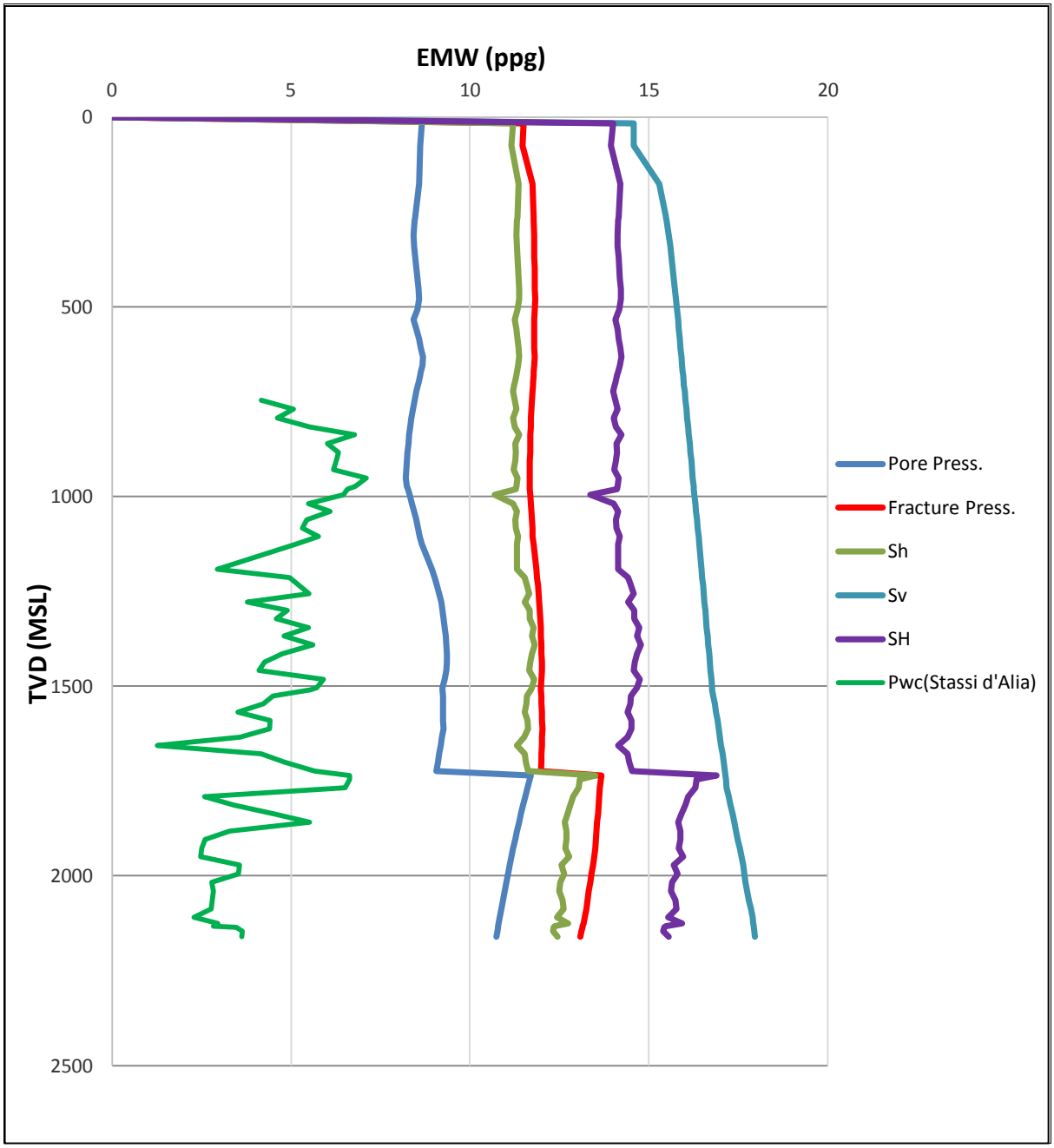

Figure 72 Stassi D' Alia Collapse Pressure Well T-2

4.7 Sensitivity Analysis in Wellbore Collapse Pressure

In this topic will analyze the impact of inclination, unconfined compressive strength (UCS) and horizontal stresses in wellbore collapse pressure using Mohr-Coulomb, Modified Lade and Stassi d' Alia methods. This is the input data that used to do the sensitivity analysis.

Table 4 Input Data Sensitivity Analysis

TVD	Azimuth	PP	ν	φ	μ	UCS	S_0	σ_v	σ_H	σ_h
MSL	Degree	Psi				Psi	Psi	Psi	Psi	Psi
1482	238.1	2348.5	0.29	29.81	0.573	1678	486.2	4233	3726.6	2981.3

4.7.1. Sensitivity Analysis toward Inclination

Data from data from tabel 3 is used to do sensitivity analysis toward inclination from 0 degrees to 90 degrees. These results of the calculation can be seen in the figure below :

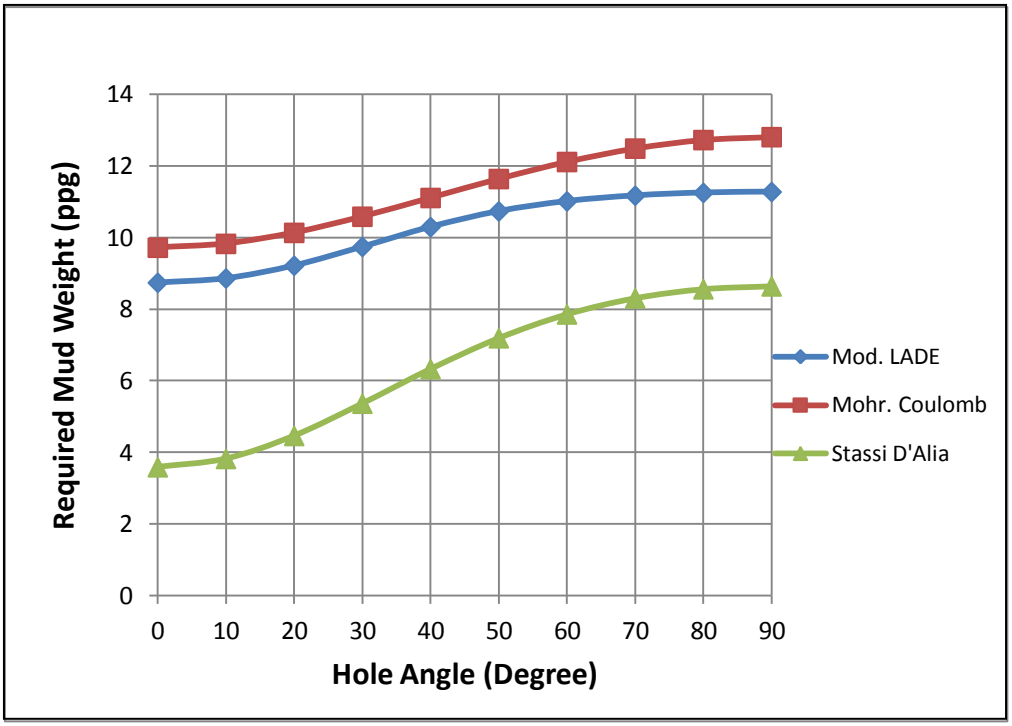

Figure 73 Well Failure Sensitivity Analysis toward Inclination

4.7.2. Sensitivity Analysis toward UCS

Data from table 3 with Inclination 20 degree is used to predict wellbore shear failure toward unconfined compressive strength (UCS) from 0 Mpa to 50 Mpa. The results of this calculation can be seen in the figure below:

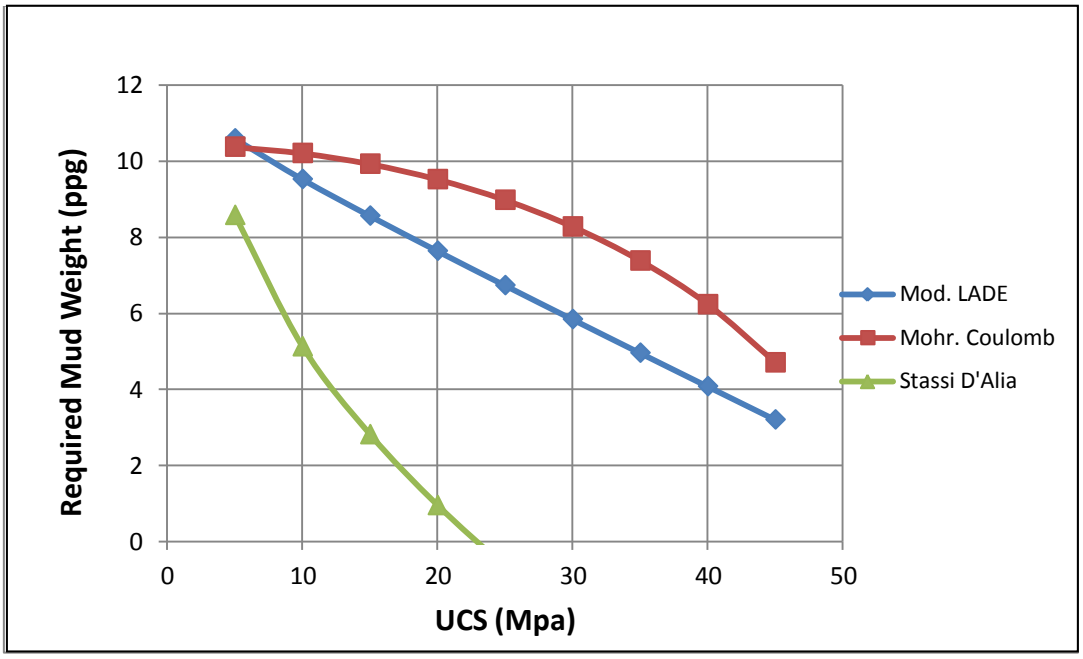

Figure 74 Well Failure Sensitivity Analysis toward UCS

4.7.3. Sensitivity Analysis in Relaxed Basin toward Horizontal Stresses

Data from table 3 with inclination 20 degree in hole angle are used to calculate wellbore collapse pressure. Firstly, the sensitivity is done toward $\sigma_H = \sigma_h = 2981.3$ psi up to $\sigma_H = \sigma v = 4233$ psi. The results of this sensitivity toward maximum horizontal stress can be seen in the figure below:

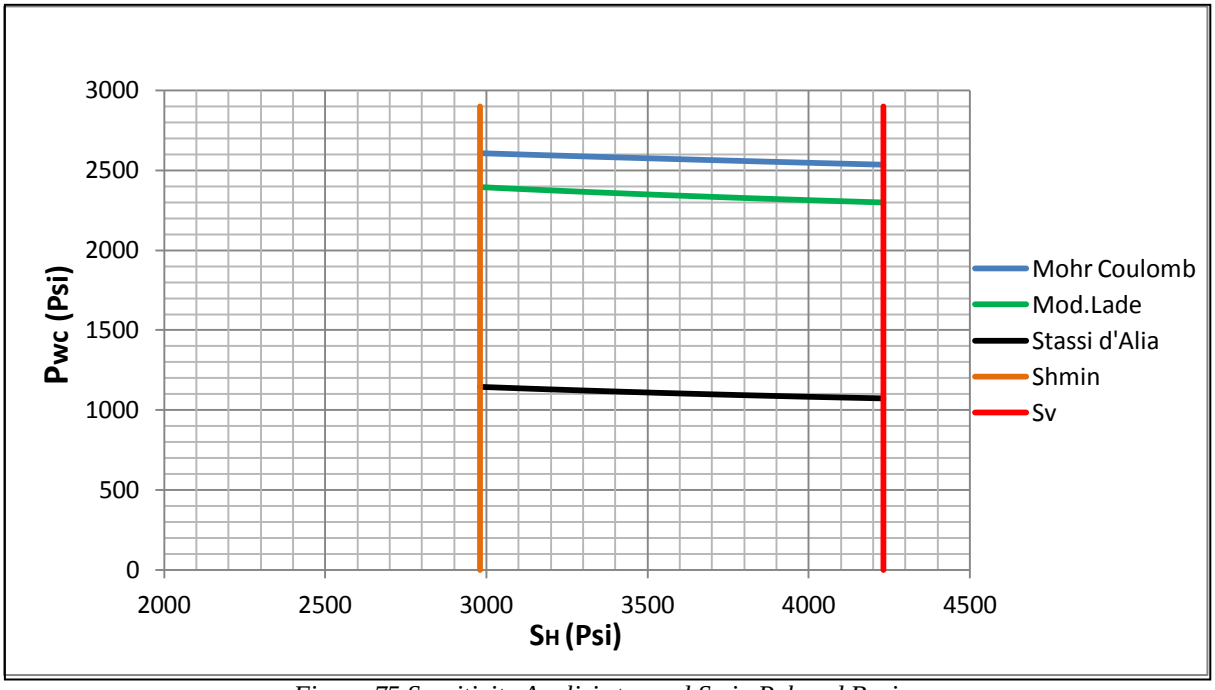

Figure 75 Sensitivity Analisis toward S_H in Relaxed Basin

Secondly, the sensitivity analysis will be done toward $\sigma_h = 2981.3$ psi up to $\sigma_h = \sigma_H = 3726.6$ psi. The result of this calculation can be seen in the figure below:

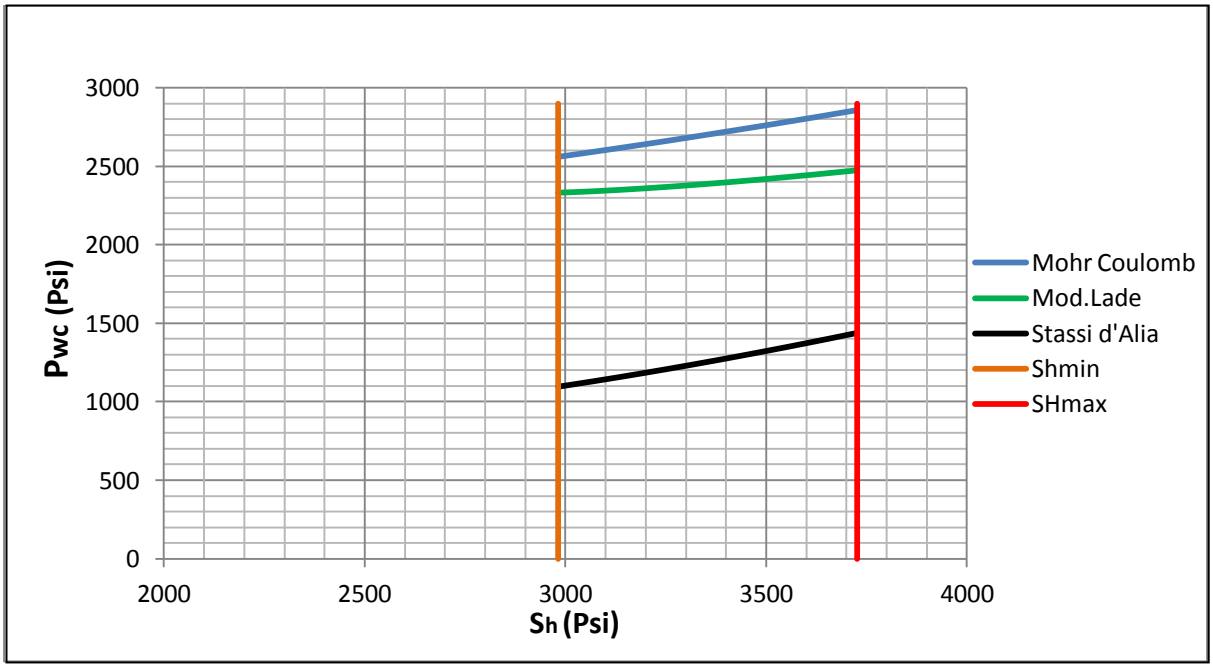

Figure 76 Sensitivity Analisis toward S_h in Relaxed Basin

4.7.4. Sensitivity Analysis in Tectonically Basin toward Horizontal Stresses

Table 5 Input Data Sensitivity Analysis in Tectonically Basin

Azimuth	PP	v	φ	μ	UCS	S_0	σ_v	σ_H	σ_h
Degree	Psi				Psi	Psi	Psi	Psi	Psi
238.1	2348.5	0.29	29.81	0.573	1678	486.2	2981.3	4233	2981.3

Data from table 4 with inclination 20 degree are used to do sensitivity. The procedure analysis toward horizontal stresses are same with sensitivity analysis in relaxed basin. Firstly, the sensitivity is done toward $\sigma_H = \sigma_h = 2981.3$ psi up to $\sigma_H = 4233$ psi. The results of this sensitivity toward maximum horizontal stress can be seen in the figure below:

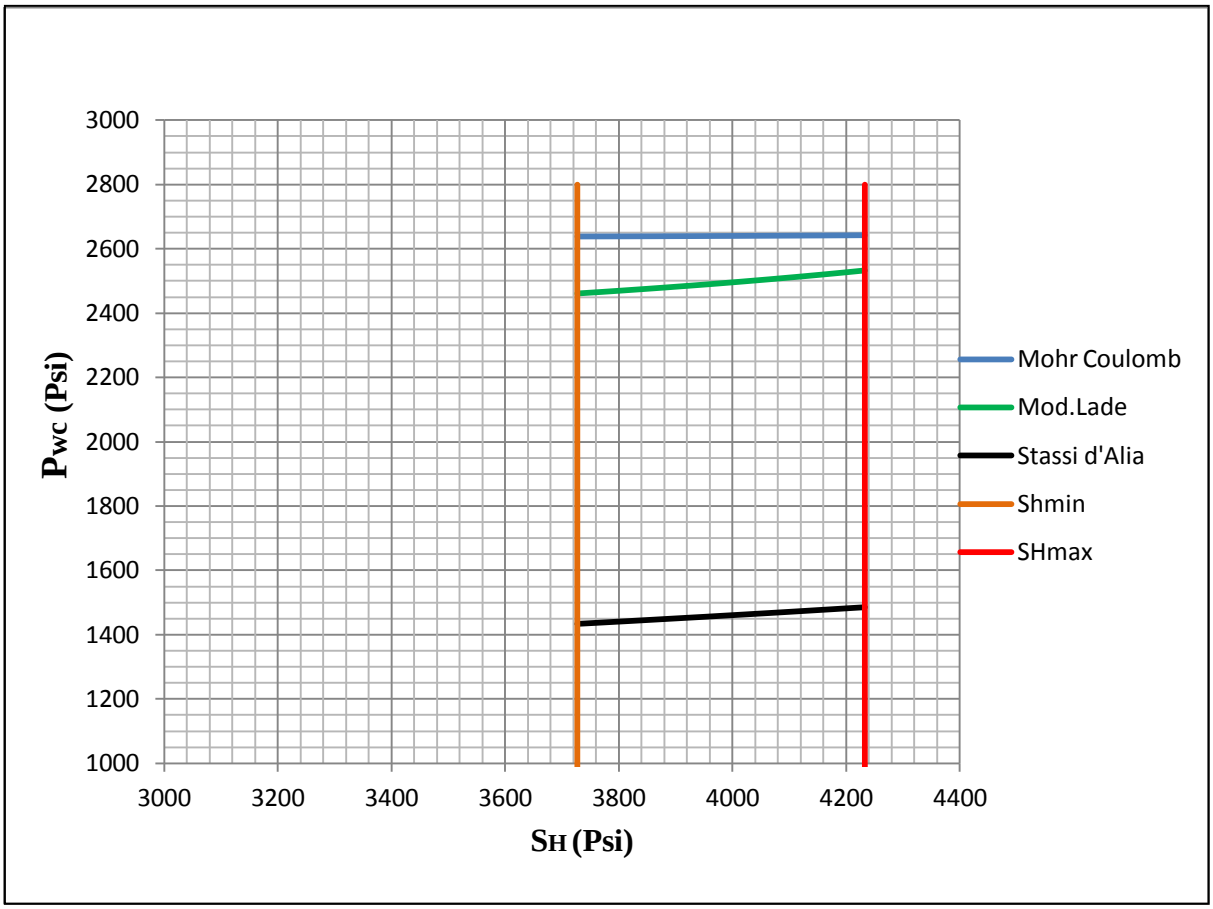

Figure 77 Sensitivity Analisis toward S_h in Relaxed Basin

Secondly, the sensitivity analysis will be done toward $\sigma_h = 3726.6$ psi up to $\sigma_h = \sigma_H = 4233$ psi. The result of this calculation can be seen in the figure below:

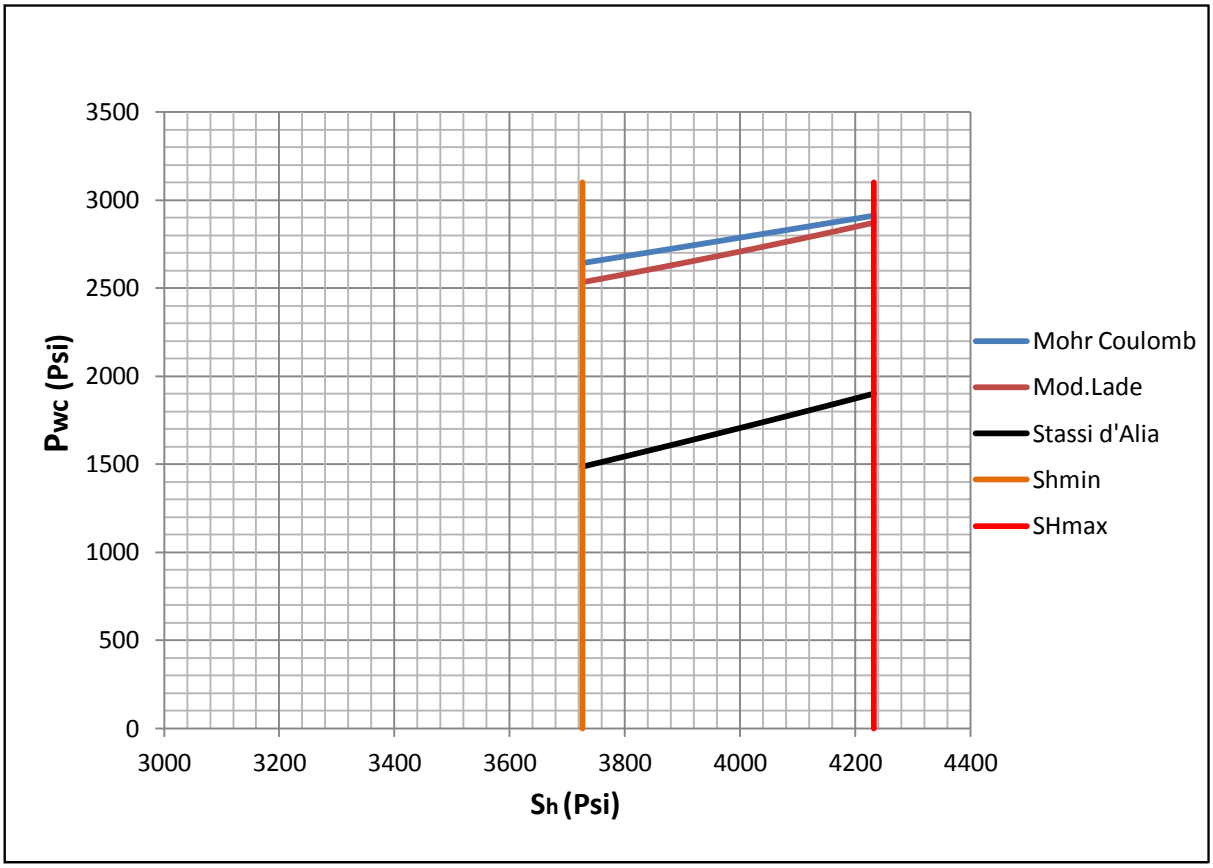

Figure 78 Well Failure Sensitivity Analysis toward Horizontal Stresses

4.8 Casing Design

The well schematic for well T-2 can be seen in the figure below:

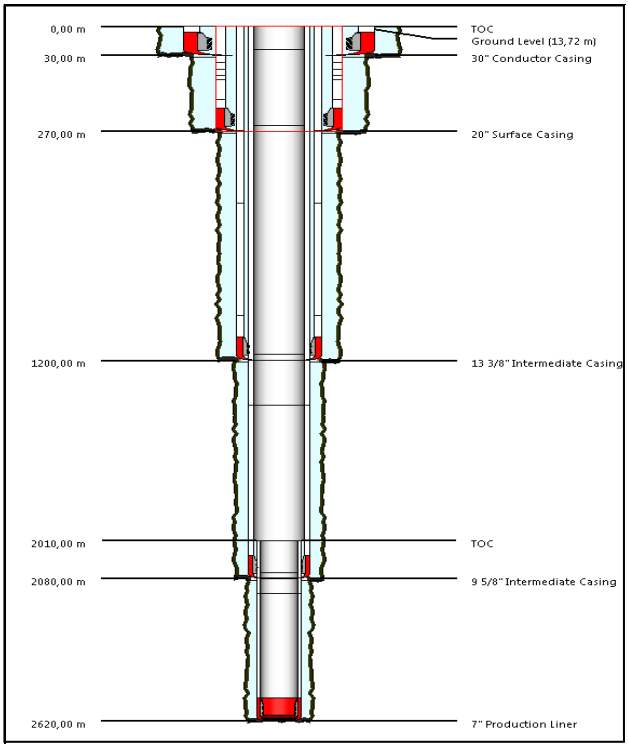

Figure 79 Well Schematic

In this case, the type of casing will be selected based on calculation from burst, collapse, axial load. Burst and collapse load line are calculated based on the greatest differential pressure between internal pressure and external pressure profile. On the other hand, the axial load line is calculated based on the maximum load between axial load profile with bending and axial load profile without bending. Triaxial load line is based on the greatest load line between burst, collapse and axial load. Finally, the design load line is calculated from load line multiply with design factor. The table below shows design factor for this calculation:

Table 6 Design Factor

Pipe Body		
Burst		1,1
Axial	Tension	1,3
	Compression	1,3
Collapse		1,1
Triaxial		1,25
Connection		
Burst		1,1
Axial	Tension	1,3
	Compression	1,3

4.8.1. Casing Design Surface Casing 20"

The initial condition for the basic calculation in this section can be seen in the table below:

Table 7 Cementing Data for Surface Casing 20"

Mix-Water Density (ppg)	8.4
Lead Slurry Density (ppg)	13.7
Displacement Fluid Density (ppg)	8.8
Float Collar Depth (m)	270

In this calculation, geothermal gradient is 1.5^0 / 100 ft with surface ambient temperature 80^0 F. This initial condition and the others parameters like pore pressure, fracture pressure and well path are used to calculate burst, collapse and axial load with different scenario using wellplan software. The results of this calculation can be seen in the figures below:

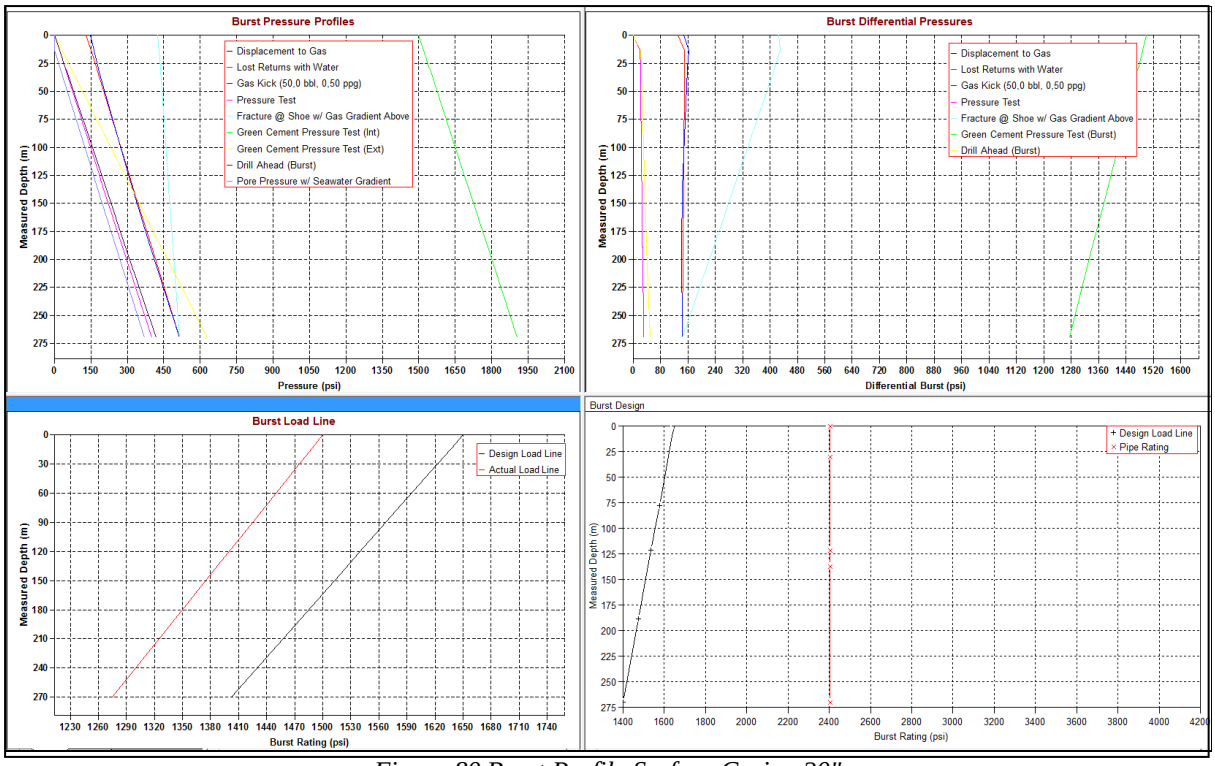

Figure 80 Burst Profile Surface Casing 20"

From figure above, burst actual load line is generated from the differential pressure between internal pressure (green cement pressure test) and external pressure (pore pressure with sea water gradient). Burst design load line is calculated by multiply actual burst load line with safety factor (1.1). In this case, casing 20" grade J-55, 106.5 ppf is safe because burst pipe rating is greater than burst design load line.

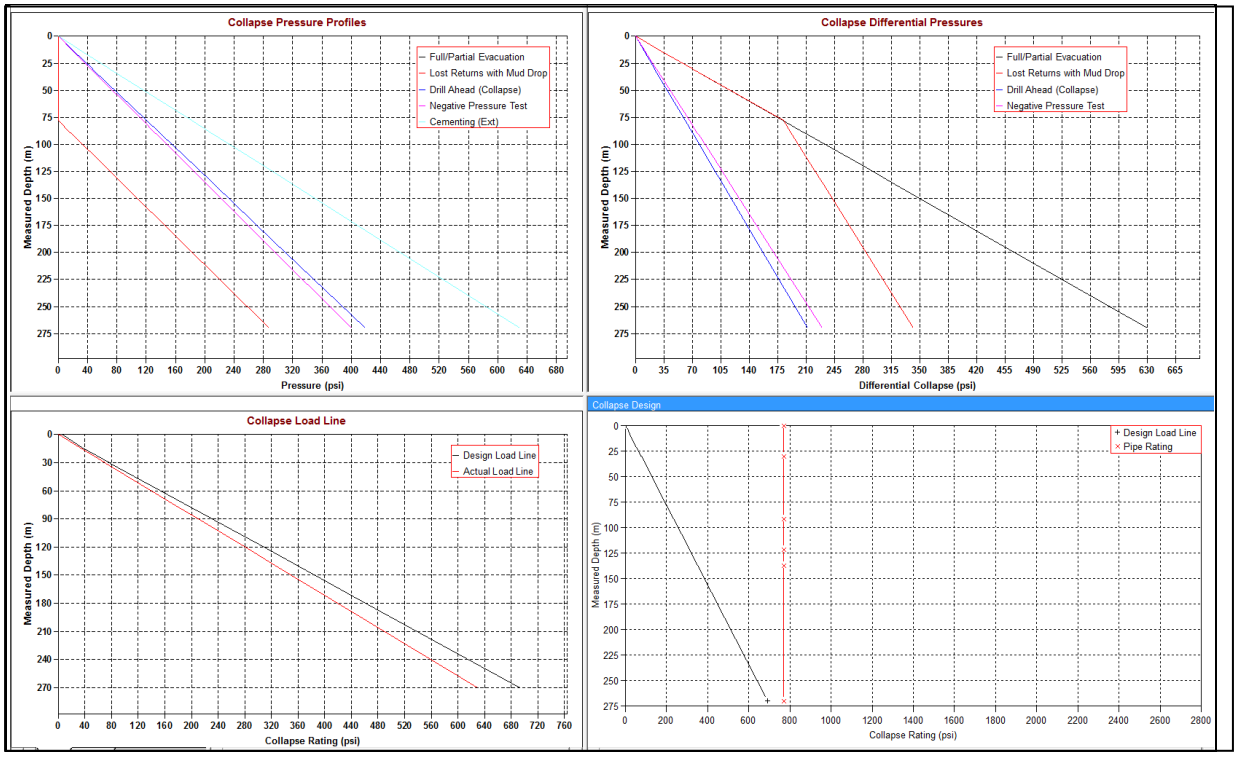

Figure 81 Collapse Profile Surface Casing 20"

From figure above, collapse actual load line is calculated from the differential pressure between external pressure (mud and cement slurry) and internal pressure (full or partial evacuation). In the worst case, collapse will happen when mud loss until at certain depth where wellbore pressure is same with pore pressure. Collapse design load line is calculated by multiply collapse actual load line with safety factor (1.1). In this case, casing 20" grade J-55, 106.5 ppf is safe because collapse pipe rating is greater than collapse design load line.

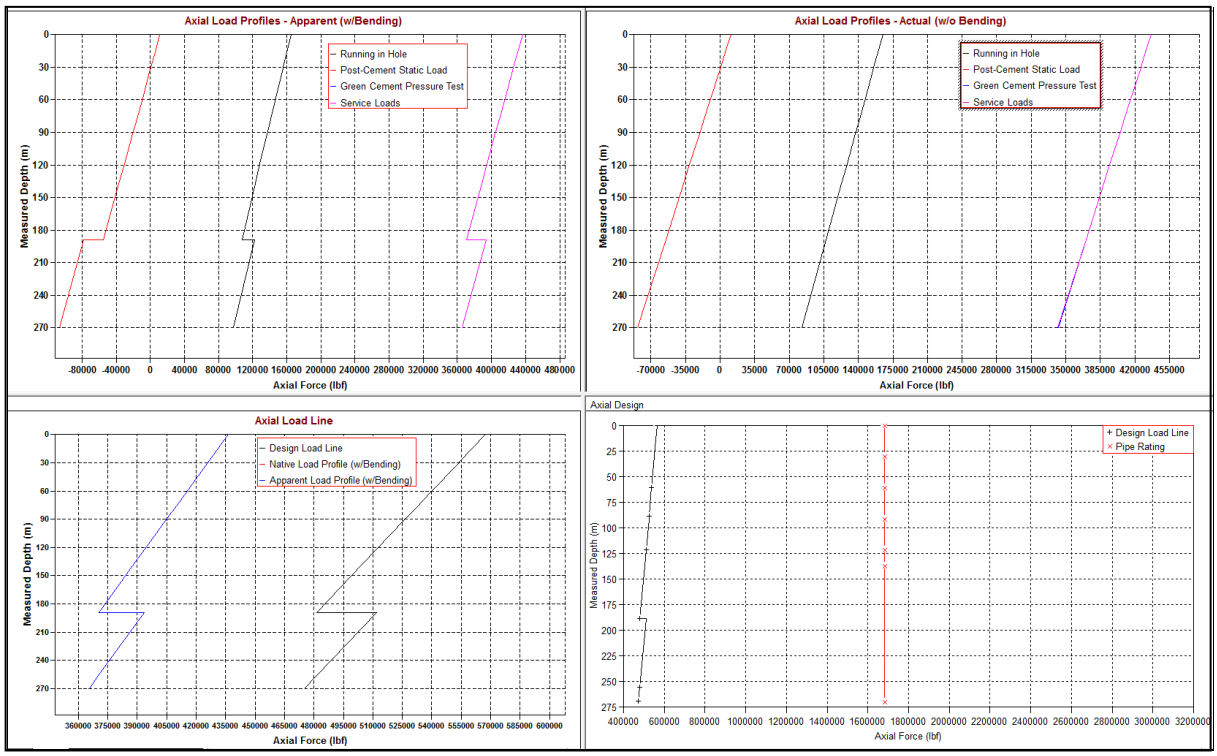

Figure 82 Axial Profile Surface Casing 20"

From figure above, native / apparent axial load line is generated from service load line profile with bending. This service load line is calculated with included effect of self weight, bouyancy, thermal strain due to temperature, piston force at end areas, pick up or slack-off loads, buckling and bending. Design load line is calculated by multiply native / apparent loan line by 1.3. Based on calculation, 20" grade J-55, 106.5 ppf is safe and it can withstand from this axial load.

4.8.2. Casing Design Intermediate Casing 13-3/8"

The initial condition for the basic calculation in this section can be seen in the table below:

Table 8 Cementing Data for Casing 13-3/8"

Mix-Water Density (ppg)	8.4
Lead Slurry Density (ppg)	13.7
Tail Slurry Density (ppg)	15.83
Tail Slurry Length (m)	400
Displacement Fluid Density (ppg)	10.5
Float Collar Depth (m)	1200

In this calculation, geothermal gradient is 1.5^0 / 100 ft with surface ambient temperature 80^0 F. This initial condition and the others parameters like pore pressure, fracture pressure and well path are used to calculate burst, collapse and axial load with different scenario using wellplan software. The results of this calculation can be seen in the figures below:

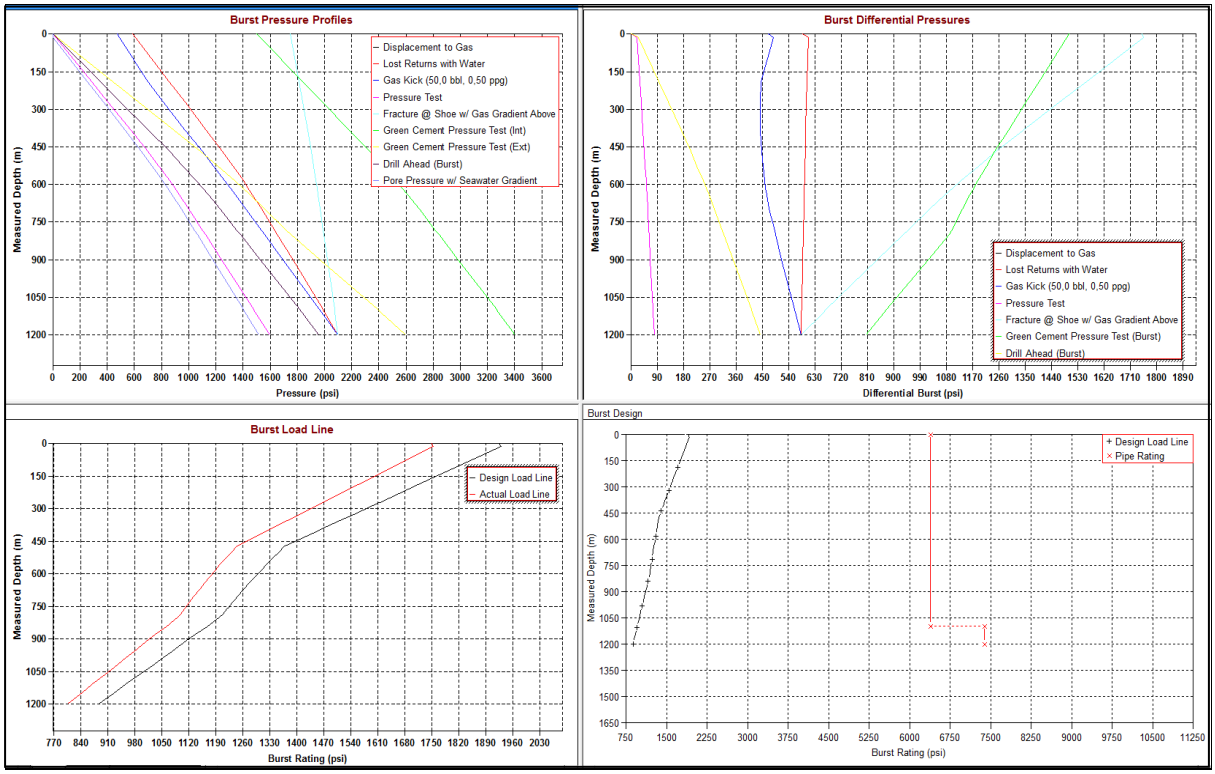

Figure 83 Burst Profile Casing 13-3/8"

From figure above, burst actual load line is generated from the differential pressure between internal pressure (green cement pressure test from depth 469 meter to 1200 meter and with case in fracture at shoe with gas gradient above from surface to depth 469 meter) and external pressure (pore pressure with sea water gradient). Burst design load line is calculated by multiply burst actual load line with safety factor (1.1). Casing 13-3/8" grade C-95, 72 ppf is safe because burst pipe rating is greater than burst design load line.

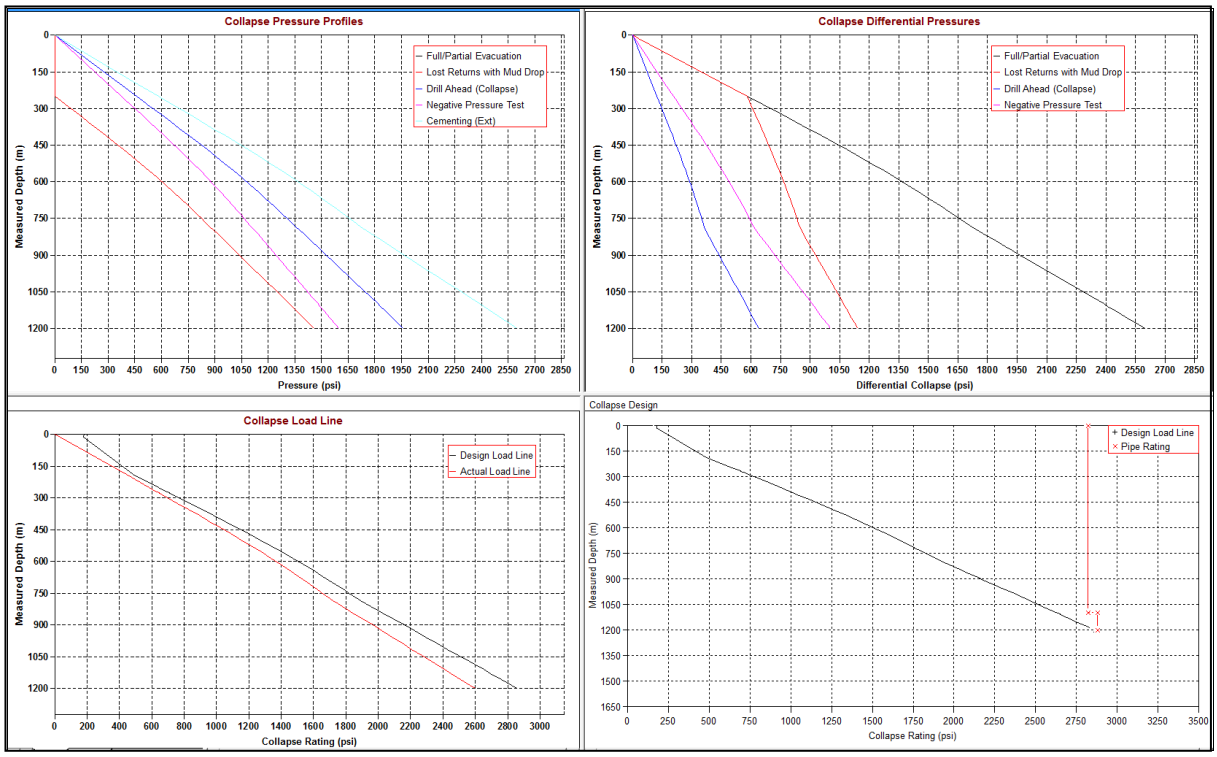

Figure 84 Collapse Profile Casing 13-3/8"

From figure above, collapse actual load line is calculated from the differential pressure between external pressure (mud and cement slurry) and internal pressure (full or partial evacuation). In the worst case, collapse will happen when mud loss until at certain depth where wellbore pressure is same with pore pressure. Collapse design load line is calculated by multiply collapse actual load line with safety factor (1.1). In this case, casing 13-3/8" grade C-95, 72 ppf can not withstand from collapse design load from surface until depth 1200 meter so it need casing with grade greater than casing grade C-95, 72 ppf. Based on analysis, it is decided to use casing 13-3/8" grade P-110, 72 ppf from depth 1100 meter to 1200 meter and use casing 13-3/8" grade C-95, 72 ppf from surface to depth 1100 meter. These casing combination can withstand from collapse load because collapse casing rating from these casing are greater than collapse design load line.

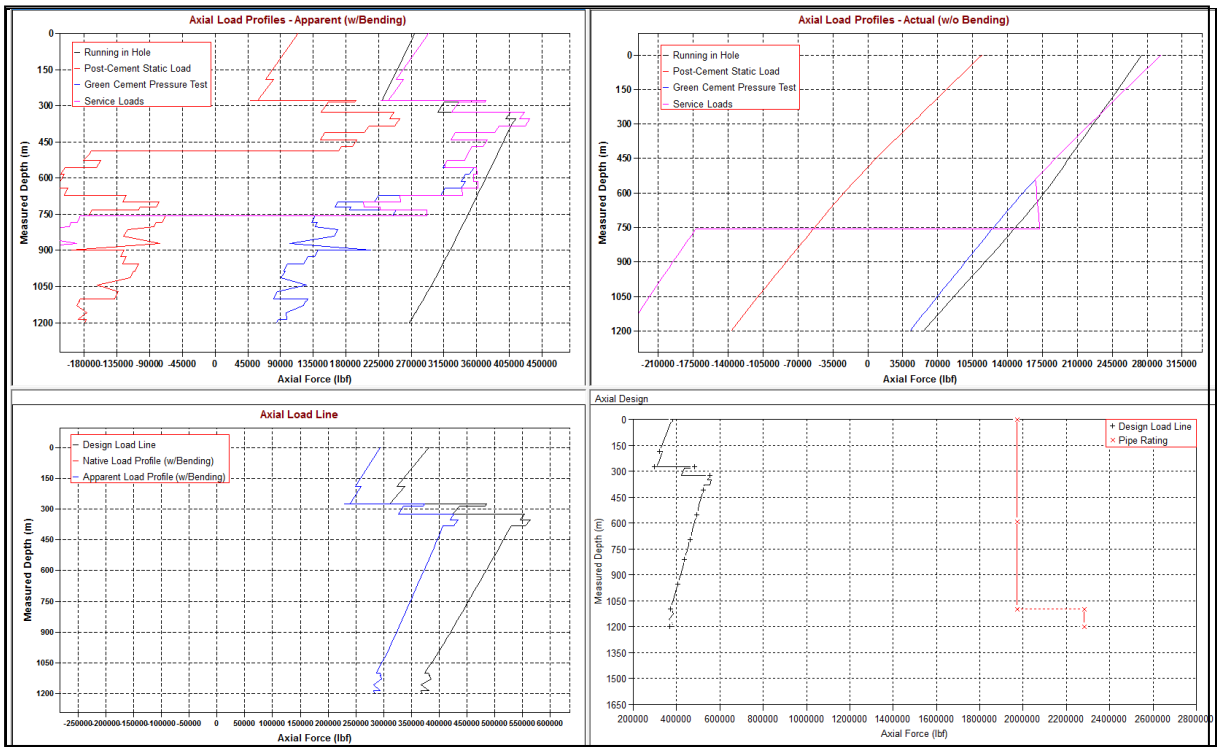

Figure 85 Axial Profile Casing 13-3/8"

From figure above, native / apparent axial load line is generated from axial load profile when running in hole. This load profile is depend on some factors like bouyed weight, wellbore inclination and bending caused by dogleg severities. Design load line is calculated by multiply native / apparent loan line by 1.3. Based on calculation, combination casing 13-3/8" grade C-95, 72 ppf and casing 13-3/8" grade P-110, 72 ppf can withstand from this design axial load.

4.8.3. Casing Design Intermediate Casing 9-5/8"

The initial condition for the basic calculation in this section can be seen in the table below:

Table 9 Cementing Data for Surface Casing 9-5/8"

Mix-Water Density (ppg)	8.4
Lead Slurry Density (ppg)	12.92
Tail Slurry Density (ppg)	15
Tail Slurry Length (m)	500
Displacement Fluid Density (ppg)	11.7
Float Collar Depth (m)	2080

In this calculation, geothermal gradient is 1.5^0 / 100 ft with surface ambient temperature 80^0 F. This initial condition and the others parameters like pore pressure, fracture pressure and well path are used to calculate burst, collapse and axial load with different scenario using wellplan software. The results of this calculation can be seen in the figures below:

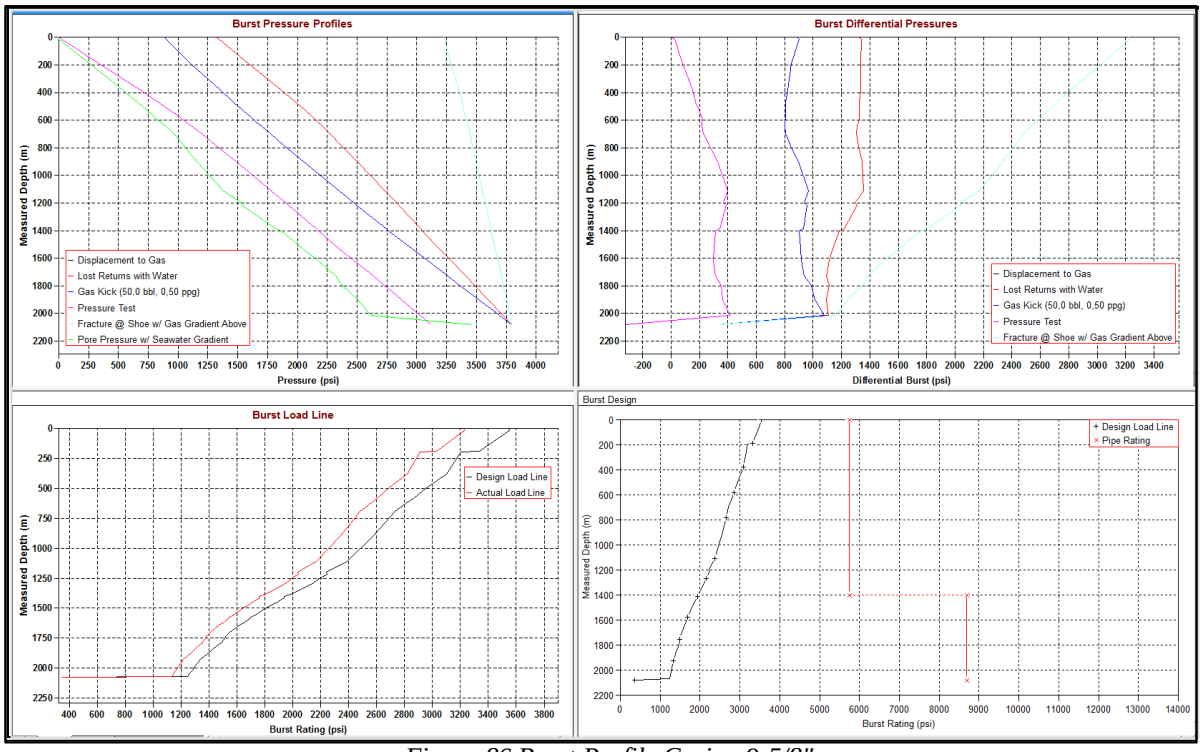

Figure 86 Burst Profile Casing 9-5/8"

From figure above, burst actual load line is generated from the differential pressure between internal pressure (fracture at shoe with gas gradient above) and external pressure pressure (pore pressure with sea water gradient). Burst design load line is calculated by multiply actual load line with safety factor (1.1). In this case, casing 9-5/8" grade N-80, 40 ppf is safe because burst pipe rating is greater than burst design load line.

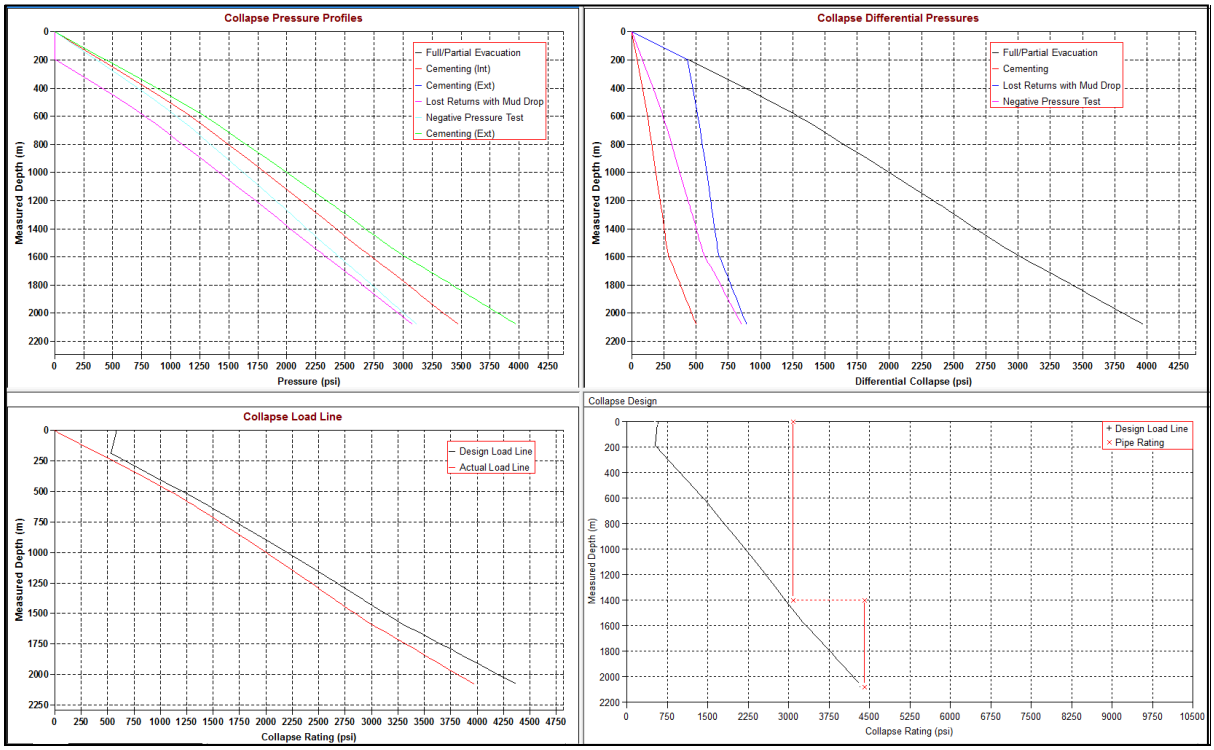

Figure 87 Collapse Profile Casing 9-5/8"

From figure above, collapse actual load line is calculated from the differential pressure between external pressure (mud and cement slurry) and internal pressure (full or partial evacuation). In the worst case, collapse will happen when mud loss until at certain depth where wellbore pressure is same with pore pressure. Collapse design load line is calculated by multiply collapse actual load line with safety factor (1.1). In this case, casing 9-5/8" grade N-80, 40 ppf can not withstand from collapse design load from surface until depth 2080 meter so it need casing with grade greater than casing grade N-80, 40 ppf. Based on analysis, it is decided to use casing 9-5/8" grade P-110, 43.5 ppf from depth 1400 meter to 2080 meter and use casing casing 9-5/8" grade N-80, 40 ppf ppf from surface to depth 1400 meter. These casing combination can withstand from collapse load because collapse pipe rating from these casing are greater than collapse design load line.

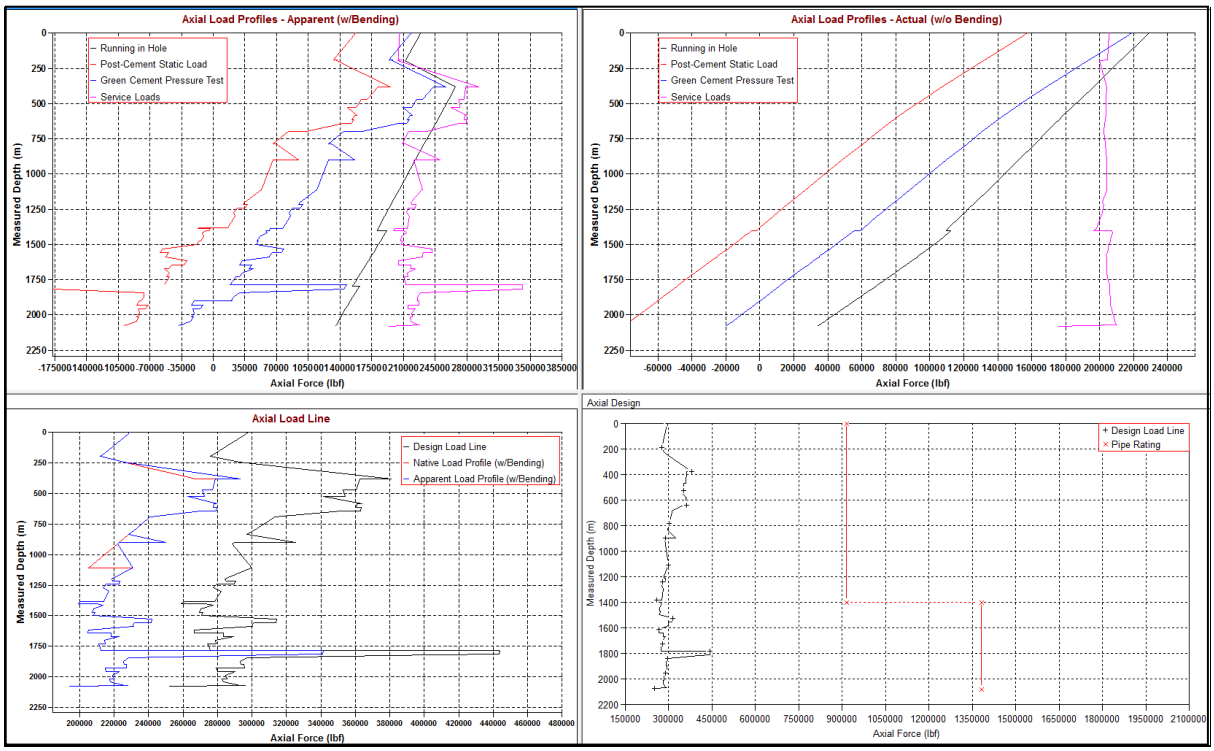

Figure 88 Axial Profile Casing 9-5/8"

From figure above, native / apparent axial load line is generated from service load line profile with bending. This service load line is calculated with included effect of self weight, bouyancy, thermal strain due to temperature, piston force at end areas, pick up or slack-off loads, buckling and bending. Design load line is calculated by multiply native / apparent loan line by 1.3. Based on calculation, combination casing 9-5/8" grade N-80, 40 ppf and casing 9-5/8" grade P-110, 43.5 ppf can withstand from this design axial load.

4.8.4. Casing Design Liner 7"

The initial condition for the basic calculation in this section can be seen in the table below:

Table 10 Cementing Data for Liner 7"

Mix-Water Density (ppg)	8.4
Lead Slurry Density (ppg)	15
Top of Cement (m)	2010
Displacement Fluid Density (ppg)	11.7
Float Collar Depth (m)	2260
Packer Fluid Density (ppg)	9
Packer Depth (m)	1870
Perforation Depth (m)	2200
Gas Gravity (sg)	0.3

In this calculation, geothermal gradient is 1.5^0 / 100 ft with surface ambient temperature 80^0 F. This initial condition and the others parameters like pore pressure, fracture pressure and well path are used to calculate burst, collapse and axial load with different scenario using wellplan software. The results of this calculation can be seen in the figures below:

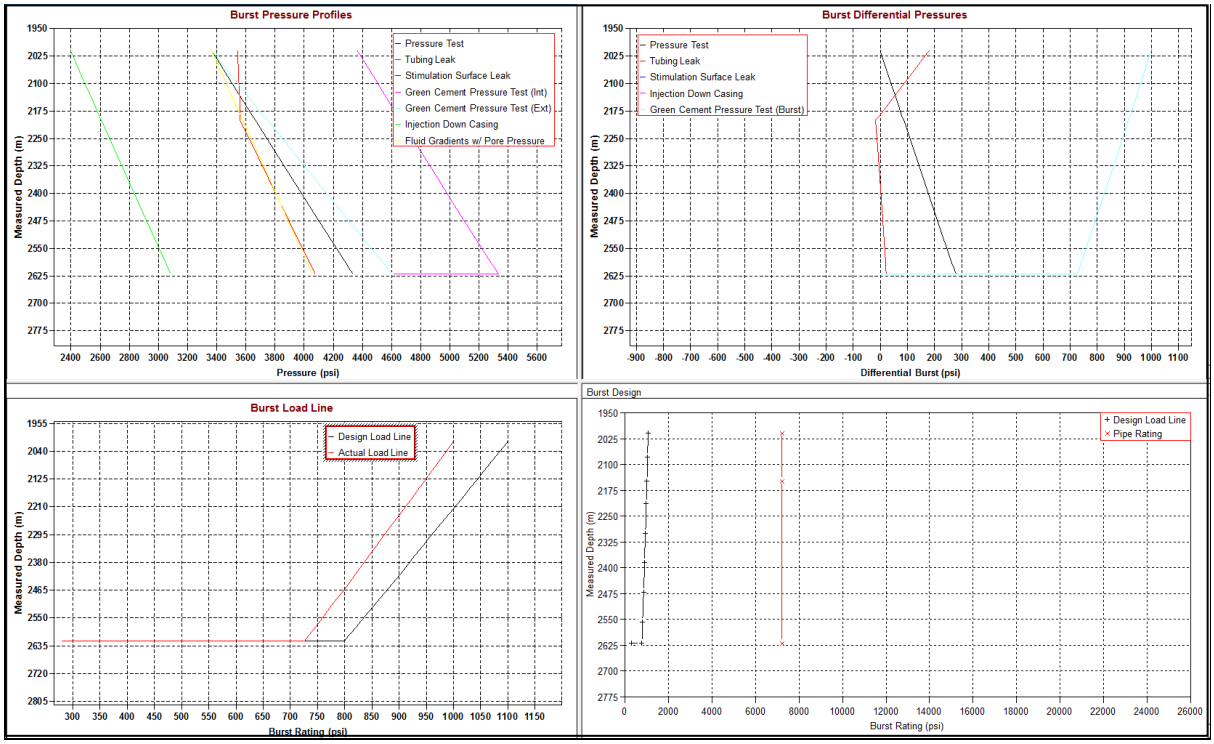

Figure 89 Burst Profile Liner Casing 7"

From figure above, burst actual load line is generated from the differential pressure between internal pressure (green cement pressure test) and external pressure (pore pressure with sea water gradient). Burst design load line is calculated by multiply burst actual load line with safety factor (1.1). In this case, liner 7" grade N-80, 26 ppf is safe because burst pipe rating is greater than burst design load line.

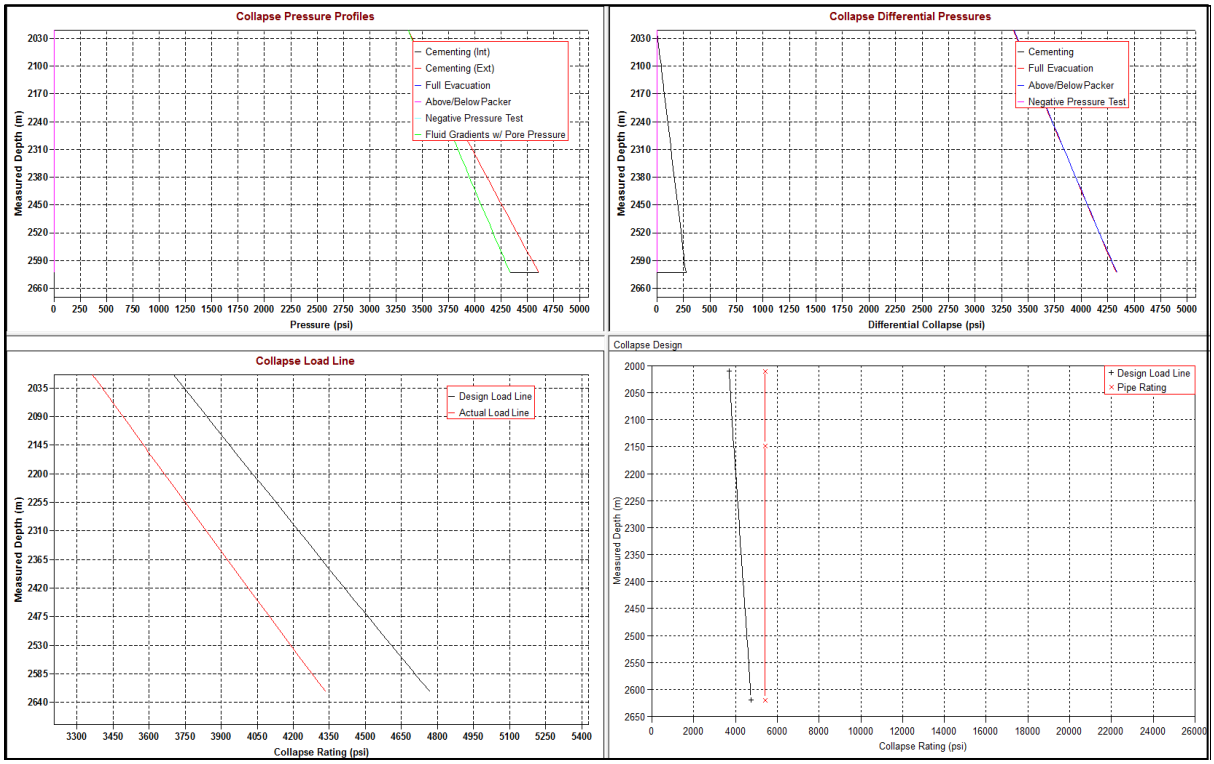

Figure 90 Collapse Profile Liner 7"

From figure above, collapse actual load line is calculated from the differential pressure between external pressure (mud and cement slurry) and internal pressure (above or below packer). In the worst case, collapse will happen when during completion or workover operations where packer or workover fluid is exposed to a depleted zone. In this case fluid drop may occur corresponding to the hydrostatic head of the fluid equillibrating with the depleted pressure at the perforation. Collapse design load line is calculated by multiply collapse actual load line with safety factor (1.1). In this case, liner N-80, 26 ppf is safe because collapse pipe rating is greater than collapse design load line.

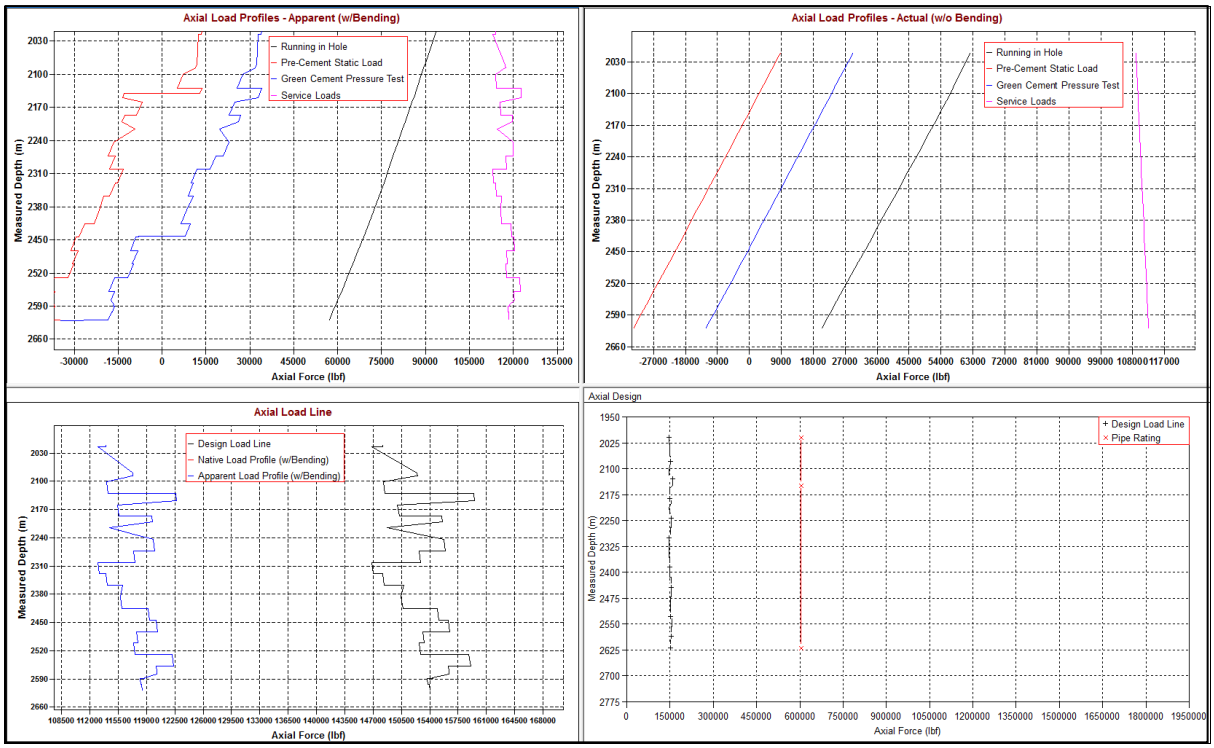

Figure 91 Axial Profile Liner 7"

From figure above, native / apparent axial load line is generated from service load line profile with bending. This service load line is calculated with included effect of self weight, bouyancy, thermal strain due to temperature, piston force at end areas, pick up or slack-off loads, buckling and bending. Design load line is calculated by multiply native / apparent loan line by 1.3. Based on calculation, liner N-80, 26 ppf is safe and it can withstand from this axial load.

4.9 Cutting Transport and Hydraulic Design

In this calculation will analyze cutting transport and hydraulic design for hole section 17-1/2", 12-1/4" and 8-1/2". This simulation using geothermal gradient 1.5^0 / 100 ft and the other parameters like cutting density, cutting size, etc used in this simulation based on the condition of formation. Mud pump is used to transport cutting from wellbore to the surface and. Maximum pump pressure should facilitate all of the pressure loss in the drillstring and annulus. This is the mud pump specification that used in this simulation :

Table 11 Mud Pump Specification

Maximum Pump Pressure	6000 Psi
Maximum Pump Power	1600 HP
Maximum Pump Rate	737 Gpm
Surface Pressure Loss	100 Psi

4.9.1. Cutting Transport and Hydraulic Design in Hole Section 17-1/2"

Table 12 Hole Section 17-1/2" Data

Section Type	MD	Length	OD	ID	Eff. Hole Diameter	FF	Vol. Excess	Items Description
	m	m	in	in	in		%	
Casing	2080	2080	9-5/8	8.835	13.137	0.25	15	Grade N-80, 40 ppf
Open Hole	2620	540		8.5	8.915	0.3	10	

Table 13 Drillstring Data for Hole Section 17-1/2"

Type	Length (m)	Depth (m)	Body		Stabilizer / Tool Joint				Weight	Material	Grade
			OD (in)	ID (in)	Avg Joint Length (m)	Length (m)	OD (in)	ID (in)			
Drill Pipe	934	934	6.625	6	9.14	0.48	8.5	4.25	29.63	CS_API 5D/7	S Class 1
Heavy Weight	165	1099	6.625	4.5	9.14	1,219	8.3	4.5	73.5	CS_1340 MOD	1340 MOD
Jar	6	1104	6	2.25	5.54				53.73	CS_API 5D/7	4145H MOD
Heavy Weight	28	1132	5	3	9.14	1,219	6.5	3,063	51.1	CS_1340 MOD	1340 MOD
Sub	1	1133	7.92	3	0.91				147	CS_API 5D/7	4145H MOD
Drill Collar	28	1161	8	2.5	9.14				152.8	SS_15-15LC	15-15LC MOD (2)
MWD	5	1166	8	3.25	5.2				141.1	SS_15-15LC	15-15LC MOD (1)
Drill Collar	28	1194	8	2.5	9.14				152.8	SS_15-15LC	15-15LC MOD (2)
Stabilizer	3	1197	9.5	2,375	2.51				363.6	CS_API 5D/7	4145H MOD
Sub	1	1198	7.92	3	0.91				147	CS_API 5D/7	4145H MOD
Mud Motor	7	1205	11.3	3	7.01				273.9	SS_15-15LC	15-15LC MOD (1)
Bit	0.31	1205	17.5		0.3				565		

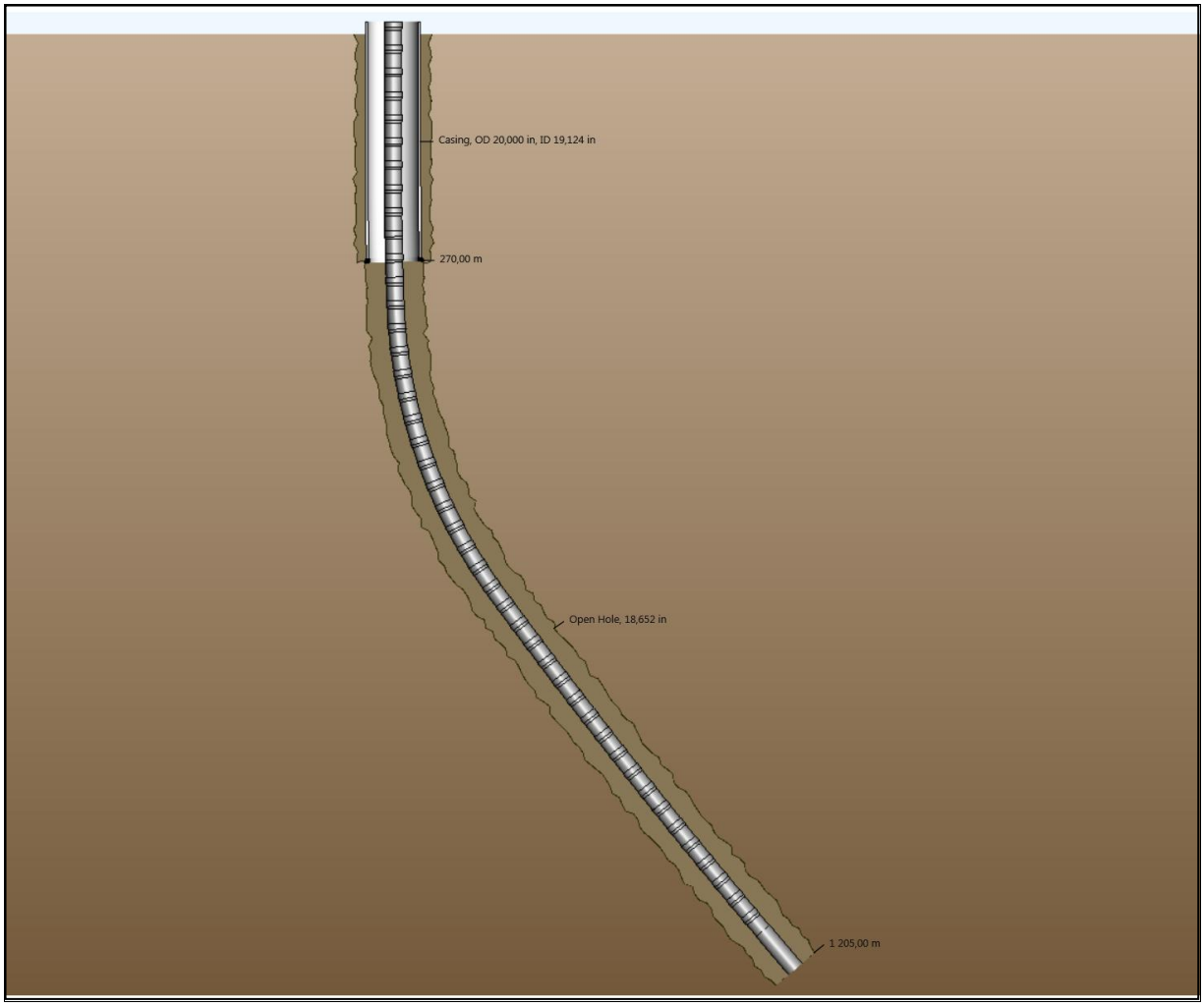

Figure 92 Wellbore Schematic Hole Section 17-1/2"

Table 14 Input Parameter for Cutting Transport Hole Section 17-1/2"

Rate of Penetration	30 m / hr
Cuttings Diameter	0.3 inch
Bed Porosity	36%
Rotary Speed	100 RPM
Cuttings Density	2 sg
Mud Density	8.8 ppg
Plastic Viscosity	15 cp
Yield Point	20 Lbf / 100 ft²
GS 10 Second	4 lbf / 100 ft²
GS 10 Minute	10 lbf / 100 ft²

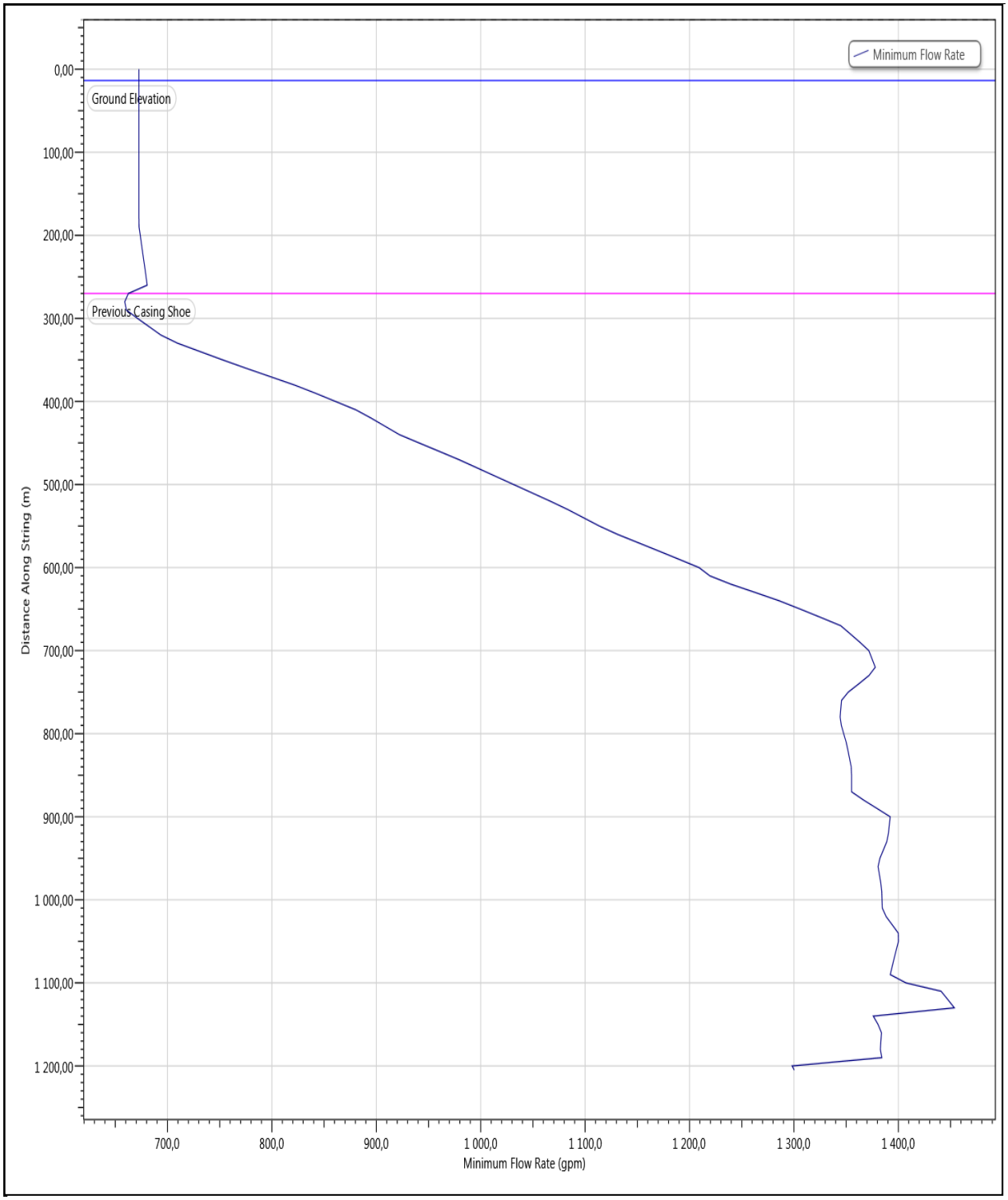

Figure 93 Minimum Flowrate Hole Section 17-1/2"

Based on the minimum flowrate calculation in this hole section, it needs a minimum flowrate 1,453.5 gallons per minute to clean this wellbore. With this flowrate, it needs two mud pumps to facilitate this flowrate. By using two mud pump and drillstring configuration, it needs to optimize the hydraulic design using jet impact force and hydraulic horsepower methods. The figure below shows the result of calculation using this method.

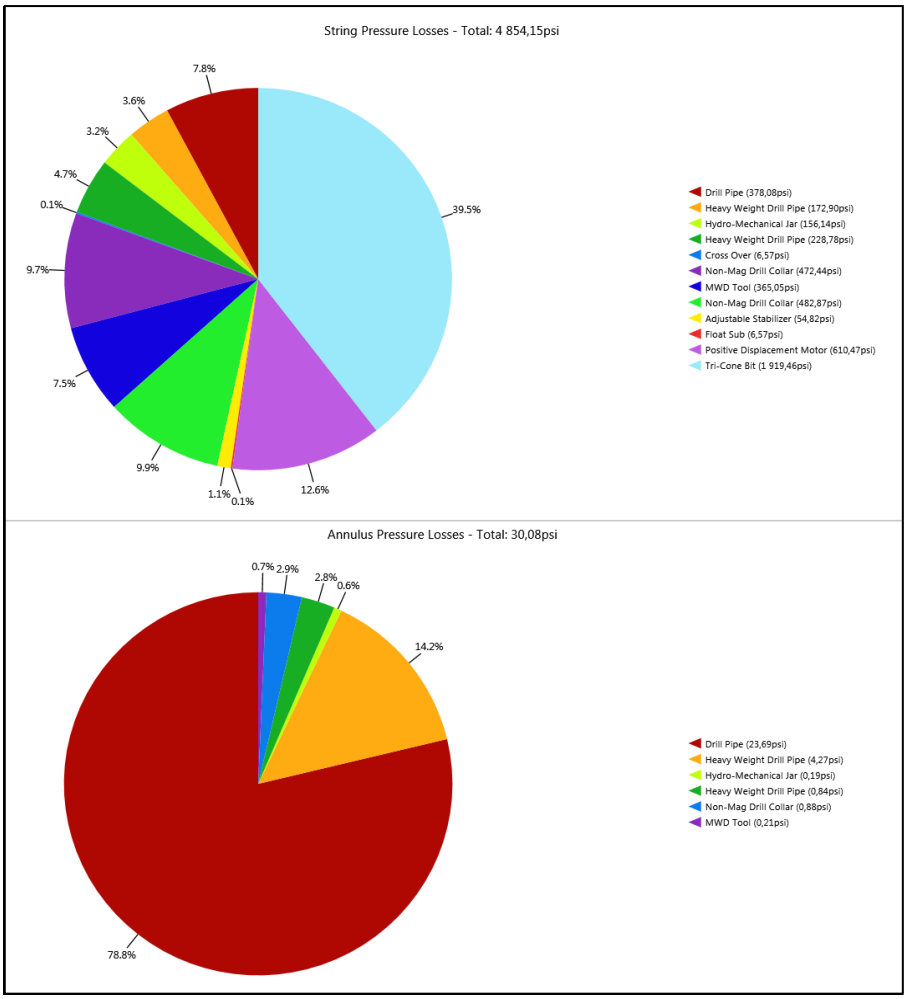

Figure 94 Component Pressure Losses Hole Section 17-1/2"

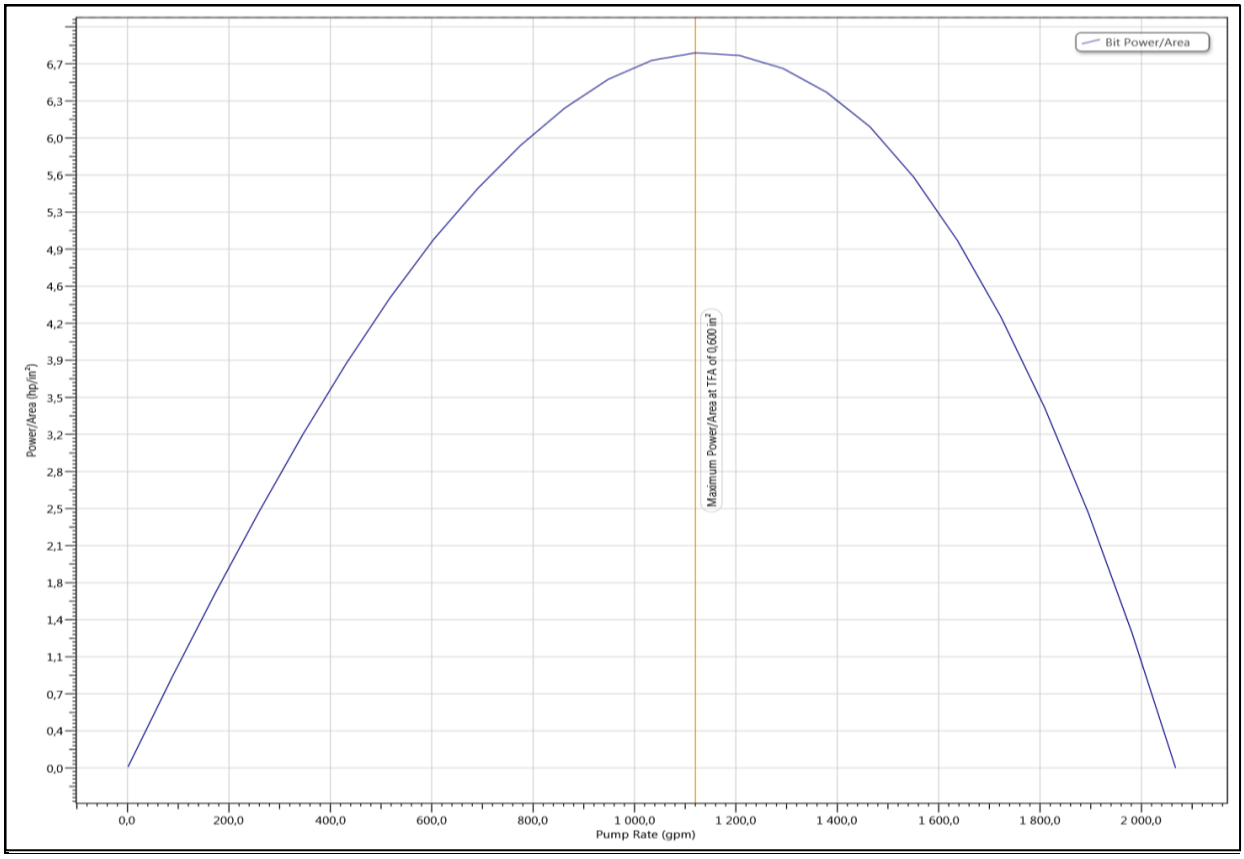

Figure 95 Hydraulic Horse Power Calculation for Hole Section 17-1/2"

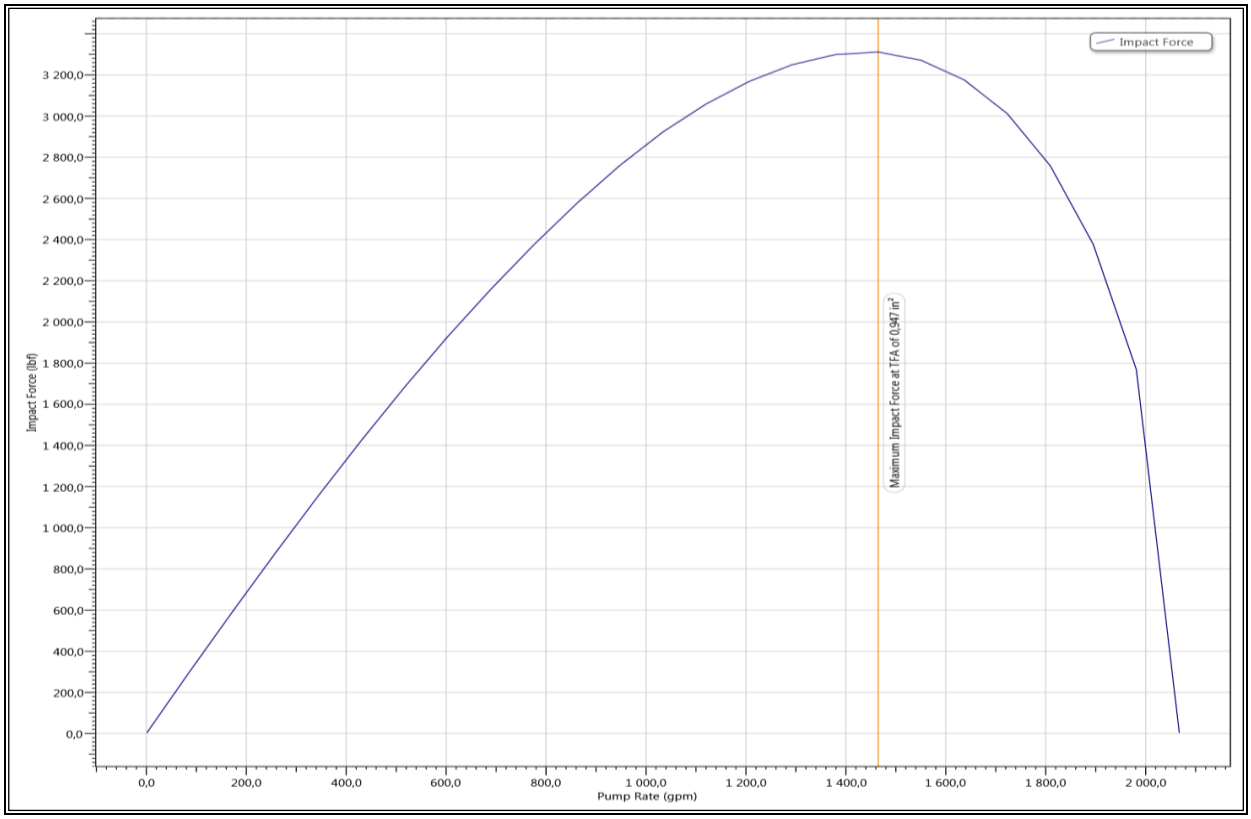

Figure 96 Jet Impact Force Calculation for Hole Section 17-1/2"

4.9.2. Cutting Transport and Hydraulic Design in Hole Section 12-1/4"

Table 15 Hole Section 12-1/4" Data

Section Type	MD	Length	OD	ID	Eff. Hole Diameter	FF	Vol. Excess	Items Description
	m	m	in	in	in		%	
Casing	1200	1200	13-3/8	12.62	18.767	0.25	15	Grade K-55, 94 ppf
Open Hole	2087	887		12.25	13.137	0.3	15	

Table 16 Drillstring Data for Hole Section 12-1/4"

Type	Length (m)	Depth (m)	Body		Stabilizer / Tool Joint				Weight	Material	Grade
			OD (in)	ID (in)	Avg Joint Length (m)	Length (m)	OD (in)	ID (in)			
Drill Pipe	2,020	2020	5	4.28	9.14	0.43	7	2.75	22.6	CS_API 5D/7	S Class 1
Jar	10.2	2030	6	2.25	10.18				53.73	CS_API 5D/7	4145H MOD
Heavy Weight	27.9	2058	5	3	9.14	1,219	6.5	3	51.1	CS_1340 MOD	1340 MOD
Sub	0.69	2058	5.4	2.76	0.69				59.71	CS_API 5D/7	4145H MOD
Drill Collar	7.51	2066	8	2.5	9.14				152.8	SS_15-15LC	15-15LC MOD (2)
MWD	6.84	2073	8	3.25	6.84				141.1	SS_15-15LC	15-15LC MOD (1)
Drill Collar	3.06	2076	8	2.5	9.14				152.8	SS_15-15LC	15-15LC MOD (2)
Stabilizer	1.73	2077	6.5	1.75	1.73				76.92	CS_API 5D/7	4145H MOD
Sub	0.81	2078	7.92	3.24	0.81				142.8	CS_API 5D/7	4145H MOD
Mud Motor	8.51	2087	8	2.5	8.51				126.9	SS_15-15LC	15-15LC MOD (1)
Bit	0.31	2087	12.25		0.3				267		

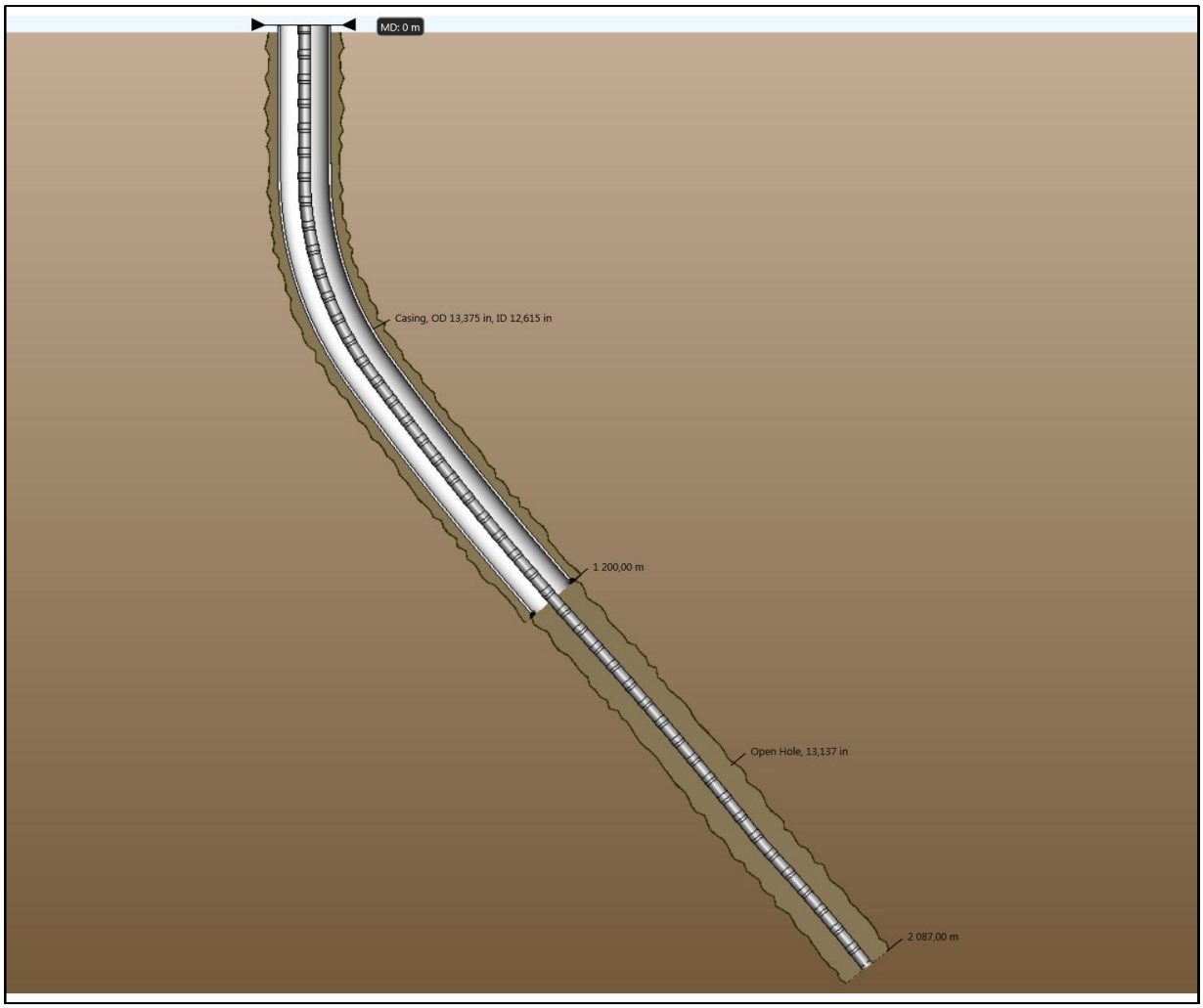

Figure 97 Wellbore Schematic Hole Section 12-1/4"

Table 17 Input Parameter for Cutting Transport Hole Section 12-1/4"

Rate of Penetration	30 m / hr
Cuttings Diameter	0.3 inch
Bed Porosity	36%
Rotary Speed	100 RPM
Cuttings Density	2.2 sg
Mud Density	10.5 ppg
PV	15 cp
Yp	19 Lbf / 100 ft²
GS 10 Second	5 lbf / 100 ft²
GS 10 Minute	12 lbf / 100 ft²

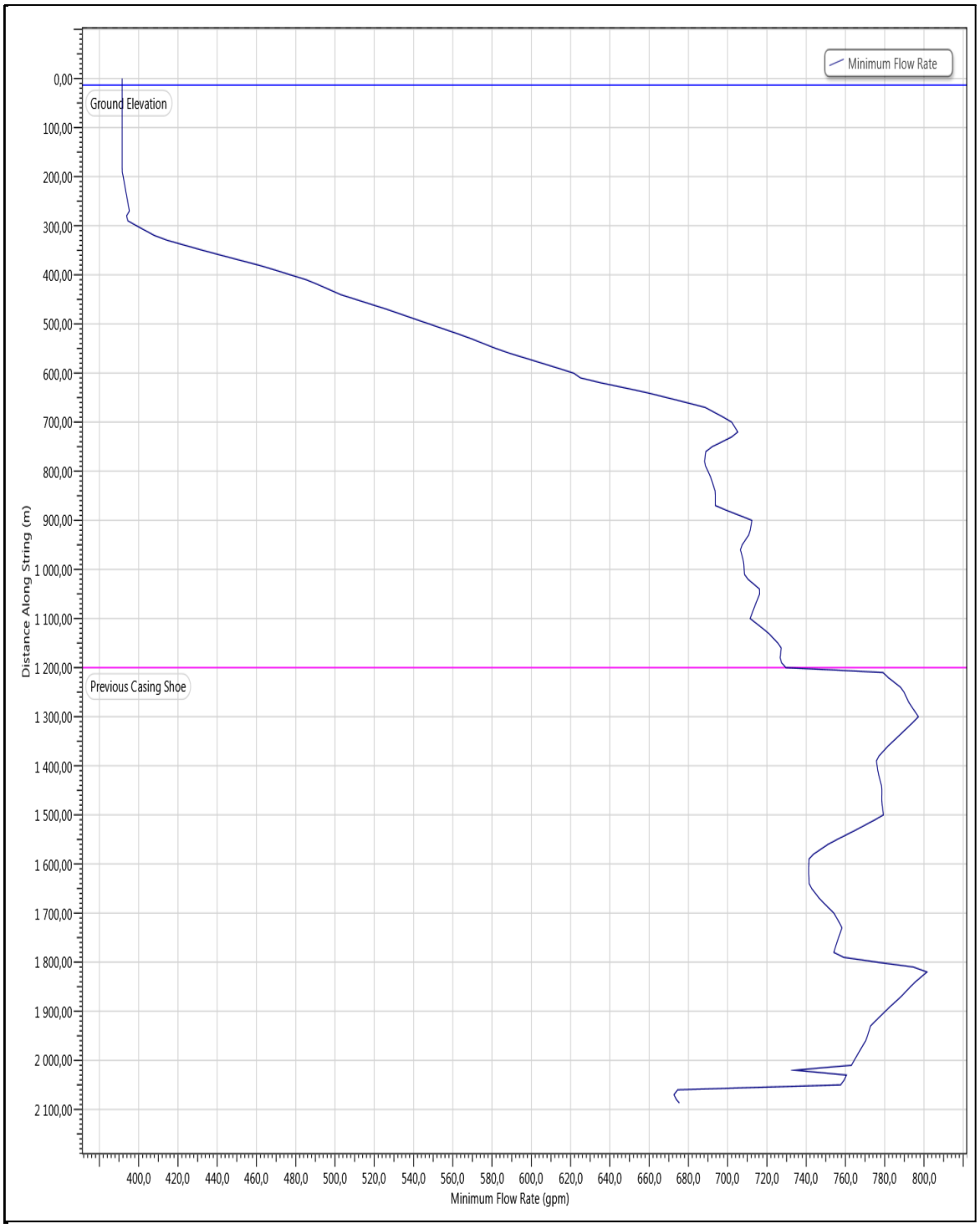

Figure 98 Minimum Flowrate Hole Section 12-1/4"

Based on minimum flowrate from calculation to transport cutting from wellbore to surface, it needs minimum 801.5 gpm to make sure wellbore clean from the cuttings. This flowrate needs two mud pump to facilitate hole cleaning in this hole section. By using two mud pumps and drillstring configuration, it needs to optimize the hydraulic design using jet impact force and hydraulic horsepower methods. The figure below shows the result of calculation using this method.

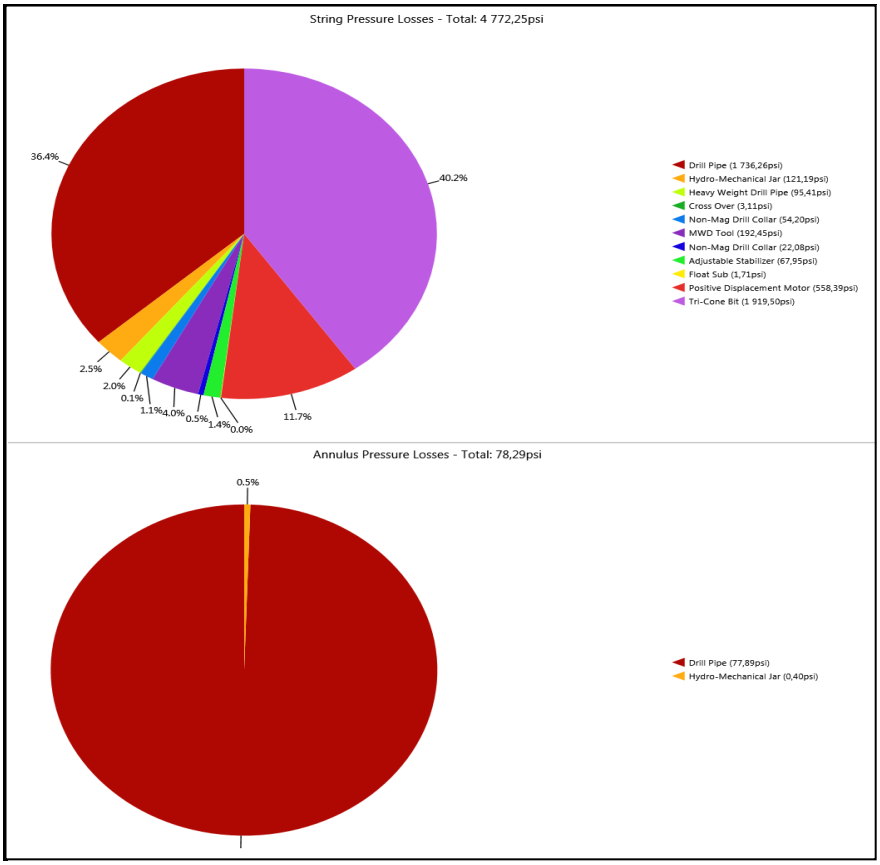

Figure 99 Component Pressure Losses Hole Section 12-1/4"

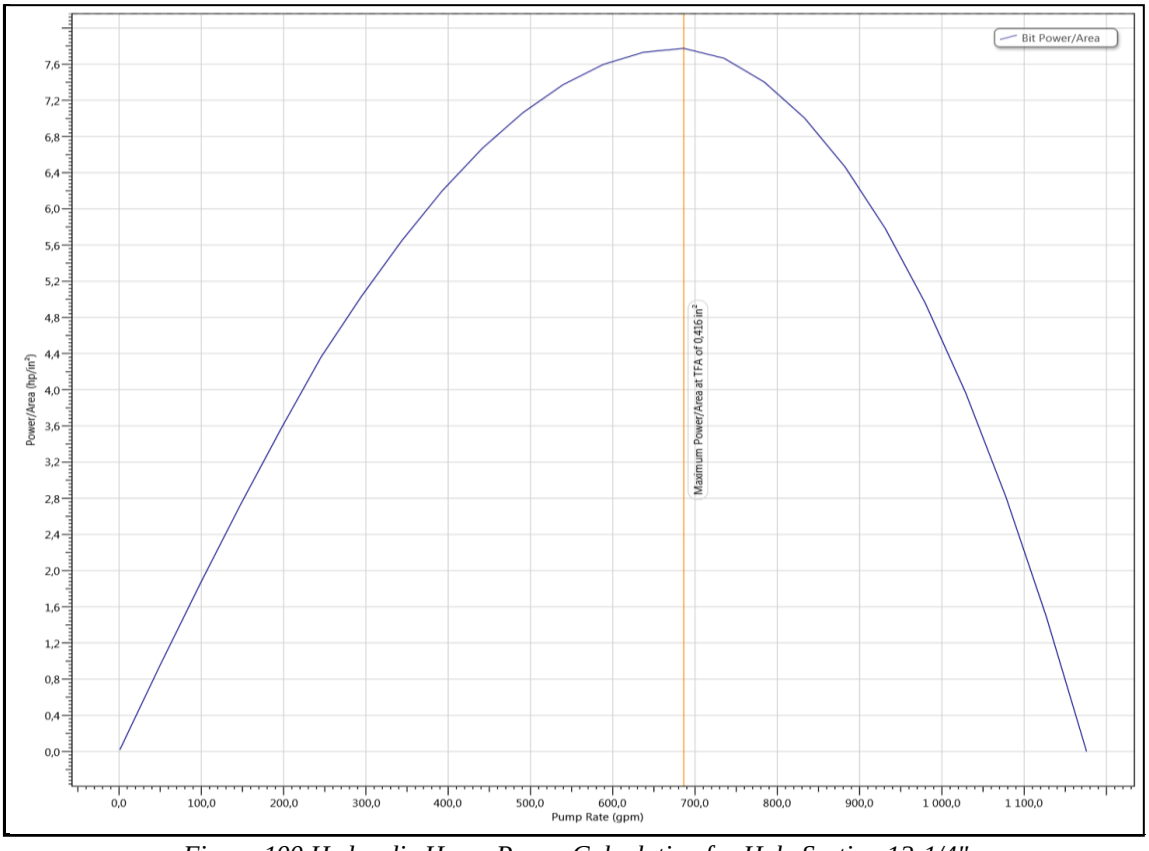

Figure 100 Hydraulic Horse Power Calculation for Hole Section 12-1/4"

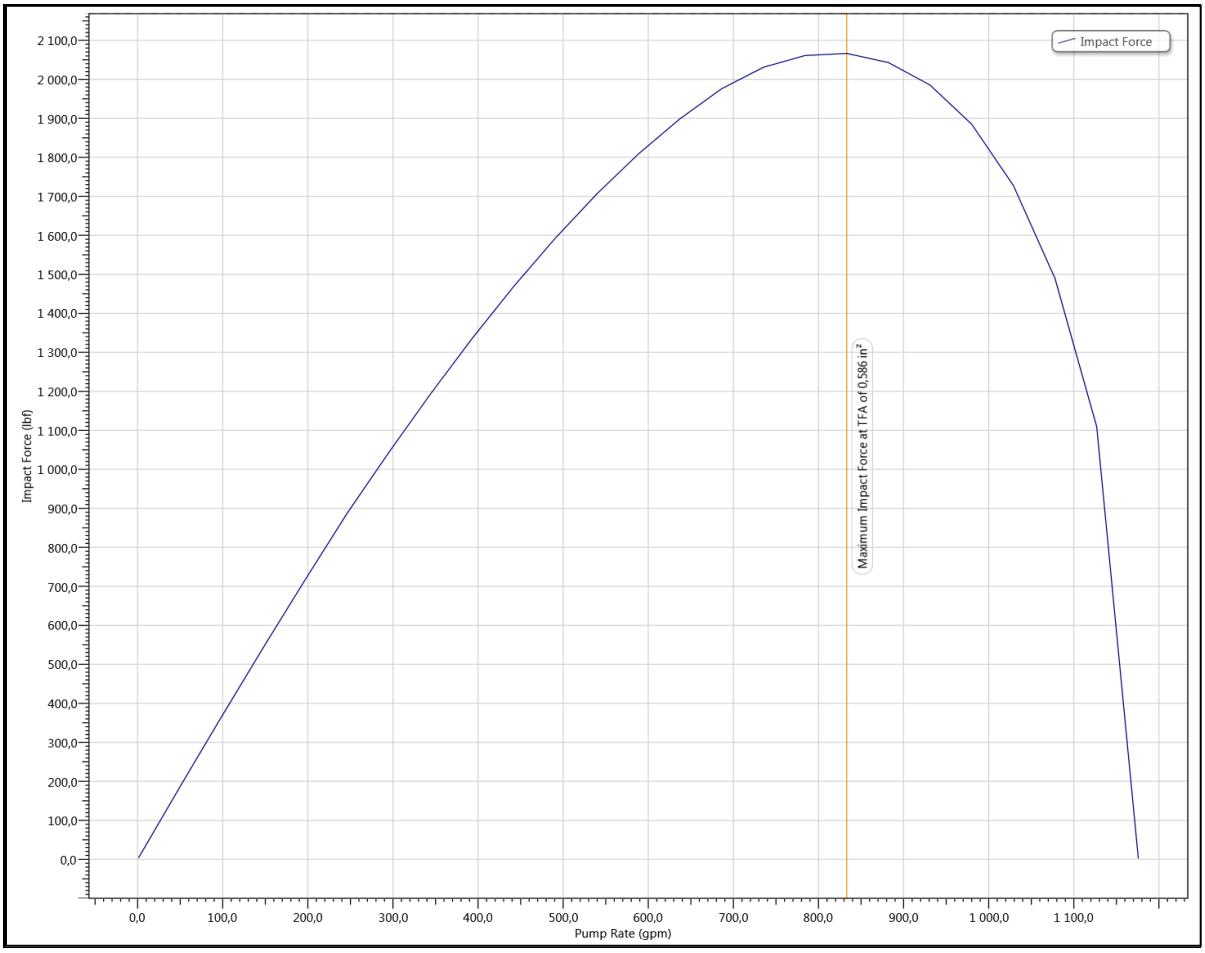

Figure 101 Jet Impact Force Calculation for Hole Section 12-1/4"

4.9.3. Cutting Transport and Hydraulic Design in Hole Section 8-1/2"

Table 18 Hole Section 8-1/2" Data

Section Type	MD	Length	OD	ID	Eff. Hole Diameter	FF	Vol. Excess	Items Description
	m	m	in	in	in		%	
Casing	270	270	20	19.12	27.805	0.25	15	Grade J-55, 54.5 ppf
Open Hole	1205	935		17.5	18.652	0.3	15	

Table 19 Drillstring Data for Hole Section 8-1/2"

Type	Length (m)	Depth (m)	Body		Stabilizer / Tool Joint				Weight	Material	Grade
			OD (in)	ID (in)	Avg Joint Length (m)	Length (m)	OD (in)	ID (in)			
Drill Pipe	1692	1692	5	4,276	9.14	0.43	6,625	2.75	22.6	CS_API 5D/7	S Class 1
Drill Pipe	700	2392	4.5	3.64	9.14	0.43	6,625	2,875	23.22	CS_API 5D/7	S Class 1
Heavy Weight	165	2557	5	3	9.14	1,219	6.5	3,063	51.1	CS_1340 MOD	1340 MOD
Jar	5.34	2563	6	2.25	5.34				53.73	CS_API 5D/7	4145H MOD
Heavy Weight	27.9	2591	5	3	9.14	1,219	6.5	3,063	51.1	CS_1340 MOD	1340 MOD
Drill Collar	9.47	2600	6.75	3	9.14				96.71	SS_15-15LC	15-15LC MOD (1)
MWD	5.99	2606	6.75	2,875	5.99				100.8	SS_15-15LC	15-15LC MOD (1)
Drill Collar	3.02	2609	6.75	3	9.14				96.71	SS_15-15LC	15-15LC MOD (1)
Stabilizer	2.03	2611	4.75	1	2.03				62.43	CS_API 5D/7	4145H MOD
Sub	0.82	2612	6.72	2.4	0.82				105.1	CS_API 5D/7	4145H MOD
Mud Motor	7.83	2620	6.75	1.5	7.83				87.5	SS_15-15LC	15-15LC MOD (1)
Bit	0.23	2620	8.5		0.23				90		

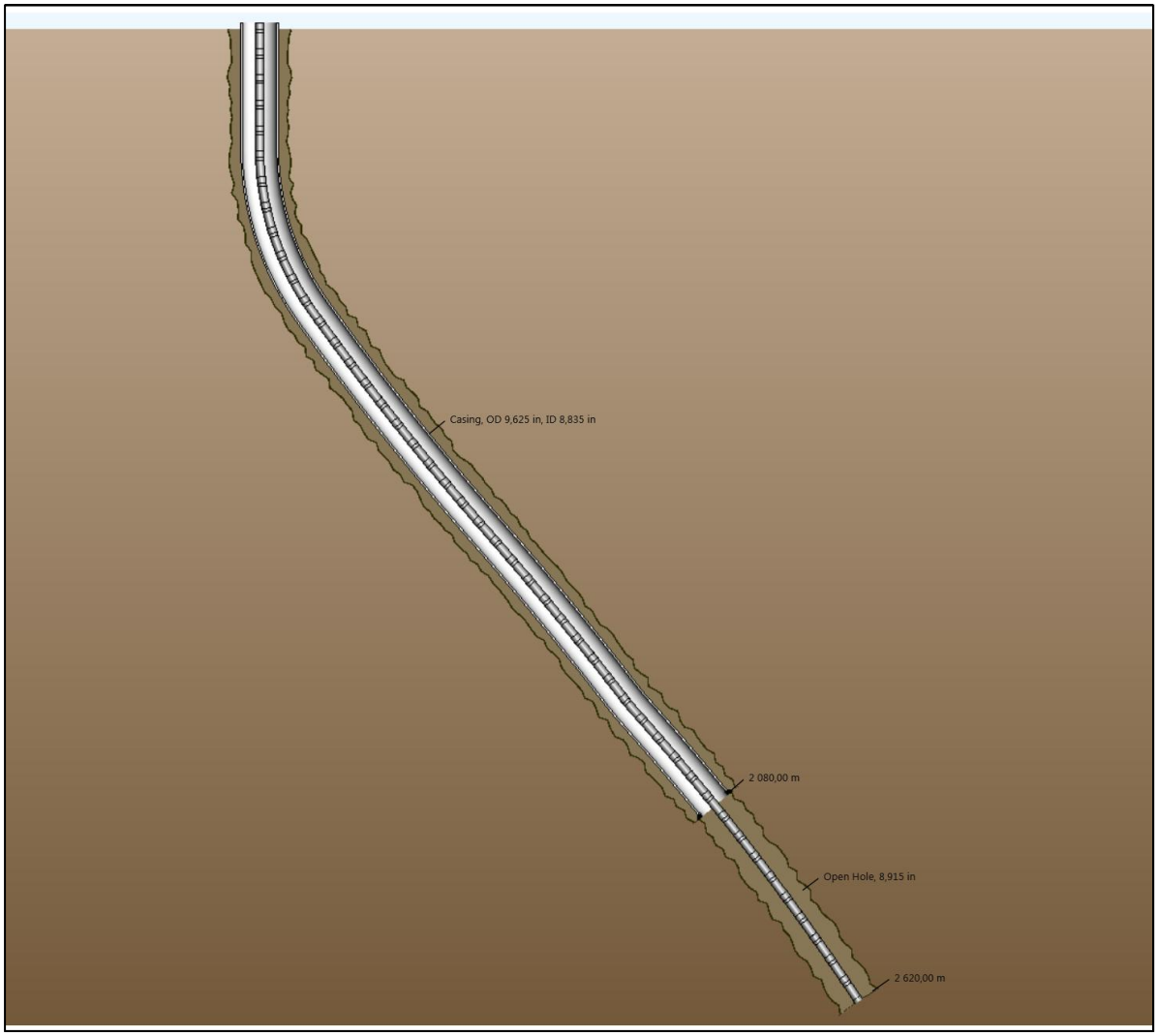

Figure 102 Wellbore Schematic Hole Section 8-1/2"

Table 20 Input Parameter for Cutting Transport Hole Section 8-1/2"

Rate of Penetration	30 m / hr
Cuttings Diameter	0.3 inch
Bed Porosity	36%
Rotary Speed	100 RPM
Cuttings Density	2.6 sg
Mud Density	11.7 ppg
PV	15 cp
Yp	22 Lbf / 100 ft²
GS 10 Second	6 lbf / 100 ft²
GS 10 Minute	18 lbf / 100 ft²

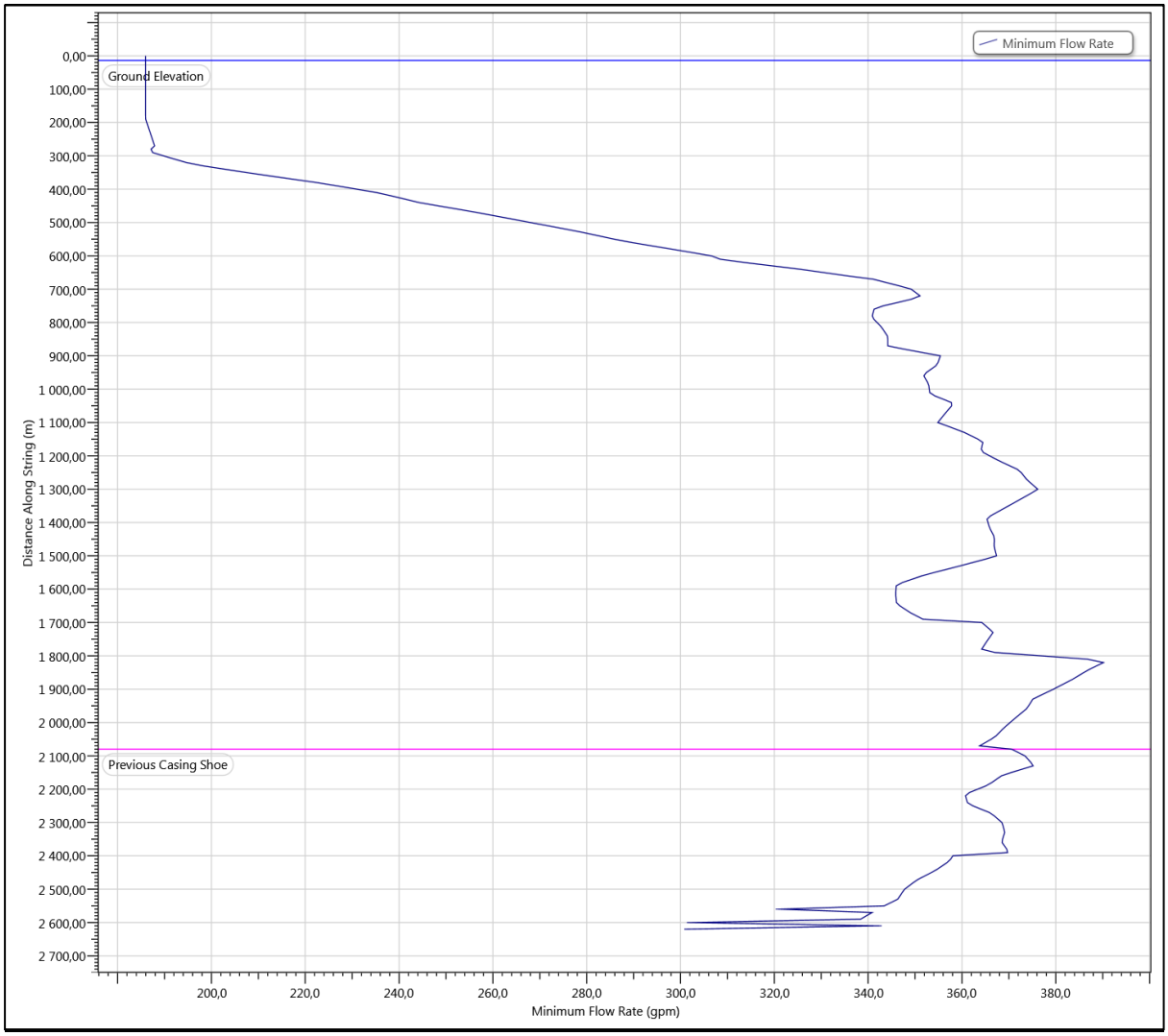

Figure 103 Minimum Flowrate Hole Section 8-1/2"

Based on minimum flowrate calculation, it needs a minimum flowrate 378 gallons per minute to clean this wellbore from the cuttings. Using this flowrate, it needs only one mud pump. The next step is to calculate the optimum hydraulic system using one mud pump and this drillstring configuration. The results of component pressure losses, hydraulic horsepower and jet impact force can be seen in the figure below :

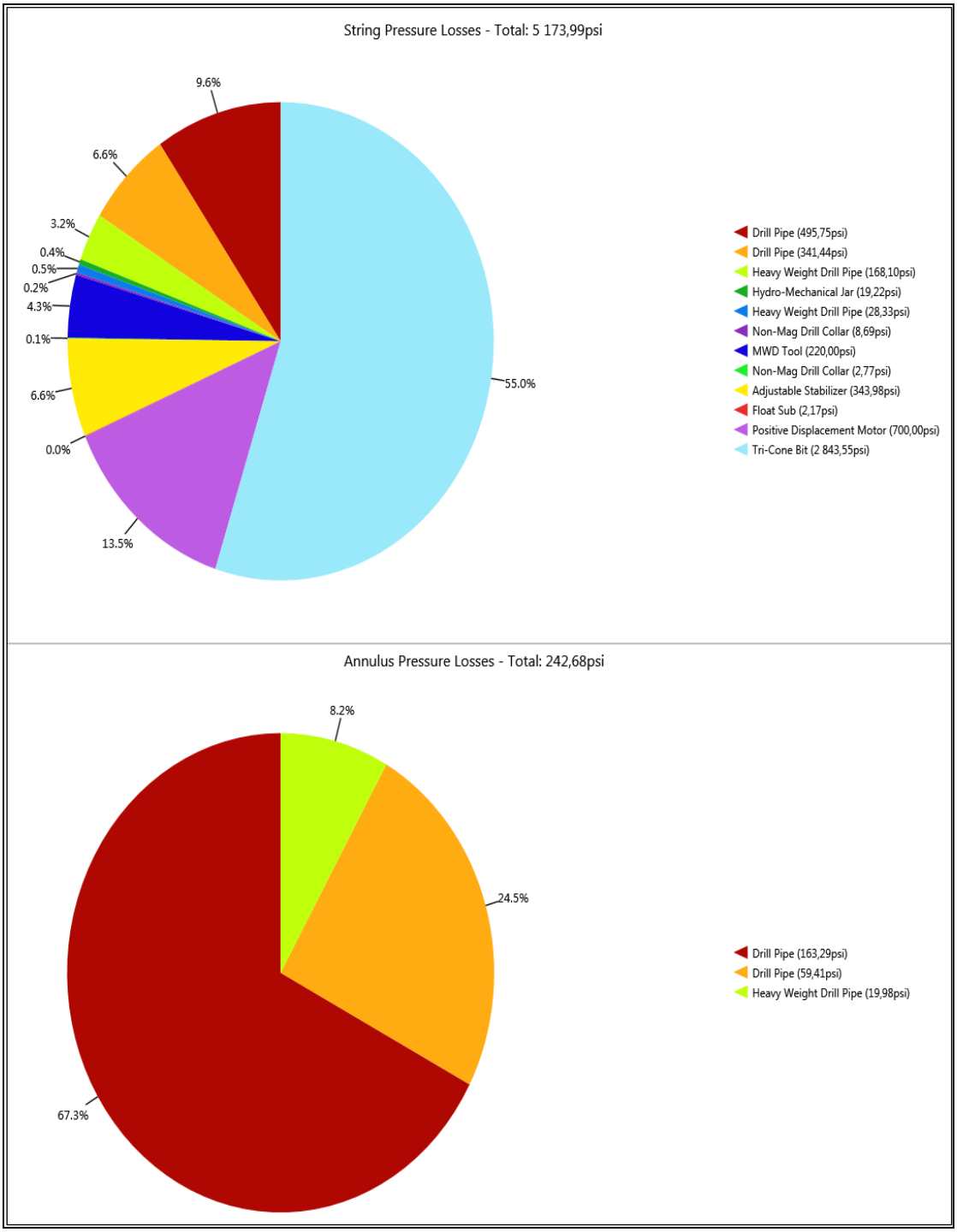

Figure 104 Component Pressure Losses Hole Section 8-1/2"

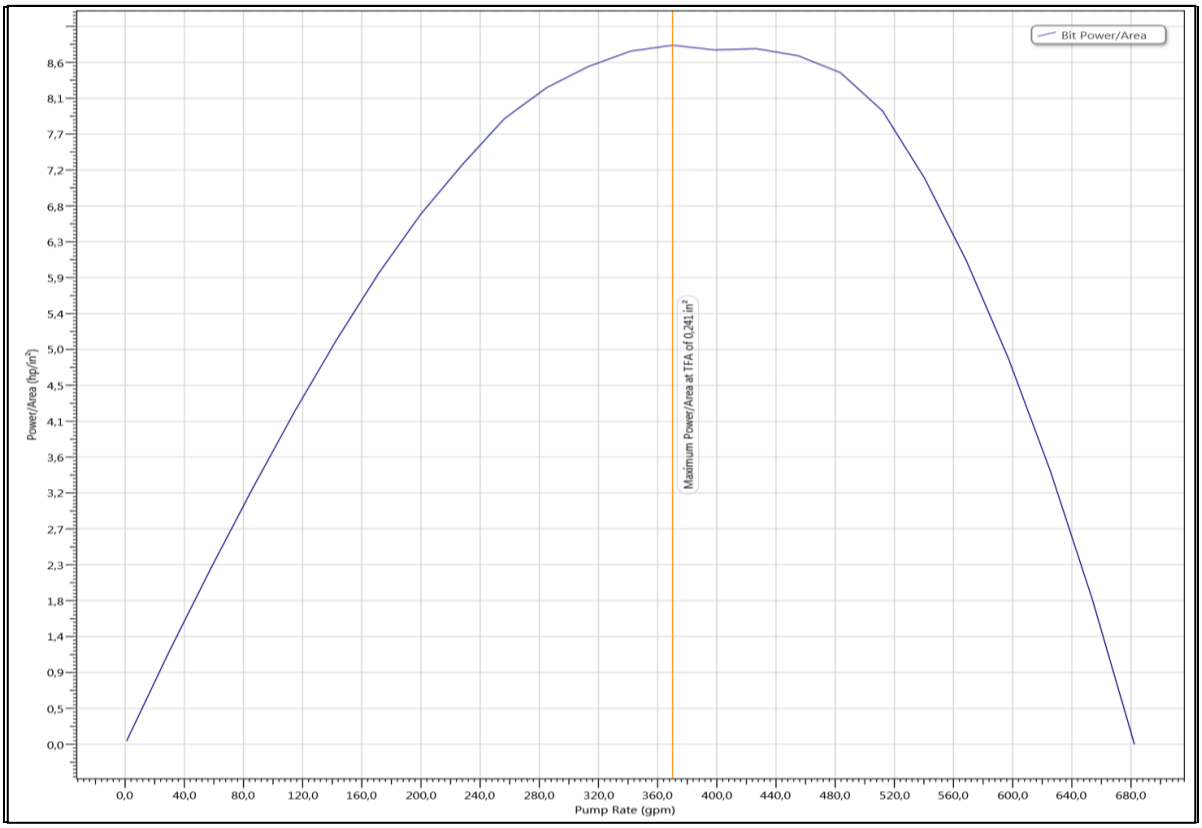

Figure 105 Hydraulic Horse Power Calculation for Hole Section 8-1/2"

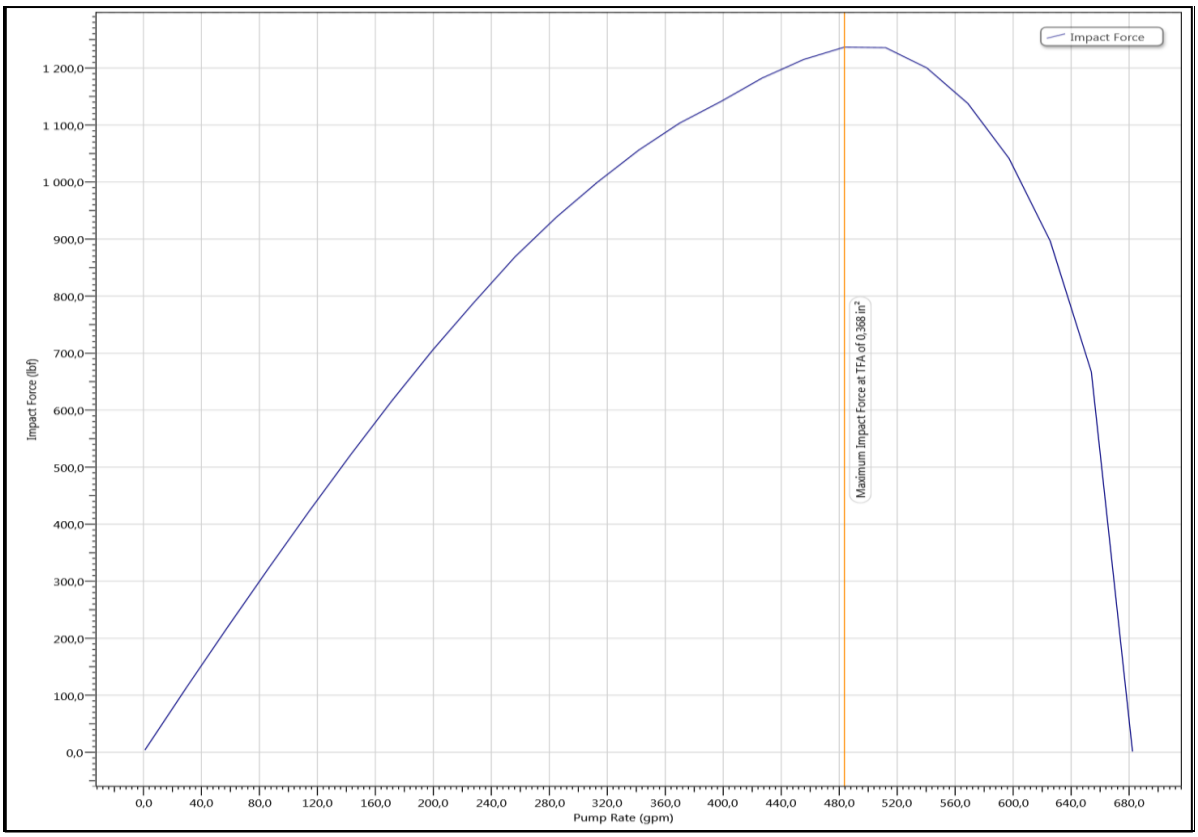

Figure 106 Jet Impact Force Calculation for Hole Section 8-1/2"

5. DISCUSSION

The results of the calculation in part 4 will discuss more details in this part. Rock mechanics properties are obtained from exploration well T-1 and these properties are used to estimate wellbore failure or wellbore collapse formation in directional well T-2. In this study will analyze more details in directional well T-2 because drilling in the directional well is more difficult than a vertical well. Furthermore, this study also will discuss about design drilling optimization in well T-2.

5.1 Wellbore Failure Sensitivity Analysis

This study will discuss wellbore failure sensitivity toward unconfined compressive strength (UCS) and inclination. UCS is the measure of the material's strength. It means that the bigger value of UCS, the stronger rock will be.

From the well Failure sensitivity analysis toward UCS chart, it can be seen that with increasing UCS value, the required mud weight become smaller. It means that to reach wellbore stability need less mud weight. From the three models to estimate wellbore collapse pressure, Stassi d' Alia gives the smallest value whereas Mohr-Coulomb gives the highest value. On the other side, Modified Lade gives the middle value between of them.

On the other hand, with increasing inclination, it needs more required mud weight. It means that wellbore will be easier in shear failure condition in higher inclination well than in vertical well. In higher inclination needs higher mud weight to keep wellbore stability. Using three methods in inclination sensitivity, Mohr coulomb gives the highest required mud weight to keep wellbore stability compare to the other methods. Whereas Stassi D' Alia gives the smallest required mud weight to keep wellbore stability compare to the other methods. Modified Lade give the middle value required mud weight.

Sensitivity toward horizontal stresses in relaxed basin where $\sigma_v > \sigma_H > \sigma_h$ give the results that wellbore collapse pressure (P_{wc}) is decrease with increasing the value of S_H. On the other hand, wellbore collapse pressure (P_{wc}) is increase with increasing the value of minimum horizontal stress (σ_h) even the increasing value is sharply. In wellbore stability application by using this analysis, drilling parallel to minimum horizontal stress is safer when drilling with high inclination or horizontal well because it need less mud weight to avoid from wellbore collapse.

In other case, sensitivity toward horizontal stresses in tectonically basin where $\sigma_H > \sigma_h > \sigma_v$ give the results that wellbore collapse pressure (P_{wc}) is increase with increasing the value of S_H. On the other hand, wellbore collapse pressure (P_{wc}) is increase with increasing the value of minimum horizontal stress (σ_h) even the increasing value is sharply.

In wellbore stability application by using sensitivity analysis in horizontal stresses, drilling parallel to minimum horizontal stress is safer than drilling parallel to maximum horizontal stress. It means that when drilling with high inclination or horizontal well, it need less mud weight to avoid from shear failure or wellbore collapse.

The results of these sensitivity analysis in this case can be seen easier through chart below:

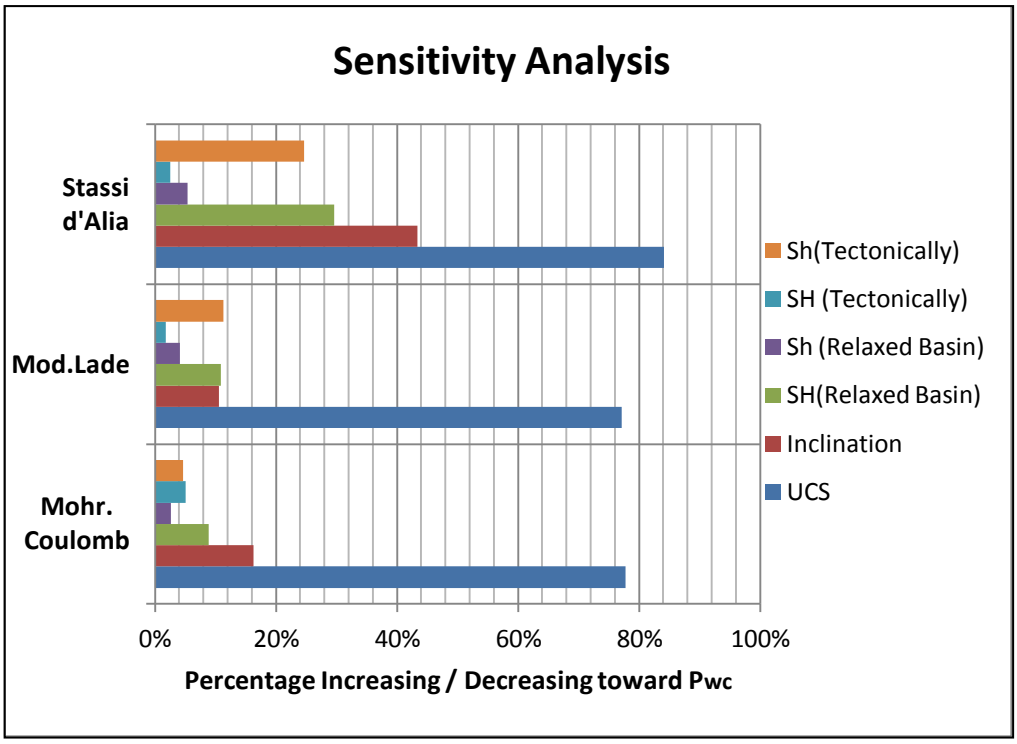

Figure 107 Summary in Sensitivity Analysis

Based on figure above show that unconfined compressive strength (UCS) gives the dominant effect in wellbore shear failure. It means that with higher UCS, it need less than mud weight to prevent shear failure. Maximum horizontal stress (S_H) in tectonically stressed basin gives the smallest effect in this sensitivity analysis using Modified Lade and Stassi d' Alia methods where these method involve three principal stresses whereas Mohr - Coulomb only involves two principal stresses.

5.2 Wellbore Stability

It is very important to avoid wellbore instability. An unstable wellbore is related to shear failure where borehole wall under compression. An unstable wellbore is happened when wellbore pressure is less than formation collapse pressure (Pwc). Consequently, wellbore will collapse and produce so much failed material from around the wellbore and sometimes these cutting materials have a bigger size and it is difficult to circulate out of wellbore. If these cutting cannot be circulated out of wellbore, it will cause hole pack off and subsequently it will cause pipe stuck.

In designing wellbore stability, a stable wellbore can be reached with increasing mud weight more than collapse pressure formation (P_{wc}) or by altering the well trajectory. In relaxed basin like in this case where $\sigma_v > \sigma_H > \sigma_h$, it is safer to drill a well with inclination more than 70^0 parallel to the minimum horizontal stress. In this case, calculation data from well T-2 will be used to design wellbore stability with keeping wellbore pressure greater than collapse pressure formation. Data from a previous calculation are plotted together to get the optimum mud weight in wellbore stability design. In this study will analyze the wellbore stability for directional well T-2. Data is normalized from original depth of reference (meter sea level) to depth of rotary kelly bushing (RKB). The elevation of kelly bushing in the rig is 13.7 meter. The results of this calculation can be seen in the figure below:

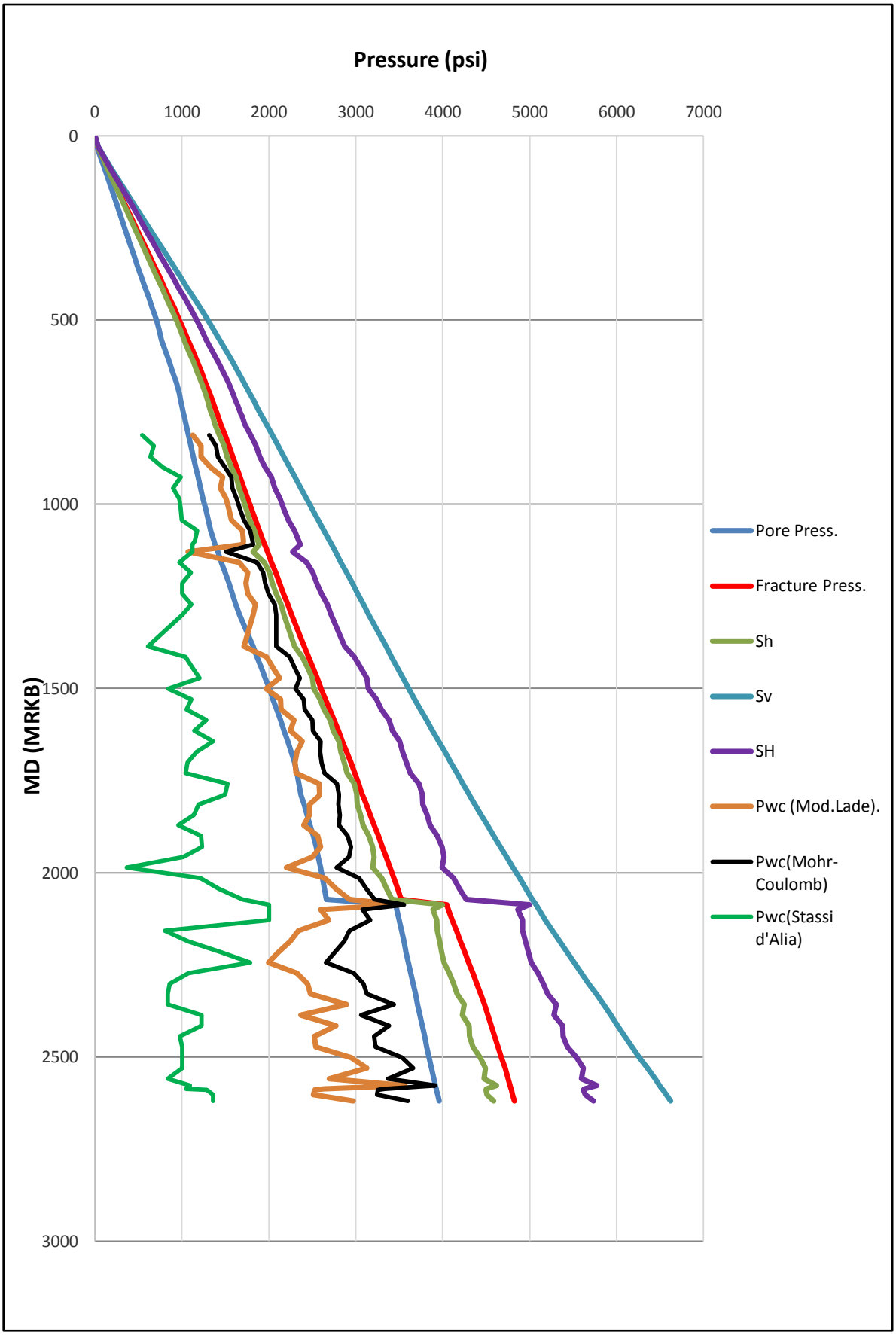

Figure 108 Wellbore Stability Design Well T-2 in Psi

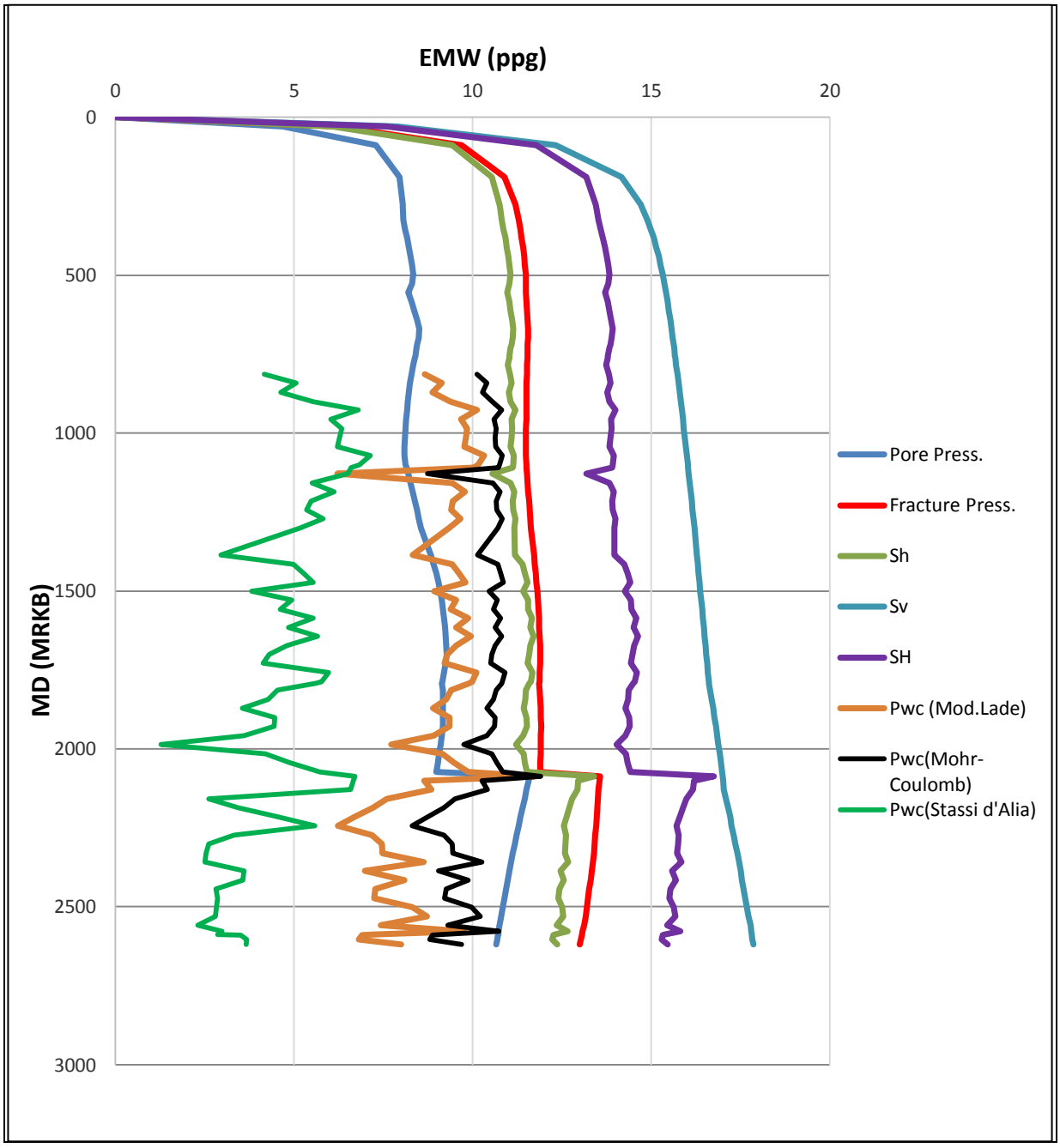

Figure 109 Wellbore Stability Design Well T-2 in EMW

From figure above, it can be seen that Mohr-Coulomb give the highest wellbore collapse pressure compare to the others because Mohr-Coulomb only uses minimum and maximum principal stress. On the other hand, Modified Lade and Stassi D' Alia use three principal stresses (σ_1, σ_2 and σ_3). From the calculation above also can be seen that in rock formation with higher cohesive strength like limestone, the value of wellbore collapse formation tends to smaller than pore pressure. It means that in a strong rock formation, there are no problems related to wellbore instability. Besides that, underbalanced drilling also can be applied in this formation without any problems related to wellbore instability as long as wellbore pressure greater than collapse pressure formation.

With knowing wellbore stability design, it will be easier to design mud weigh and design casing setting depth. In this case, will use data from calculation directional well T-2 using Modified lade method to determine the optimum mud weight to prevent wellbore instability problems during drilling. From wellbore stability design and analysis in type of formation, casing setting depth for directional well T-2 can be determined. The table below shows design casing setting depth for well T-2.

Table 21 Casing Setting Depth Well T-2

Casing Size	Hole Size	Depth	Remarks
inch	inch	M RKB	
30	36	30	Conductor Casing
20	26	270	Set to cover surface water
13⅜	17 ½	1200	Set in shale Formation to give casing integrity to drill next sect.
9⅝	12¼	2080	Set in shale Formation to give casing integrity to drill next sect.
7"	8½	2620	Liner casing to cover production zone. TOL @1870 mRKB

5.3 Casing Design

Based on fluid composition from formation, H_2S and CO_2 contents are low so the effect of corrosion that will decrease casing strength can be negligible. The results from the calculation will be used to choose the appropriate casing where this casing can withstand all of the design load. The discussion for types of casings will be explained separately.

5.3.1. Discussion in Surface Casing 20"

Before installing casing 20", conductor casing 26" is installed at depth 30 meters. The purpose to install casing 20" at depth 270 meter is to protect the water table. Based on the calculation with consider in worst case scenario, Casing with grade J-55, 94 pounds per feet (ppf) can withstand from burst, collapse and axial load.

Casing J-55, 94 pound per feet (ppf) needs to check in triaxial load and safety factor check. The results of this calculation can be seen in the figure below:

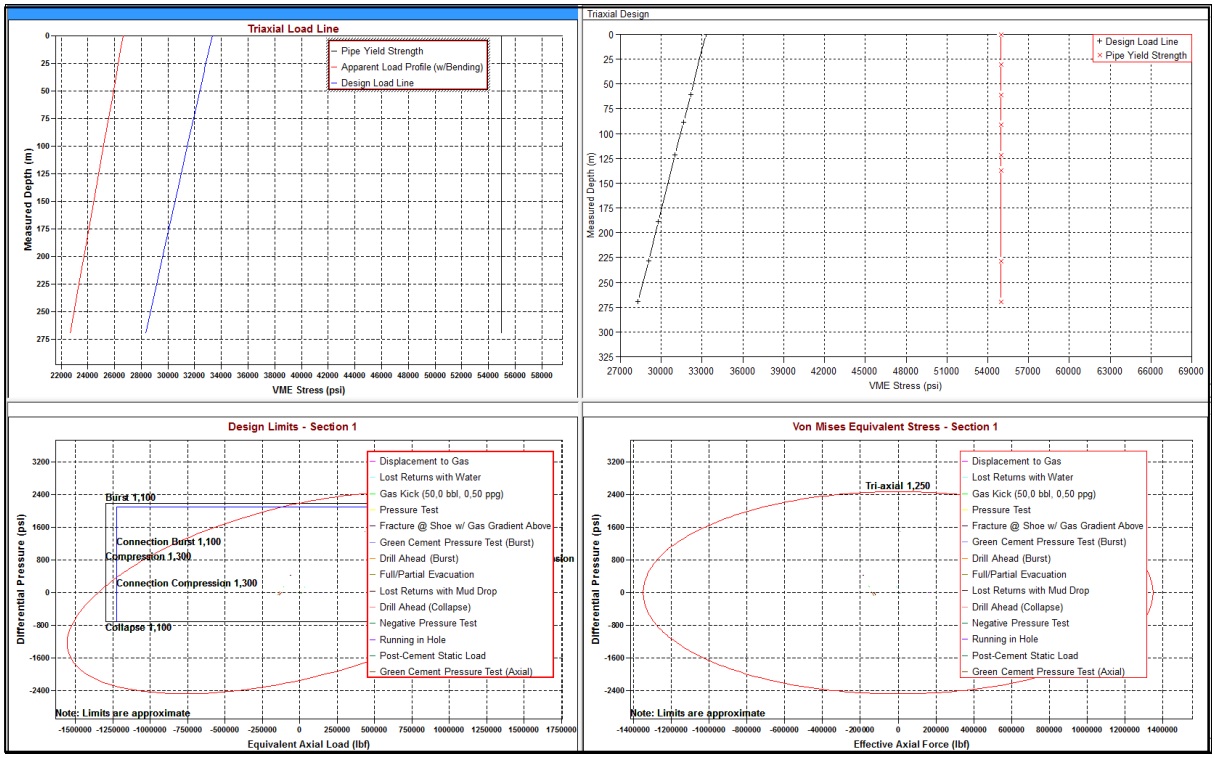

Figure 110 Triaxial and Design Factor Surface Casing 20"

From figure above, pipe yield strength casing J-55, 94 pounds per feet (ppf) greater than triaxial design. In the design limit, this casing also located in safe window between API design limit and Von Misses design limit so this casing is safe to be used and can withstand from all of the loads.

5.3.2. Discussion in Intermediate Casing 13-3/8"

The purposes to install 13-3/8" is to isolate loss circulation zone so that drilling for the next hole section will be safe from total loss circulation. Based on the calculation with consider in worst load case scenario, casing with grade C-95, 72 pounds per feet (ppf) cannot withstand from burst, collapse, axial load calculation from the surface to depth of interest so that it needs a partial section with casing grade above casing C-95, 72 ppf specification. Based on the analysis, casing P-110, 72 ppf can withstand all of these loads so that the casing configuration for this section can be seen in the table below:

Table 22 Casing 13-3/8" Configuration

Top, MD (m)	Base, MD (m)	OD (in)	Weight (ppf)	Grade
0	1100	13-3/8	72	C-95
1100	1200	13-3/8	72	P-110

These casings configuration need to check in triaxial load and safety factor check. The results of this calculation can be seen in the figure below:

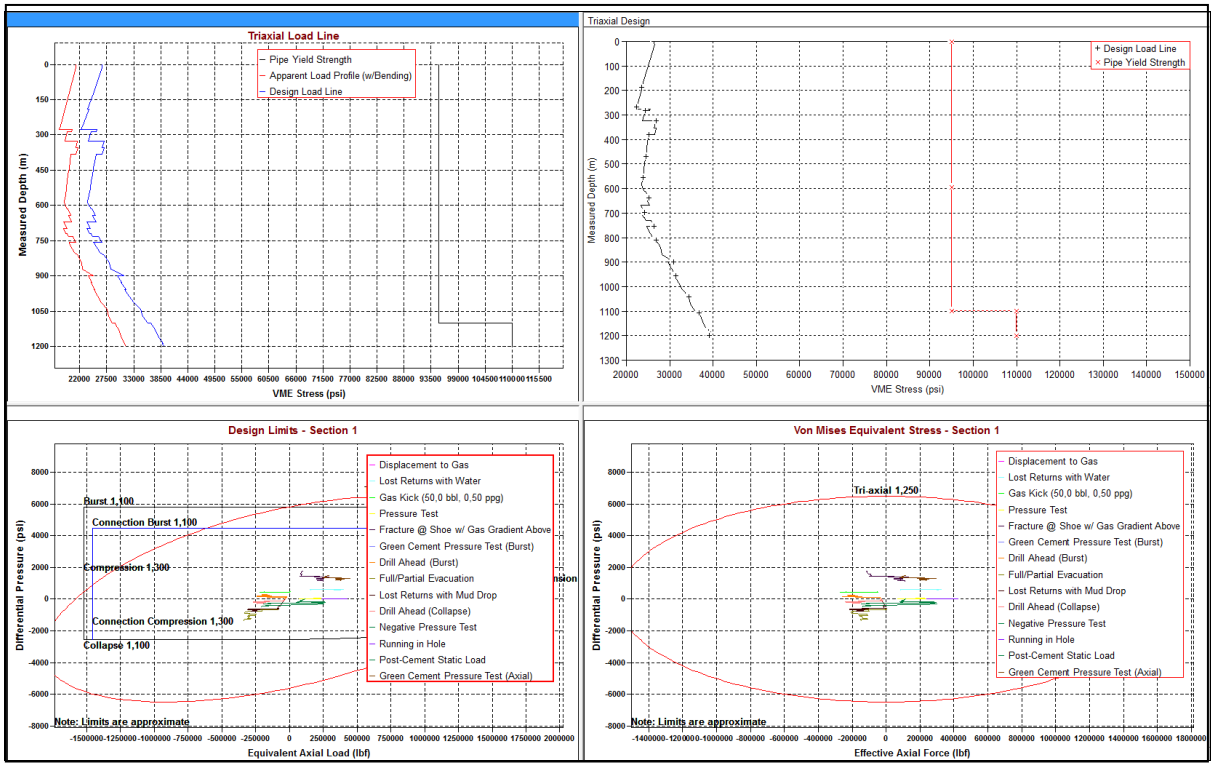

Figure 111 Triaxial and Design Factor Casing 13-3/8"

Based on figure above, these casings configurations are safe because this pipe yield strength is greater than triaxial design load line and these casing are located in a safe window between API design limit and Von Misses design limit.

5.3.3. Discussion in Intermediate Casing 9-5/8"

The main goal to install casing 9-5/8" at 2080 meter is to provide formation integrity purposes and to isolate formation before entering production zone so that it will be safe when drilling in the production zone. Based on the calculation with consider in worst load case scenario, casing with grade N-80, 40 pounds per feet (ppf) cannot withstand from burst, collapse, axial load from the surface to depth of interest so that it needs a partial section with this casing specification. Based on the analysis, casing P-110, 72 ppf can withstand all of these loads so that the casing configuration for this section can be seen in the table below:

Table 23 Casing 13-3/8" Configuration

Top, MD (m)	Base, MD (m)	OD (in)	Weight (ppf)	Grade
0	1400	9-5/8	40	N-80
1400	2080	9-5/8	43.5	P-110

These casings configuration need to check in triaxial load and safety factor check. The results of this calculation can be seen in the figure below:

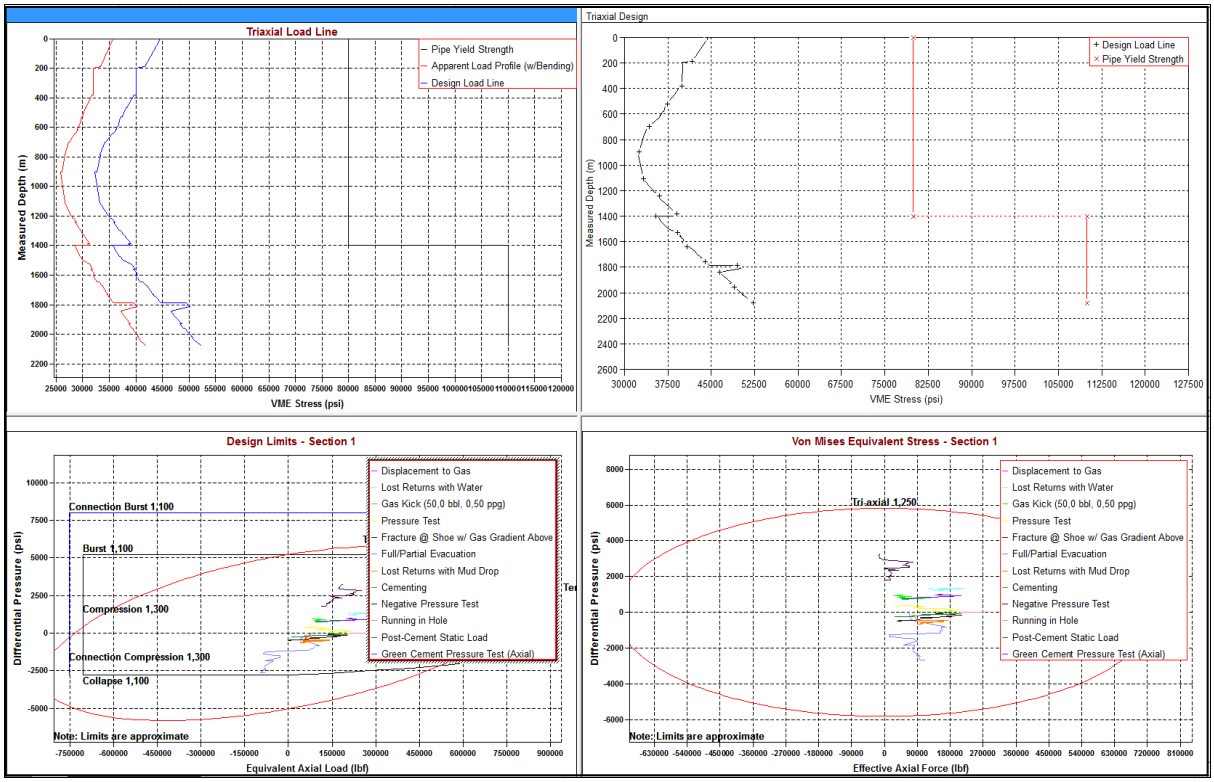

Figure 112 Triaxial and Design Factor Casing 9-5/8"

Based on figure above, these casings configurations are safe because this pipe yield strength is greater than triaxial design load line and these casing are located in a safe window between API design limit and Von Misses design limit.

5.3.4. Discussion in Liner Casing 7"

The main goal to install liner 7" is to provide formation integrity and to isolate the zone of production. Based on the calculation with consider in worst case scenario, liner 7" with grade N-80, 26 pounds per feet (ppf) can withstand from the burst, collapse and axial load. This liner is hung at depth 2010 meter.

Liner 7", N-80, 26 pounds per feet (ppf) need to check in triaxial load and safety factor check. The results of this calculation can be seen in the figure below:

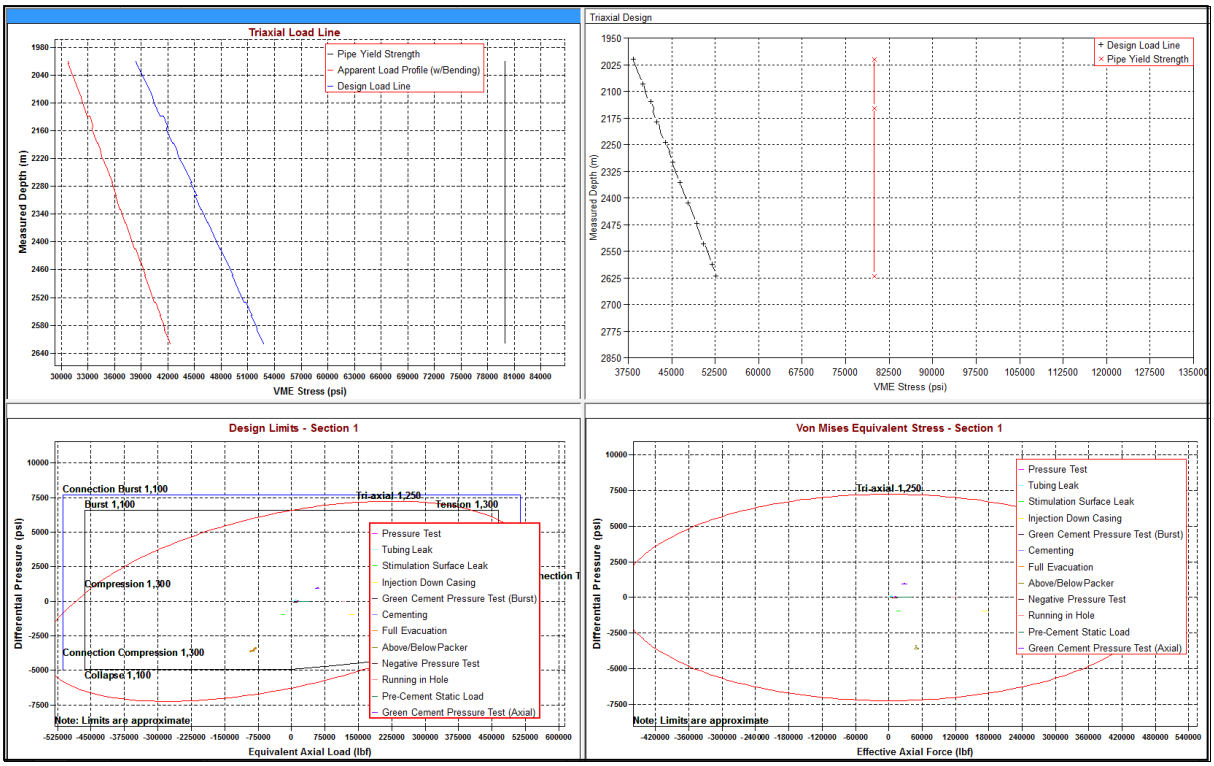

Figure 113 Triaxial and Design Factor Liner 7"

Based on figure above, these casings configurations are safe because this pipe yield strength is greater than triaxial design load line and these casing are located in a safe window between API design limit and Von Misses design limit.

5.4 Cutting Transport and Hydraulic Design

Hole cleaning or cutting transport is a complex process that involves many parameters like fluid rheology, cutting loading parameters, etc. Higher mud density, plastic viscosity, yield point have a positive impact in hole cleaning and make hole cleaning become easier. On the other hand, with higher of these parameters will give impact in higher equivalent circulating density (ECD) while pumping and the worst case this ECD will exceed fracture pressure. If ECD more than fracture formation, loss circulation will happen and this is very dangerous in drilling operation. In this thesis, ECD will be kept above collapse pressure and below minimum horizontal stress (σh) to avoid formation failure like a breakout. To reach this goal, the optimum flowrate rate must be selected. The selection of optimum flowrate also has to consider in the optimization of hydraulic design so that this is can enhance bit performance and to avoid bit balling. In this thesis, the optimization in hydraulic design will analyze in their hole section, they are hole section 17-1/2", 12-1/4" and 8-1/2". Every hole section will be discussed separately.

5.4.1. Cutting Transport and Hydraulic Design Discussion in Hole section 17-1/2"

Based on cutting transport calculation, jet impact force and hydraulic horse power graphs, the optimum flowrate 1465 gallon per minute is chosen. The results calculation using this optimum flowrate can be seen in the table below :

Table 24 Hydraulic Optimization Result in Hole Section 17-1/2"

Bit Size	Flowrate	SPP	Bit Press.Loss	Bit Impact Force	BHP	HSI
inch	gpm	psi	psi	lbf	hp	hp / in^2
17-1/2	1465	4984.23	1919.46	3297.8	1640.34	6

Using this high flowrate, the optimization in jet impact force will give maximum impact force at the bit and will enhance bit performance. To optimize Jet impact force, Based on jet impact force graph can be chosen total flow area (TFA) for bit nozzle. The table below gives the information output in determination total flow area :

Table 25 Bit Nozzle Optimization for Hole Section 17-1/2"

Bit Size	Total Flow Area	Nozzle Size	Nozzle Velocity
iinch	in^2		ft /s
17-1/2	0.952	2 x 20 1 x 21	493.8

Using this optimum flow rate, it is very important to maintain equivalent circulating density less than fracture pressure formation to avoid formation break and consequently to avoid loss circulation. Moreover, in this case, ECD will be kept greater than collapse pressure formation and less than minimum horizontal stress to maintain wellbore stability and to avoid wellbore failure from shear failure. Using software wellplan, equivalent circulating density (ECD) can be seen in the figure below:

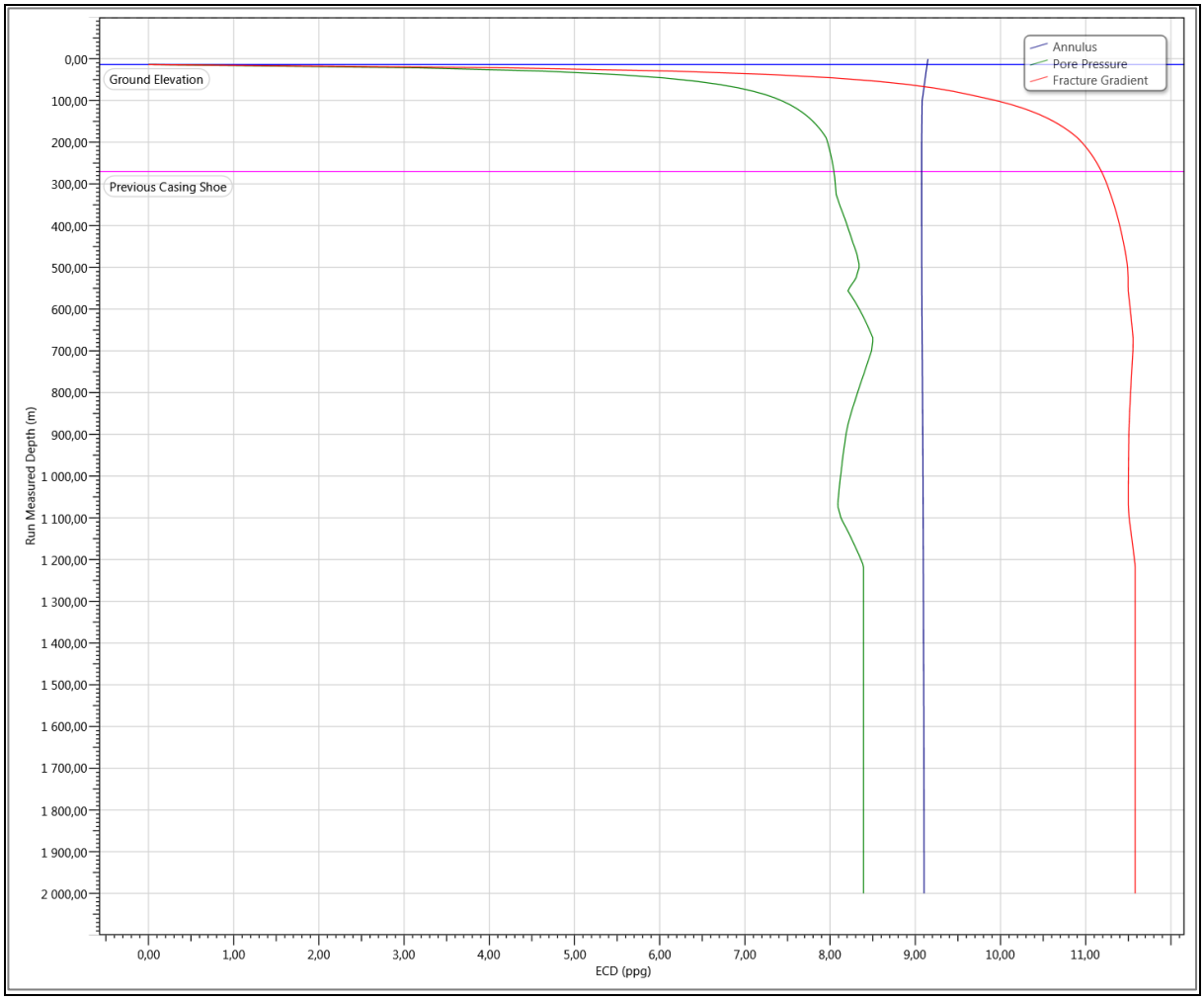

Figure 114 ECD for Hole Section 17-1/2"

In this section does not discuss detail about torque and drag, but in this section just only make sure that drillstring in this section is safe to be used in drilling. Table below shows the analysis results using wellplan software using weight ob bit (WOB) 15 Klb.

Table 26 String Analysis for Hole Section 17-1/2"

Operation	Stress Failure			Buckling Limits			Torque Failure	Measured Weight (kip)	Stretch (m)				Rotary Table Torque (ft-lbf)	Windup With Torque (revs)	Windup Without Torque (revs)	Axial Stress = 0 [From TD] (m)	Surface Neutral Point [From TD] (m)
	Fatigue	90% Yield	100% Yield	Sinusoidal	Helical	Lockup			Mechanical	Ballooning	Thermal	Total					
Tripping In								143,7	0,85	-0,34	-0,39	0,12	0,0	0,0	0,0	72,77	0,00
Tripping Out								206,4	1,08	-0,34	-0,39	0,34	0,0	0,0	0,0	72,77	0,00
Rotating On Bottom								155,8	0,88	-0,34	-0,39	0,15	11 841,1	0,9	0,7	72,77	56,86
Slide Drilling								133,2	0,79	-0,34	-0,39	0,06	2 000,0	0,2	0,0	72,77	79,69
Backreaming								270,8	1,45	-0,34	-0,39	0,72	19 204,2	1,3	1,1	7,32	0,00
Rotating Off Bottom								170,8	0,96	-0,34	-0,39	0,22	11 107,8	0,8	0,8	72,77	0,00

5.4.2. Cutting Transport and Hydraulic Design Discussion in Hole section 12-1/4"

Based on cutting transport calculation, jet impact force and hydraulic horsepower graphs, the optimum flowrate 830 gallons per minute is chosen. The results calculation using this optimum flowrate can be seen in the table below :

Table 27 Hydraulic Optimization Result in Hole Section 12-1/4"

Bit Size	Flowrate	SPP	Bit Press.Loss	Bit Impact Force	BHP	HSI
inch	gpm	psi	psi	lbf	hp	hp/in^2
12-1/4	830	4950.54	1919.50	2040.9	929.36	6.9

Using this high flowrate, the optimization in jet impact force will give maximum impact force at the bit and will enhance bit performance. To optimize Jet impact force, Based on jet impact force graph can be chosen total flow area (TFA) for bit nozzle. The table below gives the information output in determination total flow area :

Table 28 Bit Nozzle Optimization for Hole Section 12-1/4"

Bit Size	Total Flow Area	Nozzle Size	Nozzle Velocity
inch	in^2		ft /s
12-1/4	0.589	3 x 16	452.1

Using this optimum flow rate, it is very important to maintain equivalent circulating density less than fracture pressure formation to avoid formation break and consequently to avoid loss circulation. Moreover, in this case, ECD will be kept greater than collapse pressure formation and less than minimum horizontal stress to maintain wellbore stability and to avoid wellbore failure from shear failure. Using software wellplan, equivalent circulating density (ECD) can be seen in the figure below:

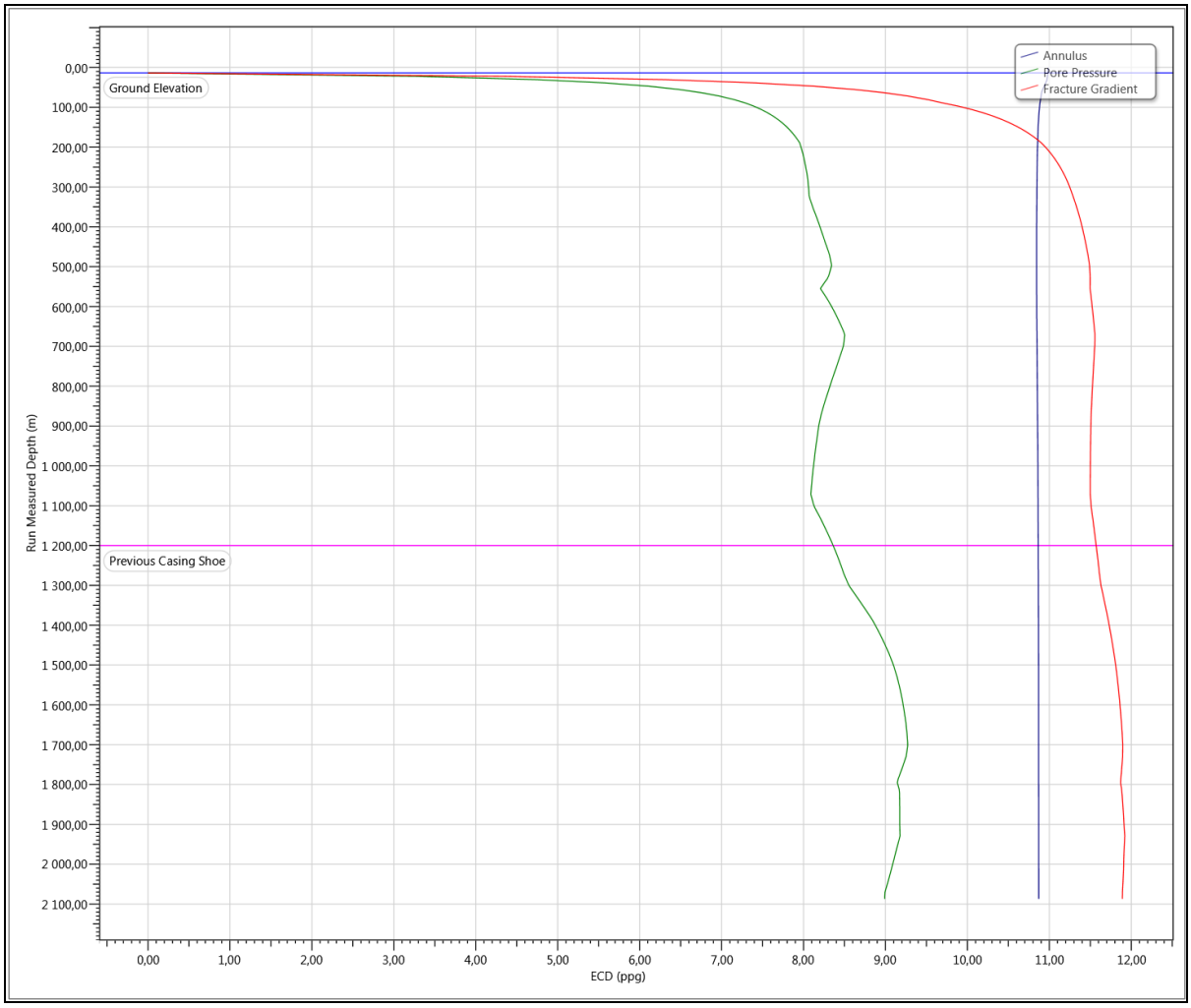

Figure 115 ECD for Hole Section 12-1/4"

In this section does not discuss detail about torque and drag, but in this section just only make sure that drillstring in this section is safe to be used in drilling. Table below shows the analysis results using wellplan software using weight ob bit (WOB) 15 Klb.

Table 29 String Analysis for Hole Section 12-1/4"

Operation	Stress Failure			Buckling Limits			Torque Failure	Measured Weight (kip)	Stretch (m)				Rotary Table Torque (ft-lbf)	Windup With Torque (revs)	Windup Without Torque (revs)	Axial Stress = 0 [From TD] (m)	Surface Neutral Point [From TD] (m)
	Fatigue	90% Yield	100% Yield	Sinusoidal	Helical	Lockup			Mechanical	Ballooning	Thermal	Total					
Tripping In								134,0	1,00	-0,30	-0,49	0,20	0,0	0,0	0,0	67,49	0,00
Tripping Out								193,8	1,39	-0,30	-0,49	0,60	0,0	0,0	0,0	67,49	0,00
Rotating On Bottom								144,5	0,99	-0,30	-0,49	0,20	8 412,6	2,3	1,9	67,49	250,85
Slide Drilling								121,4	0,82	-0,30	-0,49	0,02	1 000,0	0,4	0,0	67,49	398,43
Backreaming								259,5	2,42	-0,30	-0,49	1,62	16 537,3	3,8	3,4	9,62	0,00
Rotating Off Bottom								159,5	1,18	-0,30	-0,49	0,38	8 232,1	2,0	2,0	67,49	0,00

5.4.3. Cutting Transport and Hydraulic Design Discussion in Hole section 8-1/2"

Based on cutting transport calculation, jet impact force and hydraulic horsepower graphs, the optimum flowrate 400 gallons per minute is chosen. The results calculation using this optimum flowrate can be seen in the table below :

Table 30 Hydraulic Optimization Result in Hole Section 12-1/4"

Bit Size	Flowrate	SPP	Bit Press.Loss	Bit Impact Force	BHP	HSI
inch	gpm	psi	psi	lbf	hp	hp/in^2
8-1/2	400	5517	2844	1263.7	663.5	10.6

Using this flowrate, the optimization hydraulic horsepower method will give maximum energy dissipated at the bit and this will enhance bit performance. To optimize hydraulic horsepower, based on optimizing hydraulic horsepower graph can be chosen total flow area (TFA) for bit nozzle. The table below gives the information output in the determination total flow area :

Table 31 Bit Nozzle Optimization for Hole Section 8-1/2"

Bit Size	Total Flow Area	Nozzle Size	Nozzle Velocity
inch	in^2		ft /s
8-1/2	0.246	2 x 10 1 x 11	521.2

Using this optimum flow rate, it is very important to maintain equivalent circulating density less than fracture pressure formation to avoid formation break and consequently to avoid loss circulation. Moreover, in this case, ECD will be kept greater than collapse pressure formation and less than minimum horizontal stress to maintain wellbore stability and to avoid wellbore failure from shear failure. Using software wellplan, equivalent circulating density (ECD) can be seen in the figure below:

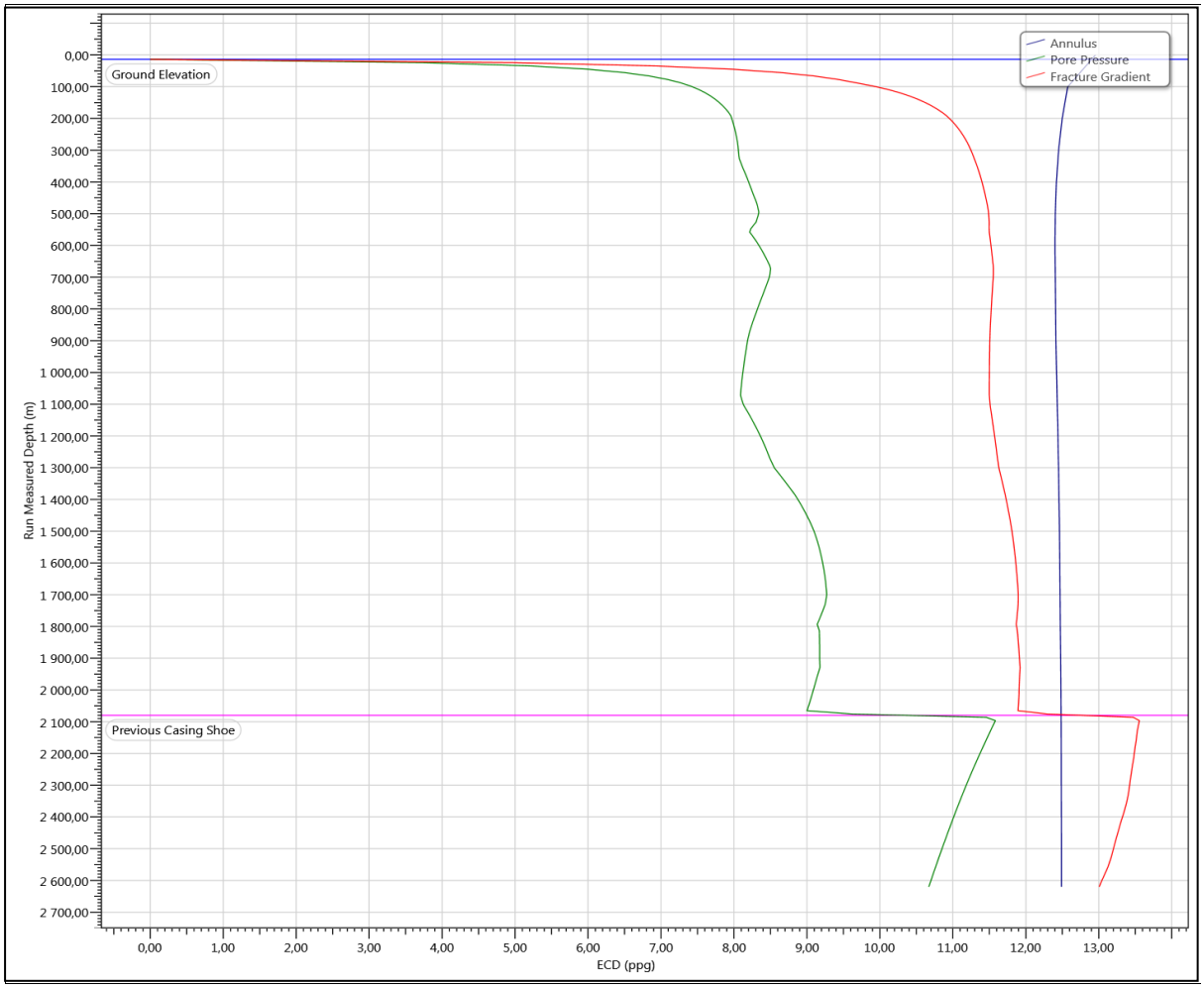

Figure 116 ECD for Hole Section 8-1/2"

In this section does not discuss detail about torque and drag, but in this section just only make sure that drillstring in this section is safe to be used in drilling. The reason using drillpipe 4-1/2" above heavy weigh drillpipe is to avoid fatigue by reducing contact angle between casing and drillpipe because if it is used drillpipe 5" above heavy weight drillpipe, it can cause fatigue. Table below shows the analysis results using wellplan software using weight ob bit (WOB) 18 Klb

Table 32 String Analysis for Hole Section 8-1/2"

Operation	Stress Failure			Buckling Limits			Torque Failure	Measured Weight (kip)	Stretch (m)				Rotary Table Torque (ft-lbf)	Windup With Torque (revs)	Windup Without Torque (revs)	Axial Stress = 0 [From TD] (m)	Surface Neutral Point [From TD] (m)
	Fatigue	90% Yield	100% Yield	Sinusoidal	Helical	Lockup			Mechanical	Ballooning	Thermal	Total					
Tripping In								809,1	1,53	-0,42	-0,15	0,96	0,0	0,0	0,0	227,66	0,00
Tripping Out								900,7	2,23	-0,42	-0,15	1,66	0,0	0,0	0,0	210,79	0,00
Rotating On Bottom								829,8	1,59	-0,42	-0,15	1,02	11 631,3	3,7	3,2	227,66	176,32
Slide Drilling								798,1	1,32	-0,42	-0,15	0,75	1 000,0	0,6	0,0	227,66	232,34
Rotating Off Bottom								847,8	1,85	-0,42	-0,15	1,28	11 819,0	3,4	3,4	227,66	0,00

6. CONCLUSION

Based on the calculation and analysis in wellbore failure criteria and drilling optimization using landmark software, it can be concluded that:

- Wellbore will be easier in failure condition in weaker formation (lower cohesive strength or lower unconfined compressive strength). It means that it is needed the higher mud weight or wellbore pressure to prevent shear failure in formation.
- The higher inclination, it requires higher mud weight to prevent shear failure in formation.
- Sensitivity in horizontal stresses in relaxed and tectonically stressed basin give the results that sensitivity in minimum horizontal stress (σ_h) needs higher pressure to avoid wellbore failure or wellbore collapse than sensitivity in maximum horizontal stress (σ_H). In wellbore stability application, it means that drilling parallel to minimum horizontal stress (σ_h) is safer than drilling parallel to maximum horizontal stress (σ_H) because when drilling parallel to minimum horizontal stress needs less wellbore pressure to keep wellbore from failure condition.
- Unconfined compressive strength (UCS) give the dominant effect in wellbore failure sensitivity. On the other hand maximum horizontal stress (S_H) in tectonically stressed basin gives the smallest effect.
- Stassi d'Alia method gives the smallest value in formation collapse pressure calculation. Mohr-Coulomb method gives the highest value in formation collapse pressure calculation and Modified Lade method give a value between of them.
- Based on drilling data and final well report from offset well T-1, Modified Lade give the best result and give near real value in using mud weight in predicting wellbore collapse failure criteria so that design wellbore stability to drill directional well T-2 use Modified Lade method to avoid wellbore problems.
- Wellbore stability problems also time dependency so it need to avoid open hole exposure time too long especially when drilling using water based mud.
- Casings configuration for well T-2 below are designed based on worst case scenario and these casing can withstand from burst, collapse, axial and triaxial load

	Top, MD (m)	Base, MD (m)	OD (in)	Weight (ppf)	Grade
Surface Casing	0	270	20	94	J-55
Intermediate Casing	0	1100	13-3/8	72	C-95
	1100	1200	13-3/8	72	P-110
Intermediate Casing	0	1400	9-5/8	40	N-80
	1400	2080	9-5/8	43.5	P-110
Liner	2010	2620	7	26	N-80

- The results of cutting transport and hydraulic optimization calculation for well T-2 can be summarized in table below:

Bit Size	Nozzle Size	Nozzle Velocity	Flow Rate	Bit Impact Force	BHP
inch		ft /s	gpm	lbf	hp
17-1/2	2 x 20 1 x 21	493.8	1465	3297.8	1640.34
12-1/4	3 x 16	452.1	830	2040.9	929.36
8-1/2	2 x 10 1 x 11	521.2	400	1263.7	663.5

- The optimization in hole section 17-1/2" and 12-1/4" use jet impact force method where by using high flowrate and optimization in bit nozzle size can maximize bit impact force and increase bit performance.
- The optimization in hole section 8-1/2" use hydraulic horse power (HHP) method where by using optimum flowrate and optimization in bit nozzle will maximize horse power loss at drilling bit and increase bit performance.
- The optimum flowrate is used to transport cutting from wellbore to surface where the optimum flow rate must be greater than minimum flow rate to transport cutting from wellbore to surface.
- It is very important to keep wellbore pressure during circulation using the optimum flow rate so that equivalent circulating density (ECD) during pumping located in between collapse pressure formation and minimum horizontal stress to prevent shear failure formation or collapse formation.

7. FUTURE WORK

Based on calculation and analysis in this thesis, below are several recommendations for future study which will be useful in the University of Stavanger:

- By knowing rock mechanic properties like cohesive strength and unconfined compressive strength can be used to design optimization in weight on a bit so that drilling optimization can be optimized.
- Study about maximum horizontal stress so that the value of maximum horizontal stress can be determined precisely.

REFERENCES

1. Aadnøy, B. S. & Hansen, A. K. , 2005. Bounds on In-situ Stress Magnitudes Improve Wellbore Stability Analyses. *Journal of Petroleum Science and Engineering*, pp. 115 - 120.
2. Aadnøy, B. S., 2003. Introduction to Special Issue Wellbore Stability. *Journal of Petroleum Science and Engineering*, pp. 79-82.
3. Aadnøy, B. S., 2010. *Modern Well Design*. 2 ed. Boca Raton: CRC Press/ Balkema .
4. Aadnøy, B. S. & Chenevert, M. E., 1987. Stability of Highly Inclined Boreholes. *Society of Petroleum Engineers*, pp. 364-374.
5. Aadnøy, B. S. & Looyeh, R., 2011. *Petroleum Rock Mechanincs* . s.l.:Gulf Professional Publishing.
6. Zoback, M. D. , 2010. *Reservoir Geomechanics*. Stanford University.
7. Amoco, 2010. *Drilling handbook* : Wellbore Stability"
8. Ewy, R.T., 1999. Wellbore-Stability Prediction by Use of a Modified Lade Criterion. *Journal SPE Drilling & Completion*. SPE-56862. Res. 14: 85-91.
9. Stassi D' Alia, F. 1967. Flow and Fracture of Materials According to a New Limiting Condition of Yielding. *J. Mechanica*. Res. 2: 178-195
10. Velocity analysis in Practice. Retrived from www.xsgeo.com
11. Clark, R. K., Bickham, K. L. A Mechanistic Model for Cuttings Transport. SPE paper 28306 presented at the *SPE 69th Annual Technical Conference and Exhibition*, New Orleans, September 25–28.
12. Luo, Yuejin and P. A. Bern, BP Research Centre; and D. B.Chambers, BP Exploration Co. Ltd. Flow-Rate Predictions for Cleaning Deviated Wells. *IADC/SPE* 23884.
13. Luo, Yuejin, P. A. Bern, D. B.Chambers, BP Exploration. Simple Charts to Determine Hole Cleaning Requirements in Deviated Wells. *IADC/SPE* 27486.
14. Peden, J. M., Heriot-Watt U., Yuejin Luo. Settling Velocity of Various Shaped Particles in Drilling and Fracturing Fluids. *SPE/IADC* 16243.
15. Rabia, H. Rig Hydraulics. Entrac Software: Newcastle, England (1989): Chapter 5.
16. Scott, K. F. A New Approach to Drilling Hydraulics. *Petroleum Engineer*. September 1972.
17. Rahimi, R. & Nygaard, R., 2014. What Difference Does Selection of Failure Criteria Make in Wellbore Stability Analysis?. *ARMA* 14-7146.
18. G. Stjern. 2000. Improving Drilling Performance in Troublesome Clay Formation in Heidrun Field. *IADC / SPE* 59219.

SYMBOLS AND ABBREVIATIONS

θ	Angle, degree
ϕ	Angle of Internal Friction, degree
D_H	Annulus diameter, inch
V_A	Average fluid velocity for annulus, ft/s
σ_a	Axial Stress, psi
D_B	Bit diameter, inch
ρ	Bulk Density, gr/cm^3
BHP	Bit hydraulic power, hp
a, b, c	Coefficients
μ	Coefficient of Friction
S_o	Cohesive Strength, psi
V_p	Compressional Velocity, m/s
K	Consistency factor
V_{afv}	Critical transport fluid velocity , ft/s
ρ_c	Cuttings density, gr / cm^3
D_C	Cuttings diameter, inch
V_{av}	Cuttings travel velocity, ft/s
z	Depth, m
Δp	Differential pressure, psi
EMW	Equivalent mud weight, ppg
F_e	Effective stress, psi
n	Flow behavior index
ρ	Fluid density, ppg
F	Force , lb
r_i	Inside radius, inch
σ_2	Intermediate Principal Stress, psi
Δt	Interval Transit Time, µs/ft
V_{int}	Interval Velocity, m/s
σ_H	Maximum Horizontal Stress, psi
S_H	Maximum Horizontal Stress, psi
σ_1	Maximum Principal Stress, psi

MD	Measured depth, m
MSL	Meter sea level, m
σ_h	Minimum Horizontal Stress, psi
S_h	Minimum Horizontal Stress, psi
σ_3	Minimum Principal Stress, psi
τ_y	Mud yield stress
l	New Length, m
σ_n	Normal Stress, psi
σ_x	Normal Stress in Plane X, psi
σ_y	Normal Stress in Plane Y, psi
σ_z	Normal Stress in Plane Z, psi
lo	Original Length, m
V_{so}	Original slip velocity, ft/s
r_o	Outside radius, inch
R_e	Particle Reynolds number
D_p	Pipe diameter, inch
PV	Plastic viscosity, cp
ν	Poisson Ratio
ppf	Pound per feet
P_0	Pore pressure, psi
Ppg	Pound per gallon
G_{pl}	Power law geometry factor
σ_r	Radial Stress, psi
V_r	Rate of penetration, m/hr
R_a	Reynolds number
V_{rms}	Root Mean Square Velocity, m/s
RKB	Rotary kelly bushing
τ	Shear Stress, psi
V_s	Shear Velocity, ft/s
V_{sv}	Slip velocity, ft/s
ε	Strain
σ	Stress, psi
A	Surface Area, $inch^2$

σ_t	Tangential Stress, psi
σ_θ	Tangential Stress, psi
T_0	Tensile Strength, psi
β	The Orientation of Failure Plane
D_{TJ}	Tool joint diameter, inch
V_{Tc}	Total cuttings velocity, ft/s
TVD	Total vertical depth, m
C_0	Unconfined Compressive Strength, psi
σ_v	Vertical Stress, psi
S_v	Vertical Stress, psi
σ_y	Von Mises stress, psi
P_{wc}	Wellbore collapse pressure, psi
YP	Yield point, lb/100ft
E	Young's modulus, psi

APPENDICES

A. Wellpath T-2 Using Calculation Method: Minimum Curvature

MD (m)	INC (°)	AZ (°)	TVD (m)	DLS (°/100ft)	AbsTort (°/100ft)	RelTort (°/100ft)	VSect (m)	NS (m)	EW (m)	Build (°/100ft)	Walk (°/100ft)
0,00	0,00	0,00	0,00	0,00	0,00	0,00	0,00	0,00	0,00	0,00	0,00
30,00	0,00	0,00	30,00	0,00	0,00	0,00	0,00	0,00	0,00	0,00	0,00
89,00	0,00	60,00	89,00	0,00	0,00	0,00	0,00	0,00	0,00	0,00	0,00
189,00	0,00	120,00	189,00	0,00	0,00	0,00	0,00	0,00	0,00	0,00	0,00
276,00	0,50	220,00	276,00	0,18	0,06	0,00	-0,29	-0,29	-0,24	0,18	0,00
277,00	0,50	220,00	277,00	0,00	0,06	0,00	-0,30	-0,30	-0,25	0,00	0,00
284,50	0,18	330,87	284,50	2,39	0,12	0,00	-0,31	-0,31	-0,28	-1,30	450,58
325,00	2,39	243,33	324,99	1,80	0,33	0,00	-0,64	-0,64	-1,06	1,66	-65,88
354,00	5,66	238,18	353,91	3,45	0,58	0,00	-1,66	-1,66	-2,82	3,44	-5,41
382,82	9,14	236,47	382,49	3,69	0,82	0,00	-3,68	-3,68	-5,93	3,68	-1,81
411,81	12,09	236,35	410,98	3,10	0,98	0,00	-6,63	-6,63	-10,38	3,10	-0,13
440,42	14,14	237,86	438,84	2,21	1,06	0,00	-10,15	-10,15	-15,84	2,18	1,61
469,07	17,01	237,44	466,44	3,06	1,18	0,00	-14,27	-14,27	-22,33	3,05	-0,45
497,65	19,64	237,90	493,56	2,81	1,27	0,00	-19,07	-19,07	-29,93	2,80	0,49
526,48	22,29	239,44	520,48	2,86	1,36	0,00	-24,43	-24,43	-38,74	2,80	1,63
555,13	24,58	238,74	546,77	2,45	1,42	0,00	-30,28	-30,28	-48,51	2,44	-0,74
584,00	27,57	238,26	572,70	3,16	1,50	0,00	-36,91	-36,91	-59,33	3,16	-0,51
613,00	30,50	238,32	598,05	3,08	1,58	0,00	-44,31	-44,31	-71,30	3,08	0,06
641,00	33,40	238,78	621,81	3,17	1,65	0,00	-52,04	-52,04	-83,94	3,16	0,50
670,00	36,05	238,27	645,64	2,80	1,70	0,00	-60,67	-60,67	-98,03	2,79	-0,54
699,00	37,34	238,71	668,89	1,38	1,68	0,00	-69,72	-69,72	-112,80	1,36	0,46
720,00	37,66	239,04	685,55	0,55	1,65	0,00	-76,33	-76,33	-123,75	0,46	0,48
731,00	37,33	239,00	694,28	0,92	1,64	0,00	-79,78	-79,78	-129,49	-0,91	-0,11
756,00	36,10	240,75	714,32	1,97	1,65	0,00	-87,28	-87,28	-142,41	-1,50	2,13
761,00	36,08	240,80	718,36	0,22	1,64	0,00	-88,72	-88,72	-144,98	-0,12	0,30
784,00	36,01	241,05	736,96	0,22	1,60	0,00	-95,29	-95,29	-156,81	-0,09	0,33
813,00	36,33	240,87	760,37	0,35	1,56	0,00	-103,60	-103,60	-171,77	0,34	-0,19
842,17	36,55	239,45	783,83	0,91	1,53	0,00	-112,22	-112,22	-186,80	0,23	-1,48
871,00	36,55	239,45	806,99	0,00	1,48	0,00	-120,95	-120,95	-201,59	0,00	0,00

MD (m)	INC (°)	AZ (°)	TVD (m)	DLS (°/100ft)	AbsTort (°/100ft)	RelTort (°/100ft)	VSect (m)	NS (m)	EW (m)	Build (°/100ft)	Walk (°/100ft)
900,00	38,37	239,25	830,01	1,92	1,50	0,00	-129,94	-129,94	-216,76	1,91	-0,21
926,85	38,26	240,26	851,08	0,72	1,47	0,00	-138,33	-138,33	-231,14	-0,12	1,15
956,68	37,77	240,72	874,58	0,58	1,45	0,00	-147,38	-147,38	-247,13	-0,50	0,47
985,48	37,96	240,82	897,32	0,21	1,41	0,00	-156,01	-156,01	-262,56	0,20	0,11
1014,07	38,00	241,18	919,85	0,24	1,38	0,00	-164,54	-164,54	-277,94	0,04	0,38
1042,75	38,84	241,03	942,32	0,90	1,36	0,00	-173,15	-173,15	-293,55	0,89	-0,16
1071,48	38,55	241,24	964,75	0,34	1,34	0,00	-181,82	-181,82	-309,28	-0,31	0,22
1100,00	38,28	241,47	987,09	0,33	1,31	0,00	-190,32	-190,32	-324,83	-0,29	0,25
1110,00	38,60	241,20	994,93	1,10	1,31	0,00	-193,30	-193,30	-330,28	0,98	-0,82
1129,00	39,20	240,69	1009,71	1,09	1,30	0,00	-199,09	-199,09	-340,71	0,96	-0,82
1157,57	39,89	240,31	1031,74	0,78	1,29	0,00	-208,05	-208,05	-356,54	0,74	-0,41
1186,05	39,81	239,01	1053,61	0,90	1,28	0,00	-217,27	-217,27	-372,29	-0,09	-1,39
1214,61	40,46	238,85	1075,44	0,70	1,27	0,00	-226,77	-226,77	-388,06	0,69	-0,17
1243,17	41,21	238,32	1097,05	0,88	1,26	0,00	-236,50	-236,50	-404,00	0,80	-0,57
1271,75	41,49	237,66	1118,51	0,55	1,24	0,00	-246,51	-246,51	-420,01	0,30	-0,70
1300,49	41,90	237,31	1139,97	0,50	1,23	0,00	-256,79	-256,79	-436,13	0,43	-0,37
1386,39	40,02	237,10	1204,83	0,67	1,19	0,00	-287,28	-287,28	-483,46	-0,67	-0,07
1415,00	40,12	237,09	1226,73	0,11	1,17	0,00	-297,29	-297,29	-498,93	0,11	-0,01
1443,48	40,30	237,25	1248,48	0,22	1,15	0,00	-307,26	-307,26	-514,38	0,19	0,17
1472,07	40,29	237,30	1270,28	0,04	1,13	0,00	-317,25	-317,25	-529,93	-0,01	0,05
1500,63	40,38	237,33	1292,05	0,10	1,11	0,00	-327,24	-327,24	-545,49	0,10	0,03
1529,12	39,11	237,76	1313,96	1,39	1,12	0,00	-337,01	-337,01	-560,86	-1,36	0,46
1557,69	37,80	237,84	1336,33	1,40	1,12	0,00	-346,48	-346,48	-575,89	-1,40	0,09
1586,20	36,84	237,95	1359,00	1,03	1,12	0,00	-355,67	-355,67	-590,53	-1,03	0,12
1614,76	36,82	237,90	1381,86	0,04	1,10	0,00	-364,76	-364,76	-605,04	-0,02	-0,05
1643,49	36,85	237,89	1404,86	0,03	1,08	0,00	-373,91	-373,91	-619,63	0,03	-0,01
1672,09	37,35	237,96	1427,67	0,53	1,07	0,00	-383,07	-383,07	-634,25	0,53	0,07
1700,72	38,01	238,11	1450,33	0,71	1,07	0,00	-392,34	-392,34	-649,10	0,70	0,16
1729,42	38,38	238,06	1472,88	0,39	1,05	0,00	-401,72	-401,72	-664,16	0,39	-0,05
1758,18	38,15	238,14	1495,46	0,25	1,04	0,00	-411,13	-411,13	-679,28	-0,24	0,08
1786,86	37,94	238,28	1518,05	0,24	1,03	0,00	-420,44	-420,44	-694,30	-0,22	0,15
1793,00	38,93	238,76	1522,86	5,13	1,04	0,00	-422,43	-422,43	-697,56	4,91	2,38
1814,43	42,40	240,29	1539,11	5,13	1,09	0,00	-429,51	-429,51	-709,59	4,94	2,18

MD (m)	INC (°)	AZ (°)	TVD (m)	DLS (°/100ft)	AbsTort (°/100ft)	RelTort (°/100ft)	VSect (m)	NS (m)	EW (m)	Build (°/100ft)	Walk (°/100ft)
1843,02	41,69	239,73	1560,34	0,86	1,09	0,00	-439,08	-439,08	-726,18	-0,76	-0,60
1871,70	41,12	239,36	1581,86	0,66	1,08	0,00	-448,69	-448,69	-742,53	-0,61	-0,39
1900,43	40,46	239,02	1603,61	0,74	1,08	0,00	-458,31	-458,31	-758,65	-0,70	-0,36
1929,38	39,75	238,63	1625,75	0,79	1,07	0,00	-467,96	-467,96	-774,61	-0,75	-0,41
1957,95	39,54	238,30	1647,75	0,32	1,06	0,00	-477,49	-477,49	-790,14	-0,22	-0,35
1986,52	39,14	237,66	1669,85	0,61	1,05	0,00	-487,10	-487,10	-805,50	-0,43	-0,68
2015,00	38,76	237,43	1691,99	0,44	1,05	0,00	-496,70	-496,70	-820,61	-0,41	-0,25
2043,56	38,44	237,44	1714,31	0,34	1,04	0,00	-506,29	-506,29	-835,62	-0,34	0,01
2072,12	37,88	237,29	1736,77	0,61	1,03	0,00	-515,81	-515,81	-850,48	-0,60	-0,16
2087,00	38,21	237,20	1748,49	0,69	1,03	0,00	-520,77	-520,77	-858,19	0,68	-0,18
2100,26	38,50	237,12	1758,89	0,68	1,02	0,00	-525,23	-525,23	-865,11	0,67	-0,18
2129,44	38,79	236,73	1781,68	0,40	1,02	0,00	-535,18	-535,18	-880,38	0,30	-0,41
2158,12	37,74	236,49	1804,20	1,13	1,02	0,00	-544,95	-544,95	-895,21	-1,12	-0,26
2186,70	37,29	236,38	1826,87	0,49	1,01	0,00	-554,58	-554,58	-909,71	-0,48	-0,12
2215,34	36,52	236,65	1849,77	0,84	1,01	0,00	-564,06	-564,06	-924,05	-0,82	0,29
2243,95	36,61	237,21	1872,75	0,37	1,00	0,00	-573,36	-573,36	-938,34	0,10	0,60
2272,43	37,38	237,26	1895,49	0,82	1,00	0,00	-582,64	-582,64	-952,75	0,82	0,05
2301,02	37,74	237,98	1918,16	0,61	0,99	0,00	-591,97	-591,97	-967,47	0,38	0,77
2329,58	37,82	238,26	1940,73	0,20	0,98	0,00	-601,21	-601,21	-982,32	0,09	0,30
2358,07	37,72	238,65	1963,25	0,28	0,98	0,00	-610,34	-610,34	-997,19	-0,11	0,42
2386,64	37,94	239,22	1985,81	0,44	0,97	0,00	-619,38	-619,38	-1012,20	0,23	0,61
2415,20	37,73	239,73	2008,37	0,40	0,96	0,00	-628,28	-628,28	-1027,29	-0,22	0,54
2443,93	37,25	240,44	2031,17	0,69	0,96	0,00	-637,00	-637,00	-1042,45	-0,51	0,75
2472,53	36,62	241,00	2054,03	0,76	0,96	0,00	-645,41	-645,41	-1057,44	-0,67	0,60
2501,16	36,20	241,47	2077,07	0,54	0,95	0,00	-653,59	-653,59	-1072,34	-0,45	0,50
2529,92	35,99	242,17	2100,31	0,49	0,95	0,00	-661,59	-661,59	-1087,27	-0,22	0,74
2558,60	35,35	243,09	2123,61	0,89	0,95	0,00	-669,28	-669,28	-1102,12	-0,68	0,98
2578,00	34,91	243,23	2139,47	0,70	0,94	0,00	-674,32	-674,32	-1112,08	-0,69	0,22
2587,10	34,70	243,29	2146,95	0,71	0,94	0,00	-676,65	-676,65	-1116,72	-0,70	0,20
2589,30	34,66	243,28	2148,75	0,56	0,94	0,00	-677,22	-677,22	-1117,84	-0,55	-0,14
2603,00	34,43	243,24	2160,04	0,51	0,94	0,00	-680,71	-680,71	-1124,78	-0,51	-0,09
2620,00	34,14	243,19	2174,09	0,52	0,94	0,00	-685,03	-685,03	-1133,32	-0,52	-0,09

B.1 Minimum Flowrate Vs ROP in Hole Section 17-1/2"

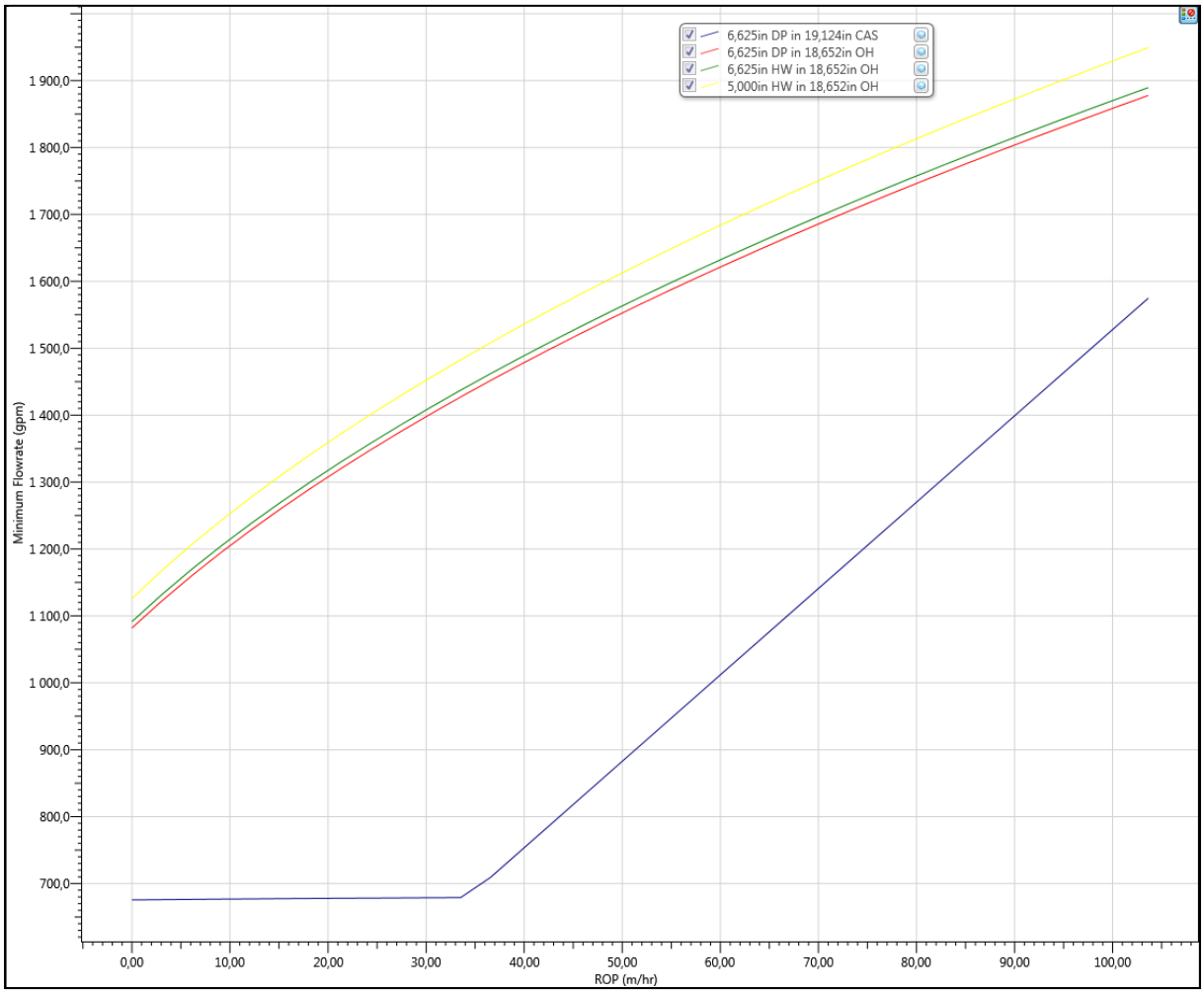

B.2 Minimum Flowrate Vs ROP in Hole Section 12-1/4"

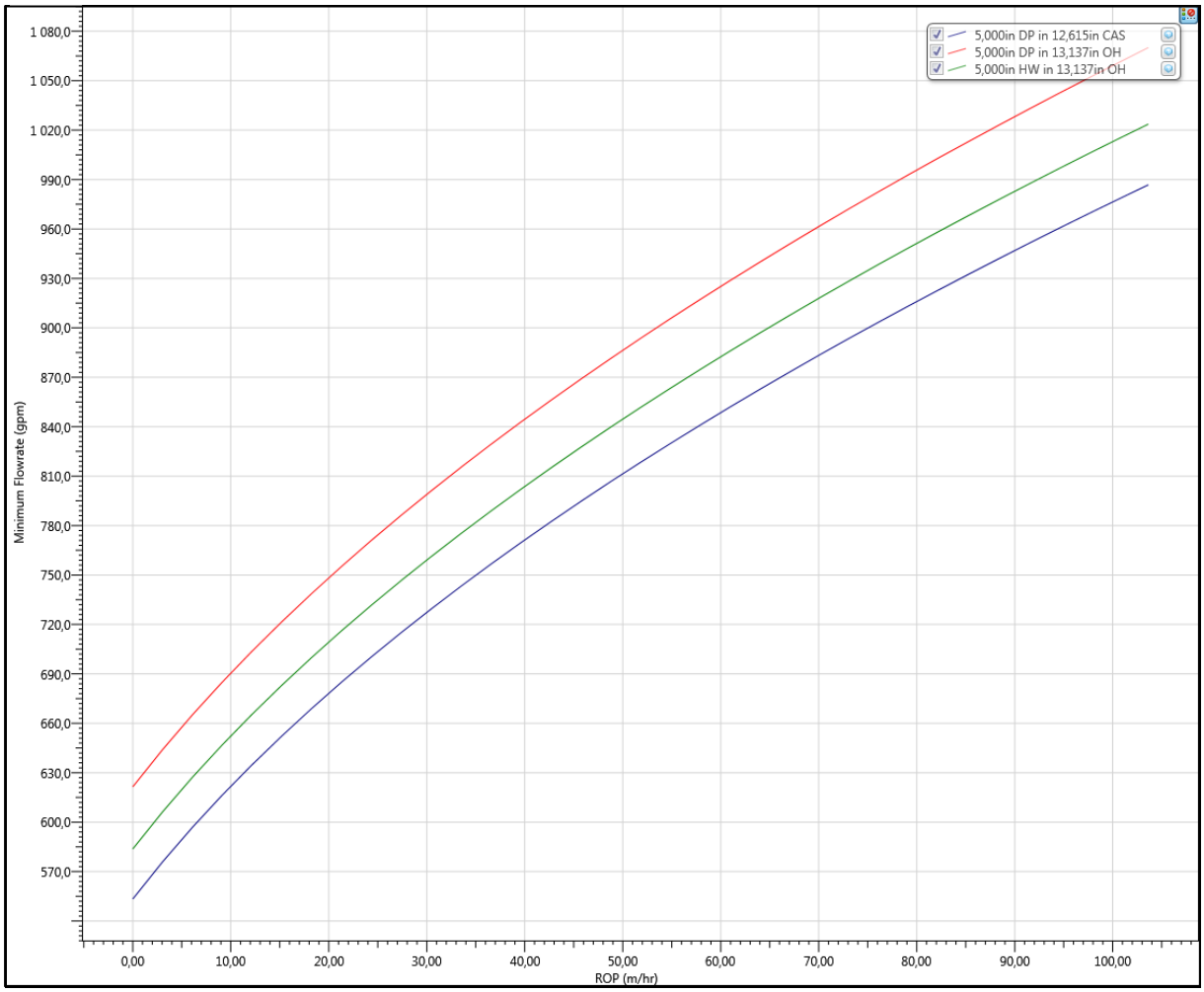

B.3 Minimum Flowrate Vs ROP in Hole Section 8-1/2"